UNIVERSIDAD COMPLUTENSE DE MADRID

FACULTAD DE GEOGRAFÍA E HISTORIA

TESIS DOCTORAL

Aproximación metodológica al estudio de la deglaciación y sus consecuencias geomorfológicas: aplicación en la Península de Tröllaskagi (Norte de Islandia)

Methodological approach to the study of deglaciation and its geomorphological consequences: application in the Tröllaskagi peninsula (Northern Iceland)

MEMORIA PARA OPTAR AL GRADO DE DOCTOR

PRESENTADA POR

José María Fernández Fernández

Bajo la dirección de los doctores

David Palacios Estremera

Nuria de Andrés de Pablo

Madrid, 2019

UNIVERSIDAD COMPLUTENSE DE MADRID

FACULTAD DE GEOGRAFÍA E HISTORIA

Departamento de Geografía

APROXIMACIÓN METODOLÓGICA AL ESTUDIO DE LA DEGLACIACIÓN Y SUS CONSECUENCIAS GEOMORFOLÓGICAS: APLICACIÓN EN LA PENÍNSULA DE TRÖLLASKAGI (NORTE DE ISLANDIA)

METHODOLOGICAL APPROACH TO THE STUDY OF DEGLACIATION AND ITS GEOMORPHOLOGICAL CONSEQUENCES: APPLICATION IN THE TRÖLLASKAGI PENINSULA (NORTHERN ICELAND)

TESIS DOCTORAL

José María Fernández Fernández

Madrid, 2019

UNIVERSIDAD COMPLUTENSE MADRID

DECLARACIÓN DE AUTORÍA Y ORIGINALIDAD DE LA TESIS PRESENTADA PARA OBTENER EL TÍTULO DE DOCTOR

D./Dña. José María Fernández Fernández,
estudiante en el Programa de Doctorado en Geografía,
de la Facultad de Geografía e Historia de la Universidad Complutense de Madrid, como autor/a de la tesis presentada para la obtención del título de Doctor y titulada:

"Aproximación metodológica al estudio de la deglaciación y sus consecuencias geomorfológicas: aplicación en la Península de Tröllaskagi (Norte de Islandia)"

y dirigida por: Dr. David Palacios Estremera y Dr. Nuria de Andrés de Pablo

DECLARO QUE:

La tesis es una obra original que no infringe los derechos de propiedad intelectual ni los derechos de propiedad industrial u otros, de acuerdo con el ordenamiento jurídico vigente, en particular, la Ley de Propiedad Intelectual (R.D. legislativo 1/1996, de 12 de abril, por el que se aprueba el texto refundido de la Ley de Propiedad Intelectual, modificado por la Ley 2/2019, de 1 de marzo, regularizando, aclarando y armonizando las disposiciones legales vigentes sobre la materia), en particular, las disposiciones referidas al derecho de cita.

Del mismo modo, asumo frente a la Universidad cualquier responsabilidad que pudiera derivarse de la autoría o falta de originalidad del contenido de la tesis presentada de conformidad con el ordenamiento jurídico vigente.

En Madrid, a 10 de junio de 2019

Fdo.: FERNANDEZ FERNANDEZ JOSE MARIA - 09062655B

Firmado digitalmente por FERNANDEZ FERNANDEZ JOSE MARIA - 09062655B
Fecha: 2019.06.07 17:04:30 +02'00'

Esta DECLARACIÓN DE AUTORÍA Y ORIGINALIDAD debe ser insertada en la primera página de la tesis presentada para la obtención del título de Doctor.

A mi padre,

A mi madre

“Nada tiene tanto poder para ampliar la mente como la capacidad de investigar de forma sistemática y real todo lo que es susceptible de observación en la vida”

Marco Aurelio (121-180)

Agradecimientos

Algunas personas creen que el destino existe, y sin embargo, otras piensan que lo que hay en realidad es el producto de todas las decisiones que tomamos, tanto aquellas de suma importancia como aquellas aparentemente insignificantes. Juzguen ustedes mismos. Cuando tan sólo contaba dos años, la persona que 26 años después escribe estas líneas, se encaprichó en una tienda de algo que veía por vez primera y que le llamó poderosamente la atención: un mapa. Ese niño, desde el carrito en que lo paseaba su madre, no imaginaba el emocionante –y en ocasiones, también difícil– camino que el mundo de la Geografía le deparaba, por lo menos en la veintena.

Hoy, cuando esta Tesis se haya en sus compases finales, me gustaría mostrar mi más sincero agradecimiento a todas las personas que han sido participes de esta experiencia, y sin las cuales, de ningún otro modo habría sido posible.

En primer lugar, quiero expresar mi más sincero agradecimiento y gratitud hacia mis directores de tesis, el Dr. David Palacios Estremera y la Dra. Nuria de Andrés de Pablo. Haberles elegido como directores de este primer trabajo de Investigación Científica es la decisión de la que más orgulloso y satisfecho me siento; y que aceptasen, probablemente el mejor premio. Ellos han sabido transmitirme una idea de Ciencia y una visión práctica de la misma que ni en el mejor de los diccionarios podría encontrarse. Debo agradecerles que me ofrecieran el tema que aborda la Tesis y el interés que me han transmitido por el mundo nórdico y las regiones polares. También agradezco que me facilitaran un espacio en la Facultad y los medios para poder trabajar en la Tesis –incluso sin ser becario al comienzo– en un entorno agradable. Por encima de todo, tengo que destacar el esfuerzo, tiempo y dedicación que en mí han invertido, así como su nivel de apoyo, exigencia y confianza. Su gran calidad humana a lo largo de estos cinco años de doctorado –también extensible a mi año de Máster– ha hecho más llevadero este sinuoso camino que supone la Tesis Doctoral. Desde el primer momento me hicieron sentir como un igual pese a la gran distancia académica que nos separa, y además, durante las continuas revisiones que han dado forma a esta Tesis han demostrado una gran paciencia y comprensión sin llegar a desesperarse. Quiero agradecerles asimismo las oportunidades que me han brindado para colaborar en distintas asignaturas de Grado (Geografía y Ordenación del Territorio) y Máster (Tecnologías de la Información Geográfica; Dinámicas Territoriales y Desarrollo; Gestión de Desastres), con las cuales he podido disfrutar de lo que siempre vi como una vocación. También quiero darles las gracias por sus invitaciones para participar en otros trabajos científicos y trabajos de campo paralelos a la Tesis, así como en distintos proyectos de investigación sin los cuales esta investigación no hubiera sido posible.

Este trabajo de investigación no se podría haber llevado a cabo sin la colaboración del "Grupo de Investigación en Geografía Física de Alta Montaña" (GFAM), al que se adscribe. El ambiente dinámico, el intercambio de ideas y su trabajo en áreas cercanas han beneficiado enormemente a esta Tesis. El resto de miembros del equipo también han contribuido a generar un entorno agradable. A Julio Muñoz, Luis Miguel Tanarro, José Úbeda, Jesús Alcalá y José Juan Zamorano (UNAM) les doy las gracias por lo bien que me acogieron dentro del grupo desde el comienzo. También les debo su total y desinteresado apoyo, así como sus interesantes discusiones científicas, sus ánimos a la hora de iniciar el estudio de la Geografía Física y la Geomorfología, el rigor científico a la hora de abordar cualquier trabajo y la importancia de la precisión y pulcritud en la aplicación de técnicas (cartografía, cálculos, etc.), sin perder la perspectiva de la Ciencia Geográfica. Tampoco me olvido de sus enseñanzas magistrales durante la Licenciatura y el Máster, junto con las del resto de profesores de las áreas Geografía Física, Análisis Geográfico Regional y Geografía Humana. A ellos les debo mi formación como geógrafo, y espero que haya podido plasmar en este trabajo sus sabias enseñanzas durante todos estos años.

Esta Tesis se ha realizado dentro del antiguo "Departamento de Análisis Geográfico Regional y Geografía Física" y el actual "Departamento de Geografía", a cuyos directores, la Dra. Cristina Montiel Molina y el Dr. Javier Gutiérrez Puebla quiero mostrar mi agradecimiento por el buen trato que siempre han tenido conmigo, el interés que mostraron en esta investigación, sus eficaces gestiones en las tareas burocráticas que implica la Tesis (permisos para ausencias, estancias, memorias anuales, etc.), por facilitarme un lugar físico en el que poder trabajar, y que me permitieran ser Colaborador Honorífico del Departamento. Mi gratitud también a la Secretaria Administrativa Dña. Mercedes García Pascual por sus labores burocráticas en el trámite de permisos y documentación asociada a las obligaciones del contrato FPU.

Me gustaría reconocer asimismo el apoyo prestado por el "Laboratorio de Geografía Física" de la Universidad Complutense de Madrid. El encomiable trabajo de la Dra. Ester Bravo Muñoz en la preparación física inicial de las muestras, y la infraestructura que poco a poco va adquiriendo el laboratorio, han sido esenciales para la posterior aplicación de las técnicas de datación en laboratorios especializados.

Durante estos cinco años, en sucesivas estancias de investigación, tuve la oportunidad de formarme asimismo en la aplicación de las dataciones por exposición a los rayos cósmicos a través de los isótopos cosmogénicos cloro-36 y berilio-10, en el "Laboratoire National des Nucléides Cosmogéniques", dependiente del "Centre Européen de Recherche et d'Enseignement des Géosciences de l'Environnement" (Aix-en-Provence,

Francia). Quiero dar las gracias especialmente a la Dra. Irene Schimmelpfennig por la amabilidad y accesibilidad que siempre mostró en cada una de mis estancias, sus pacientes y claras explicaciones e instrucciones durante los complejos tratamientos físico-químicos de rocas en el laboratorio (cloro-36l), su interés en el transcurso de esta investigación, y sus eficaces y constructivas revisiones en las publicaciones derivadas. No me olvido tampoco de Laëtitia Leanni, por su enseñanza y asesoramiento paciente durante el aprendizaje del procesado de muestras para datación mediante el isótopo cosmogénico berilio-10. Mi gratitud también a los miembros del "ASTER Team" (Didier Bourlès, Régis Braucher, George Aumaître y Karim Keddadouche) por su importante trabajo con las muestras en el Acelerador Espectrómetro de Masas (AMS). No quisiera dejar sin mencionar tampoco a otros jóvenes investigadores que conocí en las últimas estancias, el Dr. Daniel Vázquez, y Jesús Díaz, con los cuales tuve oportunidad de intercambiar pareceres sobre nuestros distintos enfoques y temas de investigación en las Ciencias de la Tierra. Debo reconocer que gracias a todas estas personas, desde el primer momento allí me sentí como en mi propia casa.

En estos cinco años, a lo largo de las diversas colaboraciones científicas, trabajos de campo y congresos, he tenido el gran honor –y suerte– de conocer fuera de la Facultad a otros grandes Investigadores y Maestros de la Geografía. Este es el caso, por ejemplo, del Dr. José María García Ruiz (IPE-CSIC), quien me mostró en los trabajos de campo de la Sierra de la Demanda y Sierra Cebollera (2015, 2016) la importancia de cartografiar "con ojo clínico" las formas del relieve *in situ*, en el propio campo, y que la Geografía es también saber leer el paisaje que se muestra ante nuestros ojos. En estos trabajos de campo, también tuve oportunidad de conocer a otros investigadores de gran calidad como Amelia Gómez Villar, Javier Santos González, José Arnáez, Javier Álvarez y Noemí Lana, de quienes también aprendí. Por su parte, en otros trabajos de campo de paralelos sobre muestreo para dataciones en la Montaña Palentina, también coincidí con los investigadores Alsonfo Pisabarro (Universidad de Valladolid) y el Dr. Ramón Pellitero, a quien doy las gracias por permitirme probar "en primicia" las *toolboxes* que estaba desarrollando, así como por sus fructíferas discusiones acerca de los métodos para la reconstrucción de paleoglaciares.

Quiero hacer especial mención también a los Dres. Skafti Brynjólfsson (Instituto Islandés de Historia Natural; Akureyri, Islandia) y Þorsteinn Sæmundsson (Universidad de Islandia), por el interés que han demostrado en las investigaciones que conforman esta tesis a través de sus valiosas revisiones y discusiones. Se agradece también al "Hólar University College" y la "Icelandic Association for Search and Rescue" (ICESAR) su soporte logístico en las campañas de campo en Tröllaskagi (Norte de Islandia).

Ha llegado el momento de mencionar a dos grandes investigadores que, gracias al GFAM, he tenido el placer de conocer, y de ello quiero dejar constancia. Se trata de los Dres. Marc Oliva Franganillo (Universidad de Barcelona) y Jesús Ruiz Fernández (Universidad de Oviedo). Dos auténticas referencias que, junto con mis directores de tesis, despertaron mi interés y fascinación por las áreas polares árticas y antárticas. A Marc le tengo que agradecer el entusiasmo y energía que transmite, así como su confianza, permitirme participar en sus proyectos de investigación y colaborar en publicaciones científicas de primerísimo nivel. A Jesús, le doy las gracias por sus enseñanzas sobre cartografía geomorfológica en campo y gabinete, por transmitirme su idea de la Geografía y por permitirme participar en su proyecto CRONOANTAR, y dentro de él en la Campaña Antártica Española, en la que tuve el placer de visitar zonas remotas del Planeta en las que jamás imaginé que estaría. Desde aquí agradezco también el magnífico trato del personal de la Base Antártica Española "Juan Carlos I" (Isla Livingston, Antártida Marítima) y los investigadores con los que coincidí, especialmente Rosana Menéndez, Susana Fernández y Javier Calleja (Universidad de Oviedo).

Para cerrar el bloque de agradecimientos en el plano académico, me gustaría reconocer la labor de los investigadores anónimos que han revisado las publicaciones que durante estos años han constituido mi trabajo. Puedo decir que con sus observaciones es mucho lo que he aprendido.

Al margen de los logros de la Tesis, este largo viaje ha servido también para conocer a muchas personas, como las que también han estado o están investigando dentro del Departamento, quienes también me han permitido ver la investigación desde otras perspectivas, y me han mostrado su más sincero y desinteresado apoyo. Entre ellos están los compañeros del "Despacho nº 16" (Jesús y Leticia al comienzo, y durante más tiempo Néstor, Juan Carlos y Jesús), el "Despacho de Investigadores del Departamento de Geografía" (Catarina –muchas gracias por tus ánimos– y Manuel), de "La Cueva" (Roberto y Tatiana) y de "La Jaula / El Mirador" (Borja, Joaquín, Claudia, Ana, Carolina, Gustavo, y más recientemente Daniela, Sofía, Elena, Onel, Julio, Marina y Oswaldo). Recientemente se incorporaron al Departamento Rocío y Rubén, quienes me han transmitido también sus experiencias sobre la Tesis doctoral en su fase final.

Mi reconocimiento debe incluir también a los compañeros que me acompañaron a lo largo de la Licenciatura en Geografía y a los que lo hicieron durante el Máster en Tecnologías de la Información Geográfica. Y en un lugar especial, destaco a tres grandes amigos y magníficas personas que también me han acompañado durante estos años: María, Yaiza y Alberto. Durante todo este tiempo me han hecho mirar la vida desde otro

ángulo, me han demostrado su cariño, y me han dado todo su apoyo y ánimos desinteresadamente, en especial en el tramo final de la Tesis, en el que el camino se hacía cuesta arriba. Y, más importante todavía, me han soportado –reconozco que a veces no ha sido fácil–. Gracias.

Llegando casi al final de esta sección, me gustaría dedicar unas palabras a otro conjunto de personas a las que les debo también mucho más allá de la vida, mi familia. Mis padres, Pablo (*D.E.P.*) y Laura, se sacrificaron y me dieron todas las oportunidades para que siguiera estudiando desde Secundaria hasta la Universidad. Mi agradecimiento también al Ministerio de Educación, por sus distintas becas. A mi madre debo agradecerle su constante e incondicional apoyo, sus ánimos y la esperanza, especialmente en aquellos momentos difíciles de bloqueo, en los que las fuerzas flaquean y nada parece ir sobre ruedas. A mi padre le debo el afán de superación, el inconformismo y el perfeccionismo que me transmitió, así como poner en mí conocimiento la palabra *geógrafo* cuando de niño pasaba las horas mirando mapas. Lamento que no haya podido ver a su hijo disfrutar todos estos años haciendo lo que siempre le ha gustado, o verle defender este trabajo, al menos del modo en el que a mí me habría gustado. La Tesis también es un logro vuestro. Más allá de mis personas más allegadas, quisiera extender toda mi gratitud a mi familia materna, por apoyarme en todo lo que hago y por animarme a conseguirlo desde que tengo uso de razón.

Finalmente, agradecer al conjunto de entidades que han financiado este trabajo de investigación. En primer lugar al Ministerio de Educación, Cultura y Deporte por darme la oportunidad de ser becario del Programa Estatal de Formación de Profesores Universitarios (FPU; proyecto FPU14/06150), con la tranquilidad económica que aporta durante estos años. El desarrollo de esta tesis tampoco habría sido el mismo sin la ayuda económica proporcionada por los proyectos CRYOCRISIS (CGL2012-35858), DEGLACIATION (CGL2015-65813-R) y EUINEUIN-2013-50924, financiados por el Ministerio de Economía y Competitividad, y dirigidos por el Dr. David Palacios. Me gustaría subrayar que gracias estos proyectos se han podido implementar en este trabajo las más novedosas –y también costosas– técnicas de datación por isótopos cosmogénicos. Gracias a dichos proyectos, también he podido disfrutar de varias estancias de investigación en el extranjero y participar en los trabajos de campo en la Península de Tröllaskagi (Norte de Islandia), y asistir a congresos científicos.

Por último, sólo me queda decir que, aunque he tratado de recoger en estas líneas a todas las personas que han hecho posible esta Tesis, probablemente me haya olvidado de

mencionar a otras que también hayan hecho méritos para aparecer. A todas ellas, deciros que de algún modo, también estáis aquí.

¡Gracias!

Índice / *Index*

Índice de tablas / *Table index*

Capítulo 1.

Chapter 3.

Chapter 4.

Chapter 5.

Chapter 6.

Índice de figuras / *Figure index*

Chapter 4.

Chapter 5.

Chapter 6.

RESUMEN

TÍTULO: "APROXIMACIÓN METODOLÓGICA AL ESTUDIO DE LA DEGLACIACIÓN Y SUS CONSECUENCIAS GEOMORFOLÓGICAS: APLICACIÓN EN LA PENÍNSULA DE TRÖLLASKAGI (NORTE DE ISLANDIA)"

Introducción.

Islandia se localiza en el contacto de las masas atmosféricas árticas frías y subtropicales cálidas y entre la corriente oceánica fría del Este de Groenlandia y la corriente cálida de Irminger. Como consecuencia, este territorio es muy sensible a los cambios atmosféricos y oceánicos, que a lo largo del tiempo han provocado constantes y bruscos cambios en su clima y en la extensión de sus glaciares, que ocupan una parte considerable de la isla. Esta variabilidad climática condiciona su dinámica medioambiental y humana. Los últimos periodos climáticos más contrastados han sido el Máximo Térmico Holoceno (MTH) y el Neoglacial, determinados por cambios en configuración atmosférica y oceánica, y por la evolución de la actividad volcánica y la insolación.

En el norte de Islandia se sitúa la Península de Tröllaskagi, caracterizada por un relieve montañoso, donde se localizan más de 160 circos, ocupados en su mayoría por glaciares cubiertos y glaciares rocosos, y sólo unos pocos por glaciares libres de una cubierta de derrubios. Éstos últimos glaciares muestran una mayor sensibilidad a las fluctuaciones climáticas. Durante el MTH, los glaciares de Tröllaskagi alcanzaron su mínima extensión Holocena y muchos de ellos desaparecieron. Con el inicio de la Neoglaciación muchos glaciares comenzaron a avanzar y otros, que habían desaparecido en el HTM, se volvieron a formar. El enfriamiento neoglacial alternó periodos de un fuerte descenso de la temperatura, principalmente en 4.7, 4.2, 3.2-3.0, 2.0, 1.5 y 1.0 ka, con periodos mucho más cálidos. Las características descritas sobre la Península de Tröllaskagi la convierten en un entorno ideal para estudiar el impacto de los cambios climáticos en los glaciares, así como las formas del relieve derivadas de ese impacto.

Objetivos y resultados.

El principal objetivo de esta Tesis doctoral es mejorar el conocimiento de la evolución de los glaciares de Tröllaskagi durante el final del Holoceno para ampliar la comprensión del cambio climático a escala global. Para lograr este objetivo, la Tesis propone una nueva estrategia metodológica que incluye la aplicación de múltiples técnicas, como la

fotointerpretación, la cartografía geomorfológica, los modelos de reconstrucción paleoglaciar, los modelos glacio-climáticos y las dataciones cosmogénicas (^{36}Cl) y liquenométricas. La estrategia busca la calibración y mejora de unas técnicas con otras para reducir considerablemente la incertidumbre de los resultados. El método propuesto también busca alternar el estudio de glaciares sin cobertura de derrubios (Gljúfurárjökull, Tungnahryggsjökull oeste y Tungnahryggsjökull este), con glaciares cubiertos (Hóladalsjökull, Hofsjökull y Héðinsdalsjökull) y glaciares rocosos (Fremri-Grjótárdalur).

Los resultados obtenidos confirman la sensibilidad de los glaciares sin cubierta de derrubios a las variaciones de la temperatura estival. Desde el final de la PEH, los glaciares tuvieron un fuerte retroceso, en especial durante las décadas más cálidas del siglo XX. Las series climatológicas y los modelos glacio-climáticos aplicados en la Tesis sugieren que el retroceso glaciar se debió a un incremento de la temperatura estival de ~1 ºC, pero que coincidió con un aumento de la precipitación anual / invernal de hasta un 40% insuficiente para evitar este retroceso. Esta tendencia se interrumpió entre los años setenta y noventa, como consecuencia de una reducción en la temperatura estival de 0,5 ºC respecto a la media actual y del incremento de la precipitación. Los resultados han permitido conocer por primera vez la existencia en Trollaskagi de importantes avances Neoglaciales ocurridos en ~400 y ~700 CE y a partir de siglos XV a XVII, ya durante la PEH, mediante dataciones cosmogénicas. Estos resultados refutan la hipótesis tradicional que fechaba el máximo Neoglacial en la PEH. Por otro lado, demuestran que los avances más importantes de la PEH en Tröllaskagi ocurrieron mucho antes de finales del siglo XIX, en contra de lo que las dataciones liquenométricas habían indicado anteriormente.

Por último, los resultados de la Tesis muestran por primera vez los grandes rasgos de la deglaciación de las montañas de Tröllaskagi, con la desaparición de los glaciares de los grandes valles hacia 16 ka y la desaparición de pequeños glaciares de circo en las cabeceras de estos valles hacia 11 ka. Justo después se formaron glaciares rocosos y glaciares cubiertos, como consecuencia de la actividad paraglacial. Los frentes de estos glaciares se estabilizaron rápidamente entre 11 y 9 ka. A continuación, se formaron nuevos glaciares rocosos en algunos circos, y se estabilizaron hacia 7-3 ka, a la vez que los glaciares cubiertos. En la mayoría de los casos, ambos grupos de formaciones permanecen estables en la actualidad, aunque no han perdido el hielo intersticial.

Conclusiones.

La Tesis ha logrado los objetivos propuestos al aportar novedosos datos sobre la evolución climática y glaciar reciente en el Norte de Islandia. Estos datos son

fundamentales para conocer el impacto del cambio climático en el Ártico, cuenca oceánica clave dentro de las tele-conexiones de la atmósfera a nivel global que están provocando el intenso calentamiento del clima en la actualidad. Además, la Tesis ha demostrado la eficacia de su propuesta metodológica para estudiar la evolución de los glaciares y deducir las casusas climáticas de esa evolución. De hecho, el carácter complementario de las técnicas aplicadas ha reducido de manera significativa el rango de incertidumbre de los resultados obtenidos. Esta nueva propuesta es apta para ser aplicada en cualquier glaciar de montaña, por lo que se propone su uso generalizado.

La Tesis, sin embrago no ha culminado y cerrado una línea de investigación. Por el contrario, los resultados aportados están pendientes de su plena confirmación mediante el contraste con nuevas investigaciones sobre el estudio de la deglaciación en valles cercanos, para fortalecer los resultados propuestos sobre la cronología del máximo Neoglacial y de la formación y estabilización de glaciares cubiertos y rocosos en el Norte de Islandia. Por otro lado, la Tesis ha resaltado la urgencia de investigar en profundidad la relación existente entre las fluctuaciones de la Oscilación del Atlántico Norte y la evolución de los glaciares, ya que todavía no está plenamente demostrada en Tröllaskagi.

ABSTRACT

TITLE: "METHODOLOGICAL APPROACH TO THE STUDY OF DEGLACIATION AND ITS GEOMORPHOLOGICAL CONSEQUENCES: APPLICATION IN THE TRÖLLASKAGI PENINSULA (NORTHERN ICELAND)"

Introduction.

Iceland is located in the meeting point of cold Arctic and warm subtropical air masses, and between the cold East Greenland and the warm Irminger sea currents. As a result, this territory is especially sensitive to the changes of the atmospheric and oceanic settings over time, which have triggered constant and abrupt changes of the Icelandic climate, and hence on the glaciers, which cover a significant part of the island. This climate variability conditions the environmental and human dynamics. The last most contrasting periods have been the Holocene Thermal Maximum (HTM) and the Neoglaciation, controlled by changes of the atmospheric and oceanic setting and the evolution of the volcanic activity and insolation.

The Tröllaskagi peninsula is characterised by a mountainous relief where over 160 cirques exist. Most of them are occupied by debris-covered glaciers and rock glaciers, and only a few are debris-free. The latter type shows a greater sensitivity to the climate fluctuations. In fact, the Tröllaskagi glaciers reached their minimum Holocene extent during the HTM, and most of them disappeared. With the onset of the Neoglaciation, many Tröllaskagi glaciers began to advance and others that had already disappeared in the HTM were re-formed. During the Neoglacial cooling, periods of strong temperature lowering at 4.7, 4.2, 3.2-3.0, 2.0, 1.5 and 1.0 ka alternated with others much warmer. The features described on the Tröllaskagi peninsula make it an ideal environment to study the impact of the climate changes on glaciers as well as the landforms derived from that impact.

Objectives and results.

The main objective of this Doctoral Thesis is to improve the knowledge on the evolution of the Tröllaskagi glaciers during the Late Holocene in order to broaden the understanding of climate change on a global scale. To achieve this objective, the Thesis proposes a new methodological strategy that integrates the application of multiple techniques such as photointerpretation, geomorphological mapping, numerical physical-based models for glacier surface reconstruction, glacier-climate models and Cosmic-Ray Exposure (^{36}Cl) and lichenometric dating. The strategy aims to calibrate and improve some

techniques with the other so that the uncertainty of the results is considerably reduced. The proposed methodology also intends to alternate the study of debris-free glaciers (Gljúfurárjökull, western Tungnahryggsjökull and eastern Tungnahryggsjökull) with debris-covered (Hóladalsjökull, Hofsjökull and Héðinsdalsjökull) and rock glaciers (Fremri-Grjótárdalur).

The results obtained confirm the sensitivity of the debris-free glaciers to the summer temperature fluctuations. Glaciers undergone a strong retreat since the end of the LIA, especially during the warmest decades of the 20th century. The climate records and the glacier-climate models applied in the Thesis suggest that the glacier retreat was due to an increase of summer temperature of ~1 ºC, which coincided with an increase of annual precipitation / winter accumulation up to 40%, insufficient to avoid the retreat. This trend was interrupted between the 1970s and 1990s as a result of a 0.5 ºC lowering of summer temperature below the current average and the increase of winter precipitation. The results have also allowed to know for the first time and throughout CRE dating (^{36}Cl) the existence of Neoglacial advances occurred in Tröllaskagi in ~400 and ~700 CE and from the 15th to 17th centuries already during the LIA. These results refute the traditional hypothesis according to which the Neoglacial maximum occurred during the LIA. On the other hand, they prove that the most important LIA advances occurred in Tröllaskagi long before the late 19th century, contrary to what had been previously stated from lichenometric dating.

Finally, the results of the Thesis show for the first time the main characteristics of the deglaciation of the Tröllaskagi mountains: the glaciers disappeared form the great valleys at around 16 ka, and the small cirque glaciers of their headwalls did it at 11 ka. Immediately after, debris-covered and rock glaciers formed due to the paraglacial activity. The fronts of these glaciers stabilized quickly between 11 and 9 ka. Then, new rock glaciers formed in some cirques. These new rock glaciers and the debris-covered glaciers stabilized between 7 and 3 ka. Both groups of formations remain stable in most of the cases, although they have not lost the inner ice.

Conclusions.

The Thesis have achieved the main objectives by providing new data on the recent climatic and glacial evolution in northern Iceland. These data are essential to know the impact of the climate change in the Arctic, i.e. a key ocean basin within the global atmospheric tele-connections that are causing intense climate warming nowadays. Moreover, the Thesis has shown the efficiency of its methodological proposal, which includes multiple techniques to study the evolution of glaciers and deduce the climatic

causes of that evolution. In fact, the complementary character of the techniques applied has significantly reduced the uncertainty range of the results obtained. This new proposal is suitable to be applied in any mountain glacier, and therefore its generalized use is proposed.

However, the Thesis has not culminated and closed a line of research. On the contrary, the results provided need to be confirmed throughout their contrast with new research on the deglaciation in nearby valleys in order to strengthen the results proposed about the Neoglacial maximum chronology and the formation and stabilization of debris-covered and rock glaciers in northern Iceland. On the other hand, the Thesis highlights the urgency of investigating in depth the relation between the fluctuations of the North Atlantic Oscillation and the glacier evolution as this relation is not entirely demonstrated in Tröllaskagi.

Capítulo 1.

Introducción. El conocimiento del Neoglacial en Islandia. Estructura y objetivos de la investigación.

1.1. La importancia de Islandia en el conocimiento de la evolución climática en los últimos milenios.

Islandia es un territorio en el que el poblamiento comenzó relativamente tarde, hacia el año 870 CE (Edudóttir et al., 2016), por lo que el estudio del paleoambiente anterior, libre de influencia antrópica, ofrece una oportunidad para comprender los cambios climáticos derivados de procesos y forzamientos naturales (Stötter et al., 1999), como los orbitales, volcánicos, atmosféricos y oceánicos.

Desde el punto de vista climático, Islandia se localiza en una posición fronteriza entre los principales sistemas de circulación atmosférica y oceánica de las zonas polar y templada. Desde el punto de vista atmosférico, en esta zona convergen los vientos (del nordeste) procedentes de las altas presiones polares, con aquellos (del suroeste) originados en las altas presiones subtropicales. Esta circulación determina hacia los 60º de latitud, en las proximidades de Islandia, el encuentro de masas de aire de características contrastadas; por un lado, las masas de aire polar frío (seco), y por otro, aquellas de aire subtropical cálido (húmedo) (Einarsson, 1984).

Por tanto, se genera un frente polar a lo largo del cual se originan sucesivas células ciclónicas subpolares (Bjerknes y Solberg, 1922), de las que la depresión de Islandia (Einarsson, 1984) es la más constante. La localización de este centro de bajas presiones oscila entre los 55º y los 70º N, y entre los 10º y los 60º O, con cambios de posición estacionales en una dirección este-oeste (Sahsamanoglou, 1990). La presión atmosférica en su núcleo (en superficie) está sujeta a variaciones entre los 994 y los 1008 hPa en enero y mayo, respectivamente (Sahsamanoglou, 1990). La intensidad de la depresión de

Islandia es máxima en invierno, con ratios de profundización hasta el doble de las observadas durante la época estival (Serreze, 1995).

La actividad ciclónica asociada y la potencia de la circulación del oeste (*westerlies*) es dependiente de la Oscilación del Atlántico Norte (NAO, del inglés *North Atlantic Oscillation*), una de las mayores fuentes de variabilidad interanual de la circulación atmosférica (Hurrel, 1995a). Las diferencias de presión en el dipolo Reykjavík – Lisboa (o Azores), con centros de presión opuestos –una depresión y un anticiclón, ambos de origen dinámico–, configuran el llamado índice NAO. En Hurrel (1995a) se indicó que los cambios de signo de este índice se asocian a cambios en los patrones de circulación atmosférica, en las rutas de tránsito de las borrascas y en la actividad sinóptica de los torbellinos (Rogers, 1990; Hurrel, 1995b), que implican asimismo cambios en el transporte y convergencia de humedad, y por tanto, cambios regionales en la precipitación.

De este modo, durante las fases positivas se incrementa el transporte de humedad en dirección suroeste-nordeste en el norte de Europa y el flujo de convergencia de humedad en Islandia, que en conjunto desencadenan períodos húmedos anómalos (Hurrel, 1995a). La situación es la opuesta en las fases negativas (ver Holmes et al., 2016). Por ello, las condiciones atmosféricas asociadas a los modos NAO disponen el régimen de masas de aire (ver Rogers, 1985), e incluso influyen en los flujos de energía atmósfera-océano (extracción de calor del océano, fusión del hielo marino, entrada de aguas frías) y en la circulación oceánica (Hurrel, 1995a).

La circulación oceánica en torno a Islandia reproduce contrastes análogos a los atmosféricos, con el encuentro entre corrientes de agua de procedencias y propiedades contrastadas. De hecho, existe un frente polar marino, también referido como «*the East Greenland front*» (Johannessen, 1986) o «*the Arctic front*» (Hansen y Meincke, 1979; Orvik et al., 2001), que se encuentra en las proximidades del borde norte de Vestfirðir, al noroeste de Islandia (Ólafsdóttir et al., 2010). Por una parte, la corriente de Irminger es una de las ramificaciones de la corriente del Golfo producida al sur de Islandia. Sus aguas, procedentes del sur, relativamente cálidas (3-8 ºC) y de alta salinidad (*ca.* 35‰), se desplazan hacia el polo a lo largo del borde oriental del canal entre Groenlandia e Islandia, bordeando las costas islandesas por el sur, oeste y norte (Stefansson, 1962; Malmberg, 1985; Malmberg et al., 1996) y suavizando las temperaturas. Por otra parte, la corriente del este de Islandia es, a su vez, una ramificación de la corriente del este de Groenlandia. En este caso, sus aguas procedentes del norte discurren por el borde occidental del canal, tienen temperaturas por debajo de los 0 ºC y una salinidad inferior al 34.5‰ (Stefansson, 1962; Malmberg, 1985; Malmberg et al., 1996). Estas aguas son portadoras de hielo

marino, que en los años más severos, alcanzan las costas del noroeste, norte y este, y hacen descender las temperaturas considerablemente (Einarson, 1984).

Del mismo modo que sucede a nivel atmosférico, la línea de contacto entre ambas corrientes oceánicas experimenta unos elevados gradientes de temperatura, así como cambios de posición a lo largo del tiempo, como recientemente se ha observado (Malmberg, 1985; Oláfsdóttir et al., 2010). Un ejemplo de ello es la llamada «*Great Salinity Anomaly*» (Dickson et al., 1988) ocurrida a finales de la década de 1960: una anomalía de presión sobre Groenlandia (Rodewald, 1967; Dickson et al., 1975) determinó un intenso flujo de viento del norte que modificó la naturaleza de las corrientes del este de Groenlandia y del este de Islandia, con una mayor presencia de aguas polares, de baja salinidad (<34.7‰), lo que permitió el transporte y formación de hielo marino (Malmberg, 1969; Dickson et al., 1988), y en última instancia, un enfriamiento de las temperaturas observadas a lo largo de Islandia (Einarsson, 1991). Anomalías de este tipo habían sucedido ya con anterioridad (Dickson et al., 1984 entre otros) en los últimos milenios (ver Bond et al., 2001; Mayewski et al., 2004; Alley y Ágúsdóttir, 2005) y demuestran cómo la variabilidad del clima de Islandia (ver Einarsson, 1991) está modulada por la compleja interacción y alternancia de las masas de aire y corrientes oceánicas, cuyos cambios de intensidad y posición repercuten en el clima islandés.

La variabilidad climática tiene serias repercusiones tanto en las actividades humanas (ver, por ejemplo, Ogilvie, 1984 y referencias incluidas; Tabla 1 en Ogilvie y Jónsdóttir, 2000), como en las dinámicas ambientales –incremento o reducción del hielo marino (Ogilvie, 1996), cambios en la vegetación (ver Wastl et al., 2001; Caseldine et al., 2006) y modificaciones en los glaciares (ver Caseldine, 1985a) –. Especialmente, los glaciares resultan ser elementos muy sensibles a las variaciones climáticas, que se reflejan en cambios en su balance de masa. Su signo determina el avance o retroceso de los frentes (por ejemplo, Thorarinsson, 1956; Jóhannesson y Sigurðsson, 1998; Sigurðsson, 2005; Oerlemans, 2005; Sigurðsson et al., 2007). Ambas respuestas dependen de los cambios en la temperatura estival y en la precipitación invernal, representativas de la ablación y acumulación, respectivamente (Sutherland, 1984; Ohmura et al., 1992; Braithwaite, 2008).

En este sentido, la temperatura estival (o de la estación de ablación), el sumatorio de temperaturas positivas y la radiación solar (radiación solar global y radiación solar neta de onda larga) determinan la fusión del hielo como mayor componente de la ablación (Sutherland, 1984; Ohmura et al., 1992; Braithwaite et al., 2008). La acumulación, por su parte, engloba la precipitación (balance de masa invernal, precipitación estival y anual; ver Ohmura et al., 1992; Braithwaite, 2008) en sus diferentes formas (líquida, sólida, derivada

de redistribución eólica, etc.), así como las avalanchas (Sissons y Sutherland, 1976; Sutherland, 1984).

Las variaciones de ambas componentes se reflejan asimismo en cambios en indicadores glaciológicos como la Altitud de la Línea de Equilibrio Glaciar (ELA, del inglés, *Equilibrium-Line Altitude*), que representa la altitud media teórica en la que el balance de masa al final de un período –normalmente un año–, es igual a cero (acumulación y ablación igualadas) (Bakke y Nesje, 2017). Es decir, indica el nivel más bajo de glaciación, donde las condiciones de temperatura y humedad son suficientes para que el hielo se mantenga (Ohmura et al., 1992).

El avance o retroceso acumulado de los glaciares, es decir, sus fluctuaciones, representan una señal de forzamiento climático filtrada y retardada (Haeberli, 1995; Haëberli et al., 2013). Este retardo o tiempo que tarda un glaciar en ajustarse a una determinada perturbación en el balance de masa se denomina *tiempo de respuesta*, un parámetro de vital importancia para conocer el efecto de los cambios climáticos en los glaciares (Jóhannesson, 1986; Jóhannesson et al., 1989a), distinto del *tiempo de reacción*, definido como el lapso de tiempo que transcurre desde que se produce una perturbación climática hasta que ésta se detecta en el frente del glaciar (Haeberli, 1995; Johanneson et al., 1989). El tiempo de respuesta de los glaciares depende, entre otros factores, fundamentalmente del tamaño de los mismos (ver categorías en Jóhannesson y Siugurðsson, 1998), la hipsometría (Jiskoot et al., 2009) o la presencia de una espesa cubierta superficial de derrubios que reduzca la fusión (ablación) y, por tanto, multiplique el *tiempo dinámico de respuesta*, al ser inversamente proporcional al balance de masa en el frente (Haeberli et al., 2013). En este sentido, la respuesta de glaciares rocosos y glaciares cubiertos a las oscilaciones climáticas sería indirecta (Robson et al., 2015) y retardada.

En Islandia, Jóhanneson y Sigurðsson (1998) clasificaron buena parte de los glaciares islandeses dentro de dos tipologías principales según la clasificación de Haeberli (1995):

- *Tipo 2*: "*Glaciares más grandes, dinámicos, de alta tensión de cizalla (glaciares de montaña, «glaciers évacuateurs»), que reaccionan dinámicamente a variaciones decenales en el clima y forzamiento del balance de masa, con una amplitud incrementada tras un retardo de algunos años*".
- *Tipo 3: "Los glaciares de valle más grandes, que dan señales fuertes y más eficientemente suavizadas de tendencias seculares con un retraso de varias décadas".*

Dadas las propiedades anteriores, a escala de décadas, los glaciares se convierten en objeto de estudio y monitorización como importantes indicadores de evolución climática, así como de los cambios en los flujos energéticos existentes en la interfaz tierra-atmósfera (Haeberli, 1995), cuando su estudio se aborda de forma retrospectiva y a escalas de miles de años (ver, por ejemplo, Sutherland, 1984; Dahl y Nesje, 1992).

Los glaciares islandeses representan una superficie de 11.100 km^2, que supone el 11% de la superficie total de la isla (Björnsson, 1978, 1979; Björnsson y Pálsson, 2008). De ellos, los de mayor tamaño son los de tipo *ice-cap*: Vatnajökull (8.100 km^2), Langjökull (900 km^2), Hofsjökull (890 km^2), Mýrdalsjökull (590 km^2) y Drangajökull (160 km^2) (Tabla 1 en Björnsson y Pálsson, 2008). En cambio, en la península de Tröllaskagi, en el norte de la isla, los numerosos glaciares (más de 150; Sigurðsson y Williams, 2008), en su mayoría de circo, son de menores dimensiones (190 km^2 en total; Tabla 1 en Björnsson y Pálsson, 2008).

Su reducida extensión es la causa de que su respuesta a las oscilaciones climáticas sea casi inmediata, cuando carecen de cobertura superficial de derrubios (*debris-free glaciers*), por lo que estos glaciares presentan la máxima sensibilidad climática. De hecho, Caseldine (1985a), basándose en las observaciones sobre el glaciar Gljúfurárjökull, uno de los pocos *debris-free* de la península, encontró un lapso de 10 años entre la ocurrencia y mantenimiento de una perturbación climática (enfriamiento de la temperatura estival), y la manifestación en el frente, en forma de avance.

En contraposición a estos glaciares altamente sensibles, en Tröllaskagi predomina una gran mayoría de *glaciares cubiertos* o *glaciares negros* (*debris-covered glaciers*) y *glaciares rocosos* (Lilleøren et al., 2013), que aunque tienen un menor dinamismo y sensibilidad climática (Tanarro et al., 2019), su formación y estabilización son importantes indicadores de fluctuaciones en el clima y/o procesos geomorfológicos (Kirkbride, 2000, 2011; Brenning, 2005; Hambrey et al., 2008; Azócar y Brenning, 2010; Benn et al., 2012; Pelto et al., 2013; Glasser et al., 2016; Mayr y Hagg, 2019), lo que también les distingue como potentes indicadores de condiciones paleoclimáticas (permafrost, temperaturas ≤4 ºC; Barsch, 1996).

Este conjunto de especificidades hacen de Islandia, y especialmente a la península de Tröllaskagi, en un «laboratorio» para estudiar el impacto de los cambios climáticos en los glaciares, así como sus consecuencias geomorfológicas.

1.2. La variabilidad climática en Islandia: el Máximo Térmico Holoceno y el Neoglacial. Estado del conocimiento.

La variabilidad atmosférica y oceánica, a través de los cambios de intensidad de los componentes de la circulación atmosférica (masas de aire, vientos) y oceánica (corrientes marinas), tiene consecuencias dramáticas en el sistema climático. De hecho, en conjunción con otros forzamientos naturales (por ejemplo, orbitales, actividad volcánica, etc.), pueden determinar bruscos cambios climáticos de regímenes cálidos a fríos, y viceversa. Es el caso del Máximo Térmico Holoceno (MTH) y el Neoglacial. El conocimiento de ambos episodios climáticos resulta clave al ser dos ejemplos de eventos climáticos extremos consecutivos, cálido y frío respectivamente, sucedidos en algunos miles de años, y que pueden servir como hipotéticos escenarios de evolución climática y glaciar en los próximos miles de años, en el contexto del actual calentamiento global.

1.2.1. El Máximo Térmico Holoceno (MTH).

El MTH es un período especialmente cálido experimentado a nivel global como consecuencia de un incremento de la insolación estival forzado orbitalmente, que determinó en altas latitudes de ambos hemisferios unas temperaturas hasta 5 ºC por encima de las propias de la era preindustrial entre 11 y 5 ka BP (Renssen et al., 2012, y referencias incluidas). Sin embargo, en el caso de regiones como Groenlandia o el norte de Europa, el efecto enfriador del *ice-sheet* Laurentino y la reducción de la insolación ocurrida hacia 9-6 ka BP, retrasaron de 1 a 2 ka el inicio del MTH, que comenzó hacia 7 ó 6 ka BP (Renssen et al., 2012).

En el caso de Islandia el desfase entre el forzamiento solar y el pico de temperaturas estivales es mayor, de 3-4 ka (Andersen et al., 2004; Geirsdóttir et al., 2013). Prueba de ello es la reconstrucción de temperaturas de Caseldine et al. (2006) basada en quironómidos, de acuerdo a la cual delimitaron el MTH en el norte de Islandia entre 8 y 6.8 cal. ka BP. Según sus resultados, el inicio de este período estaría evidenciado por las temperaturas más altas de la transición del Holoceno temprano/medio de todo el registro, en coincidencia con sendos picos de temperaturas estival en Hvítárvatn (Geirsdóttir et al., 2013) y de pólenes de *Betula* en Vatnskotsvatn (al oeste de Tröllaskagi), posiblemente en el contexto del paisaje más forestado hasta la fecha (Hallsdóttir, 1995).

Es necesario señalar que la demarcación del período varía en función de los *proxies* utilizados. Los testigos de sedimentos marinos del norte de Islandia sugieren resultados muy similares que abarcan el rango temporal 7.8-6.2 cal. ka BP (Castañeda et al., 2004) y

7.9-5.5 ka BP (Geirsdóttir et al., 2009, 2013). En cambio, los resultados de Andrews y Giraudeau (2003), obtenidos de *proxies* sedimentológicos isotópicos y cocolíticos, sugieren un posible final hacia 5-4 ka, cuando tiene lugar el máximo calentamiento del Holoceno. El final del MTH estaría marcado por el fin del desarrollo real del bosque en Vesturárdalur (Wastl et al., 2001).

Las condiciones climáticas durante este período se caracterizaron por unas temperaturas estivales hasta 4 ºC superiores a las actuales (Geirsdóttir et al., 2009). Anomalía de tal magnitud, y con un comienzo tan brusco, no parece ser resultado sólo del forzamiento orbital, sino que también intervinieron cambios en los sistemas atmosféricos y oceánicos. De hecho, las simulaciones con modelos de circulación atmosférica y oceánica revelan condiciones cálidas en el norte de Islandia, debido a un incremento del flujo de calor entre el océano y la atmósfera, propicio para la convección (Renssen et al., 2010), así como altos índices NAO hacia 6 ka BP (Wanner et al., 2008). Por su parte, en el plano oceánico, registros marinos y lacustres del nordeste de Islandia muestran la llegada de aguas más cálidas durante el período 9-6 ka. En este sentido, el máximo calentamiento holoceno ocurrido hacia 7.8-6.2 ka se vinculó al fortalecimiento de la corriente de Irminger (Geirsdóttir et al., 2009), que junto con un retroceso de las corrientes del oeste y este de Groenlandia habría contribuido asimismo a un calentamiento entre 7 y 5 ka (Andersen et al., 2004). Sin embargo, Knudsen et al. (2004), a partir de datos de foraminíferos, diatomeas e isótopos estables en sedimentos marinos, sugieren la situación opuesta, con un predominio de aguas polares/árticas e incluso picos en el flujo de *ice rafted debris* (IRD) y la presencia de especies de diatomeas árticas y asociadas a hielo marino.

Las reconstrucciones paleoclimáticas basadas en pólenes y quironómidos sugieren unas temperaturas estivales de 0.5-1.5 ºC superiores a las del periodo preindustrial en el norte de Europa hacia 7-5 ka BP (Davis et al., 2003; Seppä et al., 2009; Renssen et al., 2009, 2012). Sin embargo, en el caso de Islandia las anomalías térmicas reconstruidas son considerablemente mayores, como demuestran simulaciones glaciológicas, testigos de sedimentos marinos y datos de *treeline* (Caseldine et al., 2003; Andersen et al., 2004; Flowers et al., 2008; Anderson et al., 2018a), que han permitido inferir durante el MTH temperaturas estivales en el rango de 2-4 ºC superiores a las del período 1961-1990 (Björnsson, 2003).

Los datos anteriores evidencian la sensibilidad y variabilidad del clima islandés, que tuvo importantes repercusiones ecológicas. Una de ellas fue el ascenso de la *shrubline* y el desarrollo del bosque en altura hasta los 450 m s.n.m. durante el período 7.6-6.8 cal. ka BP (Caseldine et al., 2006), lo que explica que especies como *Betula pubescens*

alcanzaran una gran presencia entre *ca.* 6.7 y 6.0 ka BP (Wastl et al., 2001). En la misma línea, la vegetación consiguió una relativa estabilidad en el período 8.0-6.1 ^{14}C ka BP (Caseldine et al., 2003).

No obstante, quizá la mayor repercusión de este período cálido, y que más resalta la importancia de esta isla desde el punto de vista de la variabilidad climática, fue la degradación de la criosfera. Este fenómeno determinó que los glaciares de la isla alcanzasen su mínima extensión (Einarsson, 1968; Geirsdóttir et al., 2018) o incluso desaparecieran, lo que ocasionó condiciones *ice-free* en amplias regiones de Islandia durante el Holoceno temprano/medio (Kaldal y Víkingsson, 1991; Guðmundsson, 1997; Norðdahl et al., 2008; Geirsdóttir et al., 2009, 2018). Este habría sido el caso del *ice-cap* Langjökull (Geirsdóttir y Miller, 2004; Black et al., 2006; Larsen et al., 2012), como demuestra la ausencia de aguas de fusión y de erosión glaciar en su cuenca en el período comprendido entre 7.9 y 5.5 ka (Larsen et al., 2012). Lo mismo le habría sucedido al *ice-cap* Drangajökull, cuyas simulaciones glaciológicas hacen bastante improbable su persistencia del durante el MTH (Anderson et al., 2018a).

1.2.2. El clima y los glaciares islandeses durante el Neoglacial.

Después de 7-6 ka y hacia 6.2-5.0 ka ^{14}C BP, distintos *proxies* evidencian un enfriamiento del clima en el norte de Islandia, probablemente vinculado a un predominio de aguas árticas o polares (Knudsen et al., 2004). Estas condiciones de aguas frías coinciden con un descenso de las temperaturas estival e invernal hacia 6.2-5.0 ka ^{14}C BP inferido a partir de testigos sedimentarios marinos, registros de diatomeas, foraminíferos y datos de productividad biológica (Karpuz y Schrader, 1990; Eiríksson et al., 2000; Giraudeau et al., 2000).

El Neoglacial se corresponde con un enfriamiento experimentado a mediados del Holoceno, que dio lugar a la formación de nuevos glaciares y a su crecimiento tras la máxima reducción de los mismos –y casi total desaparición en el caso de Islandia– durante el MTH (Porter y Denton, 1967). Este episodio climático frío coincidió con la tendencia descendente de la insolación estival a lo largo del Holoceno (Solomina et al., 2015; Geirsdóttir et al., 2018), aunque realmente se trata de una respuesta desproporcionada a dicha circunstancia (Larsen et al., 2012).

En este sentido, el cambio abrupto que puso fin al período cálido anterior hacia 5-4 ka probablemente fue desencadenado en el plano oceánico por unas bajas temperaturas superficiales en el Atlántico Norte alrededor de Islandia (Geirsdóttir et al., 2013) y un incremento del hielo marino ártico (Guðmundsson, 1997; Geirsdóttir et al., 2009; Larsen et

al., 2012). En línea con lo anterior, Moros et al. (2006) señalaron un incremento en el hielo a la deriva en el norte de Islandia hacia 5.5 ka, que al incorporarse a la corriente del este de Groenlandia, habría desencadenado la intensificación del frente polar después de 5.5 y 4.4 ka.

Por su parte, en el plano atmosférico, ante el enfriamiento estival intervinieron cambios en la circulación atmosférica (Andersen et al., 2004), como la debilitación de la circulación del W, el desplazamiento del frente polar atmosférico hacia el sudeste, y de la depresión de Islandia hacia el sur (Harrison et al., 1992), lo que conllevó la progresiva aproximación de las líneas de paso de las depresiones asociadas, que alcanzaron su máxima cercanía entre 3 y 1 cal. ka BP (Andresen et al., 2005). Para el período posterior a 4.6 cal. ka BP, Andersen et al. (2004) hablan de un predominio de viento del norte, una reducción de la transferencia de calor a los mares nórdicos y una ralentización de la circulación termohalina. Sin embargo, en el Neoglacial también se atribuye un papel esencial a la actividad eruptiva de Hekla 4, cuyo volumen de cenizas emitido a la atmósfera pudo incrementar los efectos del enfriamiento al hacer descender la temperatura estival (Larsen et al., 2012).

El enfriamiento del clima iniciado hacia 5 ka, junto con la reducción de radiación solar que caracterizó al Holoceno, determinó el descenso de la ELA, especialmente sensible a las fluctuaciones de la temperatura estival y a la configuración topográfica, con el consiguiente surgimiento de los primeros glaciares en las *highlands* islandesas hacia 5.5 ka (Geirsdóttir et al., 2018). Es el caso de Langjökull, cuya formación marca el inicio del Neoglacial en Islandia, como demuestran los testigos de sedimentos lacustres de Hvítárvatn (Larsen et al., 2012; Geirsdóttir et al., 2013). En el este de Islandia, sedimentos lacustres del lago Lögurin sugieren un enfriamiento prácticamente síncrono hacia 5.4 ka, aunque se considera que el inicio del Neoglacial se retrasó en esta zona hasta 4.4 ka, cuando se vuelve a formar el glaciar Eyjabakkajökull (Striberger et al., 2012).

No obstante, testigos sedimentarios marinos de alta resolución procedentes de la Vøring Plateau (North Icelandic shelf) ya indicaban un enfriamiento de 3-4 ºC en las aguas superficiales de los mares nórdicos hacia 6.5 cal. ka BP, en el comienzo de lo que se ha denominado el Período de Transición Holocena (*Holocene Transition Period*, 6.5-3.0 cal. ka BP; Andersen et al., 2004), probablemente como consecuencia de una mayor influencia de la corriente del este de Islandia. Esta circunstancia ha sido confirmada por registros polínicos de Tröllaskagi (Wastl et al., 2001), que reflejan asimismo el comienzo de un enfriamiento hacia 6.4-6.0 ka BP, que culminó con las temperaturas más bajas hacia 3.5 ka BP.

Desde 5.5 ka, en el Atlántico Norte se inició un descenso de la temperatura en forma de cambios abruptos en el clima, más que una declinación monótona (Larsen et al., 2012). Estos enfriamientos, de corta duración (150 años), ocurridos hacia 4.5-4.0 ka, ca. 4-2 ka, ca. 3 ka, ca. 1.5 ka y 0.7-0.1 ka (ver Larsen et al., 2012; Geirsdóttir et al., 2013, 2018) fueron desencadenados por la intervención de erupciones volcánicas explosivas (Dugmore et al., 1995); fuentes de variabilidad interna atmosférica como la NAO (fases negativas); y factores oceánicos como las fluctuaciones en la intensidad de la circulación termohalina, la transferencia de calor hacia el norte por parte de la *Atlantic Meridional Overtuning Circulation* (AMOC), el refuerzo de la corriente del este de Groenlandia, la presencia de aguas árticas o la extensión del hielo marino (Dugmore et al., 1995; Orme et al., 2018; Geirsdóttir et al., 2013, 2018 y referencias incluidas).

Tales períodos de enfriamiento conllevaron el descenso de la temperatura estival, la desestabilización del paisaje, así como la reducción de la productividad biológica y altas tasas de sedimentación en los lagos (por ejemplo, Hvítárvatn y Haukadalsvatn; Geirsdóttir et al., 2013). No obstante, la consecuencia de mayor interés es la formación y crecimiento de glaciares. De hecho, hacia 4.5-4.0 ka y 2.5 y 2.3 ka, surgieron los grandes glaciares de la isla: el Vatnajökull (sector nordeste) y el Drangajökull (sector noroeste), respectivamente (Geirsdóttir et al., 2018). No obstante, aunque se considera que el comienzo del Neoglacial en Islandia se sitúa en 5.5 ka, se ha sugerido la ocurrencia de avances glaciares con anterioridad. Estos serían los casos de Eyjabbakajökull, cuya máxima expansión se alcanzó hacia 6.9 ka BP, o de Skálafellsjökull, del cual consta un avance cuya edad máxima es 5.7 ka BP (Sharp y Dugmore, 1985; Guðmundsson, 1997).

Ya dentro del Neoglacial propiamente dicho, hay evidencias de avances glaciares por toda Islandia. Comenzando por el sur, por ejemplo, el glaciar Sólheimajökull (glaciar *outlet* del *ice-cap* Eyjafjallajökull) experimentó períodos de avance antes de 4.5 ka BP ("estadio Drangagil"; Guðmundsson, 1997), así como antes de 3.1 ka BP y 1.4-1.2 ka BP ("estadio Ystagil"; see Gudmundsson, 1997; Dugmore, 1989; Mackintosh et al., 2002). En el mismo *ice-cap* existe constancia asimismo de avances del glaciar Gígjökull hacia 2.3 y 1.7 cal. ka BP (Kirkbride y Dugmore, 2008). Por su parte, en el centro de la isla, en el *ice-cap* Regnabuðajökull, Kirkbride y Durmore (2006) encontraron una cronología relativamente similar, con grupos de morrenas originadas hacia 5.0-4.5, 3.5-3.0 y 2.5-2.0 ka BP (Kirkbride y Dugmore, 2006).

En distintos circos de la península de Tröllaskagi, existen asimismo evidencias de avances neoglaciales anteriores a la Pequeña Edad de Hielo (PEH), en los que los frentes alcanzaron unas posiciones ligeramente más avanzadas (Meyer y Venzke, 1985;

Caseldine, 1987; Häberle, 1991, 1994; Stötter, 1991; Wastl y Stötter, 2005). La síntesis de Stötter et al. (1999) muestra una cronología de avances glaciares ocurridos hacia 4.7 (Vatnsdalur I), 4.2 (Bægisárdalur I), 3.2-3.0 (Vatnsdalur II), 2.0 (Barkárdalur I), 1.5 (Barkárdalur II) y 1.0 (Bægisárdalur II) ka BP, coincidente con los períodos de enfriamiento Neoglacial identificados por Geirsdóttir et al. (2018), y relativamente similar a la observada en el sur de Islandia (ver la correspondencia de fases de avance glaciar del norte y del sur, de Guðmundsson, 1997).

Aunque los anteriores avances representan una respuesta de los glaciares a bruscos enfriamientos en el clima, lo cierto es que el mayor enfriamiento de la segunda mitad del Holoceno ocurrió entre 0.7 y 0.1 ka (Larsen et al., 2012), es decir, durante la PEH, en correspondencia con el Evento “Bond” 0. Este enfriamiento coincidió con una reducción de la energía solar (por forzamiento orbital) y del influjo de aguas atlánticas cálidas en el ártico (Miller et al., 2010), así como probablemente con un pulso prolongado de hielo a la deriva que debilitara el transporte de calor a Europa a través de la Deriva Noratlántica (Moros et al., 2006). Estas circunstancias, junto con la ocurrencia de erupciones volcánicas que bloquearon la radiación solar (Zhong et al., 2011), dieron lugar a un mínimo térmico holoceno y permitieron en paralelo la expansión del hielo marino, así como la estabilización y avance de los glaciares (Miller et al., 2010), que en determinados casos alcanzaron su máxima extensión holocena (ver Grove, 1988). La explicación detrás de estos fenómenos está en un cambio del modo NAO de positivo (Óptimo Térmico Medieval) a negativo (Wanner et al., 2008 y referencias incluidas).

Las primeras señales de la PEH en Islandia parecen remontarse al siglo XIII. Según Ogilvie (1991), hasta el siglo XII el clima islandés habría sido suave, mientras que justo después comenzó a deteriorarse. Interesantemente, en el *foreland* del glaciar Svínafellsjökull (Öraefi) se identificaron algunas morrenas originadas probablemente en el siglo XIII (Grove, 2001), justo cuando también existe constancia del crecimiento del glaciar Langjökull (1250 CE; Larsen et al., 2011). Sin embargo, el mayor crecimiento de los glaciares coincide con la parte final de la PEH, en la que tienen lugar las condiciones más frías (ver Ogilvie, 1996; Ogilvie y Jónsson, 2001). De este modo, Kirkbride y Dugmore (2008) dataron avances glaciares en el sur de Islandia (Eyjafjallajökull) en el siglo XVIII (primera década, años cuarenta, finales de siglo), y a principios y finales del siglo XIX. Por su parte, en el centro de la isla, también hay constancia de avances entre 1690 y 1740 CE (Kirkbride y Dugmore, 2006). En el sureste de Islandia (Öraefi), Chenet et al. (2010) dataron también avances glaciares hacia 1740-1760, 1810-1820 y 1840-1880. Sin embargo, es importante señalar que buena parte de los avances glaciares de la PEH en Islandia han sido datados mediante la aplicación de la liquenometría a formaciones morrénicas, lo que

determina que las fechas tiendan a agruparse en torno a las décadas de los años sesenta y ochenta del siglo XIX, lo cual tiene más que ver con las limitaciones de la técnica (Kirkbride y Dumore, 2001), que con los eventos climáticos más fríos del último siglo de la PEH.

Este problema es el que, de hecho, sucede en la península de Tröllaskagi, donde la evolución glaciar durante la PEH se ha estudiado mediante la aplicación de la liquenometría a morrenas de pequeños glaciares de circo, cuyas edades tienden a concentrarse en el siglo XIX (Caseldine, 1983, 1985a, 1991; Kugelmann, 1991; Häberle, 1991; Caseldine y Stötter, 1993). Aunque también se han datado morrenas incluso de comienzos del siglo XX, cuando el ascenso brusco de las temperaturas (Einarsson, 1991) pone fin a la PEH y los glaciares abandonan las morrenas depositadas en los últimos avances.

1.3. Las técnicas utilizadas para el estudio de la evolución glaciar en la península de Tröllaskagi.

Los glaciares –paleoglaciares y glaciares actuales– de la península de Tröllaskagi han sido objeto de diferentes estudios con el fin de reconstruir la evolución paleoambiental a partir de la reconstrucción de la evolución glaciar a distintas escalas temporales. De este modo, los glaciares y sus formas asociadas en los valles se han investigado a través de métodos que van desde la cartografía geomorfológica glaciar hasta las dataciones y reconstrucciones paleoclimáticas.

1.3.1. Cartografía geomorfológica glaciar.

La cartografía geomorfológica de detalle es esencial para la reconstrucción de la geometría de los glaciares, la diferenciación de fases en su evolución y una aproximación a las dinámicas del hielo en glaciares ya desaparecidos (ver Pearce et al., 2017). A pesar de que las dimensiones de los glaciares de Tröllaskagi son muy reducidas (Sigurðsson, 1998; Sigurðsson y Williams, 2008), las cartografías geomorfológicas existentes en los artículos de geomorfología glaciar de Tröllaskagi, en su mayor parte, se limitan a esquemas geomorfológicos de poco detalle, en los cuales únicamente se representan las morrenas más prominentes (Kugelmann, 1991; Stötter, 1991; Häberle, 1991, 1994).

Esto contrasta, por ejemplo, con las cartografías detalladas realizadas en otras áreas de Islandia (Evans et al., 1999, 2007, 2016a, 2016b; Kjær et al., 2008; Schomacker et al., 2014; Evans y Orton, 2015; Robb et al., 2015; Chandler et al., 2016a; Everest et al., 2017; entre otros). Si se consideran las dimensiones de los glaciares o *forelands* en los que se centran los trabajos de Tröllaskagi, la escala de cartografía es inapropiada en términos de

precisión en la delimitación de formas (ver Pearce et al., 2017). Es decir, se prima la representación de la secuencia de formas (morrenas) datadas, frente a la precisión de su delimitación.

Este sesgo a favor de morrenas principales dificulta, por ejemplo, la identificación de morrenas anuales o de aquellas derivadas de perturbaciones climáticas de menor entidad y, en última instancia, repercute en una menor resolución espacial de los parámetros climáticos que puedan inferirse a partir de los glaciares. Esta es una cuestión clave pues existen glaciares con un excepcional dinamismo y sensibilidad ante las perturbaciones climáticas a escala de décadas (ver Björnsson, 1971; Caseldine, 1985a).

Excepcionalmente, los trabajos de Caseldine y Cullingford (1981) y Caseldine (1983), presentan cartografías de detalle que incluyen tanto un levantamiento topográfico del valle y el glaciar, como una representación de todas las morrenas del valle y la geometría del frente del glaciar en distintas fechas, basada en observaciones de campo. No obstante, en el caso de glaciares rocosos y glaciares cubiertos también existe una escasez de cartografías geomorfológicas detalladas. Un ejemplo es el esbozo de cartografía detallada de Kirkbride y Dugmore (2001) del glaciar rocoso ubicado en el circo Grænavatn. En ella se representan elementos característicos tanto de las laderas y paredes de los circos, como de los glaciares rocosos, si bien la base fotográfica sobre la que se realizó no fue rectificada geográficamente. En esta misma línea, sobresale asimismo la cartografía del glaciar rocoso Fremri-Grjótárdalur y el glaciar cubierto Hóladalsjökull (Tanarro et al., 2018), que identifica y representa de forma precisa aquellas formas que diferencian glaciares cubiertos y glaciares rocosos (i.e. crestas, surcos, depresiones asociadas, etc.). Además, constituye un primer paso para la elección de formas potencialmente datables, a través de las cuales conseguir una mejor comprensión del origen y posterior evolución de este tipo de formaciones.

Para poder realizar un estudio eficaz de la evolución glaciar durante los distintos enfriamientos ocurridos a lo largo del Neoglacial, es necesaria una cartografía geomorfológica de alto nivel de detalle, al menos en las formaciones morrénicas. De esta manera, la cartografía no sólo se limita a representar las morrenas más prominentes, lo cual supondría un importante sesgo a favor de las morrenas mejor conservadas o más jóvenes, en detrimento de aquellas correspondientes con eventos glaciares más alejados en el tiempo y que probablemente presenten un peor estado de conservación en un entorno geomorfológicamente muy dinámico. Un alto nivel de detalle es asimismo un requisito indispensable para detectar fluctuaciones glaciares correspondientes con escalas

temporales más cortas (escala de décadas), que se podrán correlacionar con la evolución climática.

1.3.2. Análisis de fotografías aéreas e imágenes de satélite.

Junto con la cartografía geomorfológica, también se ha empleado la fotografía aérea como registro auxiliar para estudiar la evolución de los glaciares en períodos más recientes a partir del análisis comparado entre fechas. Caseldine y Cullingford (1981) y Caseldine (1987) combinaron la cartografía geomorfológica y la geometría del frente del Gljúfurárjökull en 1946 y 1985, como apoyo a las observaciones de campo realizadas en campañas posteriores de finales de la década de 1970. En esta misma línea Sigurðsson et al. (2007) mencionan la utilización de fotografías aéreas del año 2000 e imágenes de satélite para la delimitación de la geometría de los 276 glaciares islandeses como base para la monitorización de sus futuros cambios de extensión.

No obstante, la fotografía aérea ha servido también para estudiar la evolución de glaciares menos dinámicos como los glaciares rocosos y glaciares cubiertos a través de la monitorización del desplazamiento de puntos (*orthophotos cross-correlation matching*), bloques, crestas y surcos en fotografías restituidas con técnicas fotogramétricas digitales (Wangensteen et al., 2006; Kellerer-Pirklbauer et al., 2008a; Tanarro et al., 2019; Campos et al., 2019).

Finalmente, la fotografía aérea se ha utilizado incluso como apoyo a las técnicas de datación (ver Caseldine, 1987; Häberle, 1991; Wangensteen et al., 2006; Kellerer-Pirklbauer et al., 2008a) y como documentación auxiliar para completar la historia de surges, como hicieron Brynjólfsson et al. (2012) en los glaciares Búrfellsjökull y Teigárdalur.

A la vista de esta revisión, en Tröllaskagi se ha aprovechado y desarrollado más el potencial de la fotografía aérea en los estudios de movilidad de glaciares rocosos y glaciares cubiertos, justamente los menos dinámicos y con menores variaciones ante las fluctuaciones climáticas. En cambio, pese a que los glaciares *debris-free* son los que más fluctuaciones experimentan a lo largo del tiempo, casi no se ha utilizado la fotografía aérea hasta la actualidad. La principal ventaja de esta técnica de análisis remoto es que permite actualizar el registro de las variaciones recientes de las superficies glaciares y de sus frentes sin la dependencia del grado de conservación de las evidencias geomorfológicas que dejan, como por ejemplo, las morrenas. Además, es una herramienta especialmente útil para la datación relativa de formaciones morrénicas –es decir, avances o estabilizaciones glaciares– a través de la utilización de fotografías aéreas de distintas

fechas, lo que permite la validación de dataciones derivadas de liquenometría o la conversión de sus edades relativas en edades absolutas.

1.3.3. Técnicas de datación.

La riqueza de formas derivadas de la actividad glaciar en Tröllaskagi ha convertido sus circos y valles en el foco de estudios encaminados a la reconstrucción paleoambiental holocena. Alcanzar tal objetivo implica la datación de formas glaciares, de las cuales las más frecuentemente datadas han sido las morrenas, por ser indicativas de posiciones de los frentes y de la extensión de los glaciares en el pasado. La escala temporal de las fluctuaciones y su grado de antigüedad determinan una división en las técnicas aplicadas, por lo que en el caso de fases glaciares anteriores a la PEH se han utilizado de forma conjunta el radiocarbono y la tefrocronología, mientras que en fluctuaciones ocurridas desde la PEH hasta la actualidad se ha empleado fundamentalmente la liquenometría.

1.3.3.1. Radiocarbono y tefrocronología.

Las dataciones mediante la combinación de radiocarbono y tefras se han aplicado generalmente a morrenas localizadas a escasa distancia y por delante de las correspondientes con la PEH. Las formaciones datadas han sido secciones morrénicas con suelos y depósitos de turbera e incluso restos de vegetación (madera), en Barkárdalur (Häberle, 1991), Bægisárdalur (Häberle, 1991), Vantsdalur (Stötter, 1991), þverárdalur (Wastl y Stötter, 2005) y Lambárdalur (Wastl y Stötter, 2005). Por tanto, aunque los resultados obtenidos han sido edades mínimas o máximas para la formación de turberas y suelos (ver síntesis en Wastl y Stötter, 2005), sí permitieron distinguir y delimitar importantes fases de avance glaciar dentro del Neoglacial a nivel local: Vantsdalur I, Bægisárdalur I, Vatnsdalur II, Barkárdalur II y Bægisárdalur II (ver síntesis en Stötter et al., 1999 y Wastl y Stötter, 2005).

El problema de esta combinación de técnicas es que mayoritariamente han proporcionado edades máximas o edades mínimas, y que dependen de la existencia de restos de materia orgánica y la presencia de tefras. La consecución de edades máximas o mínimas dificulta la asociación precisa de fases de avance glaciar con episodios concretos de enfriamiento, y por tanto, no permiten mejorar el conocimiento del Neoglacial, para lo que se necesitaría disponer de unas edades con un menor rango de incertidumbre. Además, en el caso de glaciares más estáticos, como los glaciares rocosos o los glaciares cubiertos, estas técnicas tampoco permiten datar momentos clave como el estancamiento de su flujo o la estabilización de los bloques una vez que el hielo ha desaparecido.

1.3.3.2. Martillo de Schmidt.

El grado de alteración de las rocas, medido a través del martillo de Schmidt o esclerómetro, también se ha utilizado para inferir edades relativas, tanto en la datación de formaciones anteriores como posteriores a la PEH. De hecho, Caseldine (1985b, 1987) lo empleó como prospección de edades relativas en una secuencia de morrenas fuera y dentro del *foreland* (anteriores a la PEH, del período 1890-1930 y posteriores a 1930) en Skíðadalur, con resultados (valores de rebote, *R- values*) satisfactorios, pero que dificultan la correlación de los avances con eventos climáticos concretos al tratarse de edades relativas. No obstante, los valores observados en la morrena más externa del valle se correlacionaron finalmente con los obtenidos en substrato de edad Preboreal, datados a su vez previamente a través de tefras. El martillo de Schmidt se ha aplicado incluso en la datación de glaciares rocosos activos e inactivos, como el caso del complejo de Fremri-Grjótárdalur (Kellerer-Pirklbauer et al., 2008a), en combinación con cálculos de campos de velocidades obtenidos por técnicas fotogramétricas.

En la misma línea merece especial mención el trabajo de Wangnsteen et al. (2006), en el que se estimó la edad de glaciares rocosos y glaciares cubiertos a través de la extrapolación de sus tasas de desplazamiento actualmente observadas mediante fotogrametría. Es decir, se calculó el tiempo necesario para que una partícula se desplazase a lo largo de una línea de corriente (*streamline*) desde la cabecera hasta una determinada posición, asumiendo que la tasa de desplazamiento fuera similar a la actual. La desventaja de este enfoque es que no permite conocer cambios clave en los glaciares como el momento de estabilización o del fin de la fusión del hielo subyacente o interno en el proceso de evolución de forma activa a inactiva.

La inserción de los resultados derivados del martillo de Schimdt en el conocimiento del Neoglacial debería pasar por una conversión de las edades relativas en edades absolutas a través de un proceso de calibración. Para ello, idealmente, se necesitan puntos de control basados en edades de exposición, no en edades mínimas o máximas derivadas, por ejemplo, de la tefrocronología.

1.3.3.3. Liquenometría.

En el caso de las fluctuaciones y fases glaciares de la PEH y posteriores se ha utilizado mayoritariamente la liquenometría, basada en especies del grupo *Rhizocarpon geographicum* al igual que en el resto de Islandia (Thompson y Jones, 1986; Evans et al., 1999; Russell et al., 2001; Kirkbride y Dugmore, 2001; Bradwell, 2001, 2004a; Harris et al., 2004; Bradwell y Armstrong, 2006; Orwin et al., 2008; Chenet et al., 2010 entre otros). Los

estudios apoyados en dataciones liquenométricas en Tröllaskagi representan el 20% de los estudios liquenométricos realizados en Islandia (Decaulne, 2016) y sus principales aportaciones son la derivación de curvas y tasas de crecimiento de la especie de liquen utilizada (Caseldine, 1983; Kugelmann, 1991), una cronología de avances glaciares durante las últimas fases de la PEH (siglo XIX) y a lo largo del siglo XX (Caseldine, 1983, 1985a, 1987; Kugelmann, 1991; Häberle, 1991, 1994; Martin et al., 1991; Caseldine y Stötter, 1993), y por último, la datación de glaciares rocosos (Martin et al., 1994; Hamilton y Whalley, 1995). Las áreas de estudio y publicaciones donde se ha aplicado la liquenometría se resumen en la Tabla 1.1.

Area	**Formas**	**Publicaciones**
Gljúfurárdalur	Morrenas	Caseldine (1983, 1985, 1987, 1991)
Vestur Tungnahryggsjökull	Morrenas	Caseldine (1985)
Heiðinnamannadalur	Morrenas	Caseldine (1985, 1987, 1991)
Vesturardalur	Morrenas	Caseldine (1987); Kugelmann (1991, Fig. 7)
Kvarnárdalur	Morrenas, glaciar rocoso	Caseldine (1987, 1991)
Skídadalur	Morrenas	Caseldine (1987, 1991)
Holárdalur	Morrenas	Caseldine (1987, 1991)
Þverardalur	Debris-flow	Caseldine (1991);
Skjóldalur	Glaciar rocoso	Chueca Cía (1991); Martin et al. (1994)
Bægisárdalur	Morrenas	Häberle (1991)
Barkárdalur	Morrenas	Häberle (1991)
Fossárdalur	Morrenas	Häberle (1991)
Myrkárdalur	Morrenas	Häberle (1991)
Skríðudalur	Morrenas	Häberle (1991)
Vindheimajökull	Morrenas	Häberle (1991)
Þverdalur	Morrenas	Kugelmann (1991)
Burfellsdalur	Morrenas	Kugelmann (1991, Fig. 7)
Grytudalur	Morrenas	Kugelmann (1991, Fig. 7)
Teigardalur	Morrenas	Kugelmann (1991, Fig. 7)
Þveradalur	Morrenas	Kugelmann (1991, Fig. 7)
Vatnsdalur	Morrenas	Kugelmann (1991, Fig. 7)
Lambárdalur	Glaciar rocoso	Martin et al. (1994)
Nautárdalur	Glaciar rocoso	Martin et al. (1994); Hamilton y Whalley (1995)
Klaengshóll	Morrenas, glaciar rocoso	Meyer y Venzke (1985); Caseldine (1991, Tabla 1)

Tabla 1.1. Síntesis de las áreas de Tröllaskagi donde se ha aplicado la liquenometría a formaciones glaciares.

Esta técnica también se ha empleado en glaciares rocosos. Así, Martin et al. (1994) dataron los glaciares rocosos de Nautárdalur, Skjóldalur y Lambárdalur, con resultados que sugieren que éstos fueron originados en la PEH. El trabajo de Hamilton y Whalley (1995) llegó a la misma conclusión aplicando también la liquenometría en Nautárdalur, con una

aportación de interesante, ya que analizó los factores ambientales que afectan al crecimiento de los líquenes.

Sin embargo, la liquenometría presenta varios problemas en Islandia. Uno de ellos es el limitado rango de aplicación, que permite datar formaciones de edades de hasta 160 o incluso 220 años (Maizels y Dugmore, 1985; Thompson y Jones, 1986; Evans et al., 1999). En Tröllaskagi, se añade además una escasez de curvas de calibración o crecimiento, cuyos puntos de control generalmente se encuentran fuera del entorno de los *forelands* glaciares (ver por ejemplo, Caseldine, 1983, 1991; Kugelmann, 1991; Häberle, 1991), sujetos a variaciones microclimáticas con posible impacto en el crecimiento y colonización de los líquenes medidos. Asimismo existe un desacuerdo en el parámetro de los líquenes que se debe medir (eje mayor, eje menor) y en el período de colonización que se asume (10-15 años; ver Caseldine, 1983; Kugelmann, 1991).

En este sentido, es vital una reducción de las incertidumbres en las edades obtenidas, fundamentalmente en las épocas recientes, pues son en las que mejor se puede evaluar la relación entre las oscilaciones climáticas y de los frentes glaciares. Ello pasa necesariamente por una combinación de las edades liquenométricas con otras técnicas complementarias, como la fotografía aérea o la observación de superficies recientemente deglaciadas, que permita evaluar la adecuación de tasas de crecimiento o períodos de colonización de los líquenes.

1.3.3.4. Dataciones por exposición a los rayos cósmicos.

Las dataciones por exposición a los rayos cósmicos (*Cosmic-Ray Exposure dating*, CRE) se han aplicado más recientemente en superficies pulidas de los fiordos que delimitan Tröllaskagi, Skagafjördur y Eyjafjördur, en sendos transectos que muestran el patrón de deglaciación de los *outlets* que discurrían por ambos valles (Andrés et al., 2019). A día de hoy no existen más publicaciones donde se apliquen las dataciones cosmogénicas en el entorno de Tröllaskagi. Los únicos precedentes de datación mediante esta técnica en Islandia se encuentran fuera de Tröllaskagi, en las *table mountains* de las zonas neovolcánicas (isótopo ^{3}He; Licciardi et al., 2007) y en Vestfirðir (isótopo ^{36}Cl; Principato et al., 2006; Brynjólfsson et al., 2015a).

La ventaja que tienen las dataciones cosmogénicas es que reducen la dependencia de la presencia de tefras o materia orgánica datable, como sucede, por ejemplo, en el caso de las dataciones de morrenas con radiocarbono. Las edades que se obtienen son de exposición, lo que permite conocer eventos clave como el descubrimiento de superficies deglaciadas, estabilización de bloques por abandono de las morrenas por parte de los

frentes o la estabilización de bloques en glaciares cubiertos o glaciares rocosos tras la desaparición definitiva del hielo intersticial o subyacente, o al reducirse el flujo hasta hacerse prácticamente nulo (estado estático). Así pues, en vista de los numerosos glaciares rocosos y cubiertos presentes en las cabeceras de los valles de Tröllaskagi, esta técnica tiene un gran potencial, por la posibilidad que ofrece para estudiar la respuesta de glaciares rocosos y glaciares cubiertos en comparación con los glaciares *debris-free* en relación a las fluctuaciones climáticas. Además, las dataciones cosmogénicas permiten estudiar la transformación de los glaciares *debris-free* en glaciares cubiertos y rocosos en el pasado y vincular estos cambios de dinámica con las variaciones climáticas pretéritas.

1.3.4. Reconstrucción de paleoglaciares y cálculo de la Altitud de la Línea de Equilibrio glaciar (ELA).

La reconstrucción de paleoglaciares incluye tanto la delimitación de la superficie ocupada (extensión horizontal), como la aproximación a su espesor y volumen (extensión vertical). A partir de las reconstrucciones se pueden derivar otros parámetros como la contribución de los glaciares a la subida del nivel del mar, como consecuencia de la fusión de hielo, y la localización de la ELA, que depende directamente de su hipsometría y que determina la distribución de las superficies de acumulación y de ablación.

Son escasos los estudios sobre los glaciares de la península de Tröllaskagi en los que se menciona de forma explícita la reconstrucción o el cálculo de ELAs. Entre ellos destacan los trabajos de Häberle (1991, 1994) con la reconstrucción de los glaciares del área de Hörgárdalur, aunque no proporcionan detalles sobre los métodos de empleados. Tan sólo se indica que *"las curvas de nivel de la antigua superficie glaciar se dibujan cada 100 m y que las áreas localizadas entre ellas [bandas altimétricas] fueron medidas con un planímetro"* y *"añadidas a una curva hipsográfica"* (Häberle, 1994). Por tanto, la técnica aplicada aquí fue el llamado "enfoque cartográfico" (Sissons, 1974; Pellitero et al., 2015), que ya había sido generalmente aceptado y utilizado en glaciares similares de otras áreas como Noruega (Dahl y Nesje, 1992), y que se basa en la experiencia y habilidades del investigador para reproducir la paleotopografía de los glaciares a partir de la interpretación de las evidencias geomorfológicas (Pellitero et al., 2015).

Häberle (1991, 1994) calculó las ELAs empleando el llamado "2:1 ratio" (Gross et al., 1978), es decir, el método *Accumulation Area Ratio* o *AAR*, en el que se asume que el área de acumulación ocupa 2/3 de la superficie del glaciar (AAR=0.67). El mismo método de cálculo ya había sido utilizado anteriormente por Caseldine (1985a) en el glaciar Gljúfurárjökull, y por otros autores en otros glaciares de la península de Tröllaskagi (Müller, 1984; Stötter, 1991). La aportación del trabajo de Häberle (1994) consistió en la utilización

de las depresiones de la ELA con respecto a un nivel de referencia (PEH) como un método para adscribir las morrenas a distintas fases glaciares de Islandia (Búði, Preboreal).

Por otro lado, Caseldine y Stötter (1993) calcularon las ELAs para 48 glaciares del sistema de valles Skíðadalur-Svarfaðardalur, basadas en el método AAR con el ratio 0.67, previamente validado por Stötter (1990) por la correspondencia entre las ELAs derivadas de este ratio y la máxima altitud de morrenas laterales datadas de la PEH en una muestra de 10 glaciares. Sin embargo, no proporcionaron detalles sobre el método que siguieron en la reconstrucción de los paleoglaciares, aunque probablemente fuera el enfoque cartográfico manual, ya que era ampliamente utilizado en otras publicaciones contemporáneas (por ejemplo, Dahl y Nesje, 1992; Häberle, 1994) sobre glaciares de circo similares. Caseldine y Stötter (1993) modelizaron también el patrón espacial de ELAs de la PEH y de mediados de la década de 1980, clasificaron los glaciares en cuanto al ascenso de dicho parámetro entre ambas fechas y correlacionaron las ELAs con la edad del comienzo del retroceso glaciar al final de la PEH.

Finalmente, el trabajo más exhaustivo, complejo y con mayor cobertura espacial hasta hoy en cuanto a ELAs es el de Ipsen et al. (2017). En él, a través de los Sistemas de Información Geográfica (SIG), se analizó la morfometría de 347 circos glaciares distribuidos en el NO, N y E Islandia, de los cuales 186 se encuentran en Tröllaskagi. En este caso, se obtuvieron las paleo-ELAs (del Último Máximo Glaciar, UMG) a partir del criterio de la altitud del fondo del circo, y se correlacionaron con la distancia de los circos a la línea de costa, como aproximación a la influencia de las fuentes de humedad. Sin embargo, este método es de los menos precisos para estimar ELAs, ya que sólo da un valor aproximado que, además, es difícil de adscribir a una fase glacial en concreto (Benn y Lehmkuhl, 2000; Benn et al., 2005). Por tanto, este enfoque sólo se puede aplicar a la última fase glaciar que ha modelado los circos, y no permite reconstruir los cambios en la ELA a lo largo del tiempo, algo que sí se logra a través de los cálculos basados en cambios en la hipsometría glaciar.

En las reconstrucciones o estimaciones de espesores generalmente no se han utilizado modelos numéricos físicos basados en la reología y flujo del hielo. Esta cuestión dificulta la obtención de reconstrucciones fiables cuando las evidencias geomorfológicas dejadas por el hielo no presentan un buen estado de conservación, lo cual es común en entornos geomorfológicamente muy dinámicos, como Tröllaskagi. Este problema tiene serias repercusiones en la estimación correcta de espesores de hielo o la reconstrucción glaciar en las áreas de acumulación.

Por ello, un buen conocimiento del Neoglacial a través del estudio del comportamiento de los glaciares requiere el ensayo de modelos numéricos (ver Nye, 1952;

Schilling y Hollin, 1981; Van der Veen, 1999; Benn y Hulton, 2010; Pellitero et al., 2016), que permiten obtener reconstrucciones más fidedignas, ya que reducen al mínimo la subjetividad y se basan en criterios objetivos y más fiables como la física del hielo. El único ejemplo de aplicación de este tipo modelos en Tröllaskagi se encuentra en el trabajo de Hamilton y Whalley (1995), en el que a partir de la reconstrucción del espesor del hielo y la pendiente, derivaron velocidades de flujo y estimaron la edad de formación del glaciar rocoso de Nautárdalur.

1.3.5. Reconstrucciones paleoclimáticas basadas en glaciares.

Hasta ahora, la mayor parte de trabajos de reconstrucción paleoclimática en Tröllaskagi, se basan en estudios de vegetación a través de registros palinológicos, variaciones en la *shrub-line* y en las tasas de acumulación en turberas (Caseldine y Hatton, 1994; Wastl et al., 2001; Caseldine et al., 2006). Llama la atención que pese a la sensibilidad de los glaciares *debris-free* de Tröllaskagi, que les convierte en *proxies* valiosos para realizar reconstrucciones paleoclimáticas de temperatura estival y precipitación invernal, tan sólo existen dos trabajos basados en esta hipótesis.

Por un lado está el artículo de Caseldine y Stötter (1993), que aporta una reconstrucción del clima de la PEH a partir de la paleo-ELA promedio de 48 glaciares de Skíðadalur-Svarfaðardalur, en términos de acumulación invernal y temperatura media de la estación de ablación. El modelo aplicado fue la ecuación exponencial expuesta por Ballantyne (1989), resultante la correlación entre la temperatura media de la estación de ablación (mayo-septiembre) y la acumulación invernal (octubre-abril) en 10 glaciares noruegos (Liestøl, 1967), y utilizado posteriormente por Dahl y Nesje (1992) en glaciares de Nordfjord (O de Noruega). Caseldine y Stötter (1993) resaltaron la discrepancia entre el incremento de la temperatura estival y de la ELA desde la PEH hasta mediados de la década de los años ochenta, en correspondencia con un incremento en la acumulación (precipitación, redistribución eólica de la nieve) que vincularon a posibles cambios en la dirección del viento predominante.

El segundo trabajo que hace una reconstrucción paleoclimática en Tröllaskagi es de Stötter et al. (1999). La principal aportación de este artículo es la reconstrucción del clima holoceno a partir del análisis de la temperatura y de la precipitación en series climatológicas de distintas estaciones meteorológicas del norte de Islandia, cuyos máximo (década de los años 30 del siglo XX) y mínimo (siglo XIX) térmicos son comparables a los óptimo y mínimo holoceno. Esta reconstrucción se explicó por medio de un sencillo modelo que relaciona la temperatura con la precipitación, el hielo marino y las ELAs de los glaciares. En este sentido, la máxima extensión de los glaciares, y avances subsecuentes, fueron tomados

como representativos de mínimos paleoclimáticos desde comienzos del Holoceno, con temperaturas comparables a las de la segunda mitad del siglo XIX.

Por otro lado, merece la pena señalar los trabajos de Björnsson (1971) y Caseldine (1985a). Aunque no tratan explícitamente la reconstrucción paleoclimática, sí que indican las condiciones (temperatura estival) que propician el avance de los glaciares de Tröllaskagi a través de la relación de las fluctuaciones glaciares y balances de masa recientes con los datos de un observatorio meteorológico cercano. En este sentido, el seguimiento de los glaciares en períodos recientes con disponibilidad de datos climatológicos es esencial para poder comprender las condiciones climáticas que determinaron la evolución glaciar en el pasado. Asimismo, es necesaria la aplicación de más modelos glacio-climáticos válidos para distintas áreas del planeta (Ohmura et al., 1992; «*degree-day*», Braithwaite, 2008), a partir de los cuales inferir condiciones paleoclimáticas (temperatura y precipitación), ya que hasta ahora sólo se ha aplicado un modelo local obtenido a partir de glaciares noruegos (ver Caseldine y Stötter, 1993; Liestøl, 1967; Ballantyne, 1989).

1.4. Objetivos de la investigación.

Considerada la idoneidad y potencial de los glaciares de la península de Tröllaskagi por su localización de borde entre sistemas atmosféricos y oceánicos de naturaleza contrastada, su alta sensibilidad a las oscilaciones climáticas y la gran riqueza de formas glaciares y periglaciares en un ambiente extraordinariamente dinámico, el *objetivo general* de la tesis es mejorar el conocimiento de la evolución de los glaciares de la península de Tröllaskagi durante el final del Holoceno como medio de aportar nuevos datos para comprender las tendencias del cambio climático actual. Para poder lograr este objetivo general, se han definido una serie de objetivos específicos:

- Proponer una secuencia metodológica que combine técnicas de distinta naturaleza para estudiar la evolución de los glaciares y entender su relación con la evolución climática.
- Diferenciar las dinámicas de los glaciares *debris-free,* de los glaciares rocosos y de los glaciares cubiertos en relación a las fluctuaciones climáticas.
- Reconstruir en tres dimensiones la extensión de los glaciares *debris-free* con el fin de conocer los cambios de sus espesores y volúmenes de hielo a lo largo del tiempo.

- Detectar fases mayores de avance o estabilización de los glaciares y conocer su extensión en aquellos intervalos temporales no cubiertos por las fotografías aéreas.
- Datar las formaciones indicativas de avances o estabilizaciones de los frentes glaciares (actuales, subactuales y holocenas), y de la estabilización definitiva de glaciares rocosos y glaciares cubiertos, a través de una propuesta de combinación de distintos técnicas aplicables a un amplio rango de edades.
- Analizar la evolución climática reciente en términos de temperatura y precipitación y evaluar su impacto en los glaciares, así como el grado de sensibilidad de éstos.
- Obtención de parámetros glaciológicos asociados a la evolución climática, susceptibles de ser utilizados como indicadores de cambio climático y para la reconstrucción de valores paleoclimáticos.
- Inferir las condiciones paleoclimáticas explicativas de fases de retroceso y avance glaciar a partir de indicadores glaciológicos, y comprender los cambios en los patrones atmosféricos de los que derivan las fluctuaciones climáticas y de los glaciares.
- Comprensión de la evolución de los glaciares en distintos valles y circos glaciares representativos de la península de Tröllaskagi, cuya interpretación pueda ser extrapolable a valles similares.
- Comprensión de la transformación de los glaciares libres de derrubios en glaciares rocosos y cubiertos a través de la datación de sus formas características.

1.5. Estrategia y estructura de la investigación.

La presente investigación se estructura del siguiente modo (Fig. 1.1):

En primer lugar, es necesario conocer las características geográficas de la península de Tröllaskagi, con especial referencia a los condicionamientos climáticos –atmosféricos y oceánicos– y los procesos geomorfológicos actuales más significativos, pues su interacción con los glaciares determina la existencia de varios tipos de glaciares con distintos niveles de dinamismo ante las fluctuaciones climáticas. Por otro lado, también se necesita conocer las características generales de los glaciares seleccionados, así como su localización, para posteriormente entender su dinámica, evolución y patrón espacial de deglaciación desde el final del Neoglacial hasta la actualidad. Esta información se presenta en el **Capítulo 2**.

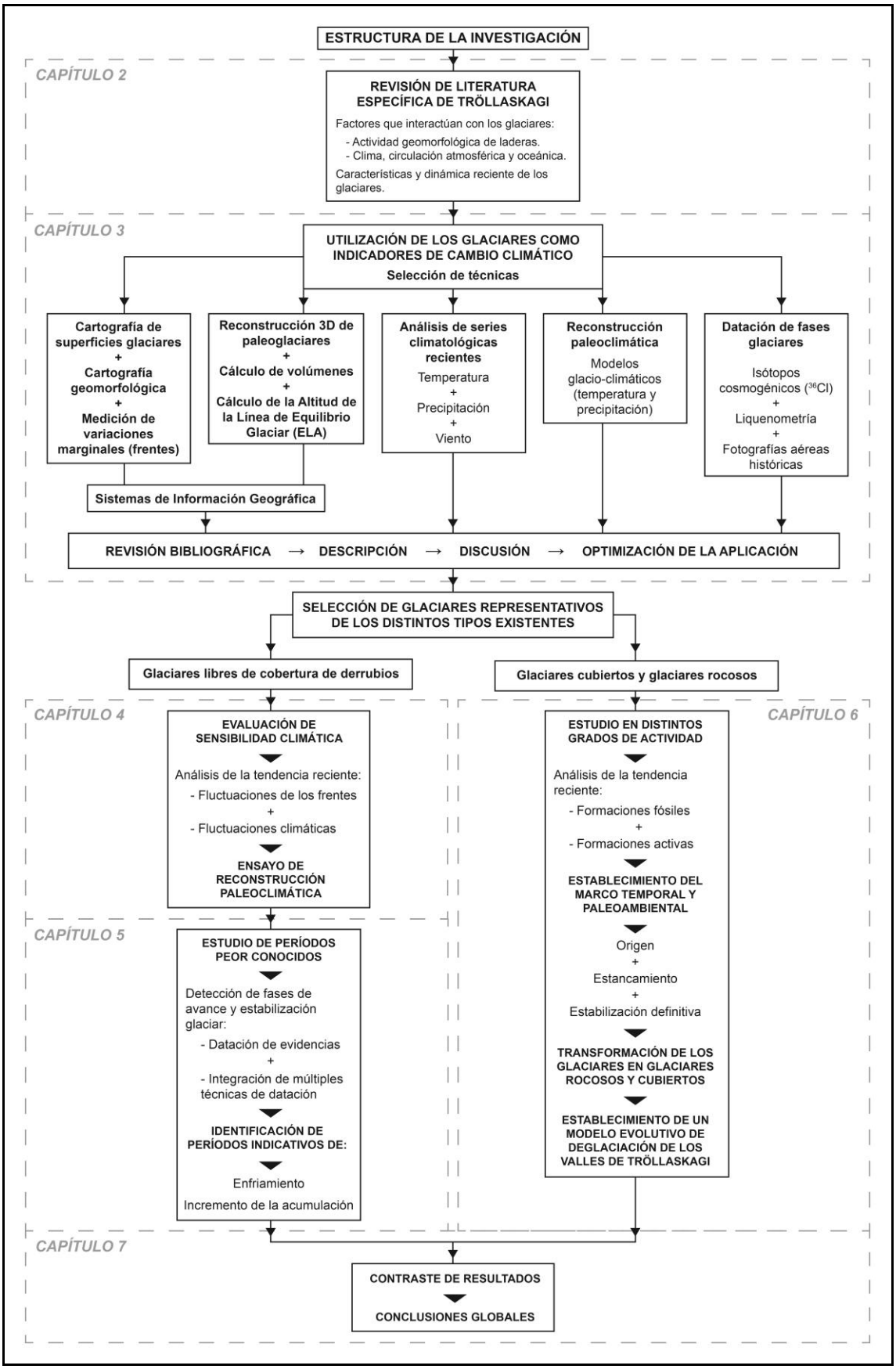

Figura 1.1. Estructura de la investigación en la Tesis Doctoral.

La consecución del objetivo general y los objetivos específicos requiere el desarrollo de una secuencia metodológica que se seguirá durante el transcurso de la investigación. Para ello, en primer lugar se hace una selección de las técnicas más adecuadas (cartografía geomorfológica, cartografía de extensiones glaciares, fotointerpretación, cálculo de volúmenes, mediciones de variaciones marginales, reconstrucción de paleoglaciares, reconstrucción paleoclimática, dataciones liquenométricas y dataciones mediante isótopos cosmogénicos) para logar cada objetivo. A continuación, para conocer bien el funcionamiento de cada técnica, se realiza una descripción y una amplia revisión bibliográfica específica. Con toda la información recabada se hizo una discusión pormenorizada de cada técnica en vistas a optimizar su aplicación individual en casos concretos. Finalmente, se establece la secuencia de aplicación de los distintos métodos. La propuesta metodológica diseñada se desarrolla en el **Capítulo 3**.

Para aplicar estas técnicas, se han seleccionado un conjunto de glaciares representativos de los distintos tipos y niveles de dinamismo presentes en los circos de Tröllaskagi: por un lado, tres glaciares sin cobertura superficial de derrubios (Gljúfurárjökull, Tungnahryggsjökull oeste y este); y por otro, tres glaciares cubiertos (Hofsdalur, Hóladalsjökull y Héðinsdalsjökull) y un complejo de glaciares rocosos (Fremri-Grjótárdalur), tanto fósiles como activos.

La comprensión del clima en el pasado a través de los glaciares requiere primero analizar la relación entre las fluctuaciones de los glaciares y la evolución del clima. De este modo, se seleccionan glaciares *debris-free* como representantes de aquellos con una máxima sensibilidad a las oscilaciones climáticas. Además, con el fin de asegurar su máxima fiabilidad como indicadores de cambio climático o fuentes de información paleoclimática, se eligieron aquellos sin evidencias ni constancia de haber experimentado surges (*non-surging glaciers*) en el pasado. Una vez elegidos los glaciares, es necesario evaluar su grado de sensibilidad climática a través del análisis conjunto de la evolución sus frentes y de las variables climáticas que controlan en mayor medida el balance de masa. En este sentido, es ideal contar con un período lo suficientemente extenso que incluya períodos fríos y cálidos registrados en series climatológicas. De esta forma, la aplicación de modelos glacio-climáticos permite tanto la evaluación del potencial de los glaciares como indicadores de cambio climático y fuentes de información paleoclimática, como la aproximación a las variaciones de temperatura y precipitación, y posibles cambios en los patrones atmosféricos. Ambas cuestiones se analizan en detalle en el **Capítulo 4**.

Cuando las relaciones entre la evolución de los glaciares y el clima ya se conocen en un período de control, como las últimas décadas, se está en condiciones de investigar en

los mismos glaciares períodos anteriores peor conocidos, sin registros climáticos instrumentales y de los que sólo quedan las huellas de los glaciares. El problema plantea en los valles y glaciares estudiados la detección de fases importantes de avance o estabilización glaciar, como indicativas de períodos de enfriamiento o incremento de la acumulación. La aproximación a períodos peor conocidos requiere la integración de distintas técnicas de datación aptas para amplios rangos temporales. Pero también exige dar solución a los aspectos más problemáticos de éstas (técnicos y específicos del área). El **Capítulo 5** investiga la evolución glaciar en fases anteriores de las que se carece de registros climáticos directos (instrumentales).

Tras analizar la evolución de glaciares *debris-free*, la investigación se centra en los glaciares rocosos y glaciares cubiertos seleccionados al comienzo. El estudio completo de su evolución requiere estudiarlos tanto en estado fósil, como en activo. Este enfoque permite establecer el marco temporal del estancamiento y la estabilización definitiva en formaciones activas y fósiles, y por tanto, la reconstrucción de la deglaciación de los valles principales y sus cabeceras, así como la progresiva transformación de los glaciares *debris-free* en glaciares rocosos y glaciares cubiertos. En este sentido, los datos obtenidos deben aportar un modelo de deglaciación de los valles estudiados extrapolable a valles con marcos geomorfológicos similares. El modelo evolutivo, la formación y estabilización de glaciares cubiertos y glaciares rocosos se describe pormenorizadamente en el **Capítulo 6**.

Una vez que se han estudiado los glaciares representativos de los distintos tipos, es necesario contrastar los resultados obtenidos y llegar a unas conclusiones globales y directrices para futuras investigaciones. Se deben demostrar asimismo los logros obtenidos, sus implicaciones en el conocimiento del Neoglacial en Tröllasakgi y las futuras líneas de investigación. Estas aportaciones se exponen en el **Capítulo 7**.

NOTA: algunos de los resultados obtenidos a lo largo de la tesis se han transmitido a la comunidad científica de forma inmediata por medio de comunicaciones a congresos internacionales y artículos científicos, por consejo de mis directores y de acuerdo con la tradición de nuestra ciencia:

Fernández, J.M., Andres, N., Tanarro, L.M., Palacios, D., 2015. Glacial and climatic evolution from the Little Ice Age last Maximum to the present in Tröllaskagi Peninsula (North Iceland): the case of Gljúlfurárjökull. Geophys. Res. Abstr. 17, EGU2015-13719–7.

Fernández-Fernández, J.M., Andrés, N., Brynjólfsson, S., Sæmundsson, Þ., 2017. Climatic implications of glacial evolution in the Tröllaskagi peninsula (northern Iceland) since the Little Ice Age maximum . The cases of the Gljúfurárjökull and Tungnahryggsjökull glaciers. Geophys. Res. Abstr. 19, EGU2017-9633.

Fernández Fernández, J.M., Andrés, N., Palacios, D., Tanarro, L.M., 2017. Glaciares libres sensibles al clima frente a los glaciares cubiertos y glaciares rocosos estáticos en la Península de Tröllaskagi (Norte de Islandia). En: Ruiz-Fernández, J., García-Hernández, C., Oliva, M., Rodríguez-Pérez, C., Gallinar, D. (Eds.), Ambientes periglaciares: avances en su estudio, valoración patrimonial y riesgos asociados, pp. 70–77. VI Congreso Ibérico de la International Permafrost Association. Mieres, 21-23 de junio.

Fernández-Fernández, J.M., Andrés, N., Sæmundsson, Þ., Brynjólfsson, S., Palacios, D., 2017. High sensitivity of North Iceland (Tröllaskagi) debris-free glaciers to climatic change from the 'Little Ice Age' to the present. The Holocene 27, 1187–1200. https://doi.org/10.1177/0959683616683262

Fernández-Fernández, J.M., Andrés, N., 2018. Methodological Proposal for the Analysis of the Evolution of Glaciers Since the Little Ice Age and Its Application in the Tröllaskagi Peninsula (Northern Iceland). Cuad. Investig. Geográfica Geogr. Res. Lett. No 44, 69–97. https://doi.org/10.18172/cig.3392

Fernández-Fernández, J.M., Palacios, D., Andrés, N., Schimmelpfennig, I., Brynjólfsson, S., Sancho, L.G., Zamorano, J.J., Heiðmarsson, S., Sæmundsson, Þ., 2019. A multi-proxy approach to Late Holocene fluctuations of Tungnahryggsjökull glaciers in the Tröllaskagi peninsula (northern Iceland). Sci. Total Environ. 664, 499–517. https://doi.org/10.1016/j.scitotenv.2019.01.364

Fernández-Fernández, J.M., Palacios, D., Andrés, N., Schimmelpfennig, I., Tanarro, L.M., Brynjólfsson, S., López-Acevedo, F.J., S., Sæmundsson, Þ., ASTER Team. Constraints on the timing of debris covered and rock glaciers - an exploratory case study in the Hólar area, northern Iceland. Global and Planetary Change (under revision).

Chapter 2.

Regional settings: topography, geomorphology and climate. Study areas and location of selected glaciers.

In order to evaluate the applicability of the methods we sought an area whose geographic configuration makes it particularly sensitive to climate change and therefore turns it into an experimental area for analysing the response of glaciers. An area with these characteristics is the Tröllaskagi Peninsula (northern Iceland) because it is the meeting place of the main atmospheric masses and ocean that determine the ocean-atmosphere interaction of the North Atlantic (Figure 2.1A).

2.1. The Tröllaskagi peninsula. Topographic and geomorphological setting.

The Tröllaskagi Peninsula extends latitudinally between the Atlantic Ocean at 66º12' N (cape of Siglunes) and the central plateaus (65º23' N), and longitudinally between the fjords of Skagafjörður (19º30' W) and Eyjafjörður (18º10' W), which separate it from the Skagi and Flateyjarskagi peninsulas respectively (Figure 2.1B). It is a 4000-km^2 plateau resulting from the accumulation of successive layers of Miocene basalts belonging to the Tertiary Basalt Formation, interspersed with 30-50 cm reddish sedimentary strata (paleosols) (Sæmundsson et al., 1980; Jóhannesson and Sæmundsson, 1989). The plateau culminates at altitudes between 1000 and 1500 meters above sea level (Kerling, 1536 m) and is dissected by deep valleys with steep slopes whose headwaters now function as glacial cirques. Deposits caused by rock-slope failure are common in Tröllaskagi valley slopes and have been considered a result of the final deglaciation during the early Holocene (Jónsson, 1976; Whalley et al., 1983; Mercier et al., 2013; Feuillet et al., 2014; Cossart et al., 2014; Coquin et al., 2015; Decaulne et al. 2016; Sæmundsson et al. 2018).

These cirques shelter over 160 small glaciers, mostly north-facing, resulting from the leeward accumulation of snow coming from the plateau (Caseldine and Stötter, 1993) and

reduced exposure to solar radiation. Glaciers are occupying cirques under similar climatic and geomorphological conditions (Björnsson and Pálsson, 2008). Most of them are rock glaciers and debris-covered glaciers, due to the intense paraglacial activity affecting the walls (Andrés et al., 2016). In this sense, it can be considered that paraglacial processes minimize cosmogenic nuclide concentrations from earlier exposure periods on the cirque headwalls (Andrés et al, 2019). These glaciers are characterized by almost static behaviour because the insulating effect of their debris cover leaves them with little or no sensitivity to the climate (Martin et al., 1991). Only a minority of glaciers lack surface debris cover and this makes them highly dynamic and sensitive to climate oscillations, especially summer temperature (Caseldine, 1985a; Häberle, 1991; Kugelmann, 1991).

2.2. Climate setting.

The 1961–1990 weather data series show a mean annual air temperature (MAAT) of 2 to 4ºC on the Tröllaskagi coasts and -2 to -4ºC on the summits (Etzelmüller et al., 2007). At Akureyri (1901-1990) MAAT is 3.4 ºC, while mean summer (June-August) and mean temperature of the ablation season (May-September) reach 9.9 and 8.4 ºC, respectively (Einarsson, 1991); in winter (January-March) the mean value drops to -1.6 ºC (Einarsson, 1991), although it can be higher if the October-April period is considered, with -0.3 ºC. Precipitation in the Tröllaskagi area oscillates between 400 mm in some lowland areas of Skagafjörður and Eyjafjörður and up to 2500 mm on the summits (1971-2000 data series; Crochet et al., 2007).

2.3. Selected glaciers.

2.3.1. Debris-free glaciers.

The frontier location of Icelandic glaciers in regard to atmosphere and ocean systems makes them exceptionally sensitive to climate oscillations (Bergþórsson, 1969; Flowers et al., 2008; Geirsdóttir et al., 2009; Brynjólfsson et al., 2015a). For this reason, they reflect the climatic evolution and the impact of climate change on the cryosphere as reliable indicators (see Jóhannesson and Sigurðsson, 1998; Bradwell, 2004b; Geirsdóttir et al., 2009; Chandler et al., 2016b). Therefore, in order to ensure maximum climate sensitivity and reliability, we selected three small debris-free glaciers (4 and 7 km^2 surfaces) with no record of having experienced surges: namely Gljúfurárjökull, and Western and Eastern Tungnahryggsjökull, located in the central sector of the Tröllaskagi peninsula (Figure 2.1B). Gljúfurárjökull (65º42'41" N, 18º39'29" W) is located at the head of the Gljúfurárdalur valley,

an eastern tributary of Skíðadalur that belongs to the Svarfaðardalur river system. The Western (65º41'3" N, 18º52'34" W) and Eastern (65º41'23"N, 18º48'38" W) Tungnahryggsjökull glaciers are located in the Vesturdalur and Austurdalur valleys respectively, which are separated by the crest of Tungnaryggur and are tributaries of Kolbeinsdalur.

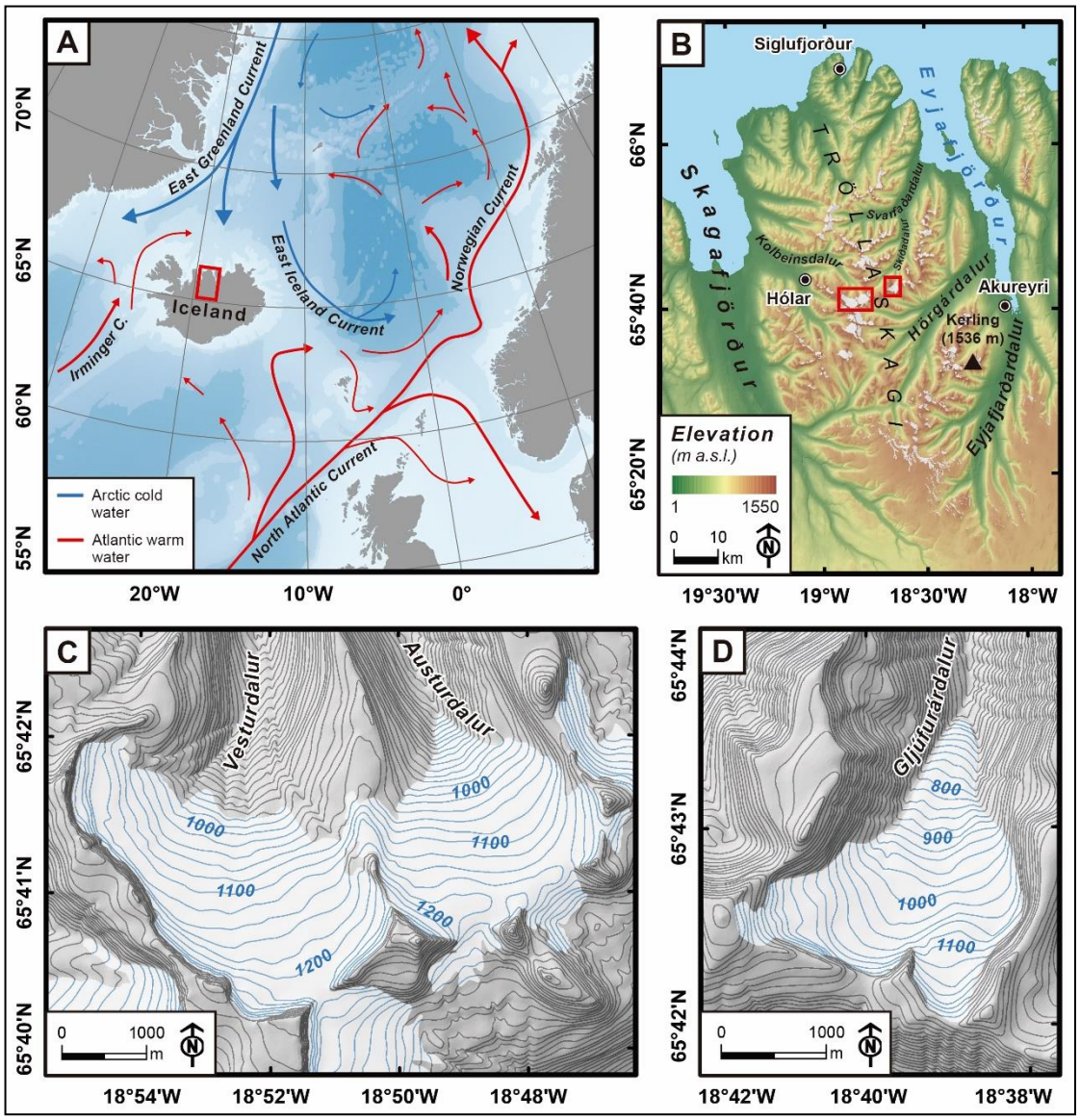

Figure 2.1. Location of the selected debris-free glaciers. (A) Iceland at the North Atlantic in the context of the meeting of cold and warm sea currents (modified from Institute of Marine Research, Norway, 2017). (B) Situation of the Tröllaskagi peninsula and the glaciers analysed (red boxes). (C) and (D) panels correspond to the enlarged boxes with the surrounding areas of Tungnahryggsjökull and Gljúfurárjökull glaciers, respectively.

2.3.2. Rock glaciers and debris-covered glaciers.

The Fremri-Grjótárdalur and Hóladalur cirques in the Víðinesdalur valley, and the Hofsdalur and Héðinsdalur valleys are the focus area of this study and are located in the

surroundings of the village of Hólar, on the western side of the Tröllaskagi peninsula (Fig. 2.2B, 2.2C). These valleys are tributaries to the main valley of Hjaltadalur, which drains into the Skagafjörður, and host both debris-free, debris-covered and rock glaciers. The summits surrounding these cirques form a flat plateau at around 1200-1330 m a.s.l. (Fig. 2.2C), hosting flat-bottomed cirques with steep 100-170 m high slopes.

In the Fremri-Grjótárdalur cirque (Fig. 2.2C), two lower fossil rock glacier sectors have been differentiated, overlapped by active rock glaciers in the western and eastern sectors of the cirque (Andrés et al., 2016; Farbrot et al., 2007; Kellerer-Pirklbauer et al., 2007). The rock glacier complex occupies an area of 0.96 km^2 with a larger rock glacier 1 km length and maximum width almost 300 m. The fronts of the fossil rock glaciers descend to an altitude of 850 m a.s.l., while the active ones descend to 950 m a.s.l. (Tanarro et al., 2018, 2019).

The Hóladalsjökull glacier, located in the adjacent cirque to the east of Fremri-Grjótárdalur (Fig. 2.2C), is formed by a debris-covered lower section, 2 km long and 1.3 km-wide, covering an area of 2.2 km^2 . The front is located at 900 m a.s.l. The upper sector is formed by 1.7 km-long debris-free glacial ice, occupying an area of 2.5 km^2 (Tanarro et al., 2018, 2019).

The Hofsjökull glacier is located at the head of the Hofsdalur valley, to the south of Hólardalur (Fig. 2.2C). Hofsjökull glacier is a 1.7 km long and 1.5 km wide debris-covered lower section and 1.3 km long debris free upper section (Campos et al., 2019).

Héðinsjökull glacier in Héðinsdalur valley (Fig. 2.2C), to the south of Hofsdalur. The distal to the present extent of Héðinsdalsjökull is a debris mantle that evidences former extent of the debris-covered glacier. The snout of this palaeo debris-covered glacier is at 640 m a.s.l. The present glacier extends from 900 m a.s.l. upwards, where ice-collapsed depressions can be observed on a debris cover mantle. The total debris-covered sector (with and without underlying ice) is 2.3 km long, being the collapsed and active sectors 1.2 and 0.9 km long respectively. The upper sector is formed by debris-free glacial ice 2.3 km long and 2.6 km wide.

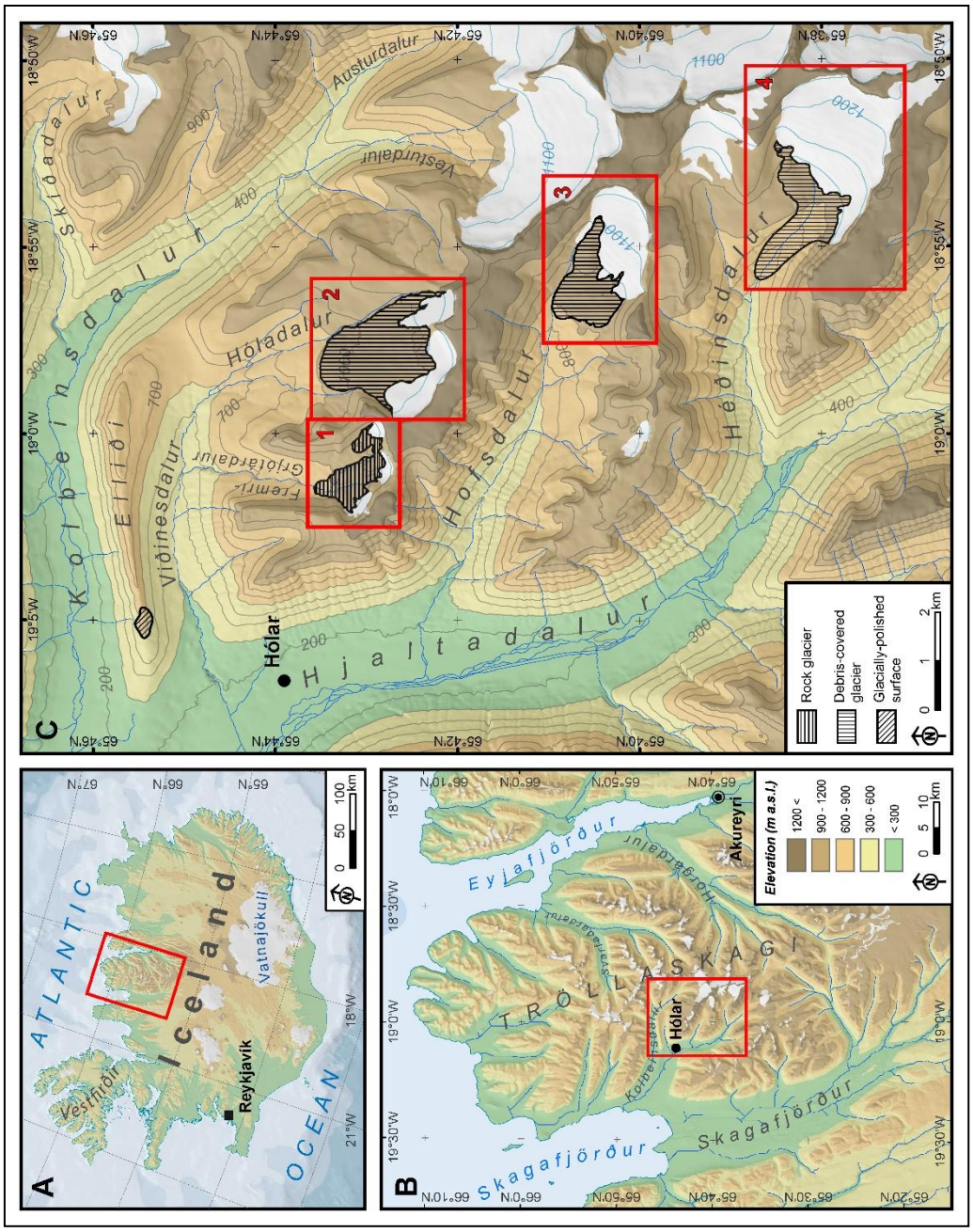

Figure 2.2. Location of the study area in central north Iceland (A) the Tröllaskagi peninsula (B) and glaciers and debris-covered glaciers under study (C). The red boxes in panels A and B refer to the extent of the panels B and C, respectively. Numbers of red boxes in panel C refer to: (1) Fremri-Grjótárdalur, (2) Hóladalsjökull, (3) Hofsjökull, and (4) Héðinsdalsjökull.

Chapter 3.

Methodology.

3.1. Glaciers as indicators of climate change.

Glaciers respond to climatic variability through changes in their length, area, volume, thickness and flow rate (Francou and Vincent, 2007; Gabbud et al., 2016). In this sense, they are highly sensitive to variations in summer temperature and winter precipitation, as these are the variables that to a greater extent control ablation and accumulation (see Ahlmann, 1924; Liestøl, 1967; Sutherland, 1984; Ohmura et al., 1992) respectively, and therefore affect the sign of mass balance and largely –but not exclusively (Gabbud et al., 2016)– front dynamics. Nevertheless, although glacier advance and retreat are considered to be indicators of climate change, it is crucial to understand the relationships between climatic variations and glacier response (Úbeda, 2011; Gabbud et al., 2016; Mal et al., 2016). The complexity of the interaction between glaciers and the climate system requires the establishment of a methodology that can analyse glacier oscillations and their relation to climate from different points of view and in an interrelated manner.

Changes in the positions of glacier fronts (i.e. retreat) are one of the indicators of climate warming and glacier change (Houghton et al., 1996; Gabbud et al., 2016) that are the simplest to measure, traditionally by placing markers or stakes that record the position of the fronts at different dates (Eythórsson, 1931, 1935; Caseldine and Cullingford, 1981; Caseldine, 1983; Caseldine, 1987; Sigurðsson, 1998; Sigurðsson et al., 2007; Icelandic Glaciological Society, 2015). The records of glacier lengths, combined with climate sensitivity and response times, are also valuable proxies for the reconstruction of temperature histories, as shown by Oerlemans (2005).

The development of Geographic Information Systems (GIS) and remote sensing have enabled the remote study of glaciers by using aerial photographs and satellite images (see Kääb, 2005; Kääb et al., 2005; Bradwell et al., 2006; Bahuguna et al., 2007; Pellika and Rees, 2009; Chandler et al., 2016b; Gachev et al., 2016), which has improved the recording of glacier surface trends (e.g. Thompson et al., 2011; Gjermundsen et al., 2011; Kaldybayev

et al., 2016; Veettil et al., 2017). Estimating glacier volumes and their spatiotemporal variations are also key aspects in the research on the impact of climate change, since the quantification of glacier melt is essential in modelling due to its global contribution to rising sea levels (Church et al., 2001; Braithwaite et al., 2006). The difficulties of accessing glaciers and surveying them through radio echo-sounding have led to the fact that estimates of volume and its variations are often carried out indirectly by applying mathematical models with a physical basis (Chen and Ohmura, 1990; Bahr et al., 1997; Klein and Isacks, 1998; Farinotti et al., 2009), because they are so easy to implement. In other cases planimetric measurements (e.g. Holmlund, 1987), remote sensing (e.g. Bahuguna et al., 2007; Rabatel et al., 2016), and the combination of GIS and photogrammetry (e.g. D'Agata and Zanutta, 2007; Diolaiuti et al., 2009; Hannesdótir et al., 2015a; Gabbud et al., 2016) have been used.

The joint study of glacier trends and climate is essential in order to assess the impact of climate change on glaciers, as well as their response to climate fluctuations. Thus, for example, the close relationship between front position variations and summer temperature oscillations is well known (Caseldine, 1985a; Kirkbride, 2002; Bradwell, 2004b; Bradwell et al., 2013). Of equally vital importance is an understanding of the climatic conditions that favor or preserve glaciation by applying glacier-climate models at the Equilibrium-Line Altitude (ELA) (e.g. Ballantyne, 1989; Ohmura et al., 1992; Braithwaite, 2008). These models are especially useful to carry out palaeoclimate reconstruction at various time scales (Ballantyne, 1989; Dahl and Nesje, 1992; Caseldine and Stötter, 1993; Hughes, 2009a; Hughes et al., 2006, 2010; Hughes and Braithwaite, 2008; Meyer and Barr, 2017) or even to explain the existence of glaciers in marginal areas that are not favorable for glaciation, especially in terms of the amount of accumulation required to make up for ablation (e.g. Hughes, 2009b; Colucci, 2016), or to interpret the effect of extreme climatic events on glaciers (e.g. Hughes, 2008).

This Thesis integrates a methodological sequence that complements most of the indicators and techniques presented in order to analyse the impact of climate change on glaciers and their response based on the analysis of different variables. Therefore, the objective of this study is to propose and evaluate a methodological approach applied in a particularly sensitive area where glaciers dynamically respond to the changes in the elements that make up the climate (Andrés et al., 2016), and applicable in any area of study. To illustrate the methodology, three glaciers have been selected (Gljúfurárjökull and Western/Eastern Tungnahryggsjökull) which are located in the interior of the Tröllaskagi Peninsula (northern Iceland).

3.2. Methodological proposal for the analysis of glacier evolution.

The effect of climate change has been analysed from different points of view, mainly including: measuring retreat and advance based on variations in the fronts position; changes in area and volume (estimated); reconstruction of glacier surfaces; calculation and time analysis of the ELAs; statistical treatment of climate series; the application of glacier-climate models to estimate precipitation in the ELA and; surface exposure dating.

3.2.1. Analysis of recent glacier variations over aerial photos and satellite imagery.

3.2.1.1. Georeferencing and photointerpretation of historical aerial photos.

Trend analysis of glacier geometry was used as an indicator of changing climate (Bahr et al., 1997). The study was carried out in the ArcGIS 10.3 (Esri) GIS work environment. The work started by identifying the positions occupied by the glacier fronts during LIA maximum, as established and validated in the literature (Caseldine and Cullingford, 1981; Caseldine, 1983, 1985a, 1985b; Caseldine and Stötter, 1993) by applying lichenometric dating methods to blocks of the most advanced moraine formations. Monitoring of the glacier extents after the LIA was based on the photointerpretation of aerial photograms (approximate scale 1:30,000) of the glaciers in 1946 (photographs taken by the United States Army Map Service), 1985 and 1994; an orthophotograph from the year 2000; and a SPOT satellite image from 2005 provided by the National Land Survey of Iceland. The photointerpretation was combined with visits to the glacier fronts in successive field campaigns in 2012, 2013, 2014 and 2015 (Figs. 3.1, 3.2 and 3.3).

The photograms were georeferenced on the orthophotograph of 2000, only for a rectangular part that includes the area surrounding the glaciers. In order to accurately observe the variations of the fronts between dates, a large number of control points (53-171) were established, evenly distributed in easily identifiable elements such as the indentations and protrusions of the topmost surfaces of the plateaus and cirque walls, as well as confluences of beds or channels of debris flows in the slopes (stable in each date covered by the photographs). The *"Adjust"* rectification method was chosen instead of third-order polynomial transformation due to: 1) the joint optimization of the global root mean squared (RMS) error and the positional accuracy of the control points (local precision); and 2) less deformation of the geometry of glacier tongues and fronts, in order to ensure that the positions of the fronts were reliable and comparable between dates. Third-order polynomial transformation only optimizes overall accuracy and not local accuracy, which is particularly important at the control points established in the vicinity of glacier fronts. RMS

errors resulting from georeferencing through *"Adjust"* transformation ranged from 3 to 6 m and were lower than those obtained from the other transformations (Table 3.1).

Figure 3.1. View of the Gljúfurárjökull snout from the left 'Little Ice Age' moraine.

Figure 3.2. View of the Eastern Tungnahryggsjökull snout from the left 1946 moraine. A number of ridges can be seen in the foreland, which shows the pulsating behaviour of the glacier in response to the recent climatic fluctuations.

Figure 3.3. View of the Western Tungnahryggsjökull glacier from the 'Little Ice Age' moraine.

Glacier	1946					1985					1994				
	No. ctrl. pts.	Pol. 1	Pol. 2	Pol. 3	Adj.	No. ctrl. pts.	Pol. 1	Pol. 2	Pol. 3	Adj.	No. ctrl. pts.	Pol. 1	Pol. 2	Pol. 3	Adj.
Gljúfurárjökull	128	96	80	68	4	103	108	76	54	6	171	110	82	63	6
Tungnahryggs-jökull (W)	78	66	48	31	3	78	67	35	28	4	90	77	53	42	5
Tungnahryggs-jökull (E)	87	58	51	34	5	53	76	39	27	6	-	-	-	-	-

Table 3.1. Summary of control points used in the georeferencing of the aerial photos and RMS error derived from the different georeferencing methods in each date. 'Pol.' refers to the polynomial transformation and the number to its order; 'Adj.' refers to the 'Adjust' method. RMS error is expressed in meters.

3.2.1.2. Glacier geometry outlining and mapping.

Once the photographs were georeferenced, the geometry of the glacier tongues was mapped at a scale of 1:1000 by means of vector polygon layers (Fig. 3.4). When mapping the glaciers' extent at the various dates the geometry of the accumulation zone (head) of the glaciers in 1946 was preserved, according to Koblet et al. (2010), assuming that the actual changes in the extent of the accumulation zone are smaller than the differences derived from the operator. In the case of Tungnahryggsjökull glaciers, whose headwaters are diffluences, it was assumed that: (i) the ice divides are the upper boundaries of the glaciers for the different stages, and (ii) the ice divide is invariant for the different

stages/dates. Likewise, in the case of the upper glacier edge constrained by the cirque wall, the glacier geometry was also assumed to be invariant from stage to stage unless the aerial photographs showed otherwise.

3.2.1.3. Glacier advance and retreat measurements.

Front advance or retreat was measured in 3D on the digital elevation model (DEM) and the layers of glacier geometry, in the ArcScene work environment, with the *"Measure Direct 3D Line"* tool. In the case of simple fronts that were clearly tongue-shaped and had a well-defined apex, such as those of Gljúfurárjökull and Eastern Tungnahryggsjökull, the distance of retreat or advance between different dates was measured between the most advanced points of the fronts at the various dates following the central axis of the longest tongue (flow line) (see Fig. 3.4).

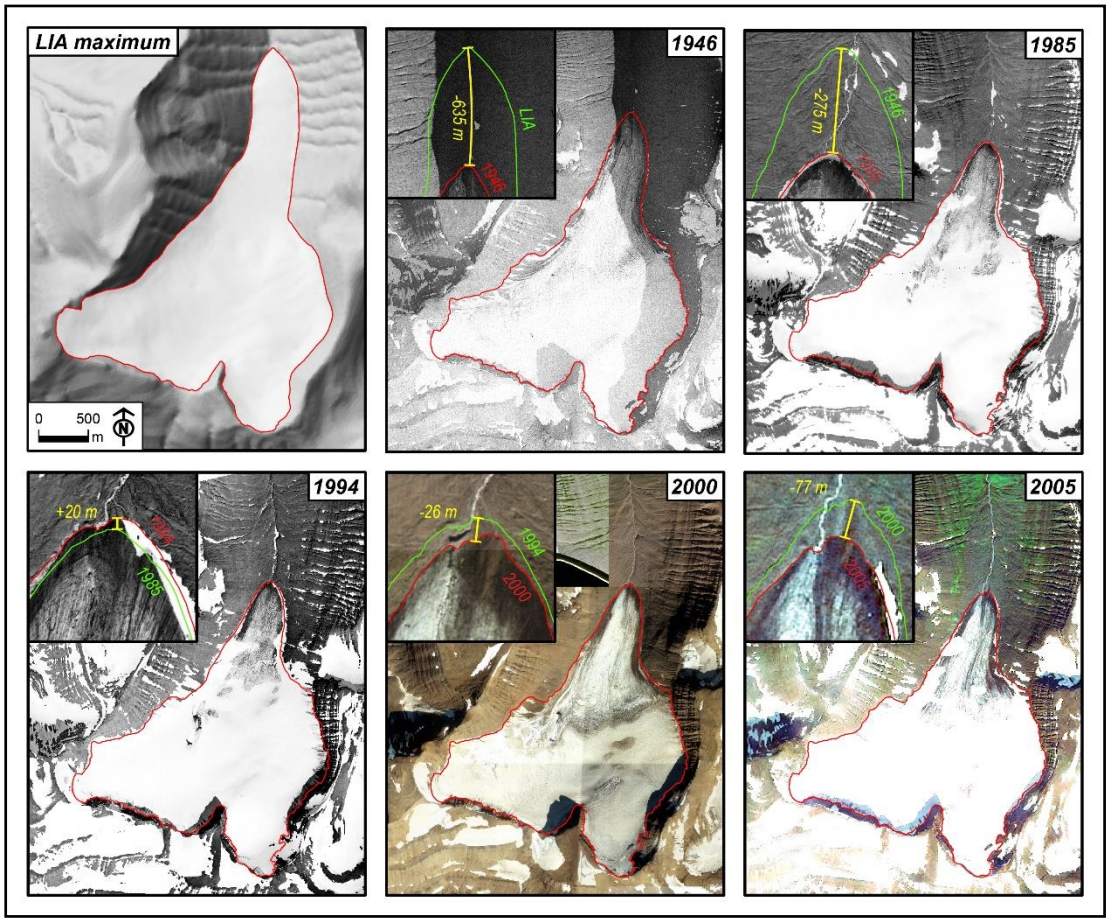

Figure 3.4. Example of glacier outline mapping of Gljúfurárjökull at different dates, based on visual inspection of georeferenced aerial photos. The yellow line and number refer to the measurement of the snout retreat/advance along the flow line. Green and red numbers correspond to the dates for which the glacier outlines were drawn.

However, in Western Tungnahryggsjökull, the retreat or advance was measured along different sectors of the front, given its greater complexity (uneven debris cover).

Lastly, with the aim of comparing the retreat between the glaciers, average rates of advance and retreat were estimated for the periods between the different dates under analysis.

3.2.2. Geomorphological mapping.

Four summer field campaigns (2012, 2013, 2014 and 2015) were conducted in Gljúfurárdalur, Vesturdalur and Austurdalur, with the objective of identifying moraines that clearly provided evidence of various glacial culminations of the western and eastern Tungnahryggsjökull glaciers. We identified the palaeo-positions of the glacier snouts, the glacier geometry and extent through photo interpretation of stereoscopic pairs and previous fieldwork. Mapping of glacial and non-glacial landforms was conducted on two enlarged 50-cm-resolution aerial orthophotos (National Land Survey of Iceland, 2015) plotted at scale ≈1:7000. These maps were imported into an ArcGIS 1.4.1 database after geo-referencing. Finally, all the glacial linear landforms were digitized, and where the moraines were prominent, continuous, or well-preserved, they were assumed to represent major culminations, and hence, glacial stages.

3.2.3. Area and volume calculation.

The areas of the glaciers were calculated in 2D using the *"Calculate Geometry"* (Area) function in ArcMap. The figures obtained were used to estimate the ice volumes through the area-volume scaling (AVS) approach according to Bahr et al. (1997). This method was chosen due to its convenience in calculating volumes when radio echo-sounding surveys are not available to estimate ice thicknesses, as is the case here. AVS is based on the existence of a proportional and exponential relation (1) between the area of the glaciers (*S*) and their volume (*V*).

$$V \propto S^{\gamma} \qquad (1)$$

where *V* and *S* are expressed in km^2 and km^3 respectively.

This relationship was demonstrated by statistical regression for 144 glaciers worldwide with reliable radio echo-sounding, excluding ice sheet and ice cap glaciers, with a regression coefficient of 1.36 (which is in turn *γ*) and squared correlation coefficient $R^2 = 0.99$ (Meier and Bahr, 1996; Bahr et al., 1997). This approach is based, on the one hand, on the proportionality between a series of geometric parameters (volume as a function of area and average thickness, area as a function of length and width, width as a function of thickness) and its association with other parameters affecting the dynamics of the ice (slope, lateral drag and mass balance). The exponential relation between area and

volume is scaled by a *γ* exponent (1) as a dimensionless quantity describing the interaction of the abovementioned parameters (2).

$$\gamma = 1 + \frac{1+m+n(f+r)}{(q+1)(n+2)} \qquad (2)$$

As a preliminary approximation to the volumes of Gljúfurárjökull and Tungnahryggsjökull, the γ exponent was calibrated in the estimates for the glaciers under study according to the considerations of Bahr et al. (1997). The width (*q*) of the glaciers was expressed as *q* = 0.6, which in turn is representative of the inventory of glaciers in Eurasia and the Alps (Bahr, 1997). The slope (*r*) was assumed to be steep (*r* = 0) because they are cirque glaciers, as opposed to the gentle slopes characteristic of large ice masses (*r* = 1). Regarding the lateral drag of the ice (*f*), depending on the values chosen in the other variables (width, slope and mass balance), *f* = 0 was assumed because it approximates *γ* ≈ 1.36 observed by statistical regression between area and volume (Meier and Bahr, 1996; Bahr et al., 1997). Mass balance was expressed as *m* = 2, agreeing with the average accumulation area ratio (AAR) obtained from Bahr's inventory of glaciers in Eurasia and the Alps (1997). Lastly, for the flow parameter (*n*), *n* = 3 was assumed as the typical ice value versus $n \rightarrow \infty$ (assuming perfect plasticity for ice sheets), according to Glenn's flow law (1958). As a result of the scaling of the above parameters, *γ* = 1.375. We applied a constant of proportionality (*c*) of *c* = 0.2055 $m^{3-2\gamma}$ for mountain glaciers (Chen and Ohmura, 1990) to the scaling of the relation expressed in (3).

$$V \propto cS^{\gamma} \qquad (3)$$

It would be possible to obtain an estimate of the uncertainty associated with the use of theoretical scaling (*γ* = 1.375) by comparing it with the results obtained with *γ* = 1.36, which is considered empirical. However, it is not calculated in the Thesis as it would need to know the specific constant of proportionality of the Tröllaskagi glaciers (which has not been stated up to now). A more detailed explanation and discussion of the physical fundamentals of AVS and the mathematical treatment and individual scaling of the variables can be found in Bahr et al. (1997) and Bahr et al. (2015).

3.2.4. Glacier reconstruction.

3.2.4.1. Cartographical «hand-drawn» contouring approach.

As a first approach with prospective aim, topography was reconstructed for the LIA from the lateral and frontal moraines, used as geomorphological evidence of the thickness and extent of the glaciers. The cartographic approach (Sissons, 1974; Pellitero et al., 2015),

based on the manual drawing of contour lines, was followed so that these lines would reproduce the topography currently observed in the glaciers, with concave (convex) curves above (below) the ELA, and all the more the further away they were. Because there was no topography for the remaining dates, reconstruction was carried out in the same way for 1946, 1985, 1994 and 2005, although only for the sectors of the tongues where changes were observed (positions that were further forward or behind), while the remainder of the glacier surface was left with the topography of the year 2000. Next, the glaciers' DEMs were created for the different dates under analysis based on the interpolation of the contour lines with the ArcGIS "Topo to Raster" tool.

3.2.4.2. Numerical physical-based modelling.

Benn and Hulton's (2010) glacier reconstruction approach using a physical-based model describing ice rheology and glacier flow (Van der Veen, 1999) was chosen in order to achieve more robust reconstructions. This model operates on deglaciated areas with non-extant glaciers. As this is not the case in our study area, we approached the glacier bedrock by tentatively estimating the ice thickness' spatial distribution on the two glaciers studied.

The "VOLTA" ("Volume and Topography Automation") ArcGIS toolbox (James and Carrivick, 2016) was applied with the default parameters. It only requires the glacier outline and its digital elevation model (DEM). In the first step, the tool "volta_1_2_centreline" creates the glacier centrelines, and then the tool "volta_1_2_thickness" estimates ice thickness at points along them, assuming perfect-plasticity rheology, and interpolates the values using a glaciologically correct routine. The final result is an ice-free DEM in which we reconstructed the glacier.

The former glacier surface topographies at the different stages/dates were reconstructed applying the semi-automatic "GLaRe" ArcGIS toolbox designed by Pellitero et al. (2016), which implements the Benn and Hulton (2010) numerical model and estimates ice-thickness along glacier flowlines. To simplify the glacier surface modelling, shear-stress was assumed to be constant along the glacier flowline and over time. Using the value 110 kPa for the shear-stress resembles best the current longitudinal profile of the glaciers in the Benn and Hulton (2010) spreadsheet. This value can be considered appropriate as it falls within the normal shear-stress range of 50-150 kPa observed in current glaciers and is very close to the standard value of 100 kPa (Paterson, 1994). The glacier contours were manually adjusted to the ice surface elevation values of the ice-thickness points estimated by "GLaRe" instead of using an interpolation routine, to obtain a more realistic surface (concave and convex contours above and below the ELA).

3.2.5. Equilibrium-Line Altitude calculation.

ELA was selected as another indicator of climate effect on glaciers (Nesje, 1992) because it marks: 1) the average altitude of a glacier's surface where the specific mass balance equals zero (Cogley et al., 2011); 2) climatic conditions sufficient for glacier survival (Ohmura et al., 1992); and because of the potential for inferring climate changes from fluctuations in its altitude (Pellitero et al., 2015), given its close connection with the local climate (Benn and Lehmkuhl, 2000). In order to observe the impact of climate change on the glaciers selected, ELAs were calculated for all the available dates since the LIA maximum, using the Accumulation Area Ratio (AAR, Brückner, 1886, 1887) and Area Altitude Balance Ratio (AABR; Osmaston, 2005) methods.

ELAs were automatically calculated in the ArcMap work environment using the "ELA calculation" toolbox designed by Pellitero et al. (2015), in which a 5 m contour interval was established. For the AAR method, the 0.67 ratio previously used in Tröllaskagi (Caseldine and Stötter, 1993) was established because its results corresponded to the maximum altitude of the lateral moraines (Stötter, 1990). Finally, for exploratory purposes, the AABR method was used. To our knowledge, it was not tested with Tröllaskagi glaciers until now due to the scarcity of current mass balance studies (e.g. Björnsson, 1971) on these glaciers, so we tentatively used the 1.5±0.4 Balance Ratio (BR) proposed for Western Norway glaciers (Rea, 2009).

3.2.6. Analysis of climate series, application of glacier-climate models and palaeoclimatic reconstruction.

In parallel with the monitoring of the glaciers, climatic evolution was analysed based on the records of two weather stations, one located in the city of Akureyri (65°41'N; 18°06' W; 23 m) in the interior of Eyjafjörður, and the other on the Öxnadalsheiði mountain road (65°28'N; 18°41' W; 540 m) in the south of the Tröllaskagi Peninsula. Although it is located 25 to 35 km away from the glaciers under study, the Akureyri climate series (Icelandic Meteorological Office, 2017) was taken as a reference of climate change from the LIA to the present day, since it covers a period from 1882 to 2015. The Öxnadalsheiði series (Icelandic Road and Coastal Administration, 2017) only covers 14 years between 2000 and 2014. The processing of the series consisted in applying 5-year running means and identifying cold and warm homogeneous periods by studying the sign of the deviation from the average (Fig. 3.5), according to Einarsson (1991). The periods identified were characterized according to their average temperatures.

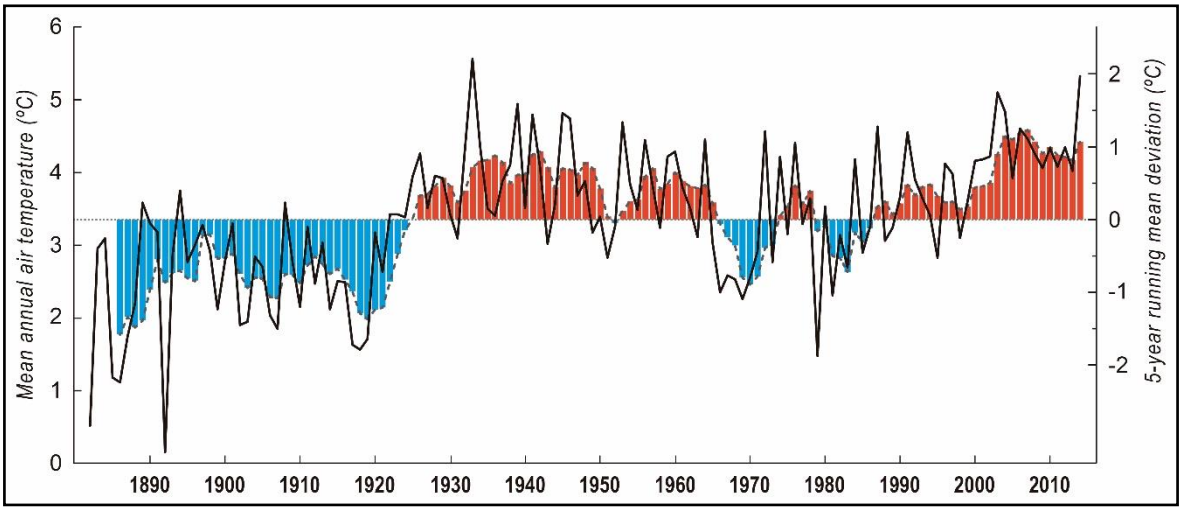

Figure 3.5. Temperature evolution, 5-year running mean and deviation from the average at Akureyri meteorological station from 1882 to 2014. The thick black line and the grey dashed line correspond to the MAAT and the 5-year running mean of the MAAT. The red (blue) bars represent the positive (negative) deviations, which correspond to warm (cold) periods.

Subsequently, with the two-fold aim of 1) carrying out a tentative reconstruction of the climate at the end of the LIA and 2) studying the influence of climate variables (temperature and precipitation, as the main controls in ablation and accumulation) at the ELA and their relationship with atmospheric circulation patterns, three glacier-climate models were applied, based on statistically validated relationships between precipitation and temperature (Liestøl, 1967; Ballantyne, 1989; Ohmura et al., 1992; Braithwaite, 2008) measured at the ELA. Such models make it possible to determine temperature or precipitation if one of the variables is known, generally temperature (Pellitero et al., 2015). The temperature values required by the different models were obtained by extrapolating the average temperatures (annual, ablation season and summer) recorded during each period at the Akureyri station at the mean ELA, assuming the vertical temperature gradient obtained from the statistical treatment of the climate series of Akureyri and Öxnadalsheiði for the 2000-2014 (common) period.

The first model is based on an exponential relationship between the mean temperature of the ablation season and the winter accumulation observed by Sutherland (1984) in a set of ten Norwegian maritime glaciers (Liestøl, 1967) and later expressed by Ballantyne (1989) with the mathematical expression (4):

$$A = 0.915e^{0.339T_a} \qquad (4)$$

where A is winter accumulation (October-April) expressed in m water equivalents; and T_a is the average temperature of the ablation season (May-September), expressed in °C.

The second model was established by Ohmura et al. (1992) based on statistical analysis of the average temperature of the three summer months (T_s) and annual precipitation (P) at the ELA of a set of 70 glaciers worldwide with mass balance monitoring. The statistical analysis of both variables characterized the climate of the ELA with the quadratic equation (5):

$$P = 645 + 296T_s + 9{T_s}^2 \qquad (5)$$

where P is the annual total precipitation (the sum of winter mass balance and summer precipitation) expressed in mm; and T_s is the average temperature of the three summer months (June, July and August) expressed in ºC. The standard error associated with this model is 200 mm; the variation of 1 °C is equivalent of 350 mm.

Lastly, we tested the degree-day model (Brugger, 2006; Braithwaite, 2008), based on the proportionality between melting snow/ice at the ELA (ablation) and the summation of positive temperatures (degree-day sum). This proportionality is expressed by the degree-day factor (*ddf*) resulting from the quotient of the two variables. The use of this third method to estimate precipitation is justified by the definition of ELA, in which the calculation of ablation is equivalent to the calculation of accumulation; in other words, it enables us to know the accumulation necessary to make up for the melt. However, depending on the amount of summer precipitation, total annual rainfall is between the winter balance and the sum of the winter balance and the summer precipitation (Ohmura et al., 1992). Therefore, Braithwaite (2008), based on the data of Ohmura et al. (1992), suggests the use of a *ddf* between 3.5±1.4 and 4.6±1.4 day^{-1} $°C^{-1}$, representing low and high accumulations. Nevertheless, in order to facilitate calculation and for exploratory purposes, we used the average *ddf* value 4.1±1.5 day^{-1} $ºC^{-1}$ previously used in palaeoclimate reconstructions (see Hughes et al., 2010). The application of this model requires knowing the average temperature of each day of the year, which was achieved by simulating in a programmed Excel spreadsheet its distribution throughout the year through a sinusoidal function (6) around the MAAT extrapolated at ELA (Fig. 3.6):

$$T_d = A \sin\left(\frac{2\pi d}{\lambda} - \phi\right) + MAAT \qquad (6)$$

where T_d is the average daily temperature; A is the amplitude (half of the annual thermal range), d is the Julian date (1-365), λ is the modelling period (1 year, 365 days), Φ is the phase angle (1.93 rad so that January is the coldest month), and MAAT is the average annual temperature.

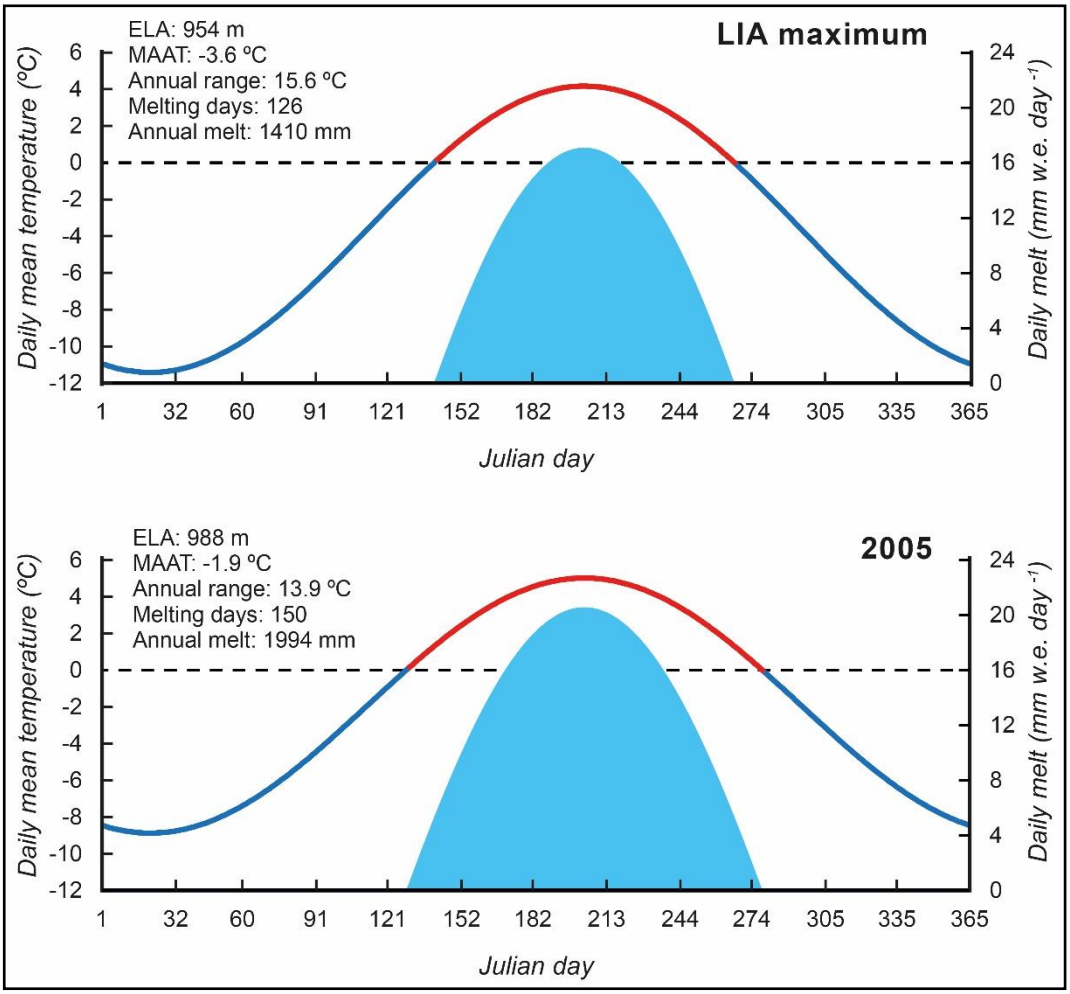

Figure 3.6. Example of the application of the degree-day model at the ELA of Gljúfurárjökull in the LIA maximum and 2005. The red (blue) line corresponds to the temperatures above (below) the freezing point. The blue polygon is the modelled distribution of the daily melt throughout the year. The melting days fairly match to the ablation season from May to September. Note the different annual temperature range, annual melting and the melting days in the two dates.

3.2.7. Surface exposure dating.

3.2.7.1. Lichenometric dating.

Lichenometry was used as a relative dating tool, assuming that the lichens increase in diameter with respect to age. The results aim to complete the age control (of recent landforms non suitable for CRE dating) on the periods between aerial photos of known date as it has been applied successfully to control lichen (Sancho et al., 2011) and bryophyte (Arróniz-Crespo et al., 2014) growth during primary succession in recently deglaciated surfaces.

First, we surveyed the moraines thoroughly, starting from the current glacier snouts downwards, looking for large stable boulders (i.e. well embedded in the moraine, not likely

of having been overturned or remobilized by slope processes which could have affected lichen growth, e.g. snow avalanches, debris-flows, rockfall, landslides or debris-flows) with surfaces valid for dating (not weathered or resulting from block break). Lichenometry was applied to date moraine ridge boulders with the following criteria and assumptions: (i) boulders must clearly belong to the moraine ridge; (ii) lichen species should be abundant enough to allow measurements of a number of thalli at each location and hence enable surfaces to be dated under favourable environmental conditions such as basaltic rocks in subpolar mountains; (iii) only the largest lichen (circular or ellipsoidal thalli) of species *Rhizocarpon geographicum*, located on smooth horizontal boulder surfaces, was measured; (iv) the lichenometric procedures should not be applied when the lichen thalli coalesce on the boulder surface and individual thalli cannot be identified.

We preferred the geomorphological criterion (stability vs. slope processes) to the establishment of lichenometry plots of a fixed area (e.g. Bickerton and Matthews, 1992) to ensure that lichens were measured on reliable boulders. This measurement strategy tries to circumvent or at least to minimize the specific problems of Tröllaskagi when dating glacial features so that: (i) snow accumulation should be lower in the moraine crest; (ii) lichen ages will be estimated only for the boulders located on the crests used to map and reconstruct the glaciers; and (iii) and lichens subjected to thalli saturation (coalescence) or high competition are not measured.

First, *Rhizocarpon geographicum* lichens were measured with a Bernier calibrator. Then, digital photographs for high-precision measurements were taken of the most representative of the largest thallus located in each selected boulder (Fig. 3.7), using an Icelandic *króna* coin (21 mm diameter) parallel to the surface of the lichen as a graphic scale. We preferred the single largest lichen approach as previously has been done in Tröllaskagi for lichenometric dating of moraines (Caseldine, 1983, 1985b, 1987; Kugelmann, 1991). The photos were scaled in ArcGIS to real size and lichen thalli were outlined manually through visual inspection of the photos and measured automatically with high accuracy according to the diameter of the smallest circle which can circumscribe the lichen outline (Fig. 3.7). We preferred the simple geometrical shape of the circle and its diameter to identify the largest axis to circumvent the problem of complex-shaped lichens. Similar procedures for lichen thalli measurement from photographs are outlined in Hooker and Brown (1977).

Then, we initially applied a 0.44 mm yr^{-1} constant growth rate and a 10-year colonization lag (Kugelmann, 1991) to the measurement of the largest *Rhizocarpon geographicum* lichen (longest axis). This growth rate is derived from the lichen growth curve

with the highest number of control points so far in Tröllaskagi (Kugelmann, 1991), and it is very similar to that reported from the near Hörgárdalur valley (Häberle, 1991). However, the authors are aware that using a constant growth rate implies not taking account the growth rate decline with increasing age. Other longer colonization lags of 15, 20, 25 and 30 years were added to the age estimate from the growth rate in order to test the colonization lag originally assumed by Kugelmann (1991), on the suspicion of longer colonization lags reported elsewhere (Caseldine, 1983; Table 1 in Evans et al., 1999). The resulting ages were compared to the dates of historical aerial photographs where the glacier snout positions constrain the maximum and minimum ages of the lichen stations.

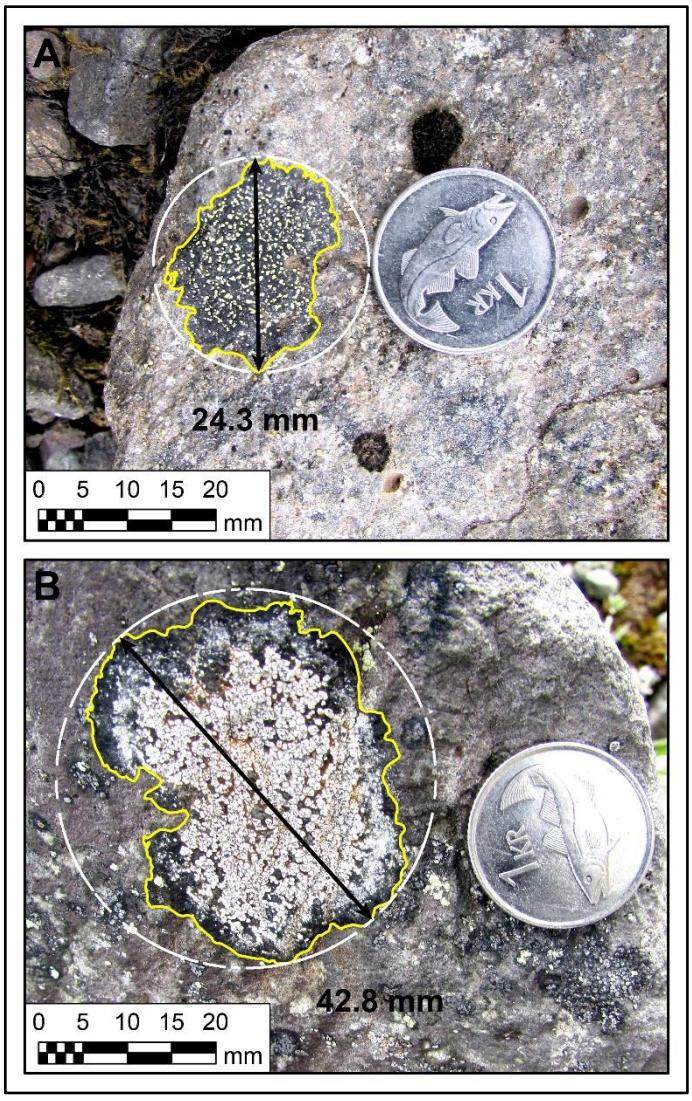

Figure 3.7. Examples of *Rhizocarpon geographicum* group and *Porpidia soredizodes* thalli measured over scaled field photos from the lichenometric station TUW-3. The lines refer to the minimum circle (white) bounding the thalli outlines (yellow) and the diameter of the circle (black). Note the contrasted size of the largest thalli in the different species.

In the case of *Porpidia* cf. *soredizodes*, since no growth rate value has been described so far, a value will be tentatively estimated in this study. For this reason, we took measurements of the two species in the same sampling locations wherever possible. It should be noted that visual distinction between *Porpidia* cf. *soredizodes* and *Porpidia tuberculosa* is not always conclusive based on morphological characteristics, but we feel confident using the measurements of the *Porpidia* cf. *soredizodes* we identified in the field.

3.2.7.2. Cosmic-Ray Exposure dating.

Where the thalli either coalesced and prevented identification of the largest thallus or dating results indicated that a formation (moraine, rock glacier, debris-covered glacier) was too old to be dated by this method, rock samples were collected for CRE dating. The criteria for boulder and surface selection where the same as for lichenometric purposes: stable boulders with no signs of being affected by slope processes (landslides, debris-flows) or postglacial overturning, well embedded in the moraine, and with no sign of surface weathering or previous boulder break. Three batches of samples were taken in 2012, 2014 and 2015.

The cosmogenic nuclide ^{36}Cl was chosen because of the basalt lithology ubiquitous in Iceland, which lacks quartz, which is needed for standard ^{10}Be CRE methods. Using a hammer and chisel, samples were collected from flat-topped surfaces of moraine boulders. The laboratory procedures applied for ^{36}Cl extraction from silicate whole rock samples were those described in Schimmelpfennig et al. (2011). Note that the samples had not enough minerals to perform the ^{36}Cl extraction on mineral separates, which is generally the preferred approach to minimize the uncertainties in age exposure estimates, as in mineral separates ^{36}Cl is often produced by less and better known production pathways than in whole rock samples (Schimmelpfennig et al., 2009). The samples were crushed and sieved to 0.25-1 mm in the “Physical Geography Laboratory” in the Complutense University, Madrid.

The batch of samples taken in 2012 was chemically processed at the “PRIME Laboratory” (Purdue University, USA), following the procedures described in Zreda et al. (1999) and Phillips (2003) for the ^{36}Cl extraction from whole rock. For the two remaining batches, sampled in the 2014 and 2015 fieldwork campaigns, chemical processing leading to ^{36}Cl extraction from the whole rock was carried out at the “Laboratoire National des Nucléides Cosmogéniques” (LN_2C) at the “Centre Europeén de Recherche et d’Enseignement des Géosciences de l’Environnement” (CEREGE), Aix-en-Provence (France).

Initial weights of about 120 g per sample were used. A chemically untreated split of each sample was set aside for analyses of the chemical composition of the bulk rocks at the “Activation Laboratories” (Ancaster, Canada) and the “Service d'Analyse des Roches et des Mineraux” (SARM, Nancy, France). First, the samples were rinsed to remove dust and fines. Then, 25-30% of the mass was dissolved to remove atmospheric ^{36}Cl and potentially Cl-rich groundmass by leaching with a mixture of ultra-pure dilute nitric (10% HNO_3) and concentrated hydrofluoric (HF) acids. In the next step, 2 g aliquots were taken to determine the major element concentrations; these were analysed by inductively coupled plasma-optical emission spectrometer (ICP-OES) at the “Activation Laboratories” and CRPG-SARM.

Then, before total dissolution, ~260 µL of a ^{35}Cl carrier solution (spike) manufactured in-house (concentration: 6.92 mg g^{-1}; $^{35}Cl/^{37}Cl$ ratio: 917) were added to the sample for isotope dilution (Ivy-Ochs et al., 2004). Total dissolution was achieved with access quantities of the above mentioned acid mixture. Following total dissolution, the samples were centrifuged to remove the undissolved residues and gel (fluoride complexes such as CaF_2). Next, chlorine was precipitated to silver chloride (AgCl) by adding 2 ml of silver nitrate ($AgNO_3$) solution at 10%.

After storing the samples for two days in a dark place to allow the AgCl to settle on the bottom, the supernatant acid solution was extracted by a peristaltic pump. To reduce the isobaric interferences of ^{36}S during the ^{36}Cl AMS measurements, the first precipitate was re-dissolved in 2 ml of ammonia (NH_3+H_2O 1:1 vol → NH_4OH), and 1 ml of a saturated solution of barium nitrate ($Ba(NO_3)_2$) was added to the samples to precipitate barium sulphate ($BaSO_4$). It was removed by centrifuging and filtering the supernatant with a syringe through acrodisc filters. AgCl was precipitated again with 3-4 ml of diluted HNO_3 (1:1 vol). The precipitate was collected by centrifuging, rinsed, and dried in an oven at 80 ºC for 2 days.

The final AgCl targets were analysed by accelerator mass spectrometry (AMS) to measure the $^{35}Cl/^{37}Cl$ and $^{36}Cl/^{35}Cl$ ratios, from which the Cl and ^{36}Cl concentration were inferred. The measurements were carried out at the “PRIME Laboratory”, and at the “Accélérateur pour les Sciences de la Terre, Environnement et Risques” (ASTER) at CEREGE in March 2017 using inhouse standard SM-CL-12 with an assigned value of 1.428 (±0.021) x 10^{-12} for the $^{36}Cl/^{35}Cl$ ratio (Merchel et al., 2011) and assuming a natural ratio of 3.127 for the stable ratio $^{35}Cl/^{37}Cl$.

When calculating exposure ages, the Excel™ spreadsheet for in situ ^{36}Cl exposure age calculations proposed by Schimmelpfennig et al. (2009) was preferred to other online

calculators (e.g. CRONUS Earth; Marrero et al., 2016) as it allows input of different ^{36}Cl production rates from spallation, referenced to sea level and high latitude (SLHL). Thus, three SLHL ^{36}Cl production rates from Ca spallation, i.e. the most dominant ^{36}Cl production reaction in our samples, were applied to allow comparisons both with other Icelandic areas (57.3±5.2 atoms ^{36}Cl (g Ca)$^{-1}$ yr^{-1}; Licciardi et al., 2008) and other areas of the world (48.8±3.4 atoms ^{36}Cl (g Ca)$^{-1}$ yr^{-1}, Stone et al., 1996; 42.2±4.8 atoms ^{36}Cl (g Ca)$^{-1}$ yr^{-1}, Schimmelpfennig et al., 2011). For ^{36}Cl production reactions other than Ca spallation, the following SLHL ^{36}Cl production parameters were applied: 148.1±7.8 atoms ^{36}Cl (g K)$^{-1}$ yr^{-1} for K spallation (Schimmelpfennig et al., 2014a), 13±3 atoms ^{36}Cl (g Ti)$^{-1}$ yr^{-1} for Ti spallation (Fink et al., 2000), 1.9±0.2 atoms ^{36}Cl (g Fe)$^{-1}$ yr^{-1} for Fe spallation (Stone et al., 2005) and 696±185 neutrons (g air)$^{-1}$ yr^{-1} for the production rate of epithermal neutrons for fast neutrons in the atmosphere at the land/atmosphere interface (Marrero et al., 2016). Elevation-latitude scaling factors were based on the time invariant “St” scheme (Stone et al., 2000). The high-energy neutron attenuation length value applied was 160 g cm^{-2}.

All production rates from spallation of Ca mentioned above are based on calibration samples with a predominant Ca composition. Iceland is permanently affected by a low-pressure cell, the Icelandic Low (Einarsson, 1984). As the atmospheric pressure modifies the cosmic-ray particle flux, and thus has an impact on the local cosmogenic nuclide production rate, the atmospheric pressure anomaly has to be taken into account when scaling the SLHL production rates to the study site. Only Licciardi et al.’s (2008) production rate already accounts for this anomaly, as the calibration sites of study are located in south western Iceland (see also Licciardi et al., 2006).

On the other hand, Stone et al.’s (1996) and Schimmelpfennig et al.’s (2011) production rates were calibrated in Tabernacle Hill (Utah, western U.S.A.) and Etna volcano (Italy), respectively, hence they need to be corrected for the atmospheric pressure anomaly when applied in Iceland. Dunai (2010) advises including any long-term atmospheric pressure anomaly at least for Holocene exposure periods. Therefore, the local atmospheric pressure at the sample locations was applied in the scaling factor calculations when using the Stone et al. (1996) and Schimmelpfennig et al. (2011) production rates. Instead of the standard value of 1013.25 hPa at sea level, a sea level value of 1006.9 hPa (Akureyri meteorological station; Icelandic Meteorological Office, 2017) was used. The atmospheric pressure correction assumed a linear variation of temperature with altitude. The results presented and discussed below are based on the ^{36}Cl production rate for Ca spallation of Licciardi et al. (2008) as it is calibrated for Iceland and considers the atmospheric pressure anomaly.

The exposure ages presented throughout the text and figures include analytical and production rate errors unless stated otherwise. No erosion or snow cover correction has been implemented. Our <2000 yr CRE ages have also been rounded to the nearest decade, and then converted to CE dates through their substraction from the year 2015 (i.e. fieldwork and sampling campaign). In order to achieve robust comparisons of our results with those obtained by radiocarbon or tephrochronology, we have calibrated the ^{14}C ages previously published in the literature through the OxCal 4.3 online calculator (https://c14.arch.ox.ac.uk/oxcal/OxCal.html) implementing the IntCal13 calibration curve (Reimer et al., 2013).

3.2.8. Mobility analysis of the boulders in active rock glaciers and debris-covered glaciers.

To determine the degree of stability of the boulders sampled for CRE dating, we followed the method previously proposed by Tanarro et al. (2019). We applied digital photogrammetry to historical aerial photographs to determine the horizontal movement and elevation changes of sampled boulders from debris-covered glaciers and rock glaciers. Aiming to know the movement uncertainty, moraine boulders (i.e. considered stable and immobile) have been surveyed in X, Y and Z values.

We used photo stereo pairs from 1980 and 1994, scanned at a high resolution (20 and 15 microns respectively), which were the only flights available of sufficient resolution quality to identify the same boulders in both years. A digital photogrammetry station was used to correct the geometric deformation and absolute orientation of the photograms and to create stereoscopic models for both dates. Our results show a mean square error in x, y, z (RMSExyz) of less than 0.32 m. The photograms covering the area of the Fremri-Grjótárdalur and Hóladalsjökull cirques present a lower error (RMSExyz 0.15-0.25 m) than those covering the Hofsjökull cirque (RMSExyz 0.17-0.32 m). With the stereoscopic models from both dates, we carried out 3D photogrammetric restitution of a set of boulders identified on the surface of the sampled landforms. Some of these boulders were the same boulders as those sampled for CRE dating and others were very close to them in the same geomorphological unit.

3.3. Discussion and evaluation of the techniques applied to study the glacier-climate evolution.

The validity of the results obtained and of the methodological proposal is supported by a correct evaluation of the techniques applied, which is developed and contextualized in

the aspects of geometric variations (area and position of the front), volume estimates, reconstruction of palaeoglaciers, calculation of ELAs and application of glacier-climate models, within the framework of previous studies with similar methodologies.

3.3.1. Variations in the glacier geometry: area and position of the front.

Photointerpretation of geomorphological features (frontal and lateral moraines, ground color changes in the foreland) allowed us to clearly reconstruct the geometry of the glaciers under study during the LIA maximum, as previously demonstrated in Iceland (Bradwell et al., 2006; Hannesdóttir et al., 2015a) and in other areas (e.g. Colucci and Žebre, 2016), which, in addition, even makes it possible to reconstruct year-by-year front positions from complete sequences of annual moraines (Bradwell, 2004b, Chandler et al., 2016b). The study of the glacial evolution since 1946, based on the manual delineation of glacial outlines from visual inspection of aerial photographs and satellite images, can be considered a valid procedure endorsed in the literature by satisfactory results with debris-free glaciers (e.g. Bradwell et al., 2006, 2013; Koblet et al., 2010; Thompson et al., 2011) as well as debris-covered glaciers (e.g. D'Agata and Zanutta, 2007; Diolaiuti et al., 2009), although it must be noted that the highest levels of precision of these studies were achieved by photogrammetric restitution. Remote sensing –in some cases aided by the application of band ratios or thresholding of ratio images– also provided good results in studies of changes in glacier areas and lengths (e.g. Bahuguna et al., 2007; Kaldybayev et al., 2016; Qureshi et al., 2017).

In this study, measurements of front position changes and calculations of retreat/advance ratios were carried out on the flow line. With a slight modification, Koblet et al. (2010) measured the length of the tongues considering the average length of the main line (flow line) and other parallel and equidistant additional lines. Changes in the position of the fronts were also analysed in other studies by crest-to-crest measurements along transects over an annual moraine sequence (Bradwell et al., 2013; Chandler et al., 2016b). Although a good statistical correlation between retreat/advance ratios and summer temperature has been found in the literature (e.g. Kirkbride, 2002; Bradwell, 2004b), it should be noted that variations of the front are not in themselves an indicator of climate change, since they depend not only on mass balance but also on ice speed as it flows from the accumulation zone to the ablation zone (Gabbud et al., 2016). This issue justifies the need to seek other complementary indicators.

3.3.2. Volume calculation.

The area-volume scaling approach (Bahr et al., 1997, 2015) used in this study is also widely accepted when estimating glacier volumes at the present time (e.g. Hughes, 2009b), studying their evolution over time (e.g. Chen and Ohmura, 1990; Colucci and Žebre, 2016) and modelling glacier volume projections in their response to climate change (e.g. Van de Wal and Wild, 2001; Radić et al., 2007; Möller and Schneider, 2010; Adhikari and Marshall, 2012). Some modifications of the implementation of the method derive from different area-volume scaling relationships: for instance, Hughes (2008, 2009b) chose the empirical area-volume relationship of Chen and Ohmura (1990) based on 63 mountain glaciers (γ = 1.357), while we use the theoretical γ = 1.375. Our application of AVS without any adjustment of γ = 1.375 can be taken as valid according to Bahr et al. (2015) because adjustments to this recommended value are possible but improbable, given that width, mass balance and AAR closures lead to the same result. In any case, the theoretical and the empirically derived values of γ are very close each other.

Even though this method has been applied to individual glaciers (e.g. Hughes, 2009b), it should be noted that maximum reliability of the calculations is obtained when applied to a large number of glaciers of different sizes and types. So when AVS is applied individually to a glacier without establishing its c it entails considerable uncertainty – up to 34% if the mean value of c = 0.034 $km^{3-2\gamma}$ (Bahr, 1997) is used (Bahr et al., 2015). Moreover, it should be borne in mind that the volume of a non-steady-state glacier is 20% smaller than the one calculated from the AVS (Van de Wal and Wild, 2001). Because of these limitations, we should treat our results with care, since no other measurements that are more accurate exist for the glaciers studied.

3.3.3. Palaeoglacier reconstruction.

The manual reconstruction of glacier topography ("hand-drawn" contours) from geomorphological evidence (or the geometry of the front visible in aerial photographs) tested in the glaciers under study can be considered a valid alternative compared with numerical physical-based models (e.g. Schilling and Hollin, 1981; Benn and Hulton, 2010; Pellitero et al., 2016) when there are no other DEMs of the surface of the glaciers, because it approximates the probable three-dimensional shape (Carr and Coleman, 2007). Many examples of its successful application existing in the literature (e.g. Sissons, 1974; Sutherland, 1984; Ballantyne, 1989; Dahl and Nesje, 1992). Dahl and Nesje (1992) stated that the error resulting from the reconstruction of the contour lines is randomly distributed

over the surface of the glacier, and considered that it does not introduce large deviations with regard to representative conditions.

3.3.4. Equilibrium-Line Altitude calculation and application of glacier-climate models.

Like in this study, ELA has been successfully used in other areas of study as an indicator of climate change (e.g. Dahl and Nesje, 1992; Styllas et al., 2016; Sagredo et al., 2017). In some occasions, however, the snowline obtained by visual inspection of satellite images (e.g. Rabatel et al., 2012; Veettil et al., 2017 and references therein) has likewise been used. Using an AAR of 0.67 based on previous experiments (Caseldine and Stötter, 1993) can be considered appropriate due to its proximity and partial overlap with the 0.64±0.04 ratio proposed by Kern and László (2010) for small glaciers over 4 km^2, as is the case of those under study. Our calculated ELAs can be considered reliable indicators of climate change due to the consistency between their fluctuations and the climate variability observed in the period analysed. The innovative testing of the AABR method in Tröllaskagi in this study with a ratio of 1.5±0.4 seems to confirm the validity of the ELAs obtained via the AAR method.

In other studies, ELAs have been inferred from meteorological records (Lie et al., 2003); this enables the estimation of the current ELA in non-glaciated areas, as well as an assessment of the connection between glaciers and climate variability (e.g. Styllas et al., 2016 in Mount Olympus, Greece). In other studies, analysis of the ELA spatial pattern (e.g. Caseldine and Stötter, 1993) and its gradient have helped to infer precipitation gradients (e.g. Chandler and Lukas, 2017 and references therein), the influence of the relief on past climates (Santos-González et al., 2013) and even past atmospheric circulation patterns and weather types (e.g. Ballantyne, 1989).

The study of climate evolution based on glacier-climate models that relate temperature and precipitation (accumulation) at the ELA can be considered a valid technique when analysing the impact of climate change, as it makes it possible to know the climatic conditions that promote or hinder glacier survival. In the literature there are numerous examples of the successful application of this type of method. Ballantyne (1989), Dahl and Nesje (1992), Caseldine and Stötter (1993) approached palaeoclimate reconstructions in Scotland, Western Norway and Tröllaskagi (Northern Iceland) respectively with the glacier-climate model designed for Norwegian maritime glaciers, which made it possible to estimate vertical precipitation gradients as well as to infer changes in atmospheric circulation. Likewise, one can find examples of applications of Ohmura et al. (1992) model in palaeoclimate reconstructions in Wales (Hughes, 2009a), in the Pindus Mountains of Greece (Hughes et al., 2006), in South Africa (Mills et al., 2012) and in the

Cantabrian Mountains of northern Spain (Pellitero, 2013; Rodríguez-Rodríguez et al., 2016). Carr et al. (2010) suggested the possibility of eliminating summer precipitation from the Ohmura et al. (1992) model, which facilitates comparison of the results obtained from the latter two methods as regards winter accumulation.

The understanding of topographic conditions that favor snow accumulation and glacier survival has improved by mapping potential avalanche/snowblow areas and calculating the so-called snowblow and avalanche ratios (e.g. Sissons and Sutherland, 1976; Sutherland, 1984; Hughes, 2008, 2009b; Mills et al., 2012; Chandler and Lukas, 2017). With this approach it is particularly useful to estimate the proportion of accumulation resulting from avalanches or redistribution by wind. Finally, simplified versions of the degree-day model such as the one used in the present study with an average *ddf* of 4.1±1.5 mm day^{-1} $ºC^{-1}$ have also been successfully applied, both in palaeoclimate reconstruction and in estimates of the accumulation needed in glaciers to make up for ablation (e.g. Hughes, 2008, 2009b; Hughes and Braithwaite, 2008; Hughes, et al., 2010). On the other hand, Brugger (2006) improved the estimates of the degree-day model applied to palaeoclimate reconstruction in the Sawatch Range (Colorado, United States) by simulating the evolution of snowfall throughout the year, alternately using different *ddf* for ice (8.0±1.0 mm day^{-1} $ºC^{-1}$) and snow (4.0±1.0 mm day^{-1} $ºC^{-1}$) depending on whether the melt rate modelled by the degree-day model exceeds snow accumulation. When comparing the results derived from the Ohmura et al. (1992) and degree-day models, it should be noted that their discrepancy depends on summer temperatures and the annual temperature range, which influence the amount of liquid or solid precipitation (Hughes, 2009a).

Chapter 4.

Recent evolution of Tröllaskagi debris-free glaciers from the Little Ice Age. Climate evolution and paleoclimate reconstruction.

4.1. Introduction.

The variations in summer temperature (Mean Ablation Season Air Temperature, T_s) and winter accumulation exert a particularly decisive influence on the dynamics of the debris-free glaciers (Eythórsson, 1935; Liestøl, 1967; Ohmura et al., 1992). For example, Caseldine (1985a) pointed out that the combined effect of a low T_s and normal winter precipitation led to a glacier advance over a 10-year period in Tröllaskagi peninsula. The debris-free glaciers are especially sensitive to climate variations and were extensively studied until the late 1980s (Caseldine and Cullingford, 1981; Caseldine, 1983, 1985a, 1985b, 1987; Caseldine and Stötter, 1993).

For many of the glaciers in the central highlands of Iceland and for the majority of those in the Tröllaskagi peninsula, the maximum glacial advance in the second half of the Holocene was reached during the Little Ice Age (LIA) (Kirkbride and Dugmore, 2001a, 2006; Schomacker et al., 2003; Flowers et al. 2007; Larsen et al., 2011).

The Holocene temperature variation range is thought to be around 3 ºC (Stötter et al., 1999): MAAT during the Holocene Thermal Maximum (HTM) is estimated to be 3 ºC higher than that for the period 1961-1990 (Caseldine et al., 2006; Geirsdóttir et al., 2009), and therefore comparable to the warmest decades of the 20th century (Stötter et al., 1999), while conditions during the post-Preboreal Holocene minimum were similar to those during the second half of the 19th century (Stötter et al., 1999). Precipitation is estimated to have doubled between both climatic extremes (Stötter et al., 1999). Caseldine and Stötter (1993) suggest that from the LIA maximum in the late 19th century to the 1980s the T_s increased by 2 ºC and winter precipitation by 600 mm (+41%, from 1450 mm) at the ELA. Climate

evolution during the last millennium, and its relationship to sea ice expansion, is relatively well known from the work of Koch (1945), Bergþórsson (1969), Ogilvie (1984, 1996, 2005, 2010), and Ogilvie and Jónsson (2001). Especially cold climatic episodes at the beginning and end of the 13th century, in much of the second half of the 14th century (1350-1380) and during the later years of the 16th century have been reported by Ogilvie (1984, 1991) and Ogilvie and Jónsson (2001). Koch (1945) suggested that between 1600 and 1900 CE the climate was particularly cold in Iceland and East Greenland, but Ogilvie (1984, 2005, 2010) pointed out that there was great variability with some mild periods and different levels of incidence of the sea-ice: a more temperate climate occurred during the 1640s, 1650s and early 18th century, while very cold climatic episodes in the late 17th century (1690s), mid-18th century (1740s in the north and 1750s in the south) and during the 19th century (1810s, 1830s and 1880s) (Ogilvie and Jónsdóttir, 2000; Ogilvie and Jónsson, 2001; Ogilvie, 2010), coinciding with the maximum sea ice extent. This is in contrast to the 20th century, which was more temperate than the three preceding centuries (Ogilvie, 1984, 1996, 2010; Ogilvie and Jónsson, 2001).

The limits and definition of the LIA are complex issues as they vary between authors, probably because of the differences in regions and the approaches applied (Grove, 2001). The origins and uses of the term "Little Ice Age" are discussed in detail in Ogilvie and Jónsson (2001). Grove (1988) considered it to have begun earlier, and extended from 1450 to 1900. However, it is suggested this period should be expanded, as much evidence has demonstrated that the LIA was under way in the early 14th century along North Atlantic regions as synthesized by Grove (2001), e.g. glacial activity found in Iceland during the 13th and 14th centuries. Nevertheless, the period from 1600 to 1900 must have been more important for the glacial activity in Iceland as it was not interrupted by major warming (Guðmundsson, 1997), except a mild period around 1640 to 1680 (Ogilvie, 2005, 2010). We define the LIA here according to Grove (2001), as the most recent period when glaciers extended globally and remained enlarged, between the Medieval period and the warming beginning in the early 20th century (Grove, 1988).

The Gljúfurárjökull and Western Tungnahryggsjökull glaciers reached their maximum extent during the LIA, more precisely during the second half of the 19th century (Caseldine and Cullingford, 1981; Caseldine, 1983, 1985a), coinciding with the Holocene maximum advance of many Icelandic ice-cap outlet glaciers (Kirkbride and Dugmore, 2008; Geirsdóttir et al., 2009). Nevertheless, the maxima of Gljúfárjökull and Tungnahryggsjökull were not synchronous: Gljúfurárjökull reached maximum extent around 1898-1903 CE, while the Western Tungnahryggsjökull reached its maximum in 1868 CE (Caseldine and Cullingford, 1981; Caseldine, 1983, 1985a). Thus, the LIA climate of the Tröllaskagi peninsula was

characterized by a T_s 2 ºC lower than at present and an average winter precipitation of 1450 mm at the Equilibrium-Line Altitude (ELA) (946 m) (Caseldine and Stötter, 1993).

Rising temperatures from the end of the 19th century caused the glaciers to retreat from their LIA positions. The retreat of the Western Tungnahryggsjökull (Caseldine, 1985a) started decades earlier than in Gljúfurárdalur, because of the steeper gradient of the Vesturdalur valley and the reduced thickness of the glacier. The retreat throughout the 19th century was interrupted by different advance phases with moraine formation: 1876-1878, 1882-1887 and 1898-1903 (Caseldine, 1985a).

Gljúfurárjökull retreated 250 m from its LIA position during the first twenty years of the 20th century (Caseldine, 1983, 1987). This retreat was interrupted with moraine formation in 1910 and 1913-1917, and later slowed down between the mid-1920s and 1930. During the early 1930s, the retreat accelerated again (ca. 200 m), and was interrupted by minor advances which enabled moraine deposition around 1935. Once again, in the late 1940s there was a short re-advance, concluding in 1950-1951 (Caseldine, 1983), which left a series of moraine arcs. Marginal measurements of the Icelandic Glaciological Society (IGS) show that Gljúfurárjökull continued to retreat 422 m until it reached its minimum extent in the mid-1970s. Glacial retreat data since the LIA obtained by Caseldine and Cullingford (1981) using photogrammetry and lichenometry show that the terminus retreated 265 m between 1939 and 1972, and 151 m between 1953 and 1960. After reaching its minimum extension, the trend reversed in 1977. The glacier commenced a new, more continuous re-advance of greater scope than the advances which had occurred during deglaciation: the snout advanced 50 m in 1977-1979, slowing in the following years to 30 m from 1979-1981 and 25 m from 1981-1983 (Caseldine and Cullingford, 1981; Caseldine, 1983, 1985a, 1985b, 1988).

The snout of Gljúfurárjökull was located at altitude 580 m with an ELA ca. 960 m in 1985 (Caseldine, 1985a). The ELA for 48 glaciers in Tröllaskagi was higher, at 992 m (Caseldine and Stötter, 1993). The last publication about Gljúfurárjökull in the late 1980s (Caseldine, 1988) pointed out the end of its advance in 1986. On the other hand, the annual IGS marginal measurements show that the Gljúfurárjökull advance ended in the late 1980s; after that, it began to retreat again, by more than 160 m between 1989 and 2013.

The relationship between the climate and glacier response (glacier termini, mass balance) was first studied in Iceland by Björnsson (1971), who proposed 8 ºC (at Akureyri) as the T_s threshold which would reflect the change in the mass balance sign in the Tröllaskagi glaciers. The temperature evolution in Iceland was studied by Einarsson (1991), who differentiated 6 thermal phases between 1901 and 1990, depending on whether these

were cold (1901-1925, 1947-1952 and 1965-1971) or warm (1926-1946, 1953-1964 and 1972-1990).

The study of the above debris-free glaciers in Tröllaskagi enabled the impact of climate change in northern Iceland to be monitored for decades and compared with the evolution of the large ice-caps in central and southern Iceland. The aim of this chapter is to extend the previous work and record the evolution of the Gljúfurárjökull and Tungnahryggsjökull glaciers (Fig. 4.1) up to the present, focusing on termini retreat, area/volume loss and ELA variation in these glaciers. In addition, the trends and relationships of these parameters with climate evolution will be analysed.

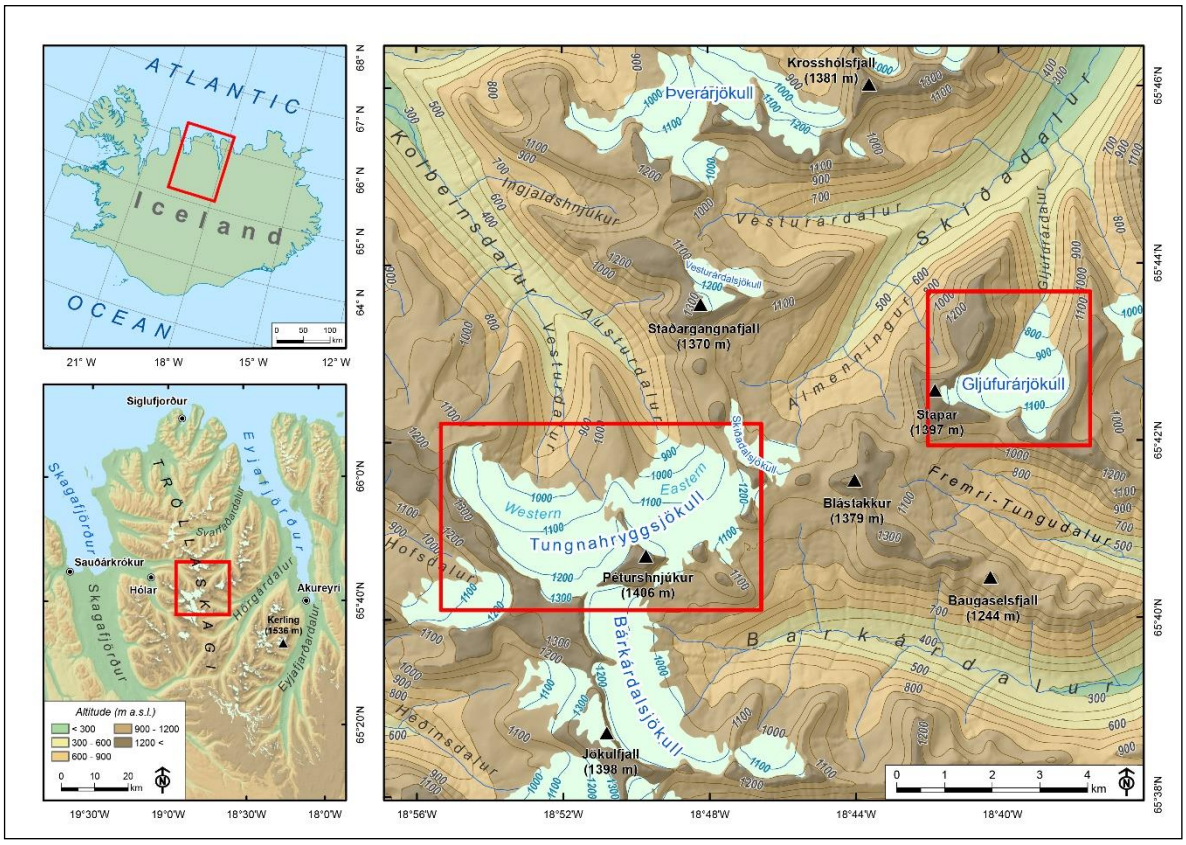

Figure 4.1. Location of the study area in the interior of the Tröllaskagi peninsula.

4.2. Results.

4.2.1. Evolution of the glacier snouts.

Studies of aerial photographs and satellite images show that the glacier snouts have retreated by more than 1300 m on average since the LIA maximum (considered to be CE 1898 in Gljúfurárjökull, and 1868 CE in both Western and Eastern Tungnahryggsjökull as explained in the publications presented in the Introduction) (Fig. 4.2), with an altitudinal rise of more than 100 m. The retreat accelerated rapidly (15.3 m yr^{-1}) during the first half of the

20th century (Fig. 4.2). In the second half of the 20th century the retreat decelerated considerably, reflected in the lowest values around 1985 (5.2 m yr^{-1}) and a trend shift in 1994, with an advance observed in Gljúfurárjökull. The trend then altered again and Gljúfurárjökull retreated in the years 1994-2005.

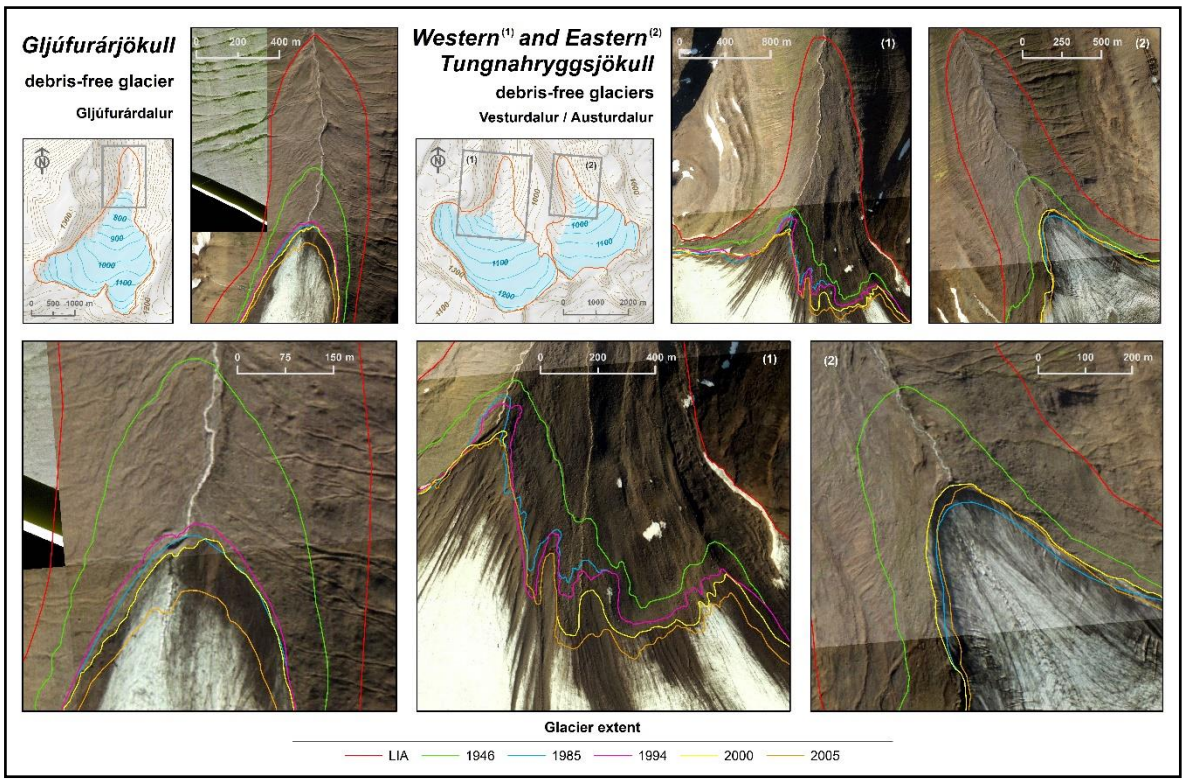

Figure 4.2. Evolution of the glacier snouts. The greatest retreat took place between the LIA maximum and 1946, and was especially significant in the Tungnahryggsjökull. LIA refers to the LIA maximum.

During the period 1898-1946, the snout of Gljúfurárjökull retreated 635 m, almost two-thirds of the total distance from the LIA maximum (1898-1903) to 2005 (Figs. 2 and 3), at an average rate of 13.2 m yr^{-1} (Table 4.1).

The rise of the snout during that period (46 m) was almost half of the total rise. By 1985 the retreat and ascent since 1898 was almost the total for the 1898-2005 period. However, the velocity of the retreat in 1946-1985 was lower than in 1898-1946. The 1994 aerial photograph reveals a change in this trend, with a snout position 20 m more advanced compared with 1985 (Fig. 2). Nevertheless, from 2000 onwards, there was a slow but continuous retreat.

The trend in Western Tungnahryggsjökull during the first half of the 20th century was a more rapid retreat, showing the highest average rates of the whole period (19.5 m yr^{-1}). By 1946 this glacier had retreated almost 90% of the total recorded between the LIA maximum (1868) and 2005 (Table 4.1).

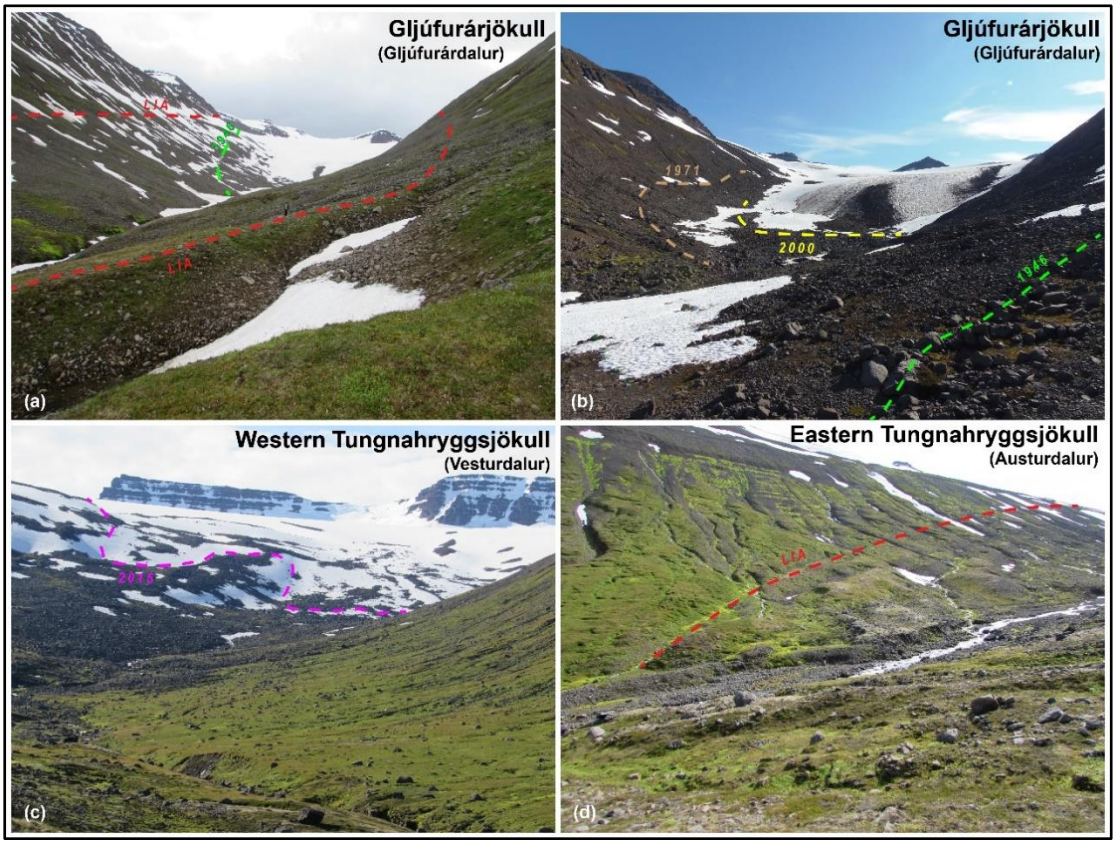

Figure 4.3. Snout and moraine positions from field observations. The Gljúfurárjökull (A, B) and Eastern Tungnahryggsjökull (D) LIA moraines are easily recognised from their sharp-crested shape. The debris cover on the Western Tungnahryggsjökull (C) determines its complex snout evolution. LIA refers to the LIA maximum.

Distance from the LIA maximum position (m)							
Glaciers	*LIA*	*1946*	*1985*	*1994*	*2000*	*2005*	*Total retreat*
Gljúfurárjökull	-	635	910	890	916	993	*993*
Tungnahr. (W)	-	1524	1584	1610	1703	1735	*1735*
Tungnahr. (E)	-	1027	1298	-	1257	1274	*1274*
Average	-	*1062*	*1264*	-	*1292*	*1334*	*1334*
Advance/retreat rate (m yr^{-1})							
Glaciers	*LIA*	*LIA-1946*	*1946-1985*	*1985-1994*	*1994-2000*	*2000-2005*	*LIA-2005*
Gljúfurárjökull	-	-13.2	-7.1	**2.2**	-4.3	-15.4	*-9.3*
Tungnahr. (W)	-	-19.5	-1.5	-2.9	-15.5	-6.4	*-12.7*
Tungnahr. (E)	-	-13.2	-6.9	-	-	-3.4	*-9.3*
Average	-	*-15.3*	*-5.2*	-	-	*-8.4*	*-10.4*
Glacier snouts elevation (m a.s.l.)							
Glaciers	*LIA*	*1946*	*1985*	*1994*	*2000*	*2005*	*↑LIA-2005*
Gljúfurárjökull	512	558	594	591	593	622	*110*
Tungnahr. (W)	540	741	786	759	779	793	*253*
Tungnahr. (E)	597	679	718	-	705	711	*114*
Average	*550*	*659*	*699*	-	*692*	*709*	*159*

Table 4.1. Glacier advance/retreat and snout elevation shift from the LIA maximum. Values in red represent glacier advances. LIA refers to the LIA maximum.

In the 1946 photo this significant retreat of the ice reveals two large moraines in the centre of the deglaciated area. The snout retreat slowed down considerably during the second half of the century, especially in 1985 (1.5 m yr^{-1}). By this date, the aerial photo shows a complex terminus covered with debris, with an uneven retreat, from 60 m in the centre to 150-170 m on the margins, and a vertical rise of more than 200 m since 1946. The 1994 aerial photo shows a similar snout, although with an advance in the western sector of ≈40 m and a retreat in the eastern sector of ≈20 m (Fig. 4.2). In 2000 the snout, still covered with debris, retreated mainly in the centre. The glacier then continued to retreat, although more slowly than Gljúfurárjökull (6.4m yr^{-1}) preserving the debris-covered snout (Figs. 4.2 and 4.3).

Just as in the glaciers described above, the retreat of the Eastern Tungnahryggsjökull from its LIA position was more intense during the first half of the 20th century (Table 4.1) and in 1946 its snout was only 200 m from its current position. The snout then continued to retreat more slowly and by 1985 had already lost its most westerly tongue (Fig. 4.2), where the margin retreated more than 400 m. The 2000 aerial photo shows that an advance of at least 41 m had taken place since 1985. Nevertheless, between 2000 and 2005 the snout retreated 17 m, even more slowly than Western Tungnahryggsjökull.

4.2.2. Evolution of ice- area and volume of the glaciers.

During the LIA maximum, the total surface area of the three glaciers exceeded 18 km^2, with almost half corresponding to the Western Tungnahryggsjökull. From then until 2005, the glaciers lost a quarter of their surface area (Table 4.2), with almost 20% lost during the first half of the 20th century. In 1985 the loss rate was considerably reduced, and slight increases in the surface area of Gljúfurárjökull and Western Tungnahryggsjökull occurred in 1994 (Table 4.2; Fig. 4.2). Since 2000 the surface loss of the glaciers has not reached 2%.

A third of the LIA maximum ice volume had been lost by 2005. The greatest volume loss (25%) occurred between the LIA maximum and 1946. The most intense volume loss rate was in Western Tungnahryggsjökull, around 2.5 x $10^{-3}km^3$ yr^{-1} (Table 4.3; Fig. 4.4). During the second half of the 20th century the losses were lower, with maximum average 7.8% (Table 4.3), although in 1985 the Eastern Tungnahryggsjökull had lost around 15% compared to 1946. In 1994 the Gljúfurárjökull and Western Tungnahryggsjökull volumes increased. However, the reduction in volume continued from 2000 onwards; the loss rate intensified during 2000-2005 with values similar to or even higher than those of the first half of the 20th century.

Area (km²)							
Glaciers	*LIA*	*1946*	*1985*	*1994*	*2000*	*2005*	*↓LIA-2005*
Gljúfurárjökull	4.372	3.540	3.407	3.413	3.384	3.335	*1.038*
Tungnahr. (W)	8.735	6.939	6.689	6.700	6.604	6.512	*2.222*
Tungnahr. (E)	5.348	4.532	4.035	-	4.054	3.940	*1.408*
Total	*18.455*	*15.011*	*14.131*	-	*14.041*	*13.787*	*4.668*
Area gain/loss rate (km² yr⁻¹)							
Glaciers	*LIA*	*LIA-1946*	*1946-1985*	*1985-1994*	*1994-2000*	*2000-2005*	*↓LIA-2005*
Gljúfurárjökull	-	-0.017	-0.003	**0.001**	-0.005	-0.010	*-0.010*
Tungnahr. (W)	-	-0.023	-0.006	**0.001**	-0.016	-0.018	*-0.016*
Tungnahr. (E)	-	-0.010	-0.013	-	-	-0.023	*-0.010*
Area gain/loss (%)							
Glaciers	*LIA*	*LIA-1946*	*1946-1985*	*1985-1994*	*1994-2000*	*2000-2005*	*↓LIA-2005*
Gljúfurárjökull	-	-19.04	-3.75	**0.18**	-0.86	-1.46	-23.73
Tungnahr. (W)	-	-20.55	-3.61	**0.16**	-1.43	-1.39	-25.44
Tungnahr. (E)	-	-15.27	-10.96	-	-	-2.79	-26.33
Total	-	*-18.67*	*-5.86*	-	-	*-1.81*	*-25.29*

Table 4.2. Ice surface evolution from the LIA maximum in the Gljúfurárjökull and Tungnahryggsjökull glaciers. Values in red represent glacier advances. LIA refers to the LIA maximum.

Volume (km³)							
Glaciers	*LIA*	*1946*	*1985*	*1994*	*2000*	*2005*	*↓LIA-2005*
Gljúfurárjökull	0.278	0.208	0.197	0.198	0.195	0.191	0.086
Tungnahr. (W)	0.720	0.524	0.498	0.500	0.490	0.481	0.239
Tungnahr. (E)	0.367	0.292	0.249	-	0.250	0.241	0.126
Total	*1.364*	*1.024*	*0.944*	-	*0.936*	*0.913*	*0.451*
Volume gain/loss rate (10⁻³ km3 y⁻¹)							
Glaciers	*LIA*	*LIA-1946*	*1946-1985*	*1985-1994*	*1994-2000*	*2000-2005*	*↓LIA-2005*
Gljúfurárjökull	-	-1.459	-0.273	**0.055**	-0.387	-0.781	*-0.808*
Tungnahr. (W)	-	-2.502	-0.663	**0.125**	-1.632	-1.863	*-1.744*
Tungnahr. (E)	-	-0.958	-1.104	-	-	-1.912	*-0.918*
Volume gain/loss (%)							
Glaciers	*LIA*	*LIA-1946*	*1946-1985*	*1985-1994*	*1994-2000*	*2000-2005*	*↓LIA-2005*
Gljúfurárjökull	-	-25.21	-5.12	**0.25**	-1.17	-2.00	*-31.10*
Tungnahr. (W)	-	-27.12	-4.93	**0.23**	-1.96	-1.90	*-33.22*
Tungnahr. (E)	-	-20.38	-14.76	-	-	-3.82	*-34.30*
Total	-	*-24.92*	*-7.77*	-	-	*-2.43*	*-33.08*

Table 4.3. Ice volume evolution from the LIA maximum in the Gljúfurárjökull and Tungnahryggsjökull glaciers. Values in red represent glacier advances. LIA refers to the LIA maximum.

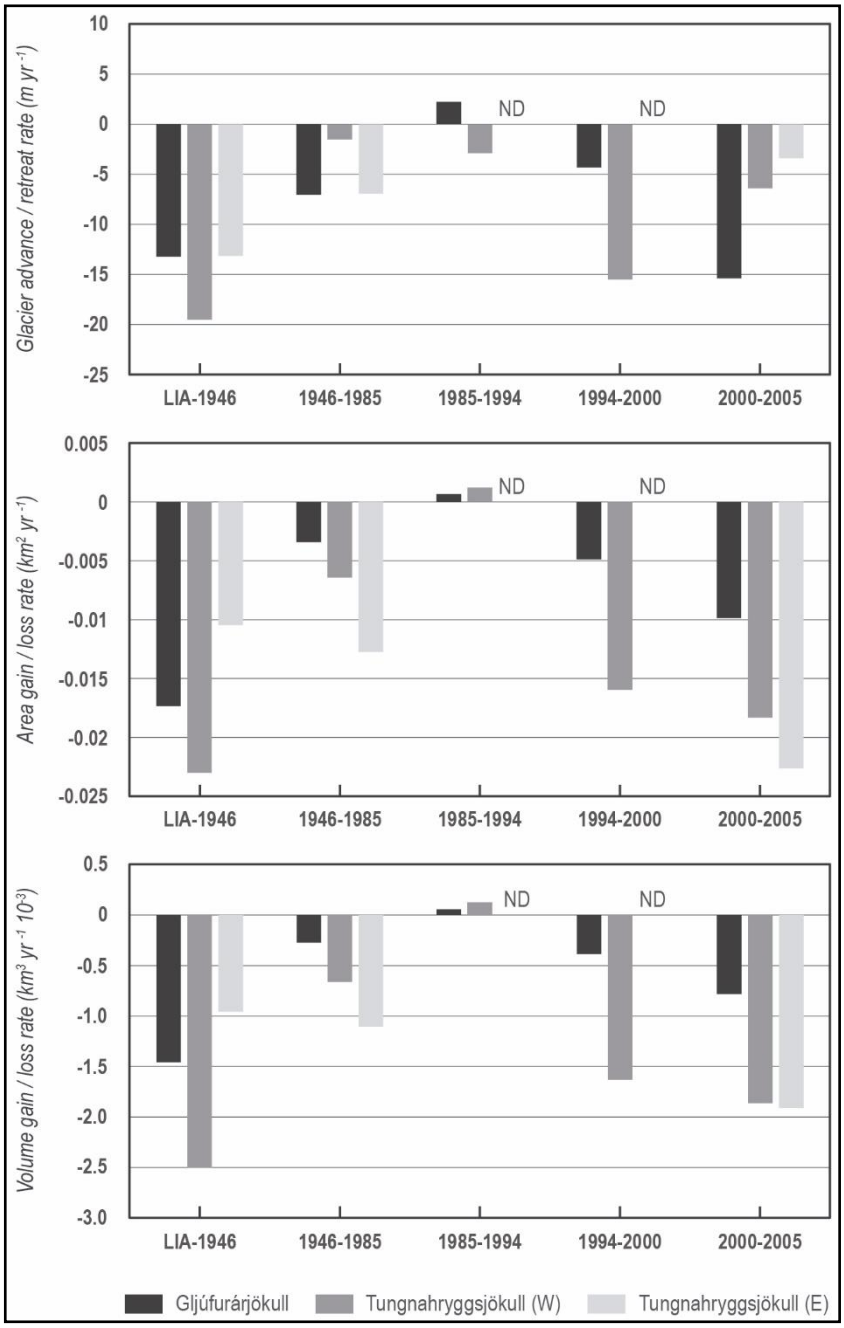

Figure 4.4. Evolution of retreat rates and area and volume loss during the different periods analysed. From 2000-2005 the rates are close to those recorded in the first half of the 20th century. LIA refers to the LIA maximum. ND refer to "no data".

4.2.3. Evolution of the Equilibrium-Line-Altitude.

Applying the AAR and AABR methods obtains a mean ELA of ≈1010 m during the LIA maximum and a rise of 40-50 m in the period analysed between LIA maximum and 2005 (Table 4.4). Using the AAR method, the greatest rise in the ELA (29 m) occurred between the LIA maximum and 1946, coinciding with the most important snout retreat and the greatest surface area and volume losses. From 1946 to 1985, there was a smaller rise (10 m), slightly more intense in Gljúfurárjökull and Western Tungnahryggsjökull. Although 1994

showed a trend shift advancing, the ELAs for the two glaciers remained stagnant. Since 2000 the ELA has remained practically stable around 1050 m Nevertheless a sharp intensification can be clearly seen in the ELA rise ratio in the last period 2000-2005, with a mean rate higher than in the period between the LIA maximum and 1946 (Table 4.4). The results obtained using the AABR method were reasonably close to those obtained using the AAR method, with maximum differences of ±10 m (Table 4.4).

ELA-AAR (0.67) *(m a.s.l.)*							
Glaciers	*LIA*	*1946*	*1985*	*1994*	*2000*	*2005*	*↑LIA-2005*
Gljúfurárjökull	954	974	985	982	984	988	*34*
Tungnahr. (W)	1046	1082	1092	1090	1091	1094	*48*
Tungnahr. (E)	1029	1061	1069	-	1071	1073	*44*
Average	*1010*	*1039*	*1049*	-	*1049*	*1052*	*42*
ELA-AAR rise rate (m yr^{-1})							
Glaciers	*LIA*	*LIA-1946*	*1946-1985*	*1985-1994*	*1994-2000*	*2000-2005*	*↑LIA-2005*
Gljúfurárjökull	-	0.42	0.28	-0.33	0.33	0.80	*0.32*
Tungnahr. (W)	-	0.46	0.26	-0.22	0.17	0.60	*0.35*
Tungnahr. (E)	-	0.38	0.21	-	-	0.40	*0.32*
Average	-	*0.42*	*0.25*	-	-	*0.60*	*0.33*
ELA-AABR (1.5±0.4) *(m a.s.l.)*							
Glaciers	*LIA*	*1946*	*1985*	*1994*	*2000*	*2005*	*↑LIA-2005*
Gljúfurárjökull	960±20	975±15	986±20	988±15	990±15	994 +15/-10	*34*
Tungnahr. (W)	1047 +20/-15	1093±10	1103±10	1101±10	1102 +10/-5	1105±10	*58*
Tungnahr. (E)	1020 +20/-15	1062±15	1075±10	-	1072 +15/-10	1079±10	*59*
Average	*1009±36*	*1043±50*	*1055±50*	-	*1055±47*	*1059±47*	*50*
ELA-AABR rise rate (m yr^{-1})							
Glaciers	*LIA*	*LIA-1946*	*1946-1985*	*1985-1994*	*1994-2000*	*2000-2005*	*↑LIA-2005*
Gljúfurárjökull	-	0.31	0.28	0.22	0.33	0.80	*0.32*
Tungnahr. (W)	-	0.59	0.26	-0.22	0.17	0.60	*0.42*
Tungnahr. (E)	-	0.54	0.33	-	-	1.40	*0.43*
Average	-	*0.48*	*0.29*	-	-	*0.93*	*0.39*

Table 4.4. ELAs and ELA changes over variable periods calculated by AAR and AABR methods for the Gljúfurárjökull and Tungnahryggsjökull glaciers. LIA refers to the LIA maximum.

4.2.4. Climate evolution.

The MAAT calculated for Akureyri (1882-2014) and Öxnadalsheiði (2000-2014) data series was 3.35 ºC and 0.97 ºC respectively. A lapse rate of 0.66 ºC 100 m^{-1} was obtained from the MAAT data series for the common period 2000-2014. Regression analysis of the two MAAT series for the period 2000-2014 showed strong correlation (r=0.79; n=15), which enabled a first approximation of the Öxnadalsheiði series reconstruction for the period 1882-2000. The least squares equation used was *y=0.9092x–3.0223* (r^2=0.63), with an overall

average (MAAT=0.02 ºC) only slightly different from the result obtained using extrapolation of the lapse rate (MAAT=-0.05 ºC).

Using the Akureyri temperature series and the 5-year running-means deviation compared with the overall series average, 9 homogeneous periods were identified (Fig. 4.5; Table 4.5).

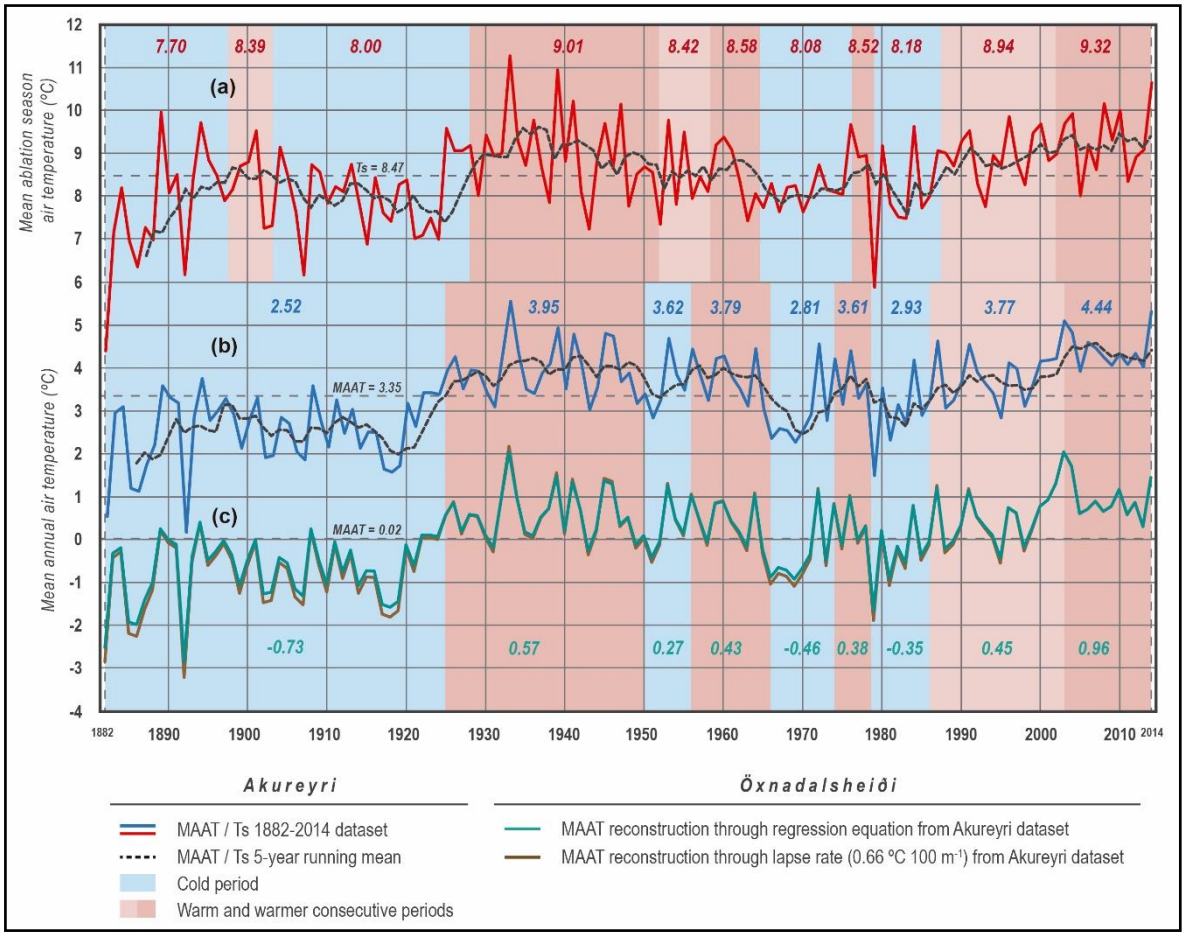

Figure 4.5. Evolution of Mean Annual Air Temperature (MAAT) (B) and Mean Ablation Season Air Temperature (T_s) at Akureyri (A), and MAAT reconstruction at Öxnadalsheiði (C). The coloured numbers in the middle of the periods are the mean value of MAAT/T_s for each period.

Thus, four cold periods with negative deviations (1882-1924; 1951-1955; 1966-1973 and 1979-1986) and five warm periods with positive deviations (1925-1950; 1956-1965; 1974-1978; 1987-1999 and 2000-2014). The MAAT was 2.5 ºC during the period 1882-1924, coinciding with the end of the LIA. This cold period ended in the early 1920s, with a sharp temperature rise and MAAT ≈4°C, maintained until the mid-1960s (Fig. 4.5). This warm period was interrupted by brief cooling, with MAAT ca. 3.6 °C, between 1950 and 1955. The temperature increase between the late LIA (1882-1924) and the period 1925-1950 was 1.4 ºC. However, the MAAT fell to 2.9 °C between 1966 and 1986, marking the first cold period with negative deviations since the end of the LIA, interrupted by higher

MAAT (3.6 °C) between 1974 and 1978. Finally, the climate trend shifted again to warmer conditions during the period 1987-2014. Two sub-periods were identified; during the first period (1987-2002) the MAAT was 3.8 ºC, while in 2003 an abrupt warming of 0.6 ºC occurred, marking the onset of the warmest period with an MAAT of 4.4 ºC from 2003-2014.

Period	Type	Akureyri				Öxnadalsheiði
		Air temperature (ºC)				
		Annual	Ablation season	Three-month summer	Annual range	Annual
1882-1924	Coldest	2.52	7.86	9.41	15.59	-0.73
1925-1950	Warm	3.95	9.05	10.38	14.80	0.57
1951-1955	Cold	3.62	8.60	9.96	14.71	0.27
1956-1965	Warm	3.79	8.38	9.52	14.56	0.43
1966-1973	Cold	2.81	8.12	9.47	15.44	-0.46
1974-1978	Warm	3.61	8.73	10.31	15.75	0.38
1979-1986	Cold	2.93	7.91	9.85	14.84	-0.35
1987-2002	Warm	3.77	8.95	10.27	14.71	0.45
2003-2014	Warmest	4.44	9.32	10.92	13.89	0.96

Table 4.5. Cold/warm periods at Akureyri and Öxnadalsheiði weather stations and seasonal values. Temperatures at Öxnadalsheiði prior to 2000 were reconstructed through the least squares equation obtained from the regression analysis between Akureyri and Öxnadalsheiði MAAT series for the common period 2000-2014.

The Akureyri climatological log shows that increases in the MAAT and T_s were 1.9 ºC and 1.5 ºC respectively between the LIA and the present (Table 4.5). The average temperature calculated from the reconstructed Öxnadalsheiði data series suggests that the MAAT was below freezing level above 500 m a.s.l. in the interior of the Tröllaskagi peninsula during the late LIA cold period, 1966-1973 and 1979-1986.

As regards precipitation, the mean annual value for the 1950-2014 period at Akureyri is 515 mm, while in the winter/accumulation season (October-April) it is 357 mm, i.e. 69% of the total. Running mean analysis (Fig. 4.6C) showed below average values from the late 1950s to the late 1960s (ca. 250 mm minima) and from the late 1970s to the early 1980s (ca. 200 mm minima in 1980). From the mid-1980s onwards, winter precipitation has been above the average, reaching maxima in the early 1990s (ca. 430 mm). Since then, winter precipitation has been relatively regular and close to average, although an increasing trend started in the mid-2000s. Individual values peaked in 1989 and 2014, at over 550 mm.

The temperatures (mean annual, May-Sep, Jun-Jul-Aug) of the above logs, averaged for the phases identified, and later extrapolated to the successive ELAs through the lapse rate of 0.66 ºC 100 m^{-1} (Table 4.6), were input into the glacio-climatic models (Ballantyne, 1989; Ohmura et al., 1992; Braithwaite, 2008). The Ballantyne (1989) model predicted

winter precipitation of 2159 mm at the 2005 mean ELA which supposes an increase of 19% 100 m^{-1} during the winter season if the Akureyri mean winter precipitation over the 30-year period 1976-2005 (357 mm) is taken into account. This result suggests an increase of ca. 50% (714 mm) in the winter precipitation compared with around 1445 mm during the late LIA (1882-1924). The results indicate that when the T_s increased by 1.2 °C since the LIA, the winter precipitation increased by 714 mm at the ELA.

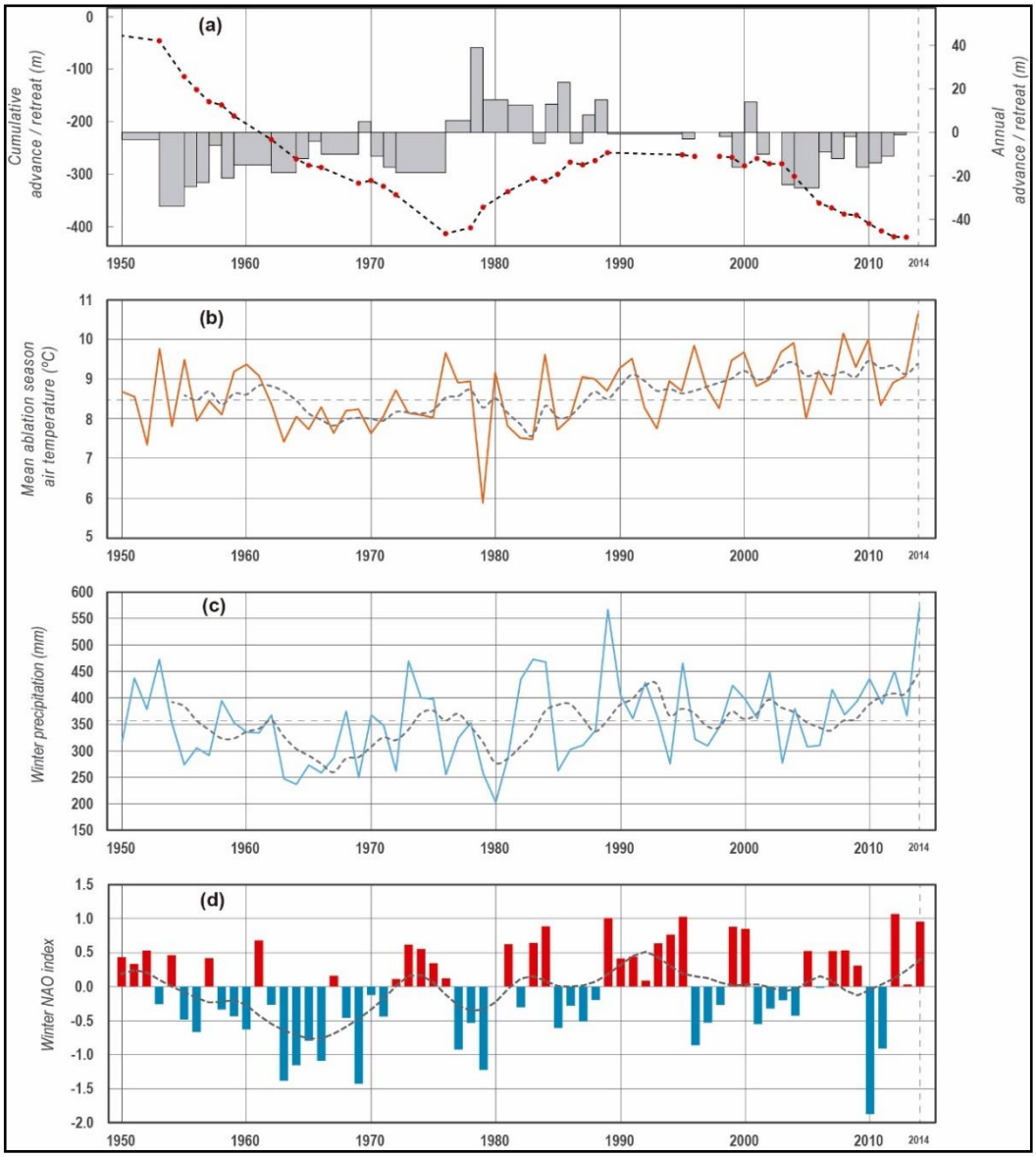

Figure 4.6. Relationship between the variations of Gljúfurárjökull snout (taken from the Icelandic Glaciological Society) (A), ablation season temperature (B) and winter precipitation (C) at Akureyri, and winter NAO index (D) since 1950. Black dotted-lines show 5-year running mean (temperature and precipitation) and LOESS-regression in the NAO index (modified from Cropper et al. (2015)). Red points in panel (A) are the years with marginal measurements. There is a clear relationship between the 1980s advance and the previous cooling of the T_s). The winter precipitation evolution shows a curve parallel to that of the NAO index (high winter precipitation, positive NAO index phase), suggesting a connection between the NAO mode and the precipitation, especially in the early 1980s and 1990s.

Period	LIA	1946	1985	1994	2000	2005	↑LIA-2005
	Mean air temperature (ºC)						
ablation season	1.35	2.35	1.13	-	2.18	2.53	1.18
three-month summer	2.90	3.67	3.08	-	3.50	4.13	1.23
mean annual	-4.00	-2.75	-3.84	-	-3.00	-2.35	1.65
	Precipitation (mm water equivalent)						
winter (model 1)	1445	2029	1344	-	1913	2159	714
annual (model 2)	1578	1854	1641	-	1791	2022	444
annual (model 3)	1223	1713	1148	-	1552	1741	518

Table 4.6. Temperature and precipitation at the ELA calculated for each year: comparison between different models: 1 (Ballantyne, 1989); 2 (Ohmura et al., 1992); 3 (Braithwaite, 2008). All models agree on a wetter climate at the present day than during the LIA maximum.

In turn, the Ohmura et al. (1992) model, with an estimated annual precipitation of 2022 mm at the 2005 mean ELA, suggests a smaller increase compared with the late LIA (1578 mm) of around 28% (444 mm). If the estimated annual precipitation for 2005 is compared with that recorded in Akureyri in the period 1976-2005 (517 mm), the pluviometric gradient obtained is lower, with an increase of 14% 100 m^{-1}. Finally, the degree-day model (Braithwaite, 2008) obtained 1741 mm annual precipitation at the ELA in 2005 (Table 4.6), an increase of 518 mm (42%) since the LIA (1223 mm). Using the degree-day model, the vertical pluviometric gradient obtained was lower than with the other models, with 13% 100 m^{-1}. This model also estimated precipitation much more sensitive to temperature variations (Table 4.6). E.g. the degree-day model estimates a reduction of 565 mm in precipitation from 1946 to 1985, due to a drop of 1.1 ºC in the MAAT between these two dates.

Mean Annual Air Temperature (ºC)						
Glacier	*LIA*	*1946*	*1985*	*1994*	*2000*	*2005*
Gljúfurárjökull	-0.71	0.42	-0.83	0.02	0.01	0.49
Tungnahr. (W)	-0.89	-0.78	-2.10	-1.09	-1.22	-0.64
Tungnahr. (E)	-1.27	-0.38	-1.65	-	-0.73	-0.10
Average	*-0.96*	*-0.25*	*-1.53*	-	*-0.65*	*-0.08*

Table 4.7. Temperature and precipitation at the ELA calculated for each year: comparison between different models. All models agree on a wetter climate at the present day than during the LIA maximum.

From the LIA to the present day, MAAT and T_s at the ELA rose by 1.7 and 1.2 ºC respectively, while in Akureyri the rise was 1.9 and 1.5 ºC. These values are much higher than the temperature increase deduced from the rise of the ELA (0.3 ºC). For most of the dates the MAAT in the glacier snouts remained close to freezing level. In Tungnahryggsjökull the MAAT of the snouts were below freezing level at all the dates and fell below -1 and -2 ºC in the coldest periods of the LIA and 1985, respectively. In the

Gljúfurárjökull snout, apart from these cold periods, the MAAT were positive, around 0.5-0.6 ºC (Table 4.7).

4.3. Discussion.

4.3.1. Interpretation of the results

The results of this research show a gradual climate warming from the end of the LIA, as well as a regressive trend for the northern Iceland glaciers. This process was not uniform, with considerable temperature variations in this region (Einarsson, 1991) which led to important changes in the debris-free glaciers studied.

The most important retreat of the Tröllaskagi glaciers between LIA maximum and the present occurred during the first half of the 20th century. The study of the three glaciers presented here shows that most of the glacier snout retreat, area reduction and volume loss had already occurred by 1946; a similar trend was observed at southeast Vatnajökull outlet glaciers, whose volume loss before 1945 represented the half of the post-LIA total loss (Hannesdóttir et al., 2015b). This is reflected in the combination of the field measurements carried out by Caseldine (1983) and the IGS at Gljúfurárdalur. However, the figures are different (Table 4.8). Our remote measurements on the aerial photos show that Gljúfurárjökull retreated 635 m in the period 1898-1946. On the other hand, the retreat reported by Caseldine (1983) would be at least 450 m if the retreat from the LIA maximum to 1915-1917 (>250 m) and the retreat during the 1930s (200 m) are considered.

Period	**Snout variation measurements (m)**	
	Remote (GIS)	*Field (IGS)*
1898-1946	-635	-450[a]
1946-1985	-275	-322
1985-1994	20	39
1994-2000	-26	-25
2000-2005	-77	-63
Total	-993	-821

[a] inferred from Caseldine and Cullingford (1981).

Table 4.8. Temperature and precipitation at the ELA calculated for each year: comparison between different models. All models agree on a wetter climate at the present day than during the LIA maximum. Note: IGS measurements have been summarized for the periods analysed. The abbreviations GIS and IGS refer to Geographical Information System and the Icelandic Glaciological Society.

The key to this glacier response is found in four main factors: 1) the sharp 1.4 ºC rise of the MAAT and 1.2 ºC rise in the T_s (Akureyri) between the cold period at the end of the LIA (1882-1924) and the warm period 1925-1950 (Fig. 4.5). 2) Warm conditions with MAAT≈4 ºC and T_s=9 ºC were maintained between 1925 and 1950 (Böðvarsson, 1955). 3) The predominant south-westerly airflow after 1920 proposed by Kirkbride (2002), which kept summers warm and caused increased ablation. 4) Other later cold periods did not last longer than 10 years (Caseldine, 1985a). This sharp increase in temperature triggered an ELA rise of ≈30 m compared to the ELA during the LIA maximum. Increased winter precipitation from the LIA maximum (Table 4.6) did not appear to have a major impact on the termini variation at that moment, but probably in further advances (e.g. mid-1970s to mid-1980s, or early 1990s) by increasing the mass flux and reducing the termini retreat rate (Kirkbride, 2002). In this context, the Western Tungnahryggsjökull glacier seems to be the most sensitive to the increased temperature of the three glaciers, as it presents the highest values for retreat rates, area and volume losses, and the greatest ELA rise.

Stötter et al. (1999) indicate that the coldest period after the LIA was from the early 1960s to the mid-1970s, when temperatures fell to levels equivalent to the warmest recorded in the 19th century. This cooling is the reason given by Caseldine (1983, 1985a, 1985b, 1988) to explain the advance of the Gjúfurárjökull between the mid-1970s and the mid-1980s, which can be clearly seen in Fig. 4.6. This would suggest a time response to T_s cooling close to 10 years. The retreat from 1946 to 1985 calculated using IGS field measurements (322 m) appears to be overestimated if we consider our results of 275 m for the same period (Table 4.8). This discrepancy can be explained by technical issues such as the accuracy of the georeferencing (RMS error), the change of field measurement procedures (estimates; see Sigurðsson et al., 2007), and the vague and scarce (incomplete) data about termini variations prior to the 1950s provided by Caseldine and Cullingford (1981) and Caseldine (1983). So the GIS measurements over a photo with snow-free termini (taken at the end of the ablation season) and properly georeferenced can provide the best results, avoiding estimates when fieldwork is not possible.

In this chapter, two points are mentioned which may clarify the glacial evolution after the 1980s: 1) the 1994 aerial photo reveals a more advanced position of the Gljúfurárjökull compared to 1985; 2) between 1979 and 1986 another cold period is identified (with temperatures not as cold as in the previous one, but separated from it by a brief warm 4-year period), characterized especially by a fall in the T_s below 8.5 and even 8 ºC in the Akureyri station (Figs. 4.5 and 4.6B). This cold period between 1979 and 1986 seems to have been the continuation of the cooling which started in the early 1960s and the reason why Gljúfurárjökull continued to advance after 1985. However, by the year 1994 the

advance had ended, due to: 1) the low advance rate of Gljúfurárjökull inferred from the positions of the snout in 1985 and 1994 (2.2 m yr^{-1}) compared with the advance velocities occurring in previous years (Caseldine and Cullingford, 1981; Caseldine 1983, 1985a, 1988); 2) the time lag (8 years) from 1994 to the end of the cooling in 1986. These findings confirm the T_s value of 8-8.5 ºC at Akureyri proposed by Björnsson (1971) and by Caseldine (1985a) as the threshold for the trend shift in the glacial mass balance, and also suggest that less than 10 years with cold summers may be required for the glacier advance. However, the increase in winter precipitation (671 mm) obtained in this study at the Gljúfurárjökull ELA between 1985 and 1994, and that obtained in Akureyri also seem to explain the glacier advance during the 1990s when the T_s in Akureyri reached over 8.5 ºC. It is reasonable to assume that a greater increase in winter precipitation reduced the number of cold summers required for the glacier snout advance. Such a clear advance was not observed in 1994 in the Western Tungnahryggsjökull, due to the difficulty in identifying precisely the lateral margins of the glacier in snow-covered areas. However, different sectors of the snout advanced or retreated compared with 1985. The explanation may be found in the uneven debris cover and the insulating effect it exerted on the ice.

From the mid-1980s there was a gradual rise of the T_s (Caseldine, 1988), which triggered the retreat of the glaciers in 2000 from their position in 1994. A sharp temperature rise occurred around the year 2003, which intensified the reduction in glacial volume and the ELA rise at rates comparable to those in the first half of the 20th century. Nevertheless, the snout retreat did not accelerate dramatically. The retreat rate intensified in the period 2000-2005 compared to 1994-2000, but did not reach the rates recorded before 1946 (Table 4.1). The glacier evolution in recent years is characterized by continuous retreat, which can be explained by the high T_s above 9 ºC since 2003. According to Caseldine and Stötter (1993), the effect of the climate warming observed from the LIA to the mid-1980s was a 50 m ELA rise in the glaciers in northern Iceland. This value is similar to the 40-50 m ELA rise obtained in the present study for Gljúfurárjökull and Tungnahryggsjökull between the LIA maximum and 2005. The AAR (0.67) and AABR (1.5) methods applied in this research to calculate the ELAs obtained homogeneous results, suggesting a good adaptation of the application of AABR=1.5, representative of the Norwegian glaciers (Rea, 2009), to the debris-free glaciers of northern Iceland.

4.3.2. Climatic implications

According to Caseldine and Stötter (1993), although the ELA is the parameter which best expresses the relationship between glaciers and climate, the use of its rise or fall to estimate T_s variations may lead to significant underestimation in results. This has been

proved in this study, observing that if the maximum depression of the ELA (41 m) and the lapse rate of 0.66º C 100 m^{-1} are taken into consideration, the rise in the ELA would indicate a lower T_s increase, approximately 0.3 ºC, assuming the precipitation remained constant. However the T_s rise recorded in Akureyri (1.5 ºC) or the rise extrapolated at the ELA (1.2 ºC) between the LIA maximum and 2005 are considerably higher. This shows that as well as temperature, other factors may have been decisive in the glacial evolution, such as precipitation and wind (Caseldine and Stötter, 1993).

The model applied by Caseldine and Stötter (1993) and by Stötter et al. (1999) suggests that the precipitation in northern Iceland during the LIA was significantly lower than at the present day. Applying the same model in this present study shows a similar trend. The model designed for Norwegian glaciers (Ballantyne, 1989) predicted winter precipitation of 1445 mm at the mean ELA (at altitude 1010 m) during the LIA maximum, and an increase of more than 714 mm (twice the modern winter precipitation at Akureyri) from then to 2005. Caseldine and Stötter (1993) estimated practically identical precipitation at the ELA during the LIA (1450 mm) and an increase of around 600 mm until the mid-1980s for the Tröllaskagi glaciers. Dahl and Nesje (1992) using the same model calculated a relatively similar increase of 690 mm in Nordfjord (Western Norway) since the LIA, where the current climate is wetter and milder (Olden, 78 m a.s.l., T_s = 12.2 ºC, winter precipitation = 812 mm; see Dahl and Nesje, 1992) because of the influence of the North Atlantic Drift and the frequent frontal precipitation associated with the polar front position.

The maritime location of the Tröllaskagi glaciers and those (Norwegian) used to devise the Ballantyne (1989) model, and also the good adaptation of a Norwegian AABR for ELA calculation, may postulate this model as the most suitable of the three to infer temperature and precipitation changes in the Tröllaskagi glaciers. This model gives higher values of precipitation than the other models (e.g., Ohmura et al., 1992) at warmer dates (e.g., 1946, 2000 and 2005) due to the exponential nature of its formula. This determines that equal values of temperature as input will give higher output precipitation in the Norwegian model than the Ohmura et al. (1992) one. Only at the coldest dates (e.g., LIA maximum and 1985) were the results inverse with higher precipitation in the Ohmura et al. (1992) model, when the T_s was far below the mean three-month summer temperature.

The precipitation pattern observed here, lower during the LIA cold period and higher during the warm periods, fully coincides with the model proposed by Stötter et al. (1999) for northern Iceland. This is also coherent with a lower ocean surface temperature (Geirsdóttir et al., 2009) linked to the greater presence of Arctic sea ice (Ogilvie, 1984, 1996; Ogilvie and Jónsdóttir, 2000; Ogilvie and Jónsson, 2001) which weakened the convective

processes (Lehner et al., 2013). Nesje and Dahl (2003) and Holmes et al. (2016) link the precipitation changes to variations in the North Atlantic Oscillation (NAO) phase (Hurrell, 1995a) and in the position of the polar front. In this sense, the dates at which high precipitation was obtained in this research (e.g. 1946, 2005) would correspond to a positive NAO phase (Fig. 4.6D) which reinforced the zonal flow of the westerlies and the W-SW winds, coinciding with a northwards displacement of the low-pressure cells and the polar front (Jansen et al., 2016). This situation facilitated the predominance of warm wet sub-tropical masses responsible for warm wet winter weather in Iceland (Holmes et al., 2016).

On the contrary, the dates when the calculated precipitation was lowest (e.g. LIA, 1985) would have coincided with the negative NAO phases (Fig. 4.6D) in which Arctic air masses predominated as a result of the southward displacement of the polar front and prevailing N-NW winds (Holmes et al., 2016). This atmospheric configuration would favour cold dry summers (Jansen et al., 2016). Thus, it is reasonable to suppose that the variations in precipitation between the cold and warm periods may also be explained by conditions that either hindered or facilitated convection, respectively (Burn et al., 2016).

However, extra accumulation from snow-blowing should also be taken into account in the corrie glaciers studied. In a deeply incised cirque surrounded by a plateau the snow may deflate from the plateau and accumulate in the cirque, either by direct accumulation or avalanching from the cirque walls (Sissons and Sutherland, 1976; Sutherland, 1984; Dahl and Nesje, 1992). Although most Tröllaskagi glaciers are surrounded by sharp peaks, ridges and summits, they receive snow blown from far out on the plateau mountains. Caseldine and Stötter (1993) suggested that up to 35% of the total winter accumulation could be attributed to the processes explained above (Tangborn, 1980). Based on this relationship between accumulation and snow-blowing, previous authors (Dahl and Nesje, 1992; Caseldine and Stötter, 1993) proposed that changes in winter accumulation may also reflect changes in the direction of the prevailing wind.

According to this reasoning, the increase in precipitation between the LIA and 2005 could be explained by a current predominance of the wind from the plateau (with snow-blowing), coherent with the changes in atmospheric circulation explained above. However, the results from the wind data processing do not provide strong support for changes in wind directions based on differences of winter accumulation, at least in the present day, with NW-NE (36%) and SW-SE (35%) as the dominating wind directions above 10 m s^{-1} during winter (October-April) at Grimsey. Further research on wind and snowfall is required to shed light on this issue.

The NAO exerts control over mass balance by influencing temperature and precipitation anomalies (Marzeion and Nesje, 2012) and therefore, a link between NAO phases and termini variations has been suggested on the literature. Bradwell et al. (2006) found that Lambatungnajökull (north-eastern outlet of Vatnajökull, South Iceland) advanced during negative NAO phases, and linked this to positive mass balances. On the contrary, Nesje et al. (2000) linked negative mass balance with negative NAO indices. Nevertheless, such relationships are not so clear, at least in Gljúfurárjökull. The continuous retreat from 1950 until the late 1970s in Fig. 4.6A is mostly characterized by negative NAO indices, so it is reasonable to think that, at least for that period, there may have been a link between negative NAO index and negative mass balance. However, this relationship during the 1980s advance is less clear as it coincides with a negative NAO phase interrupted by 3 years with positive indices (1981, 1983, 1984). We found that this advance started in the mid-1970s, i.e. 20 years after the major reversal of the NAO-index mode (negative to positive) occurred in 1955 (see Fig. 4.6), in good agreement with the reaction times at the decadal scale reported by Kirkbride (2002) and the theoretical calculations of glacier response times for small mountain glaciers (Jóhannesson et al., 1989b). The glacier termini/winter-NAO relationship at this glacier is even fuzzier if we consider the advanced position in 1994 coinciding with positive indices (since 1989), and the retreat since the late 1990s over two positive and negative NAO phases. Further, fuller and more detailed research on the past and future behaviour of the glacier termini and mass balance is needed in order to determine the future behaviour of the glaciers and elucidate the relationship with the NAO.

This research has shown the high sensitivity of the debris-free Gljúfurárjökull and Tungnhryggsjökull glaciers to climatic fluctuations (Häberle, 1991; Kugelmann, 1991), especially to the T_s (Eythórsson, 1935; Liestøl, 1967; Ohmura et al., 1992). Consequently, they experienced an important retreat during the periods characterized by warm summers and advanced during the short periods with cold summers, even when the duration of these periods was shorter than the 10 years proposed by Caseldine (1985a).

4.4. Conclusions.

The debris-free Gljúfurárjökull and Tungnahryggsjökull are important indicators of climate change, as the absence of debris and reduced dimensions mean they are highly sensitive to climate fluctuations. As a result, the abrupt climatic transition of the early 20th century and the 25-year warm period 1925-1950 triggered the most important glacier retreat

and volume loss since the end of the LIA; meanwhile, cooling during the 1960s, 1970s and 1980s altered the trend, with glacier snout advances.

Calculating the ELAs for the Tröllaskagi glaciers using the AAR and AABR methods showed a good fit of the AABR=1.5 proposed for Norwegian glaciers. Analysis of the relationships between ELA evolution and climatic data also revealed that the glacier response depends not only on the T_s, but also on other factors such as precipitation. The models applied, especially the one obtained from Norwegian glaciers, show a precipitation increase of more than 700 mm since the LIA, compatible with an increase in the surface temperature of the North Atlantic and with a change in the direction of the prevailing wind, currently from the plateau. Nevertheless, the evolution of the glaciers in the last 10 years shows an uncertain trend because of the lack of updated data (except for Gljúfurárajökull), which may become clearer with further monitoring of the glaciers over the coming years. The relationship between glacier evolution and atmospheric circulation patterns remains unclear.

Chapter 5.

Late Holocene evolution of Tungnahryggsjökull debris-free glaciers. The impact of the Neoglaciation.

5.1. Introduction and problem statement.

The Tröllaskagi Peninsula (northern Iceland) hosts over 160 small alpine cirque glaciers (Björnsson, 1978; see synthesis in Andrés et al., 2016). Only a few of these small glaciers do not have supraglacial debris cover that allows them to react quickly to small climatic fluctuations (Caseldine, 1985a; Häberle, 1991; Kugelmann, 1991), compared to the reduced dynamism of the predominant rock glaciers and debris-covered glaciers (Martin et al., 1991; Andrés et al., 2016; Tanarro et al., 2019). As a result of their high sensitivity to climatic changes, the few debris-free glaciers in Tröllaskagi fluctuated repeatedly in the past, forming a large number of moraines in front of their termini (see Caseldine, 1983, 1985a, 1987; Kugelmann, 1991 amongst others). However, the relation between glacier fluctuations and the climate is complicated due to: (i) the well-known surging potential activity in Tröllaskagi (Brynjólfsson et al., 2012; Ingólfsson et al., 2016); (ii) the possibility of glaciers being debris-covered in the past, with the subsequent change of their climate sensitivity over time; (iii) the intense and dynamic slope geomorphological activity, paraglacial to a great extent (Jónsson, 1976; Whalley et al., 1983; Mercier et al., 2013; Cossart et al., 2014; Feuillet et al., 2014; Decaulne and Sæmundsson, 2006; Sæmundsson et al., 2018) that hides and erases the previous glacial features.

5.1.1. The limitations of lichenometric dating.

In Iceland, a great part of the research on glacial fluctuations during the late Holocene, LIA (Grove, 1988; 1250-1850 CE, see Solomina et al., 2016) and later stages has been approached through application of radiocarbon dating of organic material, analysing lake sediment varves (Larsen et al., 2011; Striberger et al., 2012), dead vegetation remnants

(Harning et al., 2018a) and threshold lake sediment records (Harning et al., 2016a; Schomacker et al., 2016). These provide high-resolution records of glacier variability. In Tröllaskagi, very few reliable dates exist at present, obtained from radiocarbon and tephrochronology (Häberle, 1991, 1994; Stötter, 1991; Stötter et al., 1999; Wastl and Stötter, 2005). They suggest that late Holocene glaciers were slightly more advanced than during the LIA maximum in Tröllaskagi. However, these techniques only provide minimum or maximum ages for Holocene glacier history in northern Iceland (Wastl and Stötter, 2005). In addition, at Tröllaskagi most of the moraines are at 600-1000 m a.s.l., where the applicability of tephrochronology is very limited (Caseldine, 1990) due to the great intensity of slope geomorphological processes.

In any case, most of the moraine datings of Tröllaskagi –especially those of the last millennium– comes from lichenometry (see synthesis in Decaulne, 2016). However, the ages derived from this technique tend to be younger if they are compared to those estimated from tephra layers (Kirkbride and Dugmore, 2001). Generally, there is disagreement about the validity of the results provided by lichenometry, due to the difficulty of the lichen species identification in the field, the complexity and reliability of the sampling and measurement strategies, the uncertainty estimates, the nature of the ages provided as relative, as well as the relative reliability at producing lichen growth curves of the different species, with an extreme dependence on local environmental factors (see Osborn et al., 2015).

In fact, these problems had already been detected in northern Iceland, where in spite of the time elapsed since the first applications of this technique (Jaksch, 1970, 1975, 1984; Gordon and Sharp, 1983; Maizels and Dugmore, 1985) and contrasting with its widespread use in the south and southeast of the island (Thompson and Jones, 1986; Evans et al., 1999; Russell et al., 2001; Kirkbride and Dugmore, 2001b; Bradwell, 2001, 2004a; Harris et al., 2004; Bradwell and Armstrong, 2006; Orwin et al., 2008; Chenet et al., 2010 and others), there are still very few established growth rates for the lichen group *Rhizocarpon geographicum* (Roca-Valiente et al., 2016) from Tröllaskagi (Caseldine, 1983; Häberle, 1991; Kugelmann, 1991; Caseldine and Stötter, 1993; see synthesis in Decaulne, 2016). In general, the growth curves from Tröllaskagi suffer from a few control points (i.e. surfaces of known age) for calibration. This leads to considerable underestimation when lichen thalli sizes are beyond the calibration growth curve (Caseldine, 1990; see e.g. Caseldine, 1985a; Caseldine and Stötter, 1993; Kugelmann, 1991). That is to say, the extrapolation does not account for the decreasing growth rate with increasing age (i.e. non-linear growth). Kugelmann's (1991) growth curve has the highest number of control points to date (19 in total). In addition, the colonization lag in Tröllaskagi is poorly defined, although 10-15 years have been assumed for the *Rhizocarpon geographicum* (Caseldine, 1983; Kugelmann,

1991). Other issues, such as the absence of large thalli (Maizels and Dugmore, 1985), lichen saturation (e.g. Wiles et al., 2010), and other environmental factors (Innes, 1985 and references included; Hamilton and Whalley, 1995a) contribute to appreciable age underestimations when dating surfaces using this approach. Snow is also a major environmental factor for lichenometry in Iceland due to its long residence time on the ground (Dietz et al., 2012) and the avalanching frequency –especially in Tröllaskagi–, whose effect restricts the growth rate of lichens, and even destroys them (Sancho et al., 2017). These problems considerably limit the quality (reliability) of the lichenometric dating range of utility for applying lichenometric dating in Iceland, where the oldest ages estimated so far are between 160 and 220 years (Maizels and Dugmore, 1985; Thompson and Jones, 1986; Evans et al., 1999), thus preventing the dating of glacial advances prior to the 18th century.

In spite of the high uncertainty of the lichenometric dating, many authors working in Tröllaskagi have treated their lichenometric results as absolute ages (see Caseldine, 1983, 1985a, 1987; Kugelmann, 1991; Häberle, 1991; Caseldine and Stötter, 1993, amongst others). In fact, previously considered dates of LIA maximum glacier culmination are restricted to the very late 18th and early 19th centuries (Caseldine, 1983, 1985a, 1987; Kugelmann, 1991; Caseldine and Stötter, 1993; Caseldine, 1991; Martin et al., 1991), very close to the applicability threshold of this method. Consequently, no evidence of previous advances during phases of the LIA that were more conducive to glacier expansion (probably colder; see e.g. Ogilvie, 1984, 1996; Ogilvie and Jónsdóttir, 2000; Ogilvie and Jónsson, 2001) has been found (Kirkbride and Dugmore, 2001b).

5.1.2. The need of alternative and complementary techniques.

In the recent years, dating methods based on the Exposure to the Cosmic-Rays (CRE) have been introduced successfully to date moraines of the last millennium, and even formed during the LIA (Schimmelpfennig et al., 2012, 2014b; Le Roy et al., 2017; Young et al., 2015; Jomelli et al., 2016; Li et al., 2016; Dong et al., 2017; Palacios et al., 2019). The cosmogenic nuclides ^{36}Cl and ^{3}He have been applied previously in northern Iceland to date the Pleistocene deglaciation. Principato et al. (2006) studied the deglaciation of Vestfirðir combining ^{36}Cl CRE dating of moraine boulders and bedrock surfaces with marine records and tephra marker beds. Andrés et al. (2019) reconstructed the deglaciation at the Late Pleistocene to Holocene transition at Skagafjörður through ^{36}Cl CRE dating applied to polished surfaces along a transect from the highlands to the mouth of the fjord. Brynjólfsson et al. (2015a) applied the same isotope to samples coming from the highlands and the fjords to reconstruct the glacial history of the Drangajökull region. The other cosmogenic isotope used is ^{3}He, applied to helium-retentive olivine phenocrysts by Licciardi et al. (2007) to

determine eruption ages of Icelandic table mountains and to reconstruct the volcanic history and the thickness evolution of the Icelandic Ice Sheet during the last glacial cycle. However, CRE dating has not yet been applied to the late Holocene glacial landforms both in Iceland as a whole and the Tröllaskagi Peninsula. CRE dating is an alternative to the use of high-resolution continuous lacustrine records in northern Iceland, given the rarity of lakes in this peninsula, which limits the application of radiocarbon to date the deglaciation processes (Striberger et al., 2012; Harning et al., 2016a).

Nevertheless, CRE dating methods approach the nuclides' detection limit when applied to very recent moraines (Marrero et al., 2016; Jomelli et al., 2016). This issue precludes the application of CRE dating to the abundant post-LIA moraines existing in some of the Tröllaskagi valleys whose headwalls are occupied by climate-sensitive debris-free glaciers (Caseldine and Cullingford, 1981; Caseldine, 1983, 1985a; Kugelmann, 1991). Dating these post-LIA moraines allows to reconstruct recent climate evolution, and even to match and assess the climate reconstructions with the instrumental climate records (see Dahl and Nesje, 1992; Caseldine and Stötter, 1993). Futhermore, improving the knowledge of the recent evolution of alpine mountain glaciers, such as those of Tröllaskagi, is fundamental in the assessment of present global warming (Marzeion et al., 2014)

The use of aerial photographs from different dates is a reliable approach to the glacier evolution during the last decades (Tanarro et al., 2019). The main advantage of this technique is the possibility of studying the evolution of glacier snouts in recent dates with high accuracy. In fact, there is no dependence on the glacial features (i.e. moraines), which circumvents moraine deterioration issues derived by the geomorphological activity of the slopes. However, the main shortcoming of the aerial photo imagery is the availability only on few dates, at least in Tröllaskagi. This circumstance makes it impossible to obtain the glacier fluctuations with a high time resolution (i.e. only the periods between the available aerial photos; Tanarro et al., 2019; see Chapter 4), and hence to match them to short-term (decadal scale) climate fluctuations that are known to exert a major control especially on small mountain glaciers with short time responses (see Caseldine, 1985a; Sigurðsson, 1998; Sigurðsson et al., 2007). The only way to fill the gap between two dates with available aerial photos is through applying lichenometric dating (Sancho et al., 2011), as there is no tree species suitable to apply dendrochronology. In addition, the information provided by the aerial photo imagery (i.e. glacier snout position) constrains the period when the lichens appear and begin to grow, which circumvents many of the criticisms made on lichenometry (see Osborn et al., 2015).

Moreover, a detailed geomorphological mapping allows for identification of stable moraines, not remobilized or destroyed by glacier advances or slope processes (avalanches, slope deformations, debris-flows, etc.) and also to reconstruct the glacier snout geometry throughout different phases (see Caseldine, 1981; Bradwell, 2004b; Principato et al., 2006 amongst others). The analysis of the moraine morphology and the glacial features on the forelands is a key tool to confirm whether the glaciers were debris-free or debris-covered in the past (Kirkbride, 2011; Janke et al., 2015; Knight, et al., 2018, amongst others) as this issue determines their climate sensitivity (see Tanarro et al., 2019).

The western and eastern Tungnahryggsjökull glaciers, in the Vesturdalur and Austurdalur Valleys (central Tröllaskagi), respectively (Fig. 5.1), are two of the few debris-free glaciers –or almost debris-free in the case of the western glacier– of the peninsula that are both small and highly sensitive to climatic fluctuations (see Chapter 4). This makes them ideal for studying glacial and climatic evolution during last millennia.

The aim of our work was to apply the best methodology possible to analyse the glacial evolution of western and eastern Tungnahryggsjökull glaciers during the last millennia to the present. Applying for the first time a number of dating techniques to study the Late Holocene evolution of the two glaciers, the objectives of this chapter are:

(i) To carry out a detailed geomorphological survey of the glacier forelands in order to map accurately well-preserved glacial features. This mapping is used both to devise the sampling strategy for dating, and also to reconstruct the palaeoglaciers in 3D in order to obtain glaciological climate indicators such as the Equilibrium-Line Altitudes (ELAs). These can be used as a proxy to infer palaeoclimatic information (see Dahl and Nesje, 1992; Caseldine and Stötter, 1993; Brugger, 2006; Hughes et al., 2010, amongst others).

(ii) To use aerial photographs / satellite imagery post-dating 1946 to map the glacier extent in each available date in order to improve the information of ELA evolution in the recent decades. Aerial photographs will be used to constrain the possible periods of lichen colonization and growth over stable boulders, and will be useful to identify phases of advance, stagnation or retreat of the glacier snouts. By this way we will complete the glacier evolution from pre-instrumental glacial stages (identified from geomorphological evidence, i.e. moraines) to their current situation.

(iii) To apply CRE dating when possible depending on the preservation degree of the glacial features, and when moraines were too old to be dated by lichenometry.

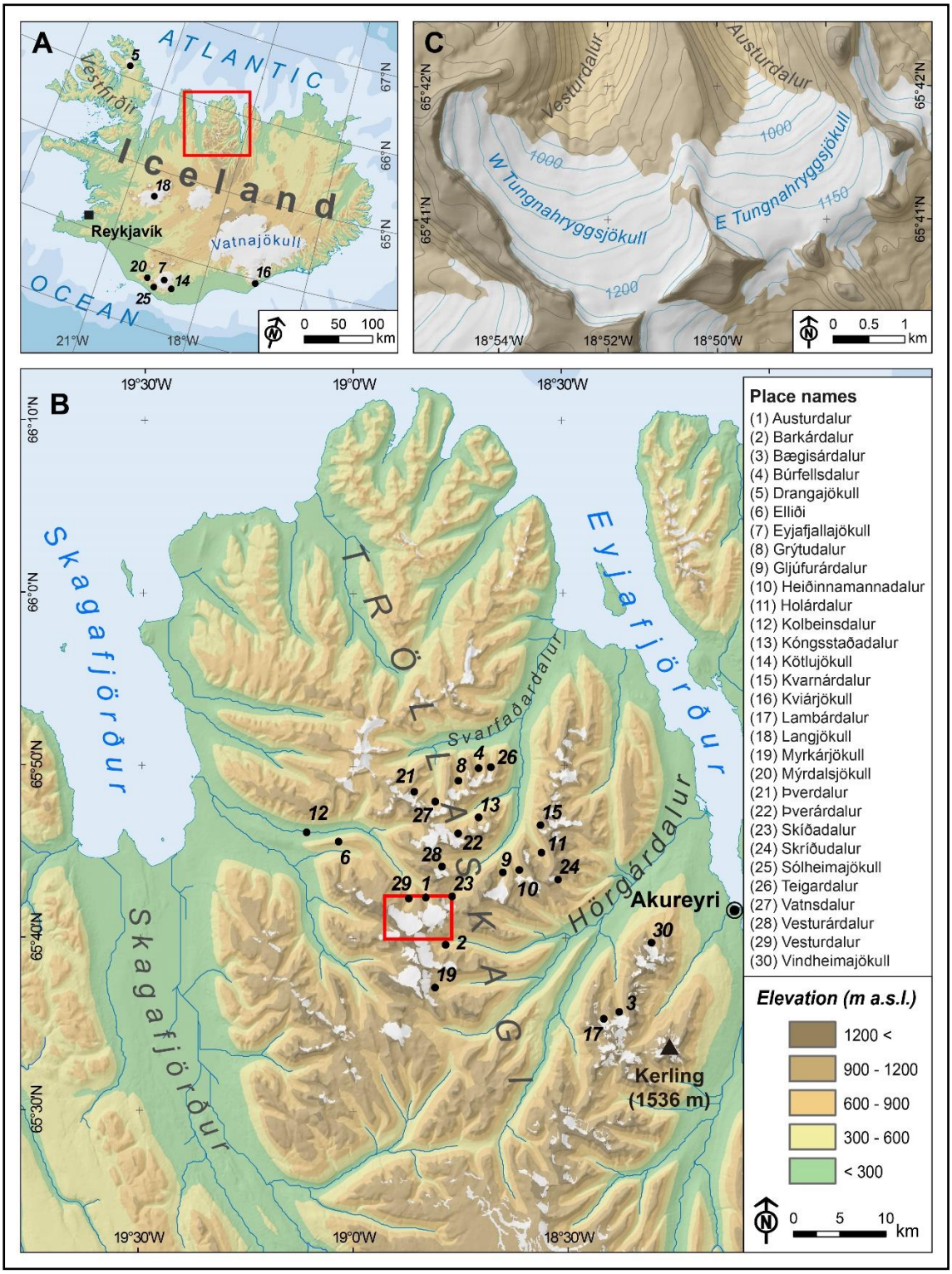

Figure 5.1. Location of the Tungnahryggsjökull glaciers and their forelands (C) (Vesturdalur and Austurdalur) in the context of Iceland (A) and the Tröllaskagi peninsula (B). The red boxes in panels A and B are panels B and C, respectively. The figure also includes the location of the place names mentioned throughout this chapter.

(iv) To apply lichenometric relative dating to recent moraines or those where CRE dating might not be suitable (i.e. limit of applicability) and provided that: 1) the geomorphological criteria evidence a good preservation of glacial features; and 2) aerial

photographs constrain the earliest and oldest possible lichen ages. This approach will also allow to check the growth rates and colonization lags of the lichen species usually used in Iceland for lichenometric dating purposes.

The experimentation and validation of this methodological purpose will help to improve the knowledge of the recent climate evolution of northern Iceland. This is of maximum interest if we consider its location within the current atmospheric and oceanic setting, strongly linked to the evolution of the Meridional Overturning Circulation (Andrews and Giraudeau, 2003; Xiao et al., 2017), a key factor in the studies for the assessment of the global climate change effects (Barker et al., 2010; Chen et al., 2015 amongst others). Moreover, if this proposal is valid, it could be applied to the research on the recent evolution of other mountain glaciers similar to those of Tröllaskagi. This aspect is a main research objective at present, as these glaciers represent the greatest contribution to the current sea-level rise (Jacob et al., 2012; Gardner et al., 2013 amongst others).

5.2. Results.

5.2.1 Geomorphological mapping, aerial photos and identified glacial stages.

Based on photo-interpretation of aerial photographs and fieldwork, two geomorphological maps were generated at ~1:7000 scale, in which well-preserved moraine segments, current glacier margins and stream network were also mapped (Figs. 5.2 and 5.3). In Vesturdalur, over 1000 moraine ridge fragments (including terminal and lateral moraine segments) were identified and mapped, with increased presence from 1.7 km upwards to the current glacier terminus. In the analysis, we retained only ridge fragments if they are at least 50 m long, protruding 2 m above the valley bottom and the alignment of glacial boulders embedded in the moraine crest is preserved, as indicators of major glacial culminations and well preservation state. Otherwise we considered either they represented insignificant glacial stages or were most probably affected by post-glacial slope reworking.

Following these criteria, we retained 12 glacial stages based on the geomorphological mapping of the Vesturdalur foreland (Fig. 5.2). We were able to verify in the field that the selected sections had not been affected by postglacial slope processes as none of these moraines was cut by debris-flows or deformated/covered by landslides. The palaeo-position of the glacier terminus was clearly defined by pairs of latero-frontal moraines in stages 1, 4 and 6.

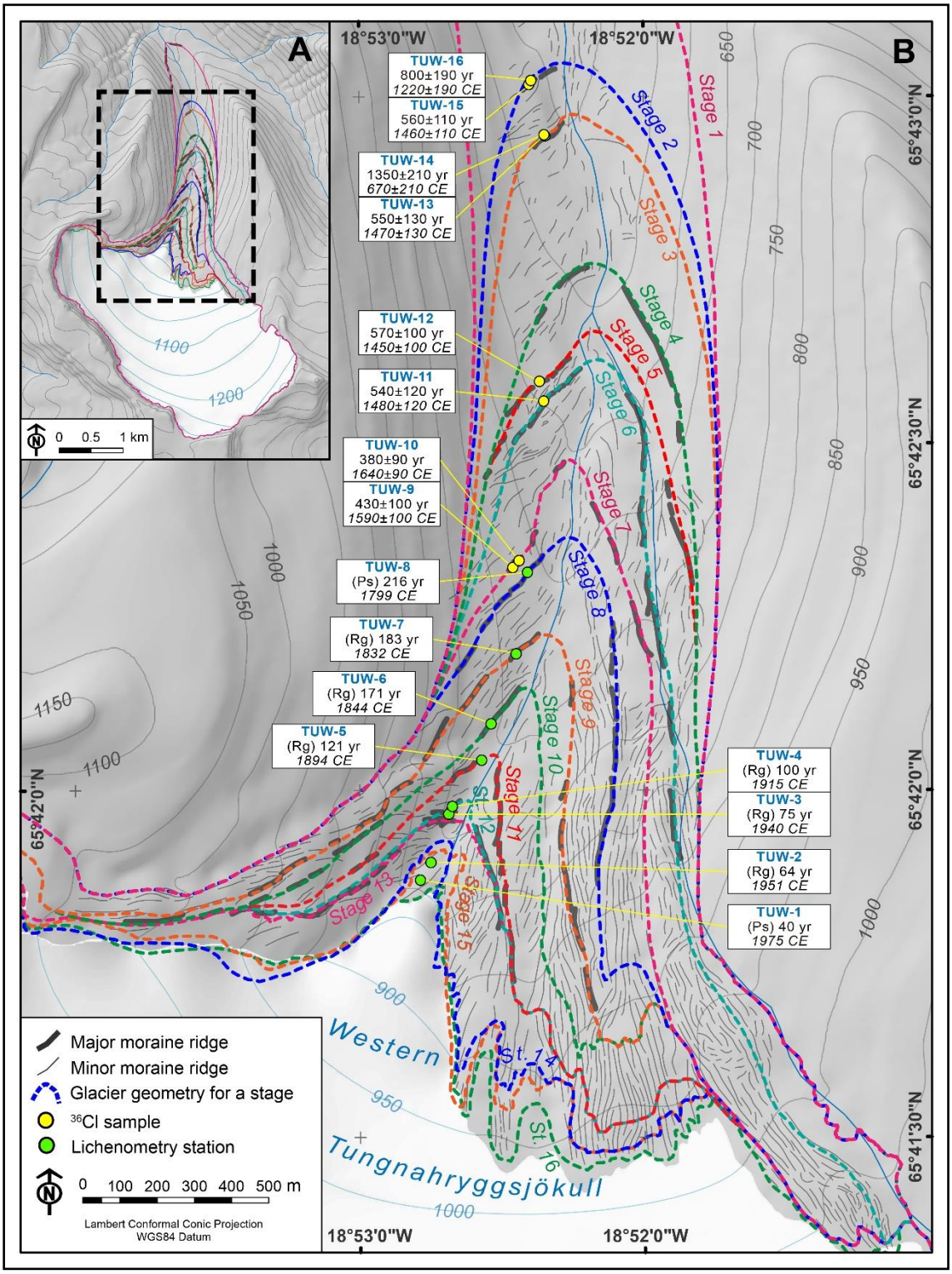

Figure 5.2. Map of the moraine ridges in the Vesturdalur foreland. (A) General view of the Western Tungnahryggsjökull foreland. (B) Detailed moraine mapping and glacier margin geometry reconstructed throughout the different glacial stages identified, and ^{36}Cl CRE and lichenometric dating results (both are expressed in ages and calendar years). Note that stages 13, 14, 15 and 16 correspond to the years 1946, 1985, 1994 and 2000. The surface-contoured glacier (white) corresponds to the year 2005 (stage 17). The abbreviations "Rg" and "Ps" in lichenometry stations indicate that the estimated dates are derived from the *Rhizocarpon geographicum* and *Porpidia soredizodes* lichens, respectively, and the number correspond to the longest axis of the largest lichen measured.

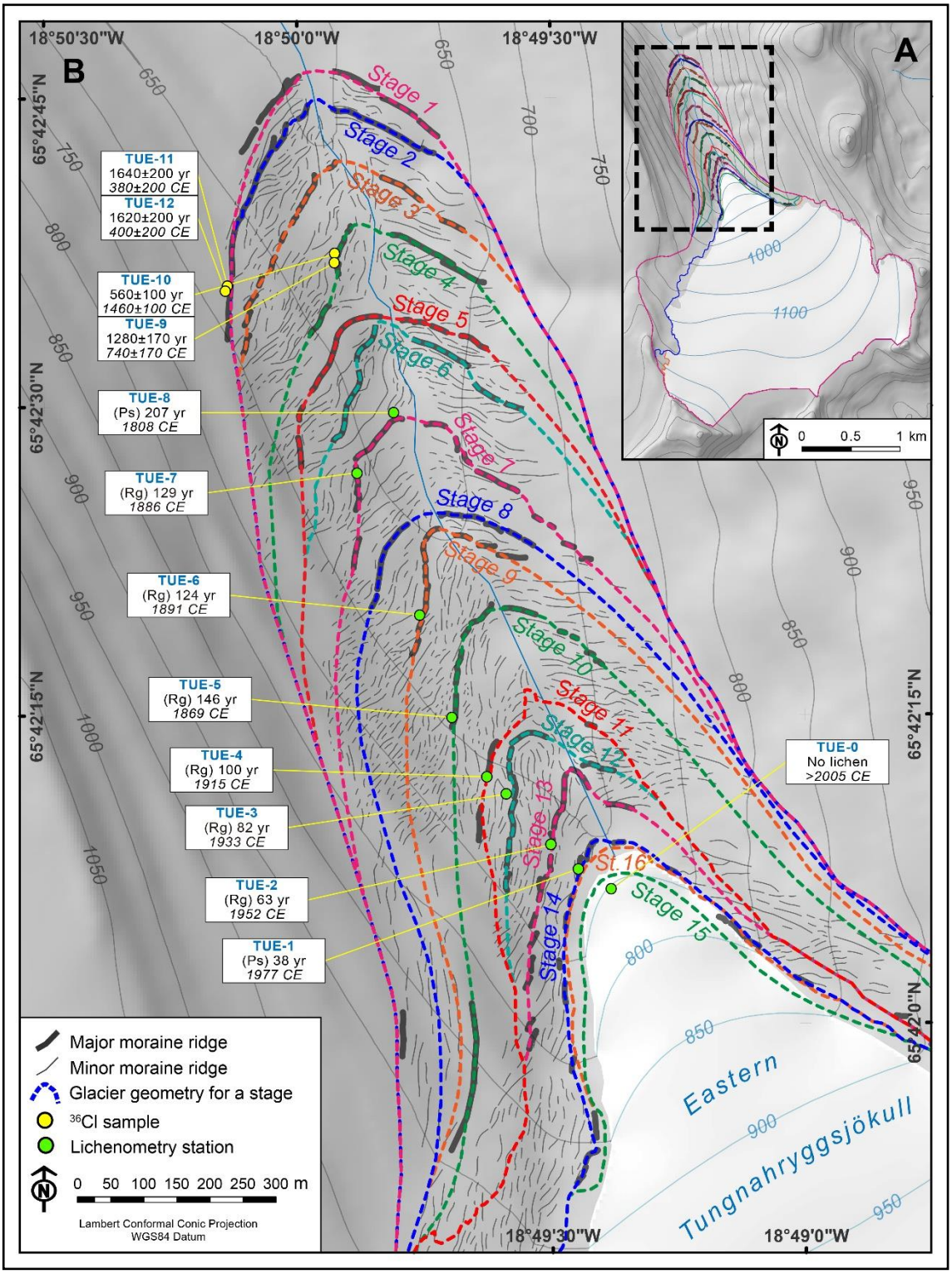

Figure 5.3. Map of the moraine ridges in the Austurdalur foreland. (A) General view of the Eastern Tungnahryggsjökull foreland. (B) Detailed moraine mapping and glacier margin geometry reconstructed throughout the different glacial stages identified, and ^{36}Cl CRE and lichenometric dating results (both are expressed in ages and calendar years). Note that stages 11, 15 and 16 correspond to the years 1946, 1985 and 2000. The surface-contoured glacier (white) corresponds to the year 2005 (stage 17). The abbreviations "Rg" and "Ps" in lichenometry stations indicate that the estimated dates are derived from the *Rhizocarpon geographicum* and *Porpidia soredizodes* lichens, respectively, and the number correspond to the longest axis of the largest lichen measured.

In stages 2, 3, 5, 9, 10, 11 and 12, it was poorly defined by short latero-frontal moraines on one side of the valley, very close to the river, with their prolongation and intersection with the river assumed to be the former apex, and so a tentative terminus geometry was drawn. The lateral geometry of the tongue was accurately reconstructed in stages 6, 8 and 9 based on long and aligned, ridge fragments, and in the other stages an approximate geometry was drawn from the terminus to the headwall. The greatest retreat between consecutive stages (1 km) occurred in the transition from the stage 1 to the stage 2. No intermediate frontal moraines were observed in the transect between the stages 1 and 2.

In Austurdalur, over 1600 moraine ridge fragments were identified and mapped. Following the same criteria as in Vesturdalur, 13 stages were identified based on the geomorphological evidence (Fig. 5.3). The furthest moraines marking the maximum extent of the eastern Tungnahryggsjökull appear at 1.3 km from the current terminus. In contrast to the other valley, moraines populate the glacier foreland more densely and regularly on both sides of the valley. Most of them are <50 m long with a few exceeding 100-200 m. The frontal moraine ridge fragments in Austurdalur clearly represent the geometry of the terminus in all the stages, as they are well-preserved and are only bisected by the glacier meltwater, with the counterparts easily identifiable. The most prominent (over 2 m protruding over the bottom of the valley) and well preserved moraines are those marking the terminus position at stages 1 to 8, with lengths ranging from 170 to 380 m.

Both glaciers were also outlined on aerial photos of 1946, 1985, 1994 (only for western Tungnahryggsjökull), and 2000, and on a SPOT satellite image (2005), and hence new recent stages from the past century were studied for the Tungnahryggsjökull, five for the western glacier (stages 13, 14, 15, 16 and 17) and four for the eastern glacier (stages 11, 15, 16 and 17) (Fig. 5.4; Table 5.1). The stages identified on the basis of the geomorphological mapping and those obtained from glacier outlining over historical aerial photos sum up to a total of 17 stages for each glacier.

W Tungnahryggsjökull		**E Tungnahryggsjökull**	
Stage	*Date*	*Stage*	*Date*
13	1946	11	1946
14	1985	15	1985
15	1994	-	-
16	2000	16	2000
17	2005	17	2005

Table 5.1. Correspondence between glacial stages mapped over historical aerial photos and the dates.

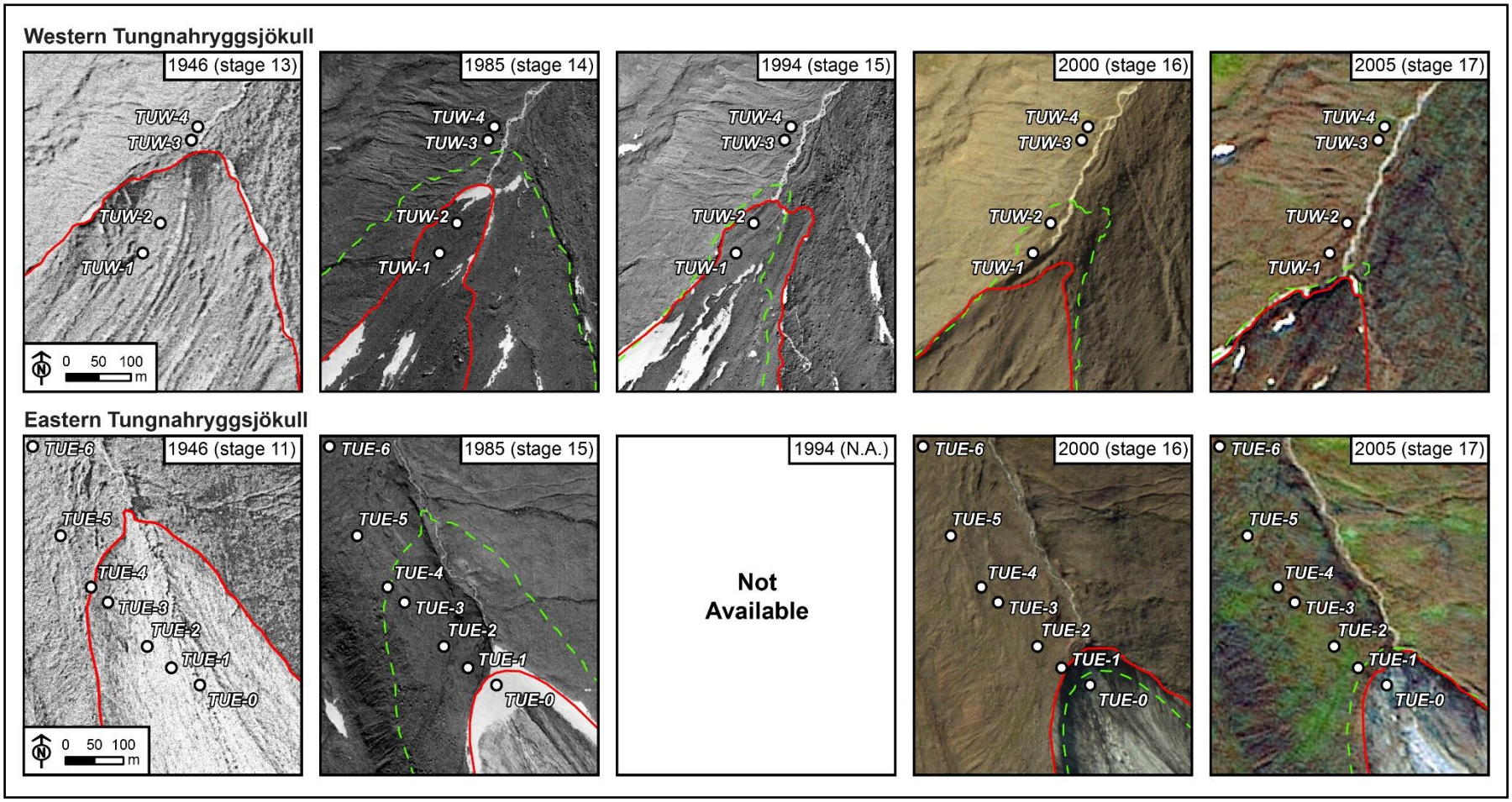

Figure 5.4. Location of the lichenometry stations in relation to the glacier snout position shown in the different aerial photographs and the satellite image. The lines refer to the glacier margin outlined over the aerial photo at a specific date (red) and at the previous date with aerial photo available (green dashed line). The points display the location of the lichenometry stations. The aerial photos provide the dating control for the validation of the lichenometric dates.

5.2.2. Glacier length, extent and volume.

The reconstructed glacier surfaces corresponding to the different glacial stages is shown in Fig. 5.5.

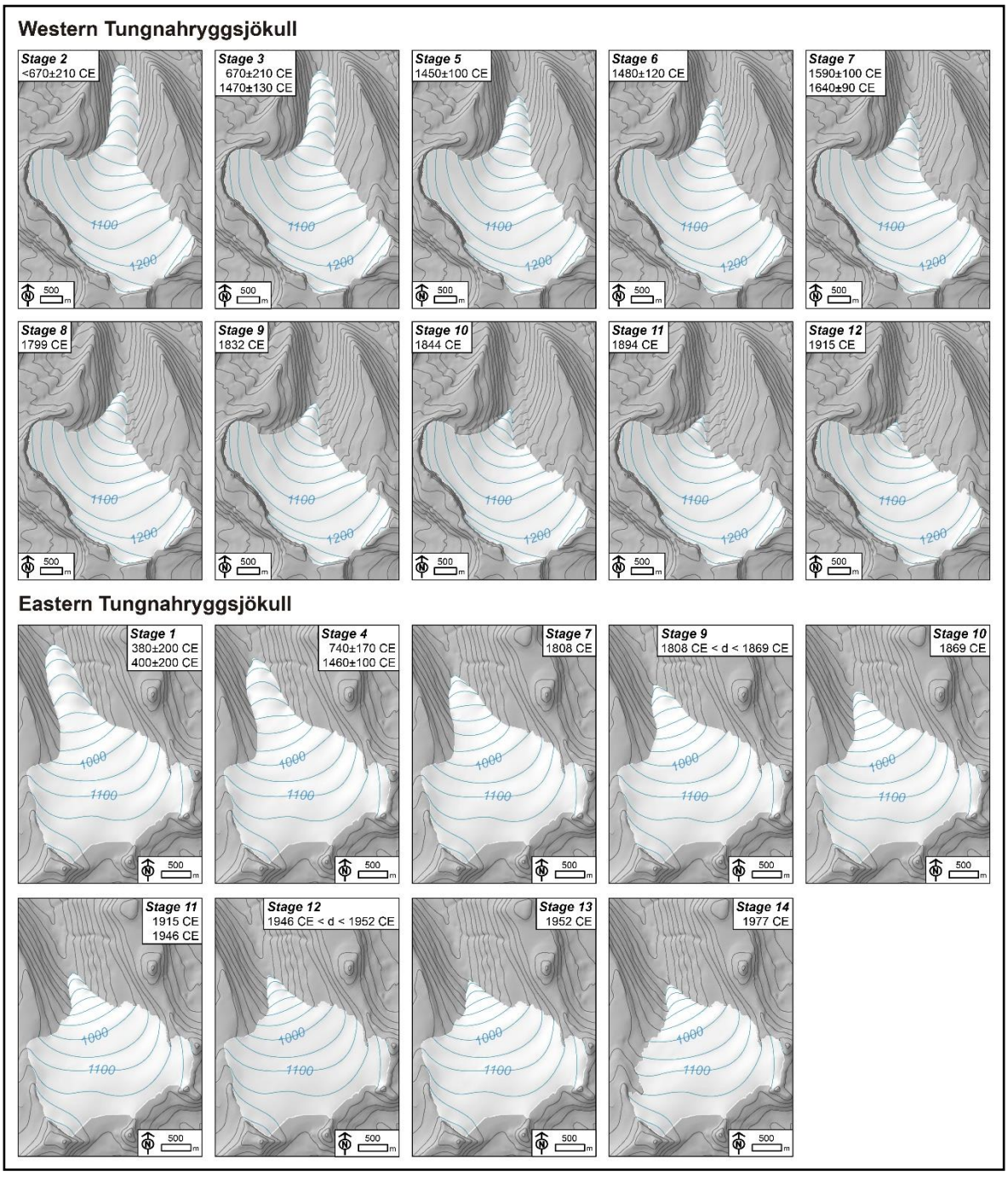

Figure 5.5. Glacier surface reconstruction for the CRE- and lichenometry-dated glacial stages.

The length of the glaciers during their reconstructed maximum ice extent was unequal, with the western Tungnahryggsjökull being 6.5 km long, and the eastern glacier being 3.8 km long (Table 5.2). The same occurred with the area, 9.4 and 5.3 km^2, respectively (Table 5.3).

Stage	W Tungnahryggsjökull		E Tungnahryggsjökull	
	Length (m)	Δ *(m)*	*Length (m)*	Δ *(m)*
1	6492	-	3777	-
2	5483	-1009	3733	-44
3	5345	-138	3627	-106
4	4946	-398	3515	-112
5	4761	-185	3398	-117
6	4682	-79	3362	-36
7	4402	-280	3237	-125
8	4218	-185	3084	-153
9	3951	-266	3057	-27
10	3800	-151	2911	-146
11	3601	-199	2755	-156
12	3452	-149	2722	-34
13	3406	-46	2618	-103
14	3338	-69	2531	-87
15	3311	-27 [a]	2477	-54
16	3203	-108	2513	+36
17	3183	-20	2485	-29

[a] The changes in the snout were uneven, with sectors retreating or advancing.

Table 5.2. Glacier length and snout position variations measured along the flowline.

Stage	W Tungnahryggsjökull				E Tungnahryggsjökull			
	Area (km^2)	Δ *(%)*	*Vol. (km^3)*	Δ *(%)*	*Area (km^2)*	Δ *(%)*	*Vol. (km^3)*	Δ *(%)*
1	9.44	-	1.103	-	5.28	-	0.466	-
2	8.87	-6.04	0.998	-9.55	5.26	-0.29	0.463	-0.49
3	8.76	-1.22	0.985	-1.33	5.22	-0.82	0.454	-1.91
4	8.46	-3.45	0.942	-4.34	5.15	-1.26	0.446	-1.97
5	8.36	-1.18	0.928	-1.47	5.09	-1.19	0.434	-2.52
6	8.14	-2.65	0.918	-1.05	5.06	-0.52	0.433	-0.27
7	7.80	-4.14	0.889	-3.24	4.98	-2.26	0.422	-2.84
8	7.64	-2.05	0.870	-2.15	4.88	-1.97	0.409	-2.99
9	7.32	-4.13	0.842	-3.22	4.81	-1.40	0.407	-0.66
10	7.18	-2.02	0.826	-1.86	4.71	-2.13	0.395	-2.77
11	6.98	-2.68	0.813	-1.58	4.56	-3.17	0.387	-2.19
12	6.94	-0.67	0.804	-1.06	4.54	-0.42	0.383	-0.86
13	6.91	-0.37	0.801	-0.49	4.51	-0.73	0.381	-0.67
14	6.67	-3.47	0.790	-1.27	4.05	-10.12	0.363	-4.78
15	6.68	+0.17	0.791	+0.09	4.02	-0.65	0.361	-0.46
16	6.57	-1.63	0.774	-2.11	4.02	-0.14	0.362	+0.16
17	6.47	-1.57	0.771	-0.43	3.88	-3.45	0.360	-0.52

Table 5.3. Glacier extent and volume variations calculated from 2D and 3D glacier reconstructions.

Over the different stages, the western glacier lost 31% of its area and retreated 51% of its total length (Tables 5.2 and 5.3) while there was less shrinkage of the eastern glacier both in area loss (26%) and length (34%). Figs. 5.2B and 5.3B and Table 5.2 show only one reversal during the general retreating trend, in the stage 15 of the western and the stage 16 of the eastern Tungnahryggsjökull. The greatest area losses occurred in the transition to the stages 2, 4, 7, 9 and 14 (>3%) on the western glacier while losses between stages in the eastern glacier were lower except for the transition between the stages 14 and 17, where a noticeable reduction of the accumulation area was observed in the aerial photos of 1946 and 1985, and the satellite image of 2005 (Fig. 5.3B). The volumes calculated from the reconstructed glacier DEM and the corrected bed DEM show that the glaciers reached ~1.10 km^3 (western) and ~0.47 km^3 (eastern) at their recorded maximum extent corresponding to their outmost moraines. From the oldest to the most recent stage they lost 30% and 23% of their ice volume, respectively. The losses between consecutive stages of the glaciers were in general lower than 3% with the exception of the stages 2, 4, 7, 9 (western) and stage 14 (eastern), where the values ranged from 3% to 10% (Table 5.3). Only one slight inversion of the volume trend is seen in the stages 15 of the western glacier and in 16 of the eastern glacier.

5.2.3. Equilibrium-Line Altitudes (ELAs).

The application of the AAR (0.67) method showed ELAs ranging from 1021 to 1099 m a.s.l. (western glacier) and from 1032 to 1065 m a.s.l. (eastern glacier) for the different reconstructed stages. This means an overall rise of 78 and 33 m respectively (Table 5.4) from the maximum to the minimum extent recorded. The results from applying the AABR (1.5) show the same trend and similar ELAs, with differences of up to ±15 m compared with those obtained from the AAR. The AABR-ELAs tend to be higher than the AAR-ELAs, especially in the second half of the reconstructed stages with the most remarkable differences occurring in the eastern Tungnahryggsjökull (Table 5.4).

However, the error derived from the uncertainties associated to the applied balance ratio (BR, ±0.4) tends to decrease as the glaciers get smaller. The greatest change in the ELA between consecutive stages is found between the stages 1 and 2 in the western glacier (+26 m), fully coincident with the largest retreat measured, about 1 km. An interesting result is that the ELA rise is attenuated in both glaciers from stage 10 onwards, with stage-to-stage variations close to zero predominating, and with only one inversion (-3 m) occurring in the western glacier between the stages 14 and 15 (Table 5.4).

Stage	W Tungnahryggsjökull				E Tungnahryggsjökull			
	AAR (0.67)	Δ	*AABR (1.5±0.4)*	Δ	*AAR (0.67)*	Δ	*AABR (1.5±0.4)*	Δ
1	1021	-	1006 +25/-20	-	1032	-	1027 ±20	-
2	1047	+26	1032 ±20	+26	1032	0	1032 ±15	+5
3	1052	+5	1037 +20/-15	+5	1034	+2	1034 ±15	+2
4	1054	+2	1049 +20/-15	+12	1037	+3	1037 ±15	+3
5	1059	+5	1059 ±15	+10	1041	+4	1041 ±15	+4
6	1067	+8	1062 +20/-10	+3	1042	+1	1042 ±15	+1
7	1072	+5	1072 +15/-10	+10	1046	+5	1046 ±15	+5
8	1076	+4	1081 ±15	+9	1047	+1	1052 ±15	+6
9	1082	+6	1087 +15/-10	+6	1054	+7	1054 +15/-10	+2
10	1086	+4	1091 +15/-10	+4	1055	+1	1060 +15/-10	+6
11	1094	+8	1099 +15/-10	+8	1061	+6	1071 ±10	+11
12	1094	0	1099 +15/-5	0	1060	-1	1070 ±10	-1
13	1094	0	1099 +15/-5	0	1061	+1	1071 +15/-10	+1
14	1100	+6	1110 ±10	+11	1060	-1	1075 ±10	+4
15	1102	+2	1107 +15/-5	-3	1061	+1	1076 +15/-10	+1
16	1098	-4	1108 +10/-5	+1	1061	0	1076 ±10	0
17	1099	+1	1109 +15/-5	+1	1065	+4	1080 ±10	+4

Table 5.4. Glacial Equilibrium-Line Altitudes (ELAs) calculated over Tungnahryggsjökull glaciers through the application of the AAR and AABR methods over the 3D glacier reconstructions.

5.2.4. Lichenometric dating.

Altogether 17 lichenometry stations (8 in Vesturdalur and 9 in Austurdalur) were set up during fieldwork in the two glacier forelands. Their spatial distribution and correspondence with the different glacial stages are given in Figs. 5.2, 5.3, and Table 5.5. The table also shows the measurements of the largest *Rhizocarpon geographicum* thalli found during fieldwork in the moraines (stages) to which the stations correspond. TUE-0 was the only station where no lichen of either species was found in 2015. Unlike *Porpidia* cf. *soredizodes* thalli, which are present in all the remaining lichenometry stations, *Rhizocarpon geographicum* thalli suitable for measuring (ellipsoidal, not coalescent) were only found in stations TUW-2 to TUW-7 in Vesturdalur, and in TUE-2 to TUE-7 in Austurdalur.

The measurements considered the diameter of the smallest circle bounding the thallus outline as representative of the longest axis (see “Lichenometric dating” section in Chapter 2). The obtained values ranged from 19.3 to 71.5 mm in Vesturdalur, and from 19.0 to 47.7 mm in Austurdalur (Table 5.5). Only one size inversion (decreasing size with increasing distance to the current terminus) was detected in Austurdalur in the station TUE-6 (Fig. 5.3). *Rhizocarpon geographicum* thalli were absent in the nearest stations (TUW-1 and TUE-1) and were coalescent in the most distant stations (TUW-8 and TUE-8) in both

glacier forelands. On the other hand, *Porpidia* cf. *soredizodes* thalli measurements ranged from 18.3 to 148.4 mm in Vesturdalur, and from 16.8 to 141.8 mm in Austurdalur (Table 5.5). A size inversion of *Porpidia cf. soredizodes* thalli is also observed in TUE-6 and in TUE-7.

Glacier foreland	**Lichen station**	**GPS location**		**Glacial stage**	***Rhizocarpon geographicum***	***Porpidia soredizodes***
		Lat. (N)	*Long. (W)*		*Min. circ. diameter (mm)*	*Min. circ. diameter (mm)*
W Tungnahr. (Vesturdalur)	TUW-1	65º41.874'	18º52.785'	15-16	- [a]	18.3
	TUW-2	65º41.899'	18º52.749'	13-15	19.3	43.7
	TUW-3	65º41.968'	18º52.686'	12-13	24.3	42.8
	TUW-4	65º41.979'	18º52.673'	12	35.2	62.1
	TUW-5	65º42.045'	18º52.571'	11	44.5	69.6
	TUW-6	65º42.097'	18º52.539'	10	66.6	106.4
	TUW-7	65º42.197'	18º52.451'	9	71.5	106.2
	TUW-8	65º42.313'	18º52.411'	8	-	148.4
E Tungnahr. (Austurdalur)	TUE-0	65º42.109'	18º49.383'	post-17	-	-
	TUE-1	65º42.125'	18º49.448'	14	-	16.8
	TUE-2	65º42.145'	18º49.502'	13	19.0	39.4
	TUE-3	65º42.186'	18º49.590'	12	27.1	53.2
	TUE-4	65º42.200'	18º49.628'	11	35.2	60.8
	TUE-5	65º42.248'	18º49.697'	10	55.6	128.2
	TUE-6	65º42.331'	18º49.760'	9	45.7	116.9
	TUE-7	65º42.446'	18º49.883'	7	47.7	100.8
	TUE-8	65º42.495'	18º49.810'	7	-	141.8

[a] Dash "-" indicates that no lichen was found.

Table 5.5. Size of the largest lichen at the lichenometry stations in the forelands of the western and eastern Tungnahryggsjökull glaciers.

When the ages of *Rhizocarpon geographicum* lichens are calculated applying a 0.44 mm yr^{-1} growth rate and a 10-year colonization lag following Kugelmann (1991), they range from 54 to 173 years in Vesturdalur, and from 53 to 119 years in Austurdalur. If longer colonization lags of 15, 20, 25 and 30 years (see Methods section) are applied tentatively, the oldest ages obtained are ~170-190 years, and the youngest ~40-70 years (Table 5.6). In general, the further away the lichenometry stations are, the older are the ages (Figs. 5.2 and 5.3), with the inversions mentioned above. Apparently the lichenometry-dated moraines are younger than the CRE-dated distal moraines.

The absence of *Rhizocarpon geographicum* lichens in 2015 at lichenometry station TUW-1 (uncovered by the glacier at some time between 1994 and 2000; Fig. 5.4) suggests a colonization lag of at least 15-21 years. In addition, it is only when the colonization lag is assumed to be longer than 10 years and shorter than 30 years that the ages obtained at

stations TUW-3 and TUE-2 are in good agreement with the ages deduced from the aerial photos (Table 5.6).

Glacier foreland	Lichen station	Glacial stage	Date deduced from photographic evidence	Surface age from growth rate (yr)				
				10-yr col. lag	*15-yr col. lag.*	*20-yr col. lag*	*25-yr col. lag.*	*30-yr col. lag*
W Tungnahr.	TUW-1	15-16	1994-2000	*35*[a]	*40*[a]	*45*[a]	*50*[a]	*55*[a]
	TUW-2	13-15	1946-1994	54	59	64	69	74 [a]
	TUW-3	12-13	<1946	65 [a]	70	75	80	85
	TUW-4	12	<1946	90	95	100	105	110
	TUW-5	11	<1946	111	116	121	126	131
	TUW-6	10	<1946	161	166	171	176	181
	TUW-7	9	<1946	173	178	183	188	193
	TUW-8	8	<1946	*211*	*216*	*221*	*226*	*231*
E Tungnahr.	TUE-0	post-17	2005<	-	-	-	-	-
	TUE-1	14	1946-1985	*33*	*38*	*43*	*48*	*53*
	TUE-2	13	1946-1985	53	58	63	68	73 [a]
	TUE-3	12	1946-1985	72 [a]	77 [a]	82	87 [a]	92 [a]
	TUE-4	11	<1946	90	95	100	105	110
	TUE-5	10	<1946	136	141	146	151	156
	TUE-6	9	<1946	114 [b]	119 [b]	124 [b]	129 [b]	134 [b]
	TUE-7	7	<1946	119 [b]	124 [b]	129 [b]	134 [b]	139 [b]
	TUE-8	7	<1946	*202*	*207*	*212*	*217*	*222*

[a] The age does not agree with the date deduced from aerial photos.

[b] The age is incoherent with the moraine chronostratigraphy.

Table 5.6. Surface ages estimated from Kugelmann's (1991) 0.44 mm yr^{-1} growth rate for different colonization lags. The ages obtained from *Rhizocarpon geographicum* lichens discussed throughout the text are those derived from a 20-yr colonization lag. The figures in italics correspond to ages tentatively inferred from the largest *Porpidia soredizodes* lichen, assuming a 0.737 mm yr^{-1} growth rate and a 15-year colonization lag.

During the 2015 field campaign, the species *Porpidia* cf. *soredizodes* was absent in station TUE-0, located on a glacially polished threshold uncovered by the glacier after 2005 (post-stage 17). However, it was found in stations TUW-1 and TUE-1, dated to 1994-2000 and 1946-1985 respectively, based on the position of the snouts in the aerial photos (Fig. 5.4). These observations suggest a colonization lag from 10 to 15-21 years, thus shorter than for *Rhizocarpon geographicum*.

5.2.5. ^{36}Cl CRE dating.

The detailed geomorphological analysis carried out on the numerous moraine ridges of both valleys has greatly limited the number of boulders reliable for successfully applying ^{36}Cl CRE and lichenometry dating methods. Due to the great intensity of the slope processes (especially snow avalanches and debris-flows), only a few boulders are well-

preserved, sometimes only one in each moraine ridge that retains its original glacier location. Thus, it should be highlighted that this issue prevented performing a statistically valid sampling for both methods (see e.g. Schaefer et al., 2009; Heyman et al., 2011).

During the fieldwork campaigns in the forelands of the western and eastern Tungnahryggsjökull glaciers, 12 samples from stable and very protrusive moraine boulders (Fig. 5.6) were collected in areas where lichenometric dating was not suitable because of lichen thalli coalescence, and also 2 samples from a polished ridge downwards the confluence of Vesturdalur and Austurdalur (Fig. 5.7). The input data for exposure age calculations, namely sample thickness, topographic shielding factor, major element concentrations of bulk/target fractions, are summarized in the Tables 5.7, 5.8, 5.9 and Table 5.10 includes the ^{36}Cl CRE ages calculated according to different Ca spallation production rates and the distance to the most recent glacier terminus position mapped. Table 5.11 includes the ^{36}Cl CRE ages converted to CE dates format presented throughout the text. The dates presented below are based on the Licciardi et al. (2008) Ca spallation production rate.

Aiming to obtain a maximum (oldest) age for the onset of the deglaciation in the valleys studied, two samples (ELLID-1 and ELLID-2) were extracted from the western sector of Elliði, a 660-m-high glacially polished crest separating Viðinesdalur and Kolbeinsdalur valleys (Fig. 5.7), and located at 11 km downstream from the confluence of Vesturdalur and Austurdalur valleys. Both samples yielded dates of 14300±1700 BCE and 14200±1700 BCE. In Vesturdalur, 8 samples were collected from 5 moraines corresponding to 5 of the stages identified on the geomorphological map (Fig. 5.2). Samples TUW-9 and TUW-10 were taken from two boulders in the moraine that correspond to the left latero-frontal edge of the glacier during the stage 7, ~1 km from the 2005 CE (stage 17) glacier terminus (measured along the flowline from the reconstructed terminus apex); they yielded consistent dates of 1590±100 CE and 1640±90 CE. Samples TUW-11 and TUW-12 were extracted from the moraines corresponding to the glacial stages 6 and 5, at 185 m and 465 m downstream respectively (~1.2 km and ~1.5 km respectively from the 2005 CE snout), and gave consistent dates 1480±120 CE and 1450±100 CE. The next ^{36}Cl samples (TUW-13 and TUW-14) were taken from two adjacent moraine boulders on the left latero-frontal moraine ridge corresponding to the stage 3, at 264 m downstream (1.8 km from the 2005 CE snout); they yielded dates of 1470±130 CE and 670±210 CE, which are significantly different from each other. The most distant samples (TUW-15 and TUW-16) were extracted from the stage 2 moraine, ~400 m downstream from the moraine ridge corresponding to stage 3 (2.2 km from the 2005 CE terminus).

Sample name	Stage	Latitude (ºN)	Longitude (ºW)	Elevation (m a.s.l.)	Shielding factor	Thickness (cm)	Dist. to terminus (m) [a]
Moraine boulders at Vesturdalur (W Tungnahryggsjökull foreland)							
TUW-9	8	65.7053	18.8744	674	0.9662	4.0	1034
TUW-10	8	65.7055	18.8740	669	0.9818	4.0	1034
TUW-11	7	65.7093	18.8725	599	0.9805	2.0	1219
TUW-12	6	65.7098	18.8728	593	0.9799	3.5	1499
TUW-13	4	65.7156	18.8725	522	0.9683	3.0	1763
TUW-14	4	65.7156	18.8725	523	0.9674	2.0	1763
TUW-15	3	65.7168	18.8734	523	0.9788	3.0	2161
TUW-16	3	65.7169	18.8733	520	0.9798	2.0	2161
Moraine boulders at Austurdalur (E Tungnahryggsjökull foreland)							
TUE-9	4	65.7103	18.8321	624	0.9848	3.0	1030
TUE-10	4	65.7104	18.8321	623	0.9849	2.5	1030
TUE-11	1	65.7101	18.8364	692	0.9667	3.0	1293
TUE-12	1	65.7100	18.8364	694	0.9756	3.5	1293
Glacially polished ridge separating Viðinesdalur and Kolbeinsdalur							
ELLID-1	-	65.7580	19.0848	608	0.9989	2.0	14370
ELLID-2	-	65.7579	19.0854	611	0.9993	3.5	14400

[a] Distance to the terminus is measured along the flowline from the reconstructed snout apex of the phase where the samples were collected.

Table 5.7. Geographic sample locations, topographic shielding factor, sample thickness and distance from terminus.

Sample name	CaO (%)	K_2O (%)	TiO_2 (%)	Fe_2O_3 (%)	Cl (ppm)	SiO_2 (%)	Na_2O (%)	MgO (%)	Al_2O_3 (%)	MnO (%)	P_2O_5 (%)	CO_2 (%)	Li (ppm)	B (ppm)	Sm (ppm)	Gd (ppm)	Th (ppm)	U (ppm)
Moraine boulders at Vesturdalur (W Tungnahryggsjökull foreland)																		
TUW-15	10.540	0.300	3.704	15.510	27	48.800	2.330	5.966	11.913	0.217	< L.D.	-	4.8	<2	2.379	2.892	0.622	0.225
TUW-16	10.388	0.377	3.239	14.930	44	49.690	2.113	6.937	11.433	0.211	< L.D.	-	3.9	<2	2.121	2.523	0.910	0.306
Average	*10.464*	*0.339*	*3.472*	*15.220*	*36*	*49.245*	*2.222*	*6.452*	*11.673*	*0.214*	*< L.D.*	-	*4.4*	*<2*	*2.250*	*2.707*	*0.766*	*0.265*
Moraine boulders at Austurdalur (E Tungnahryggsjökull foreland)																		
TUE-11	12.333	0.199	2.233	12.720	43	47.270	2.106	7.268	14.465	0.183	0.180	-	3.6	<2	4.204	4.402	0.821	0.224
TUE-12	12.325	0.229	2.219	12.617	43	47.680	2.284	6.988	14.710	0.182	0.190	-	3.6	<2	4.392	4.525	0.864	0.216
Average	*12.329*	*0.214*	*2.226*	*12.669*	*43*	*47.475*	*2.195*	*7.128*	*14.588*	*0.182*	*0.185*	-	*3.6*	*<2*	*4.298*	*4.464*	*0.842*	*0.220*
Glacially polished ridge separating Viðinesdalur and Kolbeinsdalur																		
ELLID-1	8.568	0.179	4.753	18.215	21	44.950	2.161	7.475	12.416	0.228	0.200	-	4.4	2	5.709	5.953	0.504	0.149

Table 5.8. Chemical composition of the bulk rock samples before chemical treatment. The figures in italic correspond to the average values of the bulk samples analysed and were those used for the age-exposure calculations of the samples without bulk chemical composition analysis.

Sample name	CaO (%)	K_2O (%)	TiO_2 (%)	Fe_2O_3 (%)
Moraine boulders at Vesturdalur (W Tungnahryggsjökull foreland)				
TUW-9	10.96 ± 0.22	0.27 ± 0.04	3.57 ± 0.18	13.46 ± 0.27
TUW-10	11.06 ± 0.22	0.25 ± 0.04	3.07 ± 0.15	14.31 ± 0.29
TUW-11	10.57 ± 0.21	0.37 ± 0.06	3.72 ± 0.19	15.32 ± 0.31
TUW-12	11.78 ± 0.24	0.32 ± 0.05	2.92 ± 0.15	13.62 ± 0.27
TUW-13	10.51 ± 0.21	0.37 ± 0.06	3.66 ± 0.18	15.27 ± 0.31
TUW-14	9.98 ± 0.20	0.36 ± 0.05	3.43 ± 0.17	16.16 ± 0.32
TUW-15	10.75 ± 0.21	0.33 ± 0.05	3.03 ± 0.15	15.53 ± 0.31
TUW-16	11.09 ± 0.22	0.37 ± 0.06	2.66 ± 0.13	14.34 ± 0.29
Moraine boulders at Austurdalur (E Tungnahryggsjökull foreland)				
TUE-9	10.88 ± 0.22	0.16 ± 0.02	3.21 ± 0.16	15.81 ± 0.32
TUE-10	10.75 ± 0.21	0.21 ± 0.03	3.07 ± 0.15	14.60 ± 0.29
TUE-11	11.53 ± 0.23	0.16 ± 0.02	2.82 ± 0.14	14.03 ± 0.28
TUE-12	11.90 ± 0.24	0.21 ± 0.03	2.70 ± 0.13	12.77 ± 0.26
Ellíði glacially polished ridge separating Viðinesdalur and Kolbeinsdalur				
ELLID-1	7.20 ± 0.14	0.14 ± 0.02	6.96 ± 0.35	24.28 ± 0.49
ELLID-2	7.01 ± 0.14	0.12 ± 0.02	7.18 ± 0.36	25.12 ± 0.50

Table 5.9. Concentrations of the ^{36}Cl target elements Ca, K, Ti and Fe, determined in splits taken after the chemical pre-treatment (acid etching).

They yielded dates of 1460±110 CE and 1220±190 CE, respectively, that are consistent which each other and in chronological order with sample TUW-13 from the stage 3. However, these ages are not in agreement with the oldest date of TUW-14 (670±210 CE) from the stage 3.

Four ^{36}Cl samples were taken from two prominent moraines in the Austurdalur valley (Fig. 5.3). Samples TUE-9 and TUE-10 were collected on the frontal moraine corresponding to stage 4 (1 km from the 2005 CE glacier terminus) and yield significantly different dates of 740±170 CE and 1460±100 CE. Samples TUE-11 and TUE-12 were taken from two moraine boulders located on the ridge of the left lateral moraine that records the maximum ice extent (Fig. 5.3). Their calculated ^{36}Cl dates, 380±200 CE and 400±200 CE, are consistent with each other and in stratigraphic order with the ages from stage 4.

The dates derived from Stone et al. (1996) Ca spallation production rate are similar to those presented above, only 4% older. Those derived from the Schimmelpfennig et al. (2011) production rate yielded dates older by 15% on average (Table 5.11). These small differences do not represent statistical difference given the calculated age uncertainties.

Sample name	Sample weight (g)	mass of Cl in spike (mg)	$^{35}Cl/^{37}Cl$	$^{36}Cl/^{35}Cl$ (10^{-14})	[Cl] in sample (ppm)	[^{36}Cl] (10^4 atoms g^{-1})	Age (yr) Licciardi et al. (2008) Ca spallation prod. rate	Age (yr) Stone et al. (1996) Ca spallation prod. rate	Age (yr) Schimmelpfennig et al. (2011) Ca spallation prod. rate
Moraine boulders at Vesturdalur (W Tungnahryggsjökull foreland)									
TUW-9	82.98	1.823	27.225 ± 0.729	5.700 ± 0.357	3.5	0.46 ± 0.09	430 ± 100 (*90*)	450 ± 100 (*100*)	500 ± 120 (*110*)
TUW-10	86.12	1.823	5.851 ± 0.144	0.878 ± 0.123	32.1	0.54 ± 0.10	380 ± 90 (*90*)	400 ± 90 (*90*)	440 ± 110 (*100*)
TUW-11	88.96	1.826	5.198 ± 0.110	0.987 ± 0.136	41.0	0.73 ± 0.13	540 ± 120 (*110*)	550 ± 120 (*120*)	600 ± 140 (*130*)
TUW-12	89.17	1.808	6.854 ± 0.091	1.324 ± 0.152	22.4	0.71 ± 0.10	570 ± 100 (*100*)	590 ± 110 (*100*)	650 ± 120 (*110*)
TUW-13	87.33	1.846	5.850 ± 0.147	1.014 ± 0.152	32.0	0.65 ± 0.13	550 ± 130 (*120*)	570 ± 130 (*130*)	620 ± 150 (*140*)
TUW-14	88.26	1.829	5.797 ± 0.192	2.044 ± 0.202	32.0	1.44 ± 0.17	1350 ± 210 (*190*)	1400 ± 210 (*200*)	1520 ± 250 (*210*)
TUW-15	88.61	1.828	8.869 ± 0.150	1.317 ± 0.155	14.7	0.58 ± 0.09	560 ± 110 (*100*)	590 ± 110 (*100*)	650 ± 120 (*110*)
TUW-16	88.50	1.825	4.402 ± 0.071	1.092 ± 0.164	67.0	1.19 ± 0.21	800 ± 190 (*180*)	820 ± 190 (*180*)	890 ± 210 (*200*)
Moraine boulders at Austurdalur (E Tungnahryggsjökull foreland)									
TUE-9	93.53	1.814	13.846 ± 0.153	3.402 ± 0.272	7.2	1.33 ± 0.12	1280 ± 170 (*140*)	1360 ± 170 (*150*)	1510 ± 210 (*170*)
TUE-10	85.51	1.831	12.715 ± 0.276	1.532 ± 0.172	9.0	0.60 ± 0.09	560 ± 100 (*90*)	590 ± 100 (*100*)	660 ± 120 (*110*)
TUE-11	85.80	1.835	8.621 ± 0.110	3.620 ± 0.243	15.9	1.94 ± 0.15	1640 ± 200 (*160*)	1730 ± 200 (*170*)	1910 ± 250 (*190*)
TUE-12	87.64	1.828	6.206 ± 0.088	3.172 ± 0.196	27.9	2.15 ± 0.16	1620 ± 200 (*160*)	1700 ± 190 (*160*)	1870 ± 240 (*180*)
Glacially polished ridge separating Viðinesdalur and Kolbeinsdalur									
ELLID-1	28.88	1.864	68.854 ± 0.615	11.051 ± 0.438	3.5	12.438 ± 0.516	16300 ± 1700 (*1200*)	16900 ± 1600 (*1300*)	18600 ± 2100 (*1400*)
ELLID-2	27.69	1.928	86.476 ± 0.876	10.014 ± 0.437	2.6	11.977 ± 0.547	16200 ± 1700 (*1300*)	16800 ± 1700 (*1300*)	18500 ± 2100 (*1400*)
Blanks					*Total atoms Cl* (10^{17})	*Total atoms ^{36}Cl* (10^4)			
BK-1		1.800	297.029 ± 11.372	0.545 ± 0.097	2.941 ± 0.220	16.981 ± 3.034			
BK-2		1.818	279.307 ± 3.352	0.392 ± 0.079	3.251 ± 0.170	12.347 ± 2.484			
BK-3		1.888	328.059 ± 2.892	0.359 ± 0.069	2.650 ± 0.136	11.725 ± 2.249			

Table 5.10. ^{36}Cl analytical data and CRE dating results according to different ^{36}Cl production rates from Ca spallation. $^{36}Cl/^{35}Cl$ and $^{35}Cl/_{37}Cl$ ratios were inferred from measurements at the ASTER AMS facility. The numbers in italic correspond to the internal (analytical) uncertainty at 1σ level

Sample name	Dates (CE/BCE)		
	Licciardi et al. (2008) Ca spallation prod. rate	Stone et al. (1996) Ca spallation prod. rate	Schimmelpfennig et al. (2011) Ca spallation prod. rate
Moraine boulders at Vesturdalur (W Tungnahryggsjökull foreland)			
TUW-9	1590 ± 100	1570±100	1520±120
TUW-10	1640±90	1620±90	1580±110
TUW-11	1480±120	1470±120	1420±140
TUW-12	1450±100	1430±110	1370±120
TUW-13	1470±130	1450±130	1400±150
TUW-14	670±210	620±210	500±250
TUW-15	1460±110	1430±110	1370±120
TUW-16	1220±190	1200±190	1130±210
Moraine boulders at Austurdalur (E Tungnahryggsjökull foreland)			
TUE-9	740±170	660±170	510±210
TUE-10	1460±100	1430±100	1360±120
TUE-11	380±200	290±200	110±250
TUE-12	400±200	320±190	150±240
Glacially polished ridge Elliði			
ELLID-1	14300±1700	14900±1600	16600±2100
ELLID-2	14200±1700	14800±1700	16500±2100

Table 5.11. ^{36}Cl CRE ages converted to CE/BCE dates according to the different ^{36}Cl production rates from Ca spallation. Uncertainties include the analytical and production rate error.

5.3. Discussion.

5.3.1. ^{36}Cl CRE dating.

The dates obtained in both valleys range from 380±200 CE to 1640±90 CE and are significantly younger than the ages from Elliði polished ridge (Table 5.11). TUW-14 (670±210 CE) could be the only outlier as it is significantly older than the other sample obtained from the same moraine of the stage 3 (TUW-13; 1470±130 CE) and also older than the samples TUW-15 (1460±110 CE) and TUW-16 (1220±190 CE), from the moraine of the previous stage 2 (Fig. 5.2). This would imply assuming nuclide inheritance for sample TUW-14 due to either remobilization of an earlier exposed moraine boulder (see Matthews et al., 2017) or to previous exposure periods, but the high geomorphological dynamism of the slopes limits this possibility (Andrés et al., 2019). Another possible interpretation is that the samples TUW-15 and TUW-16 (stage 2) would be the outliers since they may have experienced incomplete exposure due to post-depositional shielding (Heyman et al., 2011). The possibility of both samples being affected by proglacial processes can be ruled out given the distance to the meltwaters channel or the absence of glacial burst features (see Caseldine, 1985b) in the surroundings of the sampled boulders.

Figure 5.6. Examples of moraine boulders sampled for ^{36}Cl CRE dating in Vesturdalur ("TUW" samples) and Austurdalur ("TUE" samples) and their dates derived from the Licciardi et al. (2008) ^{36}Cl production rate from Ca spallation.

Thus, the ages of samples TUW-14 and TUW-13 would indicate that the moraine of stage 3 was built during two overlapped glacial advances at 670±210 CE and 1470±130 CE. In Austurdalur, the interpretation of the ages is also complex. Samples TUE-9 (740±170 CE) and TUE-10 (1460±100 CE) from the same moraine are significantly different, but it is

difficult to decide whether or not one of these two samples is an outlier. It is also possible that the younger age indicates the timing of a further readvance with the snout reaching the same moraine. It would be necessary to take more samples, but it will be difficult to find other sectors of these moraines that are not affected by slope processes, especially debris-flows. Other possibility to consider is that older boulders may be incorporated in the formation of push moraines as has been shown in maritime Scandinavia, and identified to give overestimated ages for LIA-moraines (Matthews et al., 2017). The hypothesis of supraglacial debris dumping can be rejected due to the lack of supraglacial debris or other features indicative of a palaeo debris-covered glacier. The synchronicity of glacial advances and retreat in both valleys should not be surprising as glaciers can retreat or advance differently in adjacent valleys due to a number of factors such as hypsometry, aspect, gradient, etc. Caseldine (1985a) suggested a high climate sensitivity of the glacier in Vesturdalur due to its steeper wally floor and thinness", which could explain a different behaviour of the glacier compared to the eastern glacier.

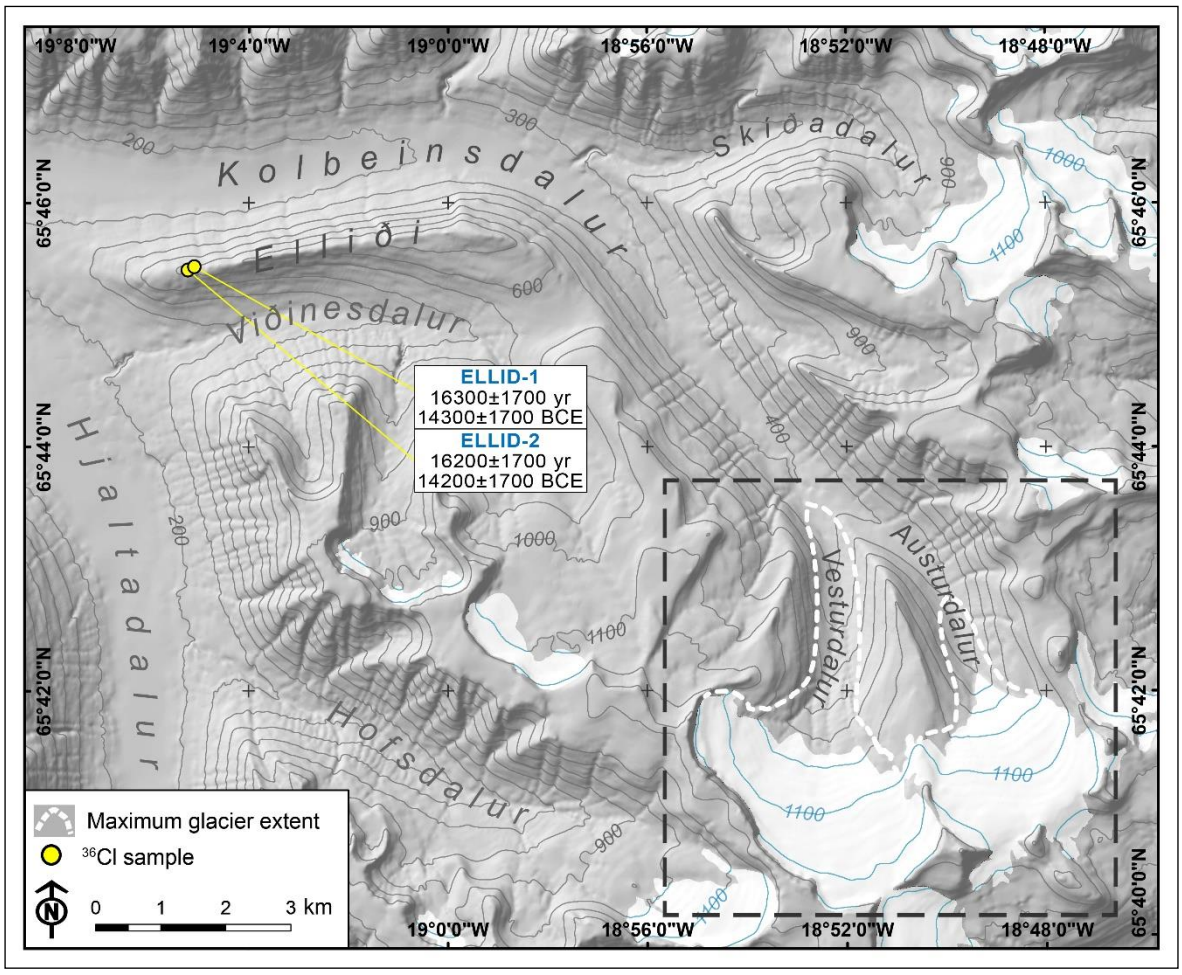

Figure 5.7. Location and BCE dates of the ^{36}Cl samples from the Ellliði crest.

5.3.1.1. Pre-LIA glacial advances.

^{36}Cl CRE dating results from glacially polished surfaces on the Elliði crest show an age of 14250±1700 yr (mean) for the Kolbeinsdalur deglaciation (Fig. 5.7). However, this should be considered as a minimum age since this probably indicates when the retreating and thinning glacier uncovered the ridge, and thus the start of the final deglaciation of the main valley. From this point to the outmost frontal moraines surveyed in this research, no glacially polished outcrops or erratic boulders suitable for ^{36}Cl sampling were found, impeding us to provide further chronological constraints for the deglaciation pattern of these valleys.

Our ^{36}Cl CRE dating results suggest late Holocene glacial advances prior to the LIA, at around ~400 and ~700 CE, in Vesturdalur and Austurdalur, respectively, coinciding with the Dark Ages Cold Period (DACP) (between 400 and 765 CE) in central Europe, according to Helama et al. (2017). In fact, recent synthesis about Icelandic lake records indicate a strong decline in temperature at 500 CE (Geirsdóttir et al., 2018).

The presence of Late Holocene moraines outside the outermost LIA moraines in other valleys of Tröllaskagi has been suggested through radiocarbon dating and tephrochronology in the Vatnsdalur (first, between 4880±325 cal. BCE (tephra Hekla 5) and 3430±510 cal. BCE, and another after 1850±425 cal. BCE; Stötter, 1991), Lambárdalur (before 3915±135 cal. BCE; Wastl and Stötter, 2005), Þverárdalur (before 3500±130 cal. BCE; Wastl and Stötter, 2005), Kóngsstaðadalur (after 1945±170 cal. BCE; Wastl and Stötter, 2005), Barkárdalur (between 375±375 cal. BCE and 190±340 cal. CE and before 460±200 cal. CE; Häberle, 1991) and Bægisárdalur (2280±205 cal. BCE and 1050±160 cal. CE; Häberle, 1991) valleys. Specifically, our oldest ^{36}Cl dates (~400 and ~700 CE) coincide with glacial advances that are radiocarbon dated from intra-morainic peat bogs in other valleys in Tröllaskagi and southern Iceland, e.g. the Barkárdalur II stage (ca. 460 CE) in Subatlantic times (Häberle, 1991, 1994), and given the uncertainties of our dates (200 yr), also with Drangajökull (NW Iceland) advancing at the same time (~300 CE; Harning et al., 2018a). On the other hand, Meyer and Venzke (1985) had already suggested the presence of pre-LIA moraines at Klængshóll (eastern cirque, tributary of Skíðadalur). Caseldine (1987, 1991) proposed a date of 5310±345 cal. BCE as the youngest for a moraine in that cirque, based on tephrochronology (tephra layer Hekla 5 dated in a similar ground in Gljúfurárdalur) and rock weathering measurements using the Schmidt hammer technique. Based on the big size of some moraines in Skíðadalur and Holárdalur, Caseldine (1987, 1991) also supports the hypothesis of pre-LIA moraines formed during several advances. All this information is not in agreement with the hypothesis that all the glaciers in Tröllaskagi

reached their maximum ice extent since the Early Holocene during the LIA (Hjort et al., 1985; Caseldine, 1987, 1991; Caseldine and Hatton, 1994).

In south and central and northwest Iceland, the ice caps reached their Late Holocene maximum advance during the LIA (Brynjólfsson, et al. 2015b; Larsen et al. 2015; Harning et al., 2016b; Anderson et al., 2018a; Geirsdóttir et al., 2018). But also pre-LIA advances have been identified and dated through radiocarbon and tephrochronology in a moraine sequence of Kvíárjökull (south-east Vatnajökull), the first of which occurred at Subatlantic times (before 110±240 cal. BCE) and the second at 720±395 CE (Black, 1990; cited in Guðmundsson, 1997). Considering the uncertainty of our ~400 and ~700 CE dates, these advances likely were coetaneous with other advances reported from southern Iceland in Kötlujökull (after 450±100 cal. CE, radiocarbon dated and supported by tephrochronology; Schomacker et al., 2003) and Sólheimajökull (southern Mýrkdalsjökull, “Ystagil stage”; Dugmore, 1989). In fact, the 669±211 CE advance of western Tungnahryggsjökull (stage 3) also overlaps with the Drangajökull and Langjökull advances at ~560 CE and 550 CE, respectively (Larsen et al., 2011; Harning et al., 2016b) during DACP, in response to the summer cooling between ~250 CE and ~750 CE (Harning et al., 2016b). These advances would correspond to the general atmospheric cooling in the North Atlantic reflected by widespread glacier advances (Solomina et al., 2016).

The timing of the stage 2 in Vesturdalur is difficult to define because the sample TUW-16 (1220±190 CE) has almost 200-year uncertainty, and thus overlaps with both the LIA and the higher temperatures of the Medieval Warm Period (MWP, Lamb, 1965; 950-1250 CE, see Solomina et al., 2016) not conducive to glacier development as it has been observed in northwest and central Iceland (Larsen et al., 2011; Harning et al., 2016b). On the other hand, moraines in Greenland Arctic environments date within the MWP, based on cosmogenic nuclide dating (Young et al., 2015; Jomelli et al., 2016), suggesting a cooling in the western North Atlantic while the eastern sector remained warm. Iceland is located in the middle of this dipole “see-saw” pattern (Rogers and van Loon, 1979). Thus, the correlations with the glacier fluctuations Greenland or Norway, are complicated as the climate anomalies in both regions show opposing signs in the different see-saw modes. To increase the difficulty of interpretation, glaciers of Tröllaskagi are known to surge occasionally (Brynjólfsson et al., 2012; Ingólfsson et al., 2016), which could explain additional complexity in the glacial advances pattern, as it would not be driven by climatic variability. Brynjólfsson et al. (2012) pointed out that only four surges from three glaciers (Teigarjökull, Búrfellsjökull, Bægisárjökull) have been reported in the Tröllaskagi peninsula, where over 160 cirque glaciers exist.

5.3.1.2. LIA glacial advances (15th-17th centuries).

The remaining ^{36}Cl ages obtained from Vesturdalur and Austurdalur are within the 1450-1640 CE range (Tables 5.10 and 5.11) and so correspond to different glacial advances or standstills during the second third of the LIA during the 15th, 16th and 17th centuries. According to our results, one of the largest glacier extents of the LIA culminated in both valleys at the latest around the mid-15th century (samples: TUW-12: 1450±100 CE / stage 6; TUE-10: 1460±100 CE / stage 4). This is a very early date compared to the LIA advances previously dated in Tröllaskagi. Earlier lichenometric research carried out in nearby valleys report more recent dates for the LIA maximum: mid-18th century in Barkárdalur (Häberle, 1991); early 19th century in Bægisárjökull and Skríðudalur (Häberle, 1991), and in Búrfellsdalur and Vatnsdalur (Fig. 7 in Kugelmann, 1991); mid-19th century (1845-1875 CE) in Myrkárjökull, Vindheimajökull (Häberle, 1991), Þverárdalur, Teigardalur, Grýtudalur, Vesturárdalur (Fig. 7 in Kugelmann, 1991), Heiðinnamannadalur and Kvarnárdalur (Caseldine, 1991); and late 19th century (1880s-1890s CE) in Gljúfurárdalur (Caseldine, 1985a, 1991). Caseldine (1991) proposed 1810-1820 CE as the date of the "outer" moraine of Vesturdalur based on a minimum lichenometric age.

According to our ^{36}Cl moraine ages, the LIA maximum of Tungnahryggsjökull glaciers occurred ~400 years earlier than these dates. This should not be surprising as Kirkbride and Dugmore (2001b) reported lichenometric ages >100 years younger than those derived from tephrochronology in the same landforms. Our results also give the earliest LIA dates based on moraine dating obtained so far in Iceland, compared to the previously published dates all obtained through lichenometric dating: 1740-1760 CE in south-east Iceland (Chenet et al., 2010). In northwestern Iceland, glaciolacustrine sediments recorded a contemporary expansion of Drangajökull at ~1400 CE (Harning et al., 2016b). Likewise a first major advance of Langjökull (western central Iceland; Fig. 5.1A) between 1450 and 1550 CE has been reported (Larsen et al., 2011), as well as advances in central Iceland between 1690 and 1740 CE (Kirkbride and Dugmore, 2006), based on varve thickness variance together with annual layer counting and C:N mass ratio, and tephrochronology (geochemical analysis), respectively.

The dates of samples TUW-13, TUW-12 and TUW-11 in Vesturdalur (average date 1470±120 CE; stages 3, 5 and 6) cannot be distinguished statistically if their internal uncertainty is considered (Fig. 5.8; Table 5.11). The spatial scatter of these sampling sites (Fig. 5.2) may indicate frequent and intense terminus fluctuations in a short time interval. Different ages obtained from the moraines of the stages 3 and 4 in Vesturdalur and Austurdalur, respectively, may indicate that in the 15th century the glacier termini reached

the moraines deposited at ~700 CE (Figs. 5.2 and 5.3) and rebuilt them, which may explain the large size of these moraines. Caseldine (1987) argued that other moraines in Skíðadalur were formed during more than one advance. Based on the size of the largest moraines, he also pointed out that many glaciers must have advanced to positions similar to those of the late 19th century earlier in the Neoglacial.

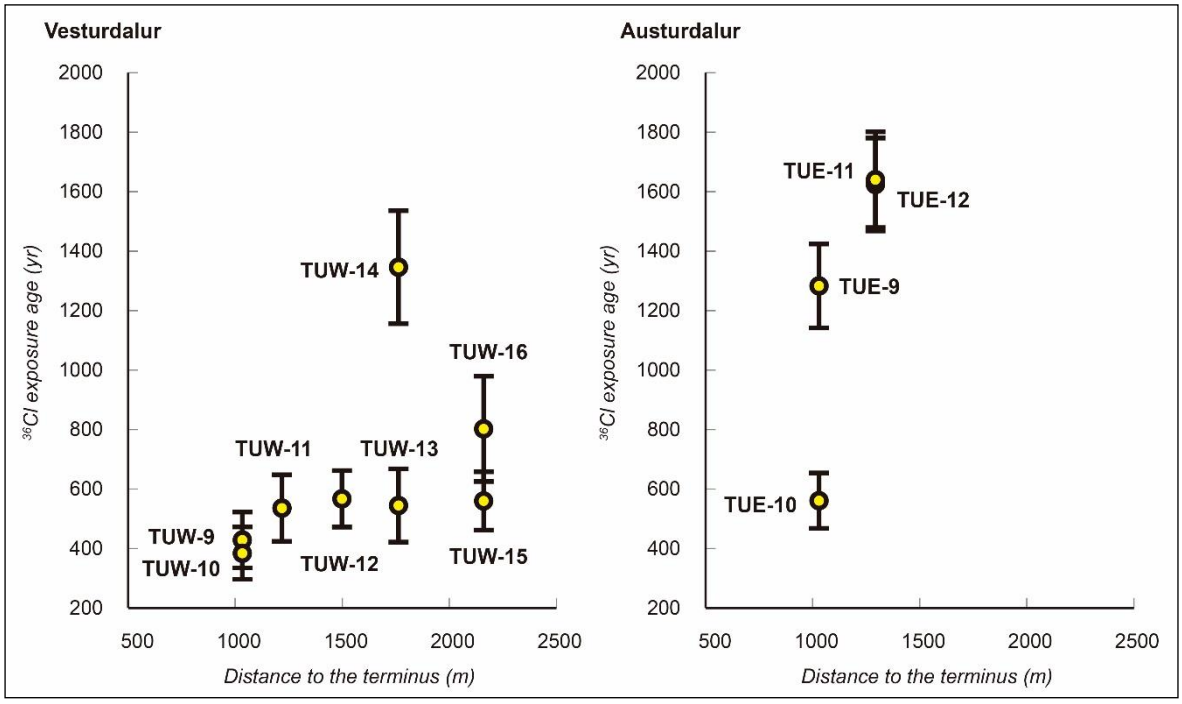

Figure 5.8. ^{36}Cl CRE ages and internal (analytical) uncertainty at 1σ level of the samples from Vesturdalur and Austurdalur. Note that the samples clustering around 500 yr (15th century) in Austurdalur are indistinguishable. Distance to the terminus (year 2005) is measured along the flowline from the reconstructed snout apex of the phase where the samples were collected.

The glacier advances in the 15th century in Vesturdalur and Austurdalur may have been the result of different climate forcings during that century: negative radiative forcing and summer cooling were linked to intense volcanic activity (Miller et al., 2012), the low solar activity of the Spörer Minimum (1460-1550 CE; Eddy, 1976), the sea-ice/ocean feedback with increased sea ice (Miller et al., 2012) and the weakening of the Atlantic Meridional Overturning Circulation (AMOC) (Zhong et al., 2011). Solar activity may have played a major role in these glacial advances if we consider that the climate in the North Atlantic is highly influenced by solar activity variability (Jiang et al., 2015). On the contrary, historical records, although not determinant, suggest a mild climate for 1430-1550 CE (Ogilvie and Jonsdóttir, 2000), and especially for 1412-1470 CE (Ogilvie, 1984). This would also be compatible with increased precipitation and hence more winter snow in warm periods (Caseldine and Stötter, 1993; Stötter et al., 1999; see Chapter 4), and also with potential surge activity with glacial advances not directly linked to specific climate periods (e.g. Brynjólfsson et al., 2012; Ingólfsson et al., 2016).

In Vesturdalur, the dates of samples TUW-9 (1590±100 CE) and TUW-10 (1640±90 CE) are compatible with a cold period from the late 1500s to 1630 CE (Ogilvie and Jónsson, 2001). Nevertheless, considering the uncertainties of these samples, their dates also overlap with the Maunder Minimum (1645-1715 CE) (Eddy, 1976), when the LIA maximum glacial advance occurred in the Alps (Holzhauser et al., 2005).

5.3.2. Lichenometric dating.

5.3.2.1. ^{36}Cl CRE dating vs. lichenometric dating. Multiple lichen species dating approach.

The contrast between our CRE dating results and earlier lichenometry-based results published elsewhere evidences the clear underestimation of the latter. This could be explained either by lichen growth inhibition due to saturation of the rock surface and competition of other thalli (Wiles et al., 2010; Le Roy et al., 2017) or a colonization lag longer than assumed up to now, from 10 to 15 years in Tröllaskagi (Kugelmann, 1991; Caseldine, 1985a, respectively). However, other factors affect the reliability of the lichen-derived ages, and may explain the differences with CRE dates. One of them is the reliability of the growth rates and lichenometric calibration curves that are commonly assumed to be linear (constant) growth in northern Iceland (e.g. Caseldine, 1983, 1985a; Häberle, 1991; Kugelmann, 1991), although it has been demonstrated that the lichen diameter growth declines with age (see e.g. Winkler, 2003, Fig. 8). This might lead to significant age underestimations for the oldest dates, putting potentially earlier dates in the 19th century

Most of the fixed control points from which lichen growth rates have been derived in northern Iceland comprise abandoned gravestones, memorial stones, old bridges and mostly abandoned farmsteads (Caseldine, 1983; Kugelmann, 1991). Time of death is commonly assumed for gravestones, and abandonment date for farmsteads. Although the latter is well known on the basis of historical documentation, the colonization lag sometimes relies on the “the likely duration” of the deterioration of the buildings after abandonment that depends on the quality and stability of the constructions (see Kugelmann, 1991), and hence affect the results. However, it should be highlighted that our approach circumvents this last issue by combining field observations with historical aerial photographs. In addition, given that lichen growth of *Rhizocarpon* subgenus depends mostly on available humidity, the location of the measured lichens has also a potential effect on the results, i.e. to micro-climatic changes (see Innes, 1985; Hamilton and Whalley, 1995a) between the location of the fixed points and the location on the moraine (crest: dryer and more exposed; green zone on the proximal slope, etc.). In the literature cited above about lichenometry-dated LIA

advances no detailed information is provided about the location of the lichen measured for dating purposes, so potential error derived from this issue cannot be assessed. Nevertheless, given that we measured lichens on horizontal flat surfaces where there is no restriction to the moisture receipt of the lichens, we can consider our results presented throughout the next sections valid. In any case, such a great difference of our CRE dates and the previous lichen-derived is more likely to be explained by the technical limitations of the technique rather than environmental factors.

Our field observations and historical aerial photos of known age restricted the dates of the moraines colonized by *Rhizocarpon geographicum* lichens. This approach would support the dates obtained from the 0.44 mm yr^{-1} growth rate of Kugelmann (1991) and the 20-year colonization lag. This rate is slightly higher than those reported from the Antarctic Peninsula (0.31 mm yr^{-1}; Sancho et al., 2017), but lower than in Tierra del Fuego (0.63 mm yr^{-1}; Sancho et al., 2011).

The correlation between the sizes of largest *Rhizocarpon geographicum* and *Porpidia* cf. *soredizodes* thalli at the same stations showed a proportionality between the largest thalli of both species: thalli of *Porpidia* cf. *soredizodes* species grow faster than those of *Rhizocarpon geographicum*. The sizes of the largest *Rhizocarpon geographicum* thalli were plotted against the sizes of the largest *Rhizocarpon geographicum* lichens (Fig. 5.9). The slope of the best-fit linear curve obtained was around 1.675 (r^2=0.82) that suggests that *Porpidia* cf. *soredizodes* lichens grow 1.675 times faster than those of *Rhizocarpon geographicum*. So if we assume 0.44 mm yr^{-1} growth rate for *Rhizocarpon geographicum* lichens, a tentative growth rate of *Porpidia* cf. *soredizodes* would be 0.737 mm yr^{-1}. However, this approach should be taken with caution due to the limited number of lichens (n=7) used of each species. Aiming to obtain a tentative date (Table 5.6), this growth rate was applied to the largest *Porpidia* cf. *soredizodes* lichens found in those stations where no *Rhizocarpon geographicum* lichens could be measured (TUW-1, TUW-8, TUE-1 and TUE-8).

Assuming colonization lags of 20 and 15 years for *Rhizocarpon geographicum* and *Porpidia* cf. *soredizodes* lichens, respectively, and the above-mentioned growth rates, several glacial advances or standstills are tentatively placed in the 19th and 20th centuries, in the context of a general retreat from the most advanced LIA positions, as discussed in the next section.

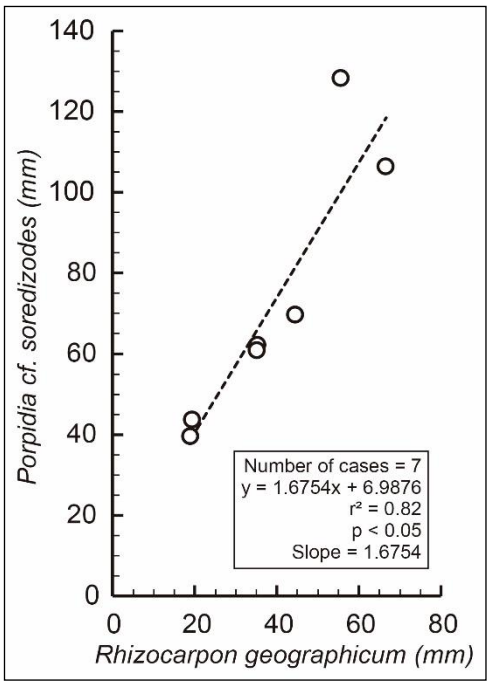

Figure 5.9. Correlation between largest thalli (longest axis) of species *Rhizocarpon geographicum* and *Porpidia* cf. *soredizodes* in several lichenometry stations. With the aim of avoiding those lichens potentially affected for any environmental factor disturbing their normal growth, the largest lichens used come from those lichenometry stations where no lichen size decrease with increasing distance to the terminus was observed (i.e., TUW-2, TUW-4, TUW-5, TUW-6, TUW-2, TUE-4 and TUE-5). From the measurements, it appears that *Porpidia* cf. *soredizodes* lichens grow faster than those of *Rhizocarpon geographicum*.

5.3.2.2. LIA glacial advances/standstills: 19th century.

Despite the low number of lichenometry stations surveyed and the limitations of this dating approach discussed in the previous sections, our results are in accordance with the geomorphological logic and with the chronological frame obtained from historical aerial photos. The ages derived from *Rhizocarpon geographicum* thalli measurements at lichenometry stations pre-dating 1946 suggest that the western and eastern Tungnahryggsjökull culminated successive advances/standstills around the 1830s, 1840s, 1860s and 1890s CE (Figs. 5.2 and 5.3, Table 5.6). Ages tentatively estimated from *Porpidia* cf. *soredizodes* thalli considering its apparently higher growth rate suggest glacial advances/standstills around the 1800s (Figs. 5.2 and 5.3, Table 5.6).

No inconsistence (age inversions) is detected in the lichenometry-dated moraine sequence, but we recognise that some age underestimation may occur since: (i) we assume linear growth when applying a growth rate; and (ii) our 19th dates were derived from >40-45 mm-diameter lichens (Tables 5.5 and 5.6), which exceed the size of the biggest control

point from which Kugelmann's growth rate was estimated (Fig. 3 in Kugelmann, 1991). This problem reinforces the need of taking lichen-derived ages as relative.

The interpretation of the chronology in Austurdalur is more complicated: the lichen sizes measured at the stations TUE-6 (1890s CE, stage 9) and TUE-7 (1880s CE; stage 7) yield more recent dates than at station TUE-5 (1860s CE; stage 10) despite being representative of earlier stages (Fig. 5.3). Given that this anomaly occurs in both lichen species, it is reasonable to conclude that it could indicate a date when the boulders may have been remobilized by postglacial processes. However, this hypothesis cannot be checked as the potential dates obtained are previous to the aerial photograph record. Thus, it would be wise to keep this possibility.

Our chronology of the 19th century glacial advances in both valleys (Table 5.6) does not coincide exactly with the phases identified by Kugelmann (1991) in Svarfaðardalur-Skíðadalur (1810, 1850, 1870-1880, 1890-1900 CE). It also differs appreciably from the chronology proposed by Caseldine (1985a) in Vesturdalur (moraines of 1868, 1878, 1887, 1898 CE). Nevertheless, it should be borne in mind that we are considering only two glaciers with their own glaciological properties. Moreover, we have estimated the ages from the growth rate (instead of a specific calibration growth curve), longer colonization lag based on field observations, and applied to the longest axis measurements (Kugelmann, 1991). On the other hand, micro-climatic differences between the location of fixed points and our lichen measured may occur. However, we recognise that the comparisons with Caseldine's (1985b) results are quite difficult since: (i) the moraines dated by Caseldine are poorly located in his mapping (and hard to identify over aerial photos and our moraine mapping); (ii) we are not able to apply the same parameters to his measurements, as he used the mean longest axis of the five largest lichen is not provided (only the average value); and (iii) he recognised the lichen growth slowdown when dating the outermost moraine, which probably is one of those dated with ^{36}Cl in this work.

Our results, despite the limitations of the applied method, largely due to the low number of moraine boulders suitable for its application can be considered compatible and in good agreement with glacial advances and cold periods during the first third of the 19th century as we show below. Martin et al. (1991) pointed out the existence of a moraine dated to ca. 1810-1820 CE in "Western Tröllaskagi Tungnahryggsjökull" (ambiguously, without providing any detail of its location), as well as others of this period in Svarfaðardalur, Búrfellsdalur and Vatnsdalur. Other dates obtained from more sophisticated statistical techniques applied to lichenometry dating procedures also evidenced a glacial advance phase 1810-1820 CE (Chenet et al., 2010).

These advance phases were coetaneous with significant sea ice persistence in the early 1800s (Ogilvie and Jónsson, 2001), decreased solar activity, and strong volcanic eruptions (Dalton Minimum, 1790-1830 CE; Wagner et al., 2005). The moraines dated in Vesturdalur to around 1830 CE (TUW-7: 1830s CE, stage 10) and the early 1890s CE (TUW-5: 1890s CE, stage 12) are in good agreement with the glacial advances in Svarfaðardalur-Skíðadalur during the 1830s and early 1890s CE (Fig. 8 in Kugelmann, 1991), as well as with the low temperatures and presence of sea ice at these dates (Koch, 1945; Ogilvie, 1996; Ogilvie and Jonsdóttir, 2000; Ogilvie and Jónsson, 2001; Kirkbride, 2002).

5.3.2.3. Post-LIA glacial advances/standstills.

Lichen-derived ages from *Rhizocarpon geographicum* thalli suggest the occurrence of glacial advances or standstills at the first half of the 20th century, culminating in 1910s, 1930s, 1940s and 1950s CE, although the 1930s CE date (TUE-3; stage 12) disagrees with the date inferred from the aerial photos, at some point between 1946 and 1985 CE (Fig. 5.4; Table 5.6). However, the 1910s CE date in both valleys is in good agreement with the moraine abandonment during the first two decades of the 20th century; it would be the result of the accumulated effect of the temperature rise since the latter half of the 19th century (Caseldine, 1987; Wanner et al., 2008). Thus, the subsequent advances would be the response to specific relative thermal minima within a warmer climate (Stötter et al., 1999). The date of TUW-3 (stage 13) representing the moraine abandonment in ~1940 CE is in agreement with the overall context of general glacier retreat as a result of the warmest decades of the 1930s and 1940s CE, which triggered an intense retreat of the glaciers (Einarsson, 1991; Martin et al., 1991; Kirkbride, 2002). The advances/standstills dated to the early 1950s CE in both Tungnahryggsjökull glaciers are likely to be synchronous given the similarity of the dates obtained (Table 5.6). They could represent glacial advances in consonance with the late 1940s – early/mid-1950s CE cooling (Einarsson, 1991; see Chapter 4), recorded both in Akureyri and many other weather stations throughout Iceland. Caseldine (1983) found a similar chronology in Gljúfurárdalur (Skíðadalur headwater, 10 km to the east), with moraine deposition between mid-1910s and 1930, around mid-1930s and late 1940s-1950 CE.

The subsequent trend of the Tungnahryggsjökull glaciers, inferred from aerial photographs, a satellite image, geomorphological mapping, and glacier reconstruction, was characterized by continuous retreat and volume loss, in line with the increasing temperature trend since the end of the LIA. This trend was only reversed between the mid-1960s and mid-1980s CE by a major cooling event (Einarsson, 1991; Sigurðsson, 2005; see Chapter

4). Two moraines have been dated after the 1950s CE. The date obtained in station TUE-1 (1970s CE; stage 14) agrees with the date deduced from the 1946 and 1985 aerial photographs (Fig. 5.4). However, the date estimated in station TUW-1 (1970s CE; between stages 15 and 16) is prior to that obtained from the 1994 and 2000 aerial photographs. The reason for this mismatch may be a non-linear growth phase of the *Porpidia* cf. *soredizodes* thalli measured (i.e. its real growth rate may have been lower than the estimated). Nevertheless, more research on this species is required to use it successfully in lichenometric dating.

The aerial photographs from 1994 (stage 15 western Tungnahryggsjökull) and 2000 (stage 16) show a reversal in the trend of both Tungnahryggsjökull glaciers (Fig. 5.4), as the positions of their termini are more advanced than in 1985 (stages 14 and 15; see Chapter 4). These advances in Vesturdalur and Austurdalur, culminating after 1985 in a period non-conducive to glacier expansion, may have been linked to above average precipitation for 1988-1995, which prevented a negative mass balance of the glaciers (Sigurðsson, 2005). The 2000 aerial photo (stage 16) and 2005 SPOT satellite image (stage 17) display the retreat of both glaciers. This trend was reinforced by the sudden warming initiated in 1995, which triggered decreased snowfall, negative mass balances for 1996-2000, and retreat of the non-surging glaciers after 2000 (Sigurðsson, 2005). In spite of these glacial fluctuations in response to the intense climatic fluctuations of the last century, the ELAs estimated in this chapter only show a general rise of 5-10 m (Table 5.4). This small ELA increase may be derived from some artifacts of the glacier reconstruction or the attenuating effect of the increase in winter precipitation suggested by glacier-climate models (Caseldine and Stötter, 1993; see Chapter 4).

5.3.3. Final remarks: Can the occurrence of pre-LIA glacial advances be confirmed? Was the LIA in northern Iceland the Holocene glacial maximum? Was it a single maximum advance?

Our results demonstrate that Tungnahryggsjökull advanced during Late Holocene glacial stages prior to the LIA and reached considerably more advanced positions, even though the Iceland large ice caps reached generally their Late Holocene maximum advance during the LIA (Larsen et al. 2015, Harning et al., 2016b; Anderson et al., 2018a, Geirsdóttir et al., 2018). The chronological data presented in the previous sections suggests that during the LIA the glaciers overlapped moraines deposited in pre-LIA glacial stages. Our results also show LIA advances since the 15th century and are thus contrary to the traditional proposal of a single maximum LIA advance occurring during either mid-18th or late-19th

centuries in Tröllaskagi peninsula, followed by subsequent minor readvances in an overall retreating trend (see Caseldine, 1983, 1985a, 1987; Kugelmann, 1991; Martin et al., 1991).

The use of the ^{36}Cl production rates from Ca spallation reported by Stone et al. (1996) does not lead to major changes in the interpretation and conclusions as the changes in the nominal dates (up to 90 yr earlier; Table 5.11) are within the external uncertainty and also overlap with the results presented above based on the Licciardi et al. (2008) production rate. Similarly, if we consider the results derived by the Schimmelpfennig et al. (2011) production rate, we obtain even earlier dates, which still overlap with the results derived by the other production rates due to a higher external uncertainty (see Table 5.11).

Although the snow cover duration is known to be high in northern Iceland (see Dietz et al., 2012), quantifying the effect of snow cover on sub-surface ^{36}Cl production is a complex issue: on the one side, snow lowers the isotopic production rates related to spallation reactions due to the shielding effect on high-energy neutrons (Benson et al., 2004; Schildgen et al., 2005), and on the other side it increases the ^{36}Cl production rate from thermal neutrons below the rock surface, due to the enhancing effect of hydrogen on these low-energy neutrons (Dunai et al., 2014). Both effects might cancel out depending on the composition of the samples, and their quantification is still debated and affected by high uncertainties (Zweck et al., 2013; Dunai et al., 2014; Delunel et al., 2014). Given this complexity, snow shielding was not applied. In any case its effect is unlikely to be higher than the uncertainty derived from extracting ^{36}Cl from whole rock instead of minerals.

Our results are in concordance with several valleys in northern Iceland, but also with the results that are being obtained in other sectors of Arctic and North Atlantic region in the last years, such as: in Baffin Island (northern Canada), where glaciers reached Late Holocene maximum positions prior to the LIA (Young et al., 2015; ^{10}Be dating), or West Greenland, with several advances or stabilizations at 1450±90 CE and 1720±60 CE (Jomelli et al., 2016; ^{36}Cl dating). However, it is striking that the early LIA advances of northern Iceland reported in the present chapter do not agree with maritime Norway, with later maximum culminations (see Nesje et al., 2008) despite being the glaciated region most comparable with Iceland in terms of climate and glaciology. Given that both Icelandic and Norwegian (western sector) climates are affected by the NAO in the same way, the time differences of the LIA culminations could be explained by variations in the response time or the hypsometry –or even different combinations of both– of glaciers in both areas. In any case, such a complex issue needs further investigation.

Our results also agree with farther and southern areas such as the Alps, with maximum advances at around 1430 CE (Schimmelpfennig et al., 2012, 2014b; ^{10}Be dates);

and Sierra Nevada (Iberian Peninsula), where LIA advances have been reported between the 14th and 17th centuries (Palacios et al., 2019; ^{10}Be dates). Culminations prior to the 19th century have also been reported in the Maritime Alps (Federici and Stefanini, 2001), with older depositional phases during the 13th and 14th centuries and major advances during the 17th century. Our detailed moraine mapping, combined with CRE dating in the surveyed valleys, clearly shows a number of advances throughout the LIA, in response to the great climatic variability of the region with alternating cold and mild/warm periods (Ogilvie, 1984, 1996; Ogilvie and Jónsdóttir, 2000; Ogilvie and Jónsson, 2001; Geirsdóttir et al., 2009) as occurred in the Alps (e.g. Schimmelpfennig et al., 2014b) or the Iberian mountains (e.g. Oliva et al., 2018). The ELA calculations show that the major long-lasting rise of the glacier ELA (24-50 m depending on the calculation method) took place prior to 1900s/1910s.

According to the results, the evolution pattern described in the Chapter 4 for the Tungnahryggsjökull glaciers should be revised as the ^{36}Cl CRE dates from the 15th and 17th centuries indicate that LIA maximum was reached earlier than previously thought. Thus, if we consider the ELA of the earliest LIA dates obtained with ^{36}Cl CRE (i.e. stages 5 and 4 of western and eastern Tungnahryggsjökull), these imply ELA depressions (with reference to the 2005 date) of 24-50 m (depending on the ELA calculation method), occurring for at least 560 years (Table 5.4) and not 150 years as had been previously assumed (Caseldine and Stötter, 1993; see Chapter 4).

5.4. Conclusions.

This chapter highlights the detailed geomorphological analysis of the glacial landforms as an essential pre-requisite prior to the application of dating methods on them. Nevertheless, this has greatly limited the number of valid moraine boulders to be dated, since the vast majority of those were affected by post-glacial processes. This issue which has prevented a statistically acceptable sampling and the validation or invalidation of the "inconsistent" ages yielded by several boulders, so a conclusive explanation cannot be given.

Applying ^{36}Cl CRE dating for the first time in the Tröllaskagi peninsula enabled us to identify pre-LIA glacial advances in Vesturdalur and Austurdalur. Thus, the western and eastern Tungnahryggsjökull glaciers did not reach their Late Holocene maximum extent during the LIA. The maximum extent for the eastern glacier was dated to ~400 CE. For the western glacier a latest date of ~700 CE and an earliest of 16300 years ago (when the Ellið crest was deglaciated) have been obtained.

The LIA maximum in Vesturdalur and Austurdalur was reached by the 15th century at the latest. A combination of detailed moraine mapping and ^{36}Cl CRE dating confirm a number of glacial advances between the 15th and 17th centuries, the earliest LIA advances dated in Tröllaskagi at present.

For the recent dates, the complementary use of aerial photographs, a satellite image and fieldwork has aided to obtain lichenometry-derived ages tentatively in good agreement with the morpho-stratigraphic order of the glacial landforms. It has also compensated some of the limitations and error sources of lichenometric dating. Thus, it has proved to be a useful tool to assess the colonization lags and the validity of the lichenometry-derived ages.

Fieldwork on recently deglaciated surfaces and historical aerial photographs have shown clearly that the colonization lag of *Rhizocarpon geographicum* lichen species is from 15-21 to 30 years, considerably longer than previously assumed in Tröllaskagi. Colonization of the *Porpidia* cf. *soredizodes* species is shorter, between 10 and 21 years.

From the measurements carried out in different lichenometry stations, growth of *Porpidia* cf. *sporedizodes* lichen appeared to be higher than in the case of *Rhizocarpon geographicum*, and proportional to that. Its growth rate has been tentatively estimated for the first time, at around 0.737 mm yr^{-1}. However, further research on the growth rates of this species is required for its potential use in lichenometric dating as a complementary species, since it also shows a shorter colonisation lag than *Rhizocarpon geographicum*.

Chapter 6.

The origin of rock glaciers and debris-covered glaciers in the context of the deglaciation.

6.1. Introduction.

Rock glaciers and debris-covered glaciers are indicative of important tipping point phases in regional climatic and geomorphological evolution (Winkler and Lambiel, 2018, Anderson et al., 2018a). In this work we follow the differentiation between debris-covered glaciers and rock glacier features proposed by Janke et al (2015), which can also be applied to their derived landforms, once the internal ice has disappeared in both cases (Fernández-Fernández et al., 2017).

6.1.1. The climatic significance of rock glaciers and debris-covered glaciers.

The existence and dynamics of rock glaciers may indicate:

(i) Permafrost in the region and a Mean Annual Air Temperature (MAAT) ≤ -4ºC at present or in the past if they are fossil rock glaciers (e.g. Barsch, 1996).

(ii) The climatic evolution that led to the transformation from debris free glaciers to rock glaciers (Johnson, 1980; Giardino and Vitek, 1988; Ackert, 1998; Janke et al., 2015; Anderson et al., 2018b; Kenner, 2019 and others), except rock glaciers which have no relationship with a glacial origin (e.g. Barsch, 1996).

(iii) The climatic evolution during their active existence (Humlum, 1998; Berger et al., 2005, Paasche et al., 2007; and others), e.g. when an increase in environmental temperature can either accelerate (Delaloye et al., 2008; Kellerer-Pirklbauer, 2012; Kellerer-Pirklbauer and Kaufmann, 2012; Kellerer-Pirklbauer et al., 2017; Wirz et al., 2016; Eriksen et al., 2018; Kenner, 2019) or paralyze the rock glacier flow (Emmer et al., 2015; Tanarro et al., 2019).

(iv) The geomorphological evolution of the walls and slopes surrounding the rock glaciers (Humlum, 2000), which can transform these rock glaciers without any direct relationship with climatic changes (Deline et al., 2015; Anderson and Anderson, 2016).

(v) The amount of water supplied to the rock glacier (Kenner et al., 2018; Jones et al., 2018).

Existence and evolution of debris-covered glaciers can also indicate climatic and geomorphological changes, such as their origin in the transformation from a debris-free glacier caused by an increase in ablation, the intensification of the geomorphological processes in the surrounding slopes, or the combination of both factors (Kirkbride, 2000, 2011; Brenning, 2005; Azócar and Brenning, 2010; Mayr and Hagg, 2019). The climate changes can also trigger changes in the dynamics of debris-covered glaciers (Benn et al., 2012; Pelto et al., 2013; Hambrey et al., 2008; Glasser et al., 2016). Nevertheless, these changes may also be due to variations in the debris supply derived from the geomorphological activity on the slopes (Anderson and Anderson, 2016; Anderson et al., 2018b; Mayr and Hagg, 2019). In fact, this dual dependence greatly complicates the interpretation of the changes that debris-covered glaciers undergo (Gibson et al., 2017). In this sense, debris-covered glaciers can evolve to rock glaciers throughout various phases driven by climatic evolution and increased debris supply in their environment (Janke et al., 2015; Monnier and Kinnard, 2015; Andrés et al., 2016, Anderson et al., 2018b; Mayr and Hagg, 2019).

Climatic, environmental and geomorphological changes can differentiate several phases of activity in rock glaciers and debris-covered glaciers (Anderson et al., 2018b). They can transform from dynamically active (with flowing ice) to become static (with stagnant internal ice) (Potter et al., 1998; Janke et al., 2013; Emmer et al., 2015; Tanarro et al., 2019). Furthermore, rock glaciers and debris-covered glaciers can melt completely and become a “fossil” feature (without internal ice), although determining when such changes occur is very difficult (Barsch, 1996; Haeberli et al., 2006). In this sense, it is important to know the dynamics and trend of these formations, which have been highlighted as authentic water reservoirs (Rangecroft et al., 2015).

6.1.2. Timing of rock glaciers and debris-covered glaciers.

Rock glaciers and debris-covered glaciers therefore contain valuable environmental information. Recent intensified studies focus on monitoring their dynamics (e.g. mobility) on a very reduced time scale, but with increasingly sophisticated techniques (Benn et al., 2012; Bosson and Lambiel, 2016; Capt et al., 2016; Emmer et al., 2015; Lippl et al., 2018 ; Kenner

et al., 2018). In spite of the great potential of long-timescale understanding that the dating of active, static or fossil rock glaciers and debris-covered glaciers might allow, it has attracted little attention of researchers in recent years in contrast with debris free glacial chronology, for example, throughout all of North America, where rock glacier landforms are common (Phillips, 2016; Briner et al., 2017; Leonard et al., 2017; Vázquez-Selem and Lachniet, 2017; Licciardi and Pierce, 2018).

Timing the formation of rock glaciers and debris-covered glaciers is often deduced by extrapolating their current dynamics to the past (Ackert, 1998; and many other subsequent studies), without considering the dynamic and morphological changes that these formations can undergo over time (Tanarro et al., 2019). Regional studies have traditionally framed the relative age of rock glaciers within the context of glacial evolution, with support from lake and moraine soil radiocarbon dating (Benedict, 1973; and others).

The need to apply more reliable dating methods to rock glaciers has been proposed for years (Haeberli et al., 2003). Dating rock glaciers methods include:

(i) Lichenometry, the method most commonly applied to rock glaciers (Benedict, 1973; Konrad and Clark, 1998; and others) obtains the stabilization point in time of the boulders, within an age range of the last few hundred years, although its application to rock glaciers presents many difficulties (Rosenwinkel et al., 2015).

(ii) Radiocarbon dating of lacustrine sediment overlapped by rock glaciers (Paasche et al., 2007) or dendrochronology of tree trunks buried by rock glacier debris (Bachrach et al., 2004), although these circumstances very seldom exist.

(iii) Schmidt Hammer dating to determine the stabilization age of rock glaciers from the rock weathering, although this method also requires complex complementary information to determine the minimum stabilization age (Matthews et al., 2013; Scapozza et al., 2014), e.g. combining this method with lichenometry (Galanin et al., 2014).

(iv) Luminescence dating, a method which also presents serious complications of interpretation when applied to rock glaciers (Fuchs et al., 2013).

Over the last ten years, Cosmic-Ray Exposure (CRE) dating methods have been applied to rock glaciers and debris-covered glaciers, although this can still be considered as an initial phase. Beryllium-10 CRE dating has been applied successfully to date stabilization time of rock glaciers in Scotland (Ballantyne et al., 2009), the Alps (Hippolyte et al., 2009) and the Iberian Peninsula (Palacios et al., 2017; Rodriguez-Rodriguez et al., 2017; Andrés et al., 2018). Correlation between ^{10}Be CRE ages and Schmidt Hammer rebound (R- values) has also been applied in recent years to date rock glaciers (Winkler,

2009) obtaining very satisfactory results (Winkler and Lambiel, 2018). ^{10}Be CRE dating has also been applied to approach the stabilization of fossil debris-covered glaciers (Fernandez-Fernandez et al., 2017) and to date rock avalanches events on active debris-covered glaciers (Deline et al., 2015). The isotope Hellium-3 has been applied to study the dynamics of debris-covered glaciers (Mackay and Marchant, 2016). Chlorine-36 CRE dating has been successfully applied to date the stabilization period of several rock glaciers in the Iberian Peninsula (Palacios et al., 2012; 2015a, 2015b; 2016), the Alps (Moran et al., 2016); and the Karçal Mountains in the Lesser Caucasus (Dede et al., 2017).

However, a recent application of the CRE methods has shown that boulders on the surface of rock glaciers and debris-covered glaciers with limited flow may have received cosmic radiation before their definitive motionless (Mackay and Marchant, 2016). In fact, active rock glaciers ice can be very old; e.g. radiocarbon dating of plant macrofossil remains in a rock glacier core in the Alps obtained >10 ka (Krainer et al., 2014). ^{10}Be dating of boulders from cold based debris-covered glaciers in the Antarctica allowed to deduce that the ice is >1 (Mackay and Marchant, 2016) or even >2 million years old (Bibby et al., 2016). However, it has been proved that due to the limited trajectory and erosion of the boulders in a rock glacier, they may retain nuclide inheritance prior to deposition (Çiner et al., 2017).

6.1.3. Cosmic-Ray Exposure dating in northern Iceland.

Chlorine-36 CRE dating has been applied in northern Iceland to date the deglaciation (Principato et al., 2006; Brynjólfsson et al., 2015a, Andrés et al., 2019). ^{36}Cl has been successfully proposed for basalts, which is the predominant bedrock in northern Iceland (Swanson and Caffee, 2001; Phillips, 2003; Principato et al., 2006; Licciardi et al., 2006, 2007, 2008; Schimmelpfennig, 2009; Schimmelpfennig et al., 2009, 2011).

Two of the cirques in the Víðinesdalur valley (Tröllaskagi peninsula) are occupied by rock glaciers and debris-covered glaciers respectively, namely the Fremri-Grjótárdalur, where there is a large rock glacier complex, and the Hóladalur, where there is essentially a large debris-covered glacier, Hóladalsjökull. These rock glaciers and debris-covered glacier have attracted the attention of researchers to determine their flow dynamics (Wangensteen et al., 2006; Farbrot et al., 2007; Kellerer-Pirklbauer et al., 2007; Lilleøren et al., 2013; Tanarro et al., 2019), although CRE dating methods have not yet been applied. A combination of multi-temporal aerial photo imagery, lichenometric procedures and ^{36}Cl CRE dating been proposed in the Chapter 4 to approach the evolution of the two nearby Tungnahryggsjökull debris-free glaciers during late Holocene.

6.1.4. Objectives.

The aim of this work is:

(i) To investigate whether CRE dating method can be applied to determine the formation timing of rock glaciers and debris-covered glaciers.

(ii) To illuminate about their evolution in order to see the potential for future research contributing to our knowledge of the climatic and glacial evolution of the Tröllaskagi peninsula.

Before applying CRE dating, we carried out high-precision boulder mobility measurements of active rock glaciers and debris-covered glaciers, aiming to relate the results to the stability degree of the analysed features. This method was applied to the rock glaciers of the Fremri-Grjótárdalur cirque and the debris-covered glaciers of the Hóladalur cirques in the Víðinesdalur valley, and Hofsdalur and Héðinsdalur valleys (see Fig. 2.2 in Chapter 2).

6.2. Previous research.

6.2.1. Permafrost, temperature and precipitation.

The snout of the debris-covered and rock glaciers in Tröllaskagi are found at 900-950 m a.s.l., where the MAAT is -1.8 to -2.6 ºC (Kellerer-Pirklbauer et al., 2007) and precipitation around 1500-2000 mm (Crochet et al., 2007). The continuous permafrost limit is located between 850-950 m a.s.l. (Etzelmüller et al., 2007; Wangensteen et al., 2006). The current ELA of the main debris-free glaciers close to the study cirques is 1010-1060 m a.s.l., with the MAAT around -2.3 ºC (see Chapter 4). These glaciers reached their LIA maximum ca. 1865-1900, according to Caseldine (1985a) or in the 15th century or early according to the CRE results of the Chapter 5. During this maximum the ELA was about 950-1010 m a.s.l. and the MAAT 1.7-1.9 ºC lower than at present (Caseldine and Stötter, 1993; see Chapter 4).

6.2.2. The deglaciation of the main valleys of Tröllaskagi.

The CRE dating (Andrés et al., 2019), combined with previous radiocarbon results (see synthesis in Pétursson et al., 2015), indicates that the glacier outlet of the Skagafjörður fjord, flowing down from the Icelandic Ice Sheet (IIS), was situated in the outermost sector of the fjord at approximately 17-15 ka. Subsequently, this glacier outlet retreated and occupied the central part between 15-12 ka, and then the innermost part of the fjord around

11 ka. After 11ka, rapid deglaciation affected the fjord, when the IIS outlet glacier almost reached dimensions similar to the Hofsjökull ice-cap in central Iceland. Norðdahl (1991a, 1991b) emphasized that most of the Tröllaskagi valleys run N-S, thus facilitating the flow of the IIS outlets, but important secondary valleys in these mountains were outside these flows. Ingólfsson (1991) and Norðdahl (1991a, 1991b) summarized the studies carried out on the possible glaciation of the Tröllaskagi summits and show how most geomorphologists and palaeobotanists in the early 20th century argued for an ice-free scenario for these summits during the LGM. This hypothesis was supported by simulation models (Hubbard et al., 2006). In fact, ice-free plateaus on the Tröllaskagi summits during the LGM may have served as refugia for flora and fauna (Rundgren and Ingólfsson, 1999).

6.2.3. Rock glaciers and debris-covered glaciers of the Tröllaskagi peninsula.

6.2.3.1. Origin.

The origin of Fremri-Grjótárdalur and Hóladalsjökull rock glaciers and debris-covered glaciers is still under discussion. Their age has been inferred from headwall recession, based on a rate of 0.4-1.2 mm yr^{-1} (Farbrot et al., 2007). Through streamline interpolations from present surface velocities, Wangensteen et al. (2006) estimated maximum age of the rock glaciers to be about 4.5-5 ka BP, with reactivation of the higher lobes about 1.0-1.5 ka BP. Using a combination of the same method and Schmidt hammer dating, Kellerer-Pirklbauer et al. (2007, 2008b) proposed an age contemporary with the 8.2 ka event (8.6-8.0 cal. ka BP according to Greenland stratigraphy; Alley and Ágústsdóttir, 2005) for Fremri-Grjótárdalur fossil rock glaciers. Kellerer-Pirklbauer et al. (2007, 2008b) proposed that the origin of the active rock glacier was related to one of the first neoglacial advances occurred in Tröllaskagi about 5.9-5.2 cal. ka BP, with reactivation during the second neoglacial advance by 3.2-3.0 ka (Kellerer-Pirklbauer et al., 2007). From a combination of headwall recession rate and lichenometric dating, the Nautárdalur rock glacier, located a few km to the east, was considered to be about 0.2 ka old and related to the Little Ice Age glacial expansion (Martin et al., 1994; Hamilton and Whalley, 1995a, 1995b).

6.2.3.2. Dynamics.

The dynamics of these rock and debris-covered glaciers are also under discussion. Using data obtained by digital photogrammetry, Wangensteen et al. (2006), proposed block displacement rates ranging from less than 0.10 m yr^{-1} to a maximum of 0.84 m yr^{-1} in the Hóladalsjökull debris-covered glacier and a maximum of 0.74 m yr^{-1} in the Fremri-Grjótárdalur rock glacier. Kellerer-Pirklbauer et al. (2007) used similar techniques in the Fremri-Grjótárdalur rock glacier and obtained rates of 0.06 m yr^{-1} - 0.74 m yr^{-1}. Lilleøren et

al. (2013) used satellite radar interferometry and reported block displacement rates of 0.2–0.5 m yr^{-1} in some rock glaciers in Tröllaskagi. Tanarro et al. (2019) applied jointly manual and digital photogrammetry, obtaining a mean velocity of 0.33 m yr^{-1} for the Hóladalsjökull debris-covered glacier, mainly connected to surface lowering processes derived from ice degradation, and insignificant movement for the Fremri-Grjótárdalur rock glacier. These results are similar to those obtained in the Nautárdalur glacier, where boulder movement measured by theodolite during a 17-year period ranged from <0.05 m yr^{-1} - 0.31 m yr^{-1}, with the snout advancing <1 m during this period (Whalley et al., 1995a, 1995b).

6.3. Field strategy.

Three complementary methodological steps of this Chapter focus on the Fremri-Grjótárdalur rock glaciers and the Hóladalsjökull, Hofsjökull and Héðinsdalsjökull debris-covered glaciers. The first step was to determine when the deglaciation occurred in these valleys and in each of the two cirques. The second step was to determine the exposure age of the boulders of the fossil rock glaciers located in the Fremri-Grjótárdalur cirque. In this sense, the fossil rock / debris-covered glaciers are representative of the first landforms generated after deglaciation inside the cirques. The application of this strategy, following a clear chronological sequence indicated by the geomorphological landform disposition, will allow the reconstruction of the deglaciation phases and the rock glacier formation.

The final step was to determine the stabilization period of the frontal boulders of the debris-covered glaciers that still conserve underlying ice. For sufficiently representative sampling, it was decided to take samples from boulders of both the Hofsjökull and Héðinsdalsjökull debris-covered glaciers. By this way, we will be able to deduce whether the stabilization moment of these debris-covered glaciers is synchronous in different valleys of Tröllaskagi.

Previous to CRE sampling of the fronts at the active debris-covered glaciers and rock glaciers, a photogrammetric analysis was applied to these boulders to measure their flow and hence their stability degree in the last decades, in order to avoid that high-mobility or potentially overturned boulders are sampled. We were able to identify boulders in the following units:

I. Two moraine boulders in the Hóladalsjökull cirque (representative of samples HO-1, HO-2).

II. A boulder in the moraine of the Fremri-Grjótárdalur cirque (sample FDG-11), and two further boulders from the same ridge.

III. Three boulders on the crest of the lobe of the western fossil rock glacier in Fremri-Grjótárdalur (samples FGD-1, FDG-2).

IV. (iv) Three boulders on the lowest lobe of the eastern fossil rock glacier in Fremri-Grjótárdalur cirque (samples FGD-4B, FDG-5B).

V. Five boulders on the steep transversal ridge in the western lobe of the active Fremri-Grjótárdalur rock glacier (samples FGD-1B, FGD-2B, FDG-3B).

VI. Ten boulders in one ridge at the front of the Hofsjökull debris-covered glacier (samples HOFS-1, HOFS-2, HOFS-3).

Finally, we compiled a database including X and Y coordinates, and altitude (Z) of each boulder in both dates. These data were then processed to obtain the horizontal displacement and elevation difference for each boulder.

6.4. Results.

6.4.1. Movement of boulders from rock glaciers and debris-covered glaciers with internal ice.

The results of the horizontal movement and elevation changes of the analysed boulders are presented in Table 6.1.

The moraine boulders HOL-1 and HOL-2, located in the Hóladalsjökull cirque, have remained stable during the 14 year observation period. Horizontal movement (0.052 and 0.022 m yr^{-1}) and elevation changes (-0.04 and 0.06 m yr^{-1}) are negligible and within the RMSE of our analysis. We obtained similar results from the analysis of the moraine boulders in the Fremri-Grjótárdalur cirque, where sample FDG-11 was collected. There is the exception of one boulder, which indicates a slight horizontal movement of 0.108 m yr^{-1}, while the rest hardly show any movement, with maximum about 0.05 m yr^{-1}.

We obtained similar results from the boulders located on the ridges at the Fremri-Grjótárdalur fossil rock glaciers. For example, in the western rock glacier from which samples FDG-1 and FDG-2 were collected, we obtained displacement rates of less than 0.047 m yr^{-1} and maximum elevation difference of -0.43 m yr^{-1}. In the eastern rock glacier by samples FGD-4B and FGD-5B, we obtained a movement of 0.022 m yr^{-1}, and maximum elevation changes of -0.36 m yr^{-1}.

Geomorphological units	CRE sample	Analized boulders	Year 1980			Year 1994			1980-1994 period			
			X (m)	Y (m)	Elevation (m a.s.l.)	X (m)	Y (m)	Elevation (m a.s.l.)	Horizontal displacement		Elevation changes	
									Abs. (m 14 yr^{-1})	Velocity (m yr^{-1})	Abs. (m 14 yr^{-1})	Velocity (m yr^{-1})
Moraine boulders at Hóladalsjökull cirque	HOL-1	B-1	501384.27	581422.77	835.36	501384.99	581422.70	835.32	0.723	0.052	-0.04	-0.003
	HOL-2	B-2	501393.24	581350.79	839.98	501392.94	581350.62	840.04	0.345	0.025	0.06	0.004
Moraine boulders at Fremri-Grjótárdalur cirque	FDG-11	B-4	499246.73	580783.27	897.57	499247.03	580781.79	897.53	1.510	0.108	-0.04	-0.003
		B-5	499248.00	580769.41	898.00	499247.80	580768.72	897.93	0.718	0.051	-0.07	-0.005
		B-6	499266.84	580740.85	899.42	499267.27	580740.50	899.74	0.554	0.040	0.32	0.023
Frontal ridge at Fremri-Grjótárdalur western fossil rock glacier	FDG-1, FDG-2	B-7	498805.31	580940.54	871.31	498804.97	580940.22	871.04	0.467	0.033	-0.27	-0.019
		B-8	498828.64	580944.99	866.63	498828.92	580944.85	866.20	0.313	0.022	-0.43	-0.031
		B-9	498871.17	580933.82	867.89	498871.83	580933.79	867.78	0.661	0.047	-0.11	-0.008
Transverse ridge at upper lobe of Fremri-Grjótárdalur western rock glacier with internal ice	FGD-1B, FGD-2B, FGD-3B	B-10	499163.16	580369.13	950.27	499161.8	580370.94	950.20	2.264	0.162	-0.07	-0.005
		B-11	499153.50	580345.39	951.61	499153.30	580347.20	951.57	1.821	0.130	-0.04	-0.003
		B-12	499172.04	580338.82	953.45	499171.96	580340.40	953.62	1.582	0.113	0.17	0.012
		B-13	499221.77	580333.74	952.24	499221.59	580334.79	952.16	1.065	0.076	-0.08	-0.006
		B-14	499153.33	580314.13	956.72	499152.87	580315.89	956.53	1.819	0.130	-0.19	-0.014
Frontal ridge at Fremri-Grjótárdalur eastern fossil rock glacier	FGD-4B, FGD-5B	B-15	499645.82	580131.39	989.73	499645.73	580131.51	989.76	0.150	0.011	0.03	0.002
		B-16	499659.70	580127.30	993.74	499659.43	580127.46	993.38	0.314	0.022	-0.36	-0.026
		B-17	499651.98	580097.27	992.21	499651.94	580097.29	992.00	0.045	0.003	-0.21	-0.015

Table 6.1. Inventory of the photogrammetry-tracked boulders surveyed in the different geomorphological units their mobility measurements for the 1980-1994 period. Note that the low mobility figures pose the sampled boulders as highly reliable.

Geomorphological units	CRE sample	Analized boulders	Year 1980			Year 1994			1980-1994 period			
			X (m)	Y (m)	Elevation (m a.s.l.)	X (m)	Y (m)	Elevation (m a.s.l.)	Horizontal displacement		Elevation changes	
									Abs. (m 14 yr^{-1})	Velocity (m yr^{-1})	Abs. (m 14 yr^{-1})	Velocity (m yr^{-1})
Frontal ridges at Hosfdalur debris-covered glacier	HOFS-1, HOFS-2, HOFS-3	B-18	502428.88	575959.77	887.63	502424.46	575959.28	887.04	4.447	0.318	-0.59	-0.042
		B-19	502393.88	575939.80	884.95	502390.67	575943.19	883.69	4.669	0.333	-1.26	-0.090
		B-20	502400.52	575931.57	887.51	502396.74	575934.19	886.48	4.599	0.329	-1.03	-0.074
		B-21	502411.46	575920.45	891.44	502407.88	575923.78	890.89	4.889	0.349	-0.55	-0.039
		B-22	502413.24	575917.63	892.38	502409.12	575920.74	891.60	5.162	0.369	-0.78	-0.056
		B-23	502416.01	575675.23	926.16	502412.97	575677.98	925.85	4.099	0.293	-0.31	-0.022
		B-24	502382.18	575667.46	923.25	502379.86	575669.72	923.06	3.239	0.231	-0.19	-0.014
		B-25	502408.02	575627.08	933.75	502406.13	575628.55	933.42	2.394	0.171	-0.33	-0.024
		B-26	502400.35	575616.67	934.97	502398.34	575618.54	934.54	2.745	0.196	-0.43	-0.031
		B-27	502425.77	575603.09	940.43	502423.72	575604.54	940.39	2.511	0.179	-0.04	-0.003

Table 6.1. (cont.)

Logically, different results were obtained from the analysis of the boulders located on the rock glacier ridges that still contain internal ice (representative for samples FGD-1B, FGD-2B and FGD-3B), although the movement is very slow, between 0.076 m yr^{-1} and maximum 0.162 m yr^{-1}. These values, therefore, would indicate displacements of 1.6 and 2.2 m in 14 years. The elevation differences are negative, but negligible, between -0.04 and -0.19 m yr^{-1}.

We also obtained very small displacements on the front of the Hofsjökull debris-covered glacier (boulders from which samples HOFS-1, HOFS-2 and HOFS-3 were collected). The horizontal displacement rates of the boulders ranges from 0.18 m to 0.37 m yr^{-1}, indicating about 2.5 and 5.16 m displacement and elevation changes of -0.19 to -1.26 m.in 14 years.

Our results suggest that the sampled boulders located in rock glaciers and debris-covered glaciers with internal ice have a minimum displacement rate in the last decades, mainly related to ice degradation and subsidence, not to horizontal flow.

6.4.2. Deglaciation of the Tröllaskagi internal valleys: geomorphology and CRE dating.

Fieldwork and moraine mapping was carried out in the Víðinesdalur valley, and Hofsdalur and Héðinsdalur valleys, during the summers of 2012, 2014 and 2015, exploring for erratic boulders or glacially polished bedrock surfaces suitable for applying the CRE method. The high number of landslides and other slope processes have transformed and covered the glacial landforms of the valley. No bedrock outcrops, or any existing outstanding block in the relief were observed, with the exception of those generated by post-glacial rock avalanches. The only exceptions observed during the fieldwork were two polished bedrocks located on the Elliði ridge, which separates the Víðinesdalur valley to the south from the Kolbeinsdalur valley to the north (Fig. 6.1). The polished surfaces are at around 600 m a.s.l., i.e. 300 m above the bottom of the Víðinesdalur valley. Samples were collected from each of these polished surfaces (ELLID-1 and ELLID-2; see Chapter 5), whose ages indicate the start of deglaciation of these valleys studied. Both samples gave very similar ages: 16.3 ± 1.2 ka (ELLID-1) and 16.3 ± 0.9 ka BP (ELLID-2). The location, chemical composition and calculated exposure ages of the samples is included in the Tables 6.2, 6.3, 6.4 and 6.5.

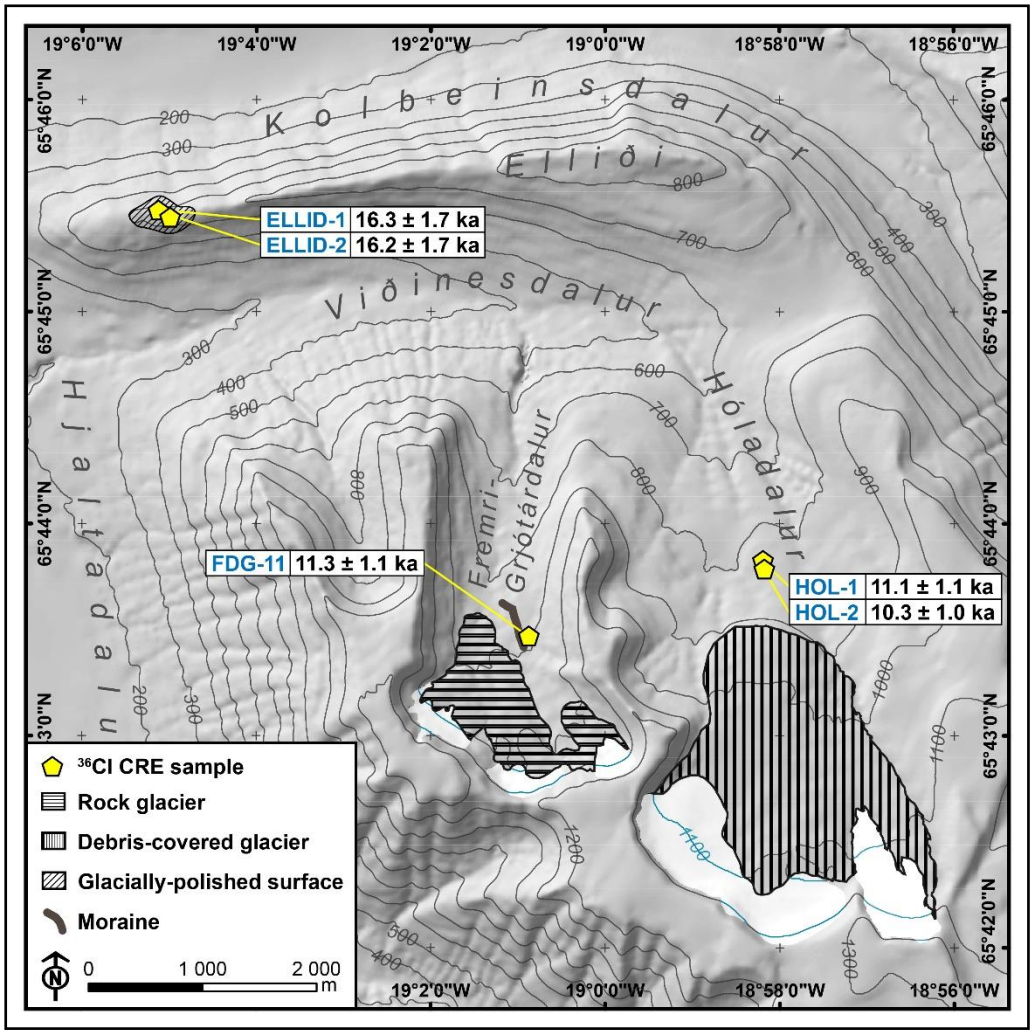

Figure 6.1. Location of samples describing the deglaciation pattern of the study area.

6.4.3 Deglaciation of the Tröllaskagi cirques: geomorphology and CRE dating results.

To determine the timing of the deglaciation of the Fremri-Grjótárdalur and Hóladalsjökull cirques, glacial landforms located in front of the rock glaciers and the debris-covered glacier were studied. No polished surfaces are preserved, only remnants of a highly degraded moraine ridge in each cirque. In the Fremri-Grjótárdalur cirque is a degraded lateral moraine in front of the rock glaciers (Figs. 6.1, 6.2 and 6.3). One prominent glacial boulder (FDG-11) was considered suitable for exposure dating and yielded an age of 11.3±0.8 ka BP. A similar highly degraded moraine is located about 900 m distal and 100 m lower to the Hóladalsjökull debris-covered glacier (Figs. 6.1 and 6.4). Two large stable blocks with glacially polished surfaces were considered suitable for exposure dating (Fig. 6.4B). From those, samples HOL-1 and HOL-2 yielded ages of 11.1±1.1 and 10.3±0.7 ka BP respectively. The three ages are indistinguishable from each other within their 1 sigma analytical uncertainties, and are in chronostratigraphical order with the ELLID samples (Fig. 6.1).

Sample name	Sample type	Latitude (ºN)	Longitude (ºW)	Elevation (m a.s.l.)	Shielding factor	Thickness (cm)	Distance from the headwall (m)
Glacially polished ridge Ellið							
ELLID-1	Polished bedrock	65.7580	19.0848	597	0.9986	2.0	16000
ELLID-2	Polished bedrock	65.7579	19.0854	597	0.9994	3.5	15900
Moraine boulders of Hóladalur							
HOL-1	Moraine boulder	65.7303	18.9698	833	0.9629	3.0	3400
HOL-2	Moraine boulder	65.7297	18.9696	841	0.9931	3.0	3480
Fremri-Grjótárdalur rock glacier complex							
FGD-1	Rock glacier (inactive) boulder	65.7259	19.0245	869	0.8889	4.0	1480
FGD-2	Rock glacier (inactive) boulder	65.8003	19.0200	874	0.9765	4.5	1640
FGD-11	Moraine boulder	65.7242	19.0159	912	0.9843	5.0	1680
FGD-1B	Rock glacier (active) boulder	65.7207	19.0172	960	0.9932	2.0	1030
FGD-2B	Rock glacier (active) boulder	65.7209	19.0186	960	0.9741	4.0	1080
FGD-3B	Rock glacier (active) boulder	65.7205	19.0186	966	0.9929	3.5	1035
FGD-4B	Rock glacier (inactive) boulder	65.7184	19.0079	1005	0.9841	3.5	830
FGD-5B	Rock glacier (inactive) boulder	65.7187	19.0073	1030	0.9880	4.0	780
Hofsjökull debris-covered glacier							
HOFS-1	Debris-covered glacier (active) boulder	65.6812	18.9481	893	0.9758	2.5	2950
HOFS-2	Debris-covered glacier (active) boulder	65.6811	18.9478	894	0.9557	4.0	2920
HOFS-3	Debris-covered glacier (active) boulder	65.6811	18.9479	903	0.9856	3.5	2930
Héðinsdalsjökull debris-covered glacier							
HEDIN-1	Moraine boulder	65.6454	18.9292	640	0.9758	3.5	4690
HEDIN-2	Moraine boulder	65.6455	18.9272	660	0.9764	2.0	4580
HEDIN-3	Moraine boulder	65.6455	18.9278	653	0.9775	2.5	4610

Table 6.2. Geographic sample locations, topographic shielding factor, sample thickness and distance from headwall.

Sample name	CaO (%)	K_2O (%)	TiO_2 (%)	Fe_2O_3 (%)	SiO_2 (%)	Na_2O (%)	MgO (%)	Al_2O_3 (%)	MnO (%)	P_2O_5 (%)	Li (ppm)	B (ppm)	Sm (ppm)	Gd (ppm)	Th (ppm)	U (ppm)	Cl (ppm)
Glacially polished ridge Elliði																	
ELLID-1	8.568	0.179	4.753	18.215	44.950	2.161	7.475	12.416	0.228	0.20	4.4	2	5.709	5.953	0.504	0.149	21
Fremri-Grjótárdalur rock glacier complex																	
FGD-1B	11.738	0.356	2.590	13.300	47.670	2.395	6.702	13.844	0.194	0.24	4.3	< 2	5.120	5.280	1.131	0.314	37
FGD-4B	9.580	0.465	3.529	16.270	47.200	2.808	5.223	12.798	0.239	0.34	6.1	< 2	6.930	7.122	1.605	0.437	44
Hofsjökull debris-covered glacier																	
HOFS-1	9.345	0.359	4.267	18.150	48.770	2.225	5.772	10.288	0.250	< L.D	5.4	< 2	2.756	3.213	1.017	0.336	77
Héðinsdalsjökull debris-covered glacier																	
HEDIN-1	10.773	0.262	2.880	14.920	47.290	2.282	6.423	12.918	0.213	0.24	4.4	< 2	5.447	5.704	1.143	0.317	40

Table 6.3. Chemical composition of the bulk rock samples before chemical treatment.

Sample name	CaO (%)	K_2O (%)	TiO_2 (%)	Fe_2O_3 (%)
Glacially polished ridge Elliði				
ELLID-1	7.20 ± 0.14	0.14 ± 0.02	6.96 ± 0.35	24.28 ± 0.49
ELLID-2	7.01 ± 0.14	0.12 ± 0.02	7.18 ± 0.36	25.12 ± 0.50
Moraine boulders of Hóladalur				
HOL-1	12.05 ± 0.24	0.29 ± 0.04	2.53 ± 0.13	13.16 ± 0.26
HOL-2	11.07 ± 0.22	0.35 ± 0.05	2.93 ± 0.15	14.13 ± 0.28
Fremri-Grjótárdalur rock glacier complex				
FGD-1	11.01 ± 0.22	0.28 ± 0.04	2.66 ± 0.13	14.07 ± 0.28
FGD-2	11.57 ± 0.23	0.33 ± 0.05	2.52 ± 0.13	12.79 ± 0.26
FGD-11	10.92 ± 0.22	0.28 ± 0.04	2.59 ± 0.13	13.70 ± 0.27
FGD-1B	11.37 ± 0.23	0.33 ± 0.05	3.15 ± 0.16	12.68 ± 0.25
FGD-2B	11.73 ± 0.23	0.31 ± 0.05	2.80 ± 0.14	10.60 ± 0.21
FGD-3B	9.88 ± 0.20	0.31 ± 0.05	4.06 ± 0.20	16.71 ± 0.33
FGD-4B	8.59 ± 0.17	0.40 ± 0.06	4.55 ± 0.23	19.70 ± 0.39
FGD-5B	8.96 ± 0.18	0.29 ± 0.04	4.75 ± 0.24	20.58 ± 0.41
Hofsjökull debris-covered glacier				
HOFS-1	9.91 ± 0.20	0.39 ± 0.06	3.54 ± 0.18	17.06 ± 0.34
HOFS-2	9.66 ± 0.19	0.39 ± 0.06	4.50 ± 0.22	18.43 ± 0.37
HOFS-3	9.63 ± 0.19	0.44 ± 0.07	4.37 ± 0.22	18.07 ± 0.36
Héðinsdalsjökull debris-covered glacier				
HEDIN-1	10.28 ± 0.21	0.18 ± 0.03	3.70 ± 0.18	16.91 ± 0.34
HEDIN-2	7.87 ± 0.16	0.80 ± 0.04	2.65 ± 0.13	13.36 ± 0.27
HEDIN-3	8.06 ± 0.16	0.76 ± 0.04	3.05 ± 0.15	14.50 ± 0.29

Table 6.4. Concentrations of the ^{36}Cl target elements Ca, K, Ti and Fe, determined in splits taken after the chemical pre-treatment (acid etching).

6.4.4 Stabilization of boulders from the fossil rock glaciers (with no internal ice): geomorphology and CRE dating results.

Two large boulders (samples FDG-1 and FDG-2) were collected at the frontal margin of the fossil rock glacier located below the active rock glaciers of the western sector of Fremri-Grjótárdalur cirque about 870 m a.s.l. (Figs. 6.1, 6.2 and 6.3). The samples yielded exposure ages of 10.5±0.7 and 11.1±0.7 ka respectively. Two more boulders (samples FDG-4B and FDG-5B) yielded ages of 9.3±0.7 and 9.5±0.7 ka BP respectively. They were located at the front edge of the other fossil rock approximately 1005 m a.s.l., about 150 m higher than FDG-1 and FDG-2, in the eastern sector of the cirque (Figs. 6.2 and 6.3).

6.4.5 Stabilization of boulders from active rock glaciers and debris-covered glaciers (with stagnant internal ice): CRE dating results.

Three samples were collected from boulders at the front of the active rock glacier, with internal ice, of the western sector of Fremri-Grjótárdalur (FGD-1B, FGD-2B and FDG-

3B), at an altitude of approx. 960 m (Figs. 6.2, 6.3 and 6.5). These samples gave ages, 2.5±0.2, 5.2±0.4 and 6.5±0.5 ka respectively, in good chronostratigraphical agreement with previous samples of the cirque (moraine and fossil rock glacier). To determine the timing of the stabilization of the debris-covered glaciers, three samples were taken from the boulders at the frontal part of the Hofsjökull debris-covered glacier, located at the bottom of Hofsdalur. The front of Hofsjökull presents a glacial ice wall of around 20 m, covered by a 2 m thick debris mantle. Three samples were collected from boulders at the front of the glacier located at about 900 m a.s.l. (HOFS-1, HOFS-2 and HOFS-3; Figs. 6.1, 6.6 and 6.7). The results of these samples yielded ages of 5.4±0.5, 5.6±0.5 and 6.7±0.6 ka, respectively. These ages are similar to the samples FGD-2B and FDG-3B from the active rock glaciers.

Finally, three samples were taken from debris-covered glacier of Héðinsdalur, in the distal sector of Héðinsdalsjökull, where is no internal ice at present (HEDIN-1, HEDIN-2 and HEDIN-3), at about 650 m a.s.l. (Fig. 6.8 and 6.9), and yielded ages of 3.0±0.3, 2.6±0.3 and 2.2±0.2 ka respectively.

6.5. Discussion.

6.5.1 Deglaciation of the Tröllaskagi internal valleys and beginning of the formation of the rock glaciers and debris-covered glaciers into the cirques.

The intense degradation of the Tröllaskagi glacial landscape, due to slope mass movements together with ash and aeolian sediments which have partly covered the slopes, greatly limits the possibility of obtaining a sufficient number of reliable CRE samples to map/reconstruct the deglaciation pattern of the three studied valleys. The only samples obtained from the Elliði ridge summits (ELLID-1, ELLID-2) yielded the same age (16.3±1.0 ka) (Fig. 6.10). This age may indicate the definitive retreat of the glaciers that descended through the Hóladalur valley. The datings of the moraine remains observed in the Fremri-Grjótárdalur and Hóladalur cirques yielded almost similar ages: 11.3±0.7, 11.1±1.0 and 10.3±0.7 ka (Figs. 6.1 and 6.3) which is around 5 ka younger than those from the Elliði ridge.

The results obtained in this study reflect a similar deglaciation pattern to that observed elsewhere in Iceland. In fact, the onset of the deglaciation in Iceland can be determined around 18.6 cal. ka BP, in concordance with the global sea level rise (Andrews et al 2000; Ingólfsson and Norðdahl 2001), which increased sharply during the Bølling interstadial (14.7 to 14.1 ka BP), when the Icelandic Ice Sheet IIS collapsed and retreated from the north (Norðdahl et al., 2008; Norðdahl and Ingólfsson, 2015; Pétursson et al., 2015).

Sample name	Sample weight (g)	Mass of Cl in spike (mg)	$^{35}Cl/^{37}Cl$	$^{36}Cl/^{35}Cl$ (10^{-14})	[Cl] in sample (ppm)	[^{36}Cl] (10^4 atoms g^{-1})	^{36}Cl CRE age (yr)
Glacially polished ridge Elliði							
ELLID-1	28.88	1.864	64.854 ± 0.615	11.051 ± 0.438	3.5	12.438 ± 0.516	16254 ± 1685 (*1217*)
ELLID-2	27.69	1.928	86.476 ± 0.876	10.014 ± 0.437	2.6	11.977 ± 0.547	16174 ± 1713 (*925*)
Moraine boulders of Hóladalur							
HOL-1	30.41	1.012	10.718 ± 0.037	17.257 ± 0. 435	15.6	15.060 ± 0.384	11096 ± 1092 (*1057*)
HOL-2	30.89	0.992	9.528 ± 0.066	15.669 ± 0.364	18.3	14.055 ± 0.336	10328 ± 993 (*668*)
Fremri-Grjótárdalur rock glacier complex							
FGD-1	31.96	1.018	7.805 ± 0.131	13.071 ± 0.399	25.7	13.311 ± 0.444	10534 ± 1048 (*720*)
FGD-2	30.2	0.985	6.026 ± 0.035	13.066 ± 0.395	43.9	17.536 ± 0.547	11092 ± 1111 (*734*)
FGD-11	30.69	1.000	9.585 ± 0.096	17.206 ± 0.568	18.4	15.604 ± 0.525	11341 ± 1133 (*782*)
FGD-1B	70.54	1.883	6.135 ± 0.648	48.960 ± 0.269	36.7	4.304 ± 0.287	2509 ± 290 (*227*)
FGD-2B	70.34	1.880	5.649 ± 0.646	83.750 ± 0.343	43.8	8.330 ± 0.444	5176 ± 565 (*411*)
FGD-3B	67.66	1.882	5.888 ± 0.568	10.512 ± 0.412	41.6	10.414 ± 0.521	6546 ± 696 (*505*)
FGD-4B	26.52	1.851	14.293 ± 0.150	87.158 ± 0.394	25.1	12.908 ± 0.627	9274 ± 951 (*715*)
FGD-5B	25.78	1.870	11.531 ± 0.115	86.801 ± 0.361	35	14.353 ± 0.655	9450 ± 977 (*706*)
Hofsjökull debris-covered glacier							
HOFS-1	84.09	1.822	4.289 ± 0.532	68.219 ± 0.356	77.4	9.128 ± 0.670	5417 ± 669 (*509*)
HOFS-2	85.46	1.832	5.189 ± 0.100	89.175 ± 0.466	43.0	8.026 ± 0.552	5596 ± 644 (*508*)
HOFS-3	86.23	1.819	4.374 ± 0.671	90.595 ± 0.430	70.2	11.279 ± 0.809	6748 ± 817 (*625*)

Table 6.5. ^{36}36Cl CRE dating results. The numbers in italics correspond to the internal (analytical) uncertainty at one standard level

Sample name	Sample weight (g)	Mass of Cl in spike (mg)	$^{35}Cl/^{37}Cl$	$^{36}Cl/^{35}Cl$ (10^{-14})	[Cl] in sample (ppm)	[^{36}Cl] (10^4 atoms g^{-1})	^{36}Cl CRE age (yr)
Héðinsdalsjökull debris-covered glacier							
HEDIN-1	67.56	1.878	8.846 ± 0.853	45.314 ± 0.258	19.9	3.167 ± 0.202	2953 ± 334 (260)
HEDIN-2	64.38	1.875	4.706 ± 0.454	25.226 ± 0.165	76.5	3.571 ± 0.286	2591 ± 337 (266)
HEDIN-3	63.98	1.893	4.717 ± 0.438	22.065 ± 0.157	77.1	3.136 ± 0.269	2221 ± 300 (241)
Blanks [a]					*Total atoms Cl* (10^{17})	*Total atoms ^{36}Cl* (10^4)	
BK-1		1.800	297.029 ± 11.372	0.545 ± 0.097	2.941 ± 0.220	16.981 ± 3.034	
BK-2		1.884	356.675 ± 7.637	0.575 ± 0.135	2.313 ± 0.139	18.738 ± 4.384	
BK-3		1.888	328.059 ± 2.892	0.359 ± 0.069	2.650 ± 0.136	11.725 ± 2.249	
Cblk3125-1		1.897	98.243 ± 1.536	14.248 ± 0.301			
Cblk3125-2		1.859	85.103 ± 0.398	2.228 ± 0.175			

[a] BK-1 was processed with samples HOFS-1, HOFS-2 and HOFS-3; BK-2 was processed with samples FGD-1B, FGD-2B and FGD-3B; BK-3 was processed with samples ELLID-1, ELLID-2, HEDIN-1, HEDIN-2, HEDIN-3, FGD-4B and FGD-5B. Cblk3125-1 and Cblk3125-2 were processed

Table 6.5. (cont.)

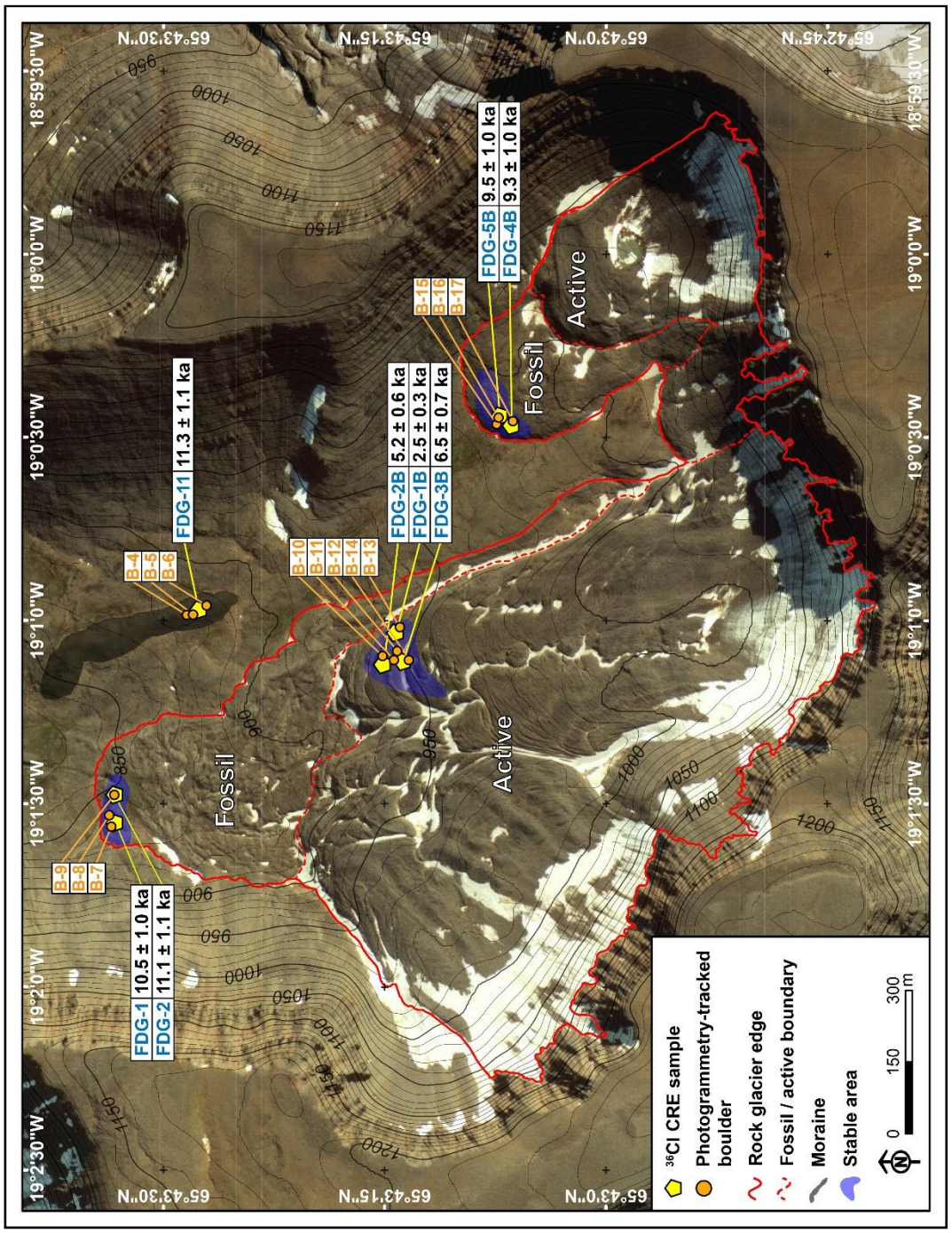

Figure 6.2. View of the Fremri-Grjótárdalur rock glacier complex and spatial distribution of ^{36}Cl CRE samples and photogrammetry-tracked boulders. Stable area refers where it is known that the boulder movement of less than 0.16 m yr^{-1}.

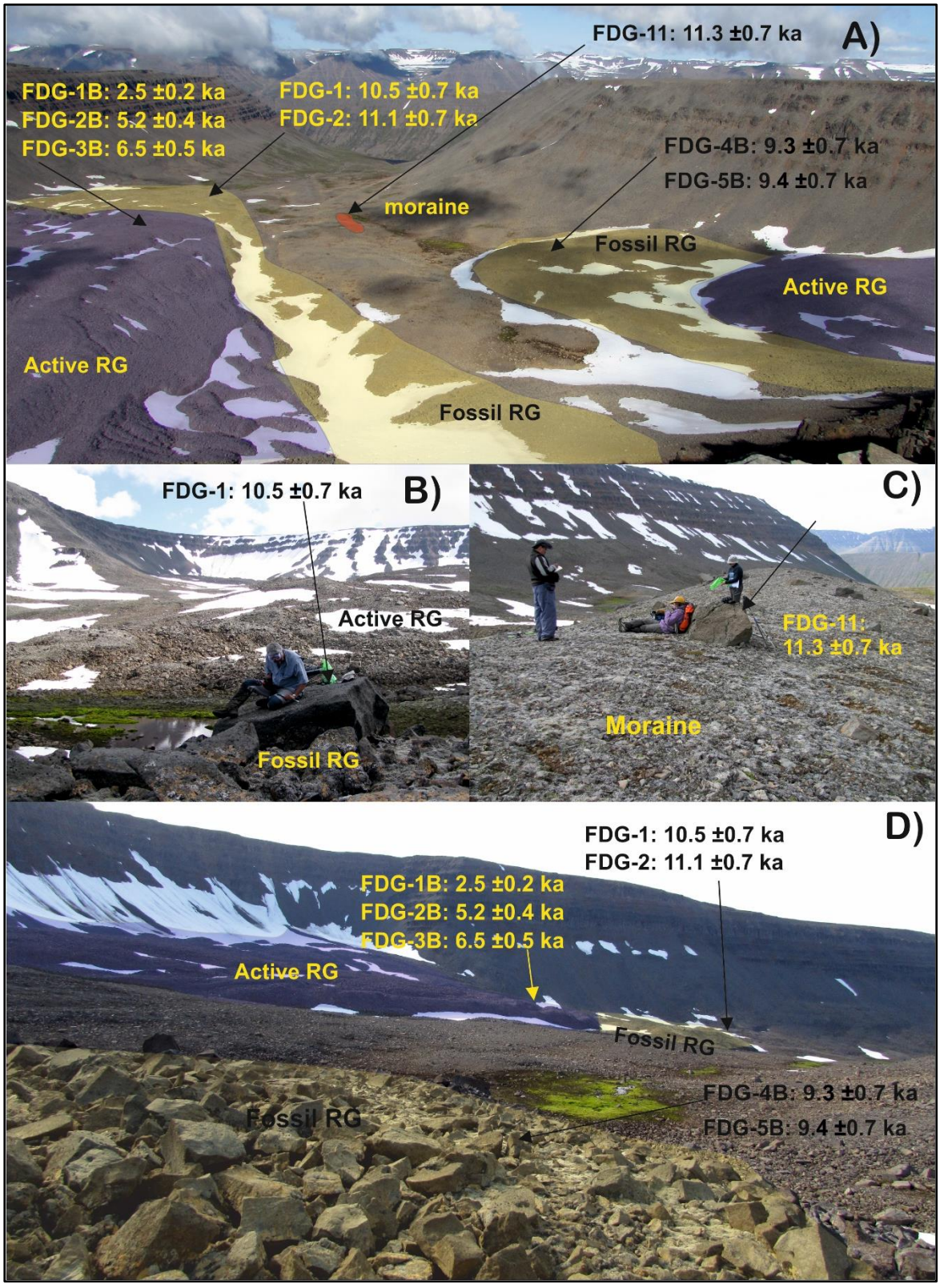

Figure 6.3. Photos of the Fremri-Grjótárdalur rock glacier complex. (A) View of the rock glacier complex from the summit area to the north. (B) Sample FDG-1 in the fossil rock glacier. (C) Sample FDG-11 in the lateral moraine located in front of the rock glaciers. (D) View of the rock glacier complex from the eastern sector of the cirque.

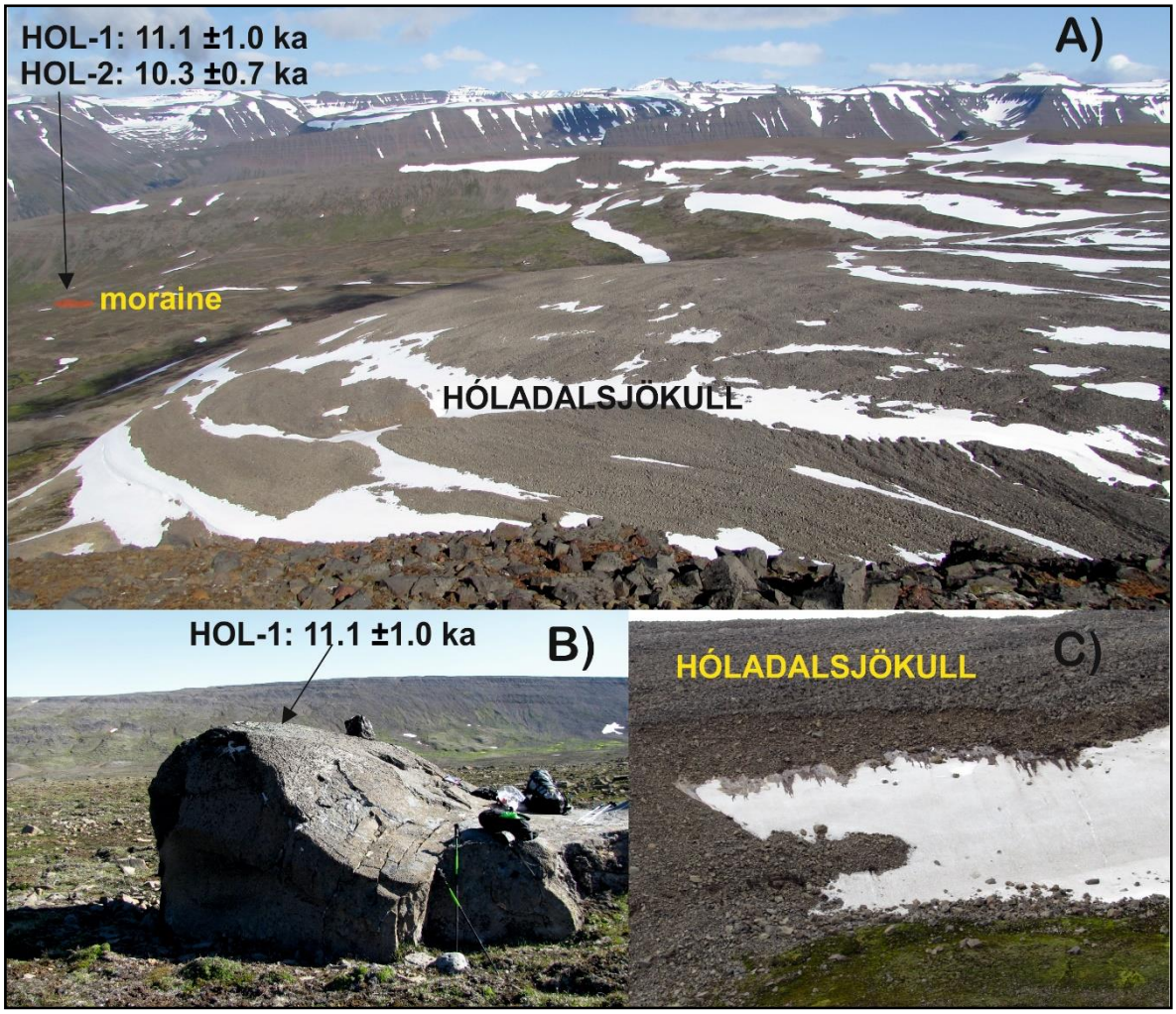

Figure 6.4. Field photos of Hóladalur cirque. (A) Oblique view of the Hóladalsjökull debris-covered glacier from the western summit area. (B) Sample HOL-1 in a moraine in front of the debris-covered glacier. (C) Close up view of the debris-covered glacier snout.

The ages obtained in this study suggest that the retreat of the glaciers in Tröllaskagi coincided with the retraction of the main tongue of the IIS in this area, which flowed down from the highlands throughout the Skagafjörður fjord. This glacier retreated from the mouth of the fjord (161 km north of the present Hofsjökull ice-cap) in 15.9±1.2 ka, based on ^{36}Cl dating (Andrés et al., 2019). This indicates that from the Bølling interstadial, the glaciers in the internal Tröllaskagi valleys and the Skagafjörður IIS outlet glacier were already disconnected. This may show that from the Allerød interstadial (13.9-12.9 ka) at least some of the Tröllaskagi glaciers behaved as alpine glaciers, already disconnected from the IIS. The Tröllaskagi plateau therefore, may have remained ice-free, as it has been widely proposed (Ingólfsson, 1991; Norðdahl, 1991a, 1991b; Rundgren and Ingólfsson, 1999; Andrés et al., 2016).

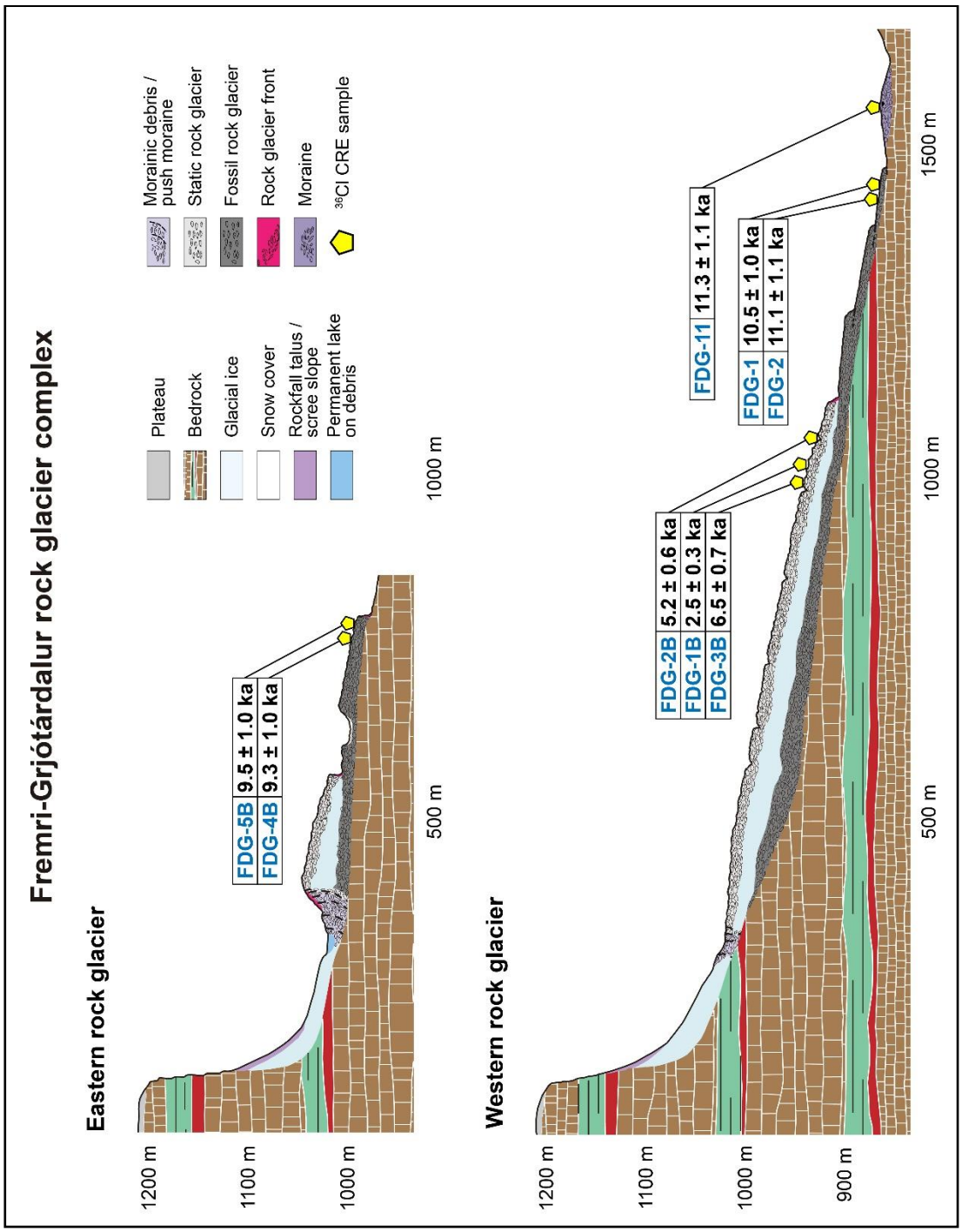

Figure 6.5. Idealized longitudinal profile of the Fremri-Grjótárdalur rock glaciers and the relative position of the ^{36}Cl CRE samples.

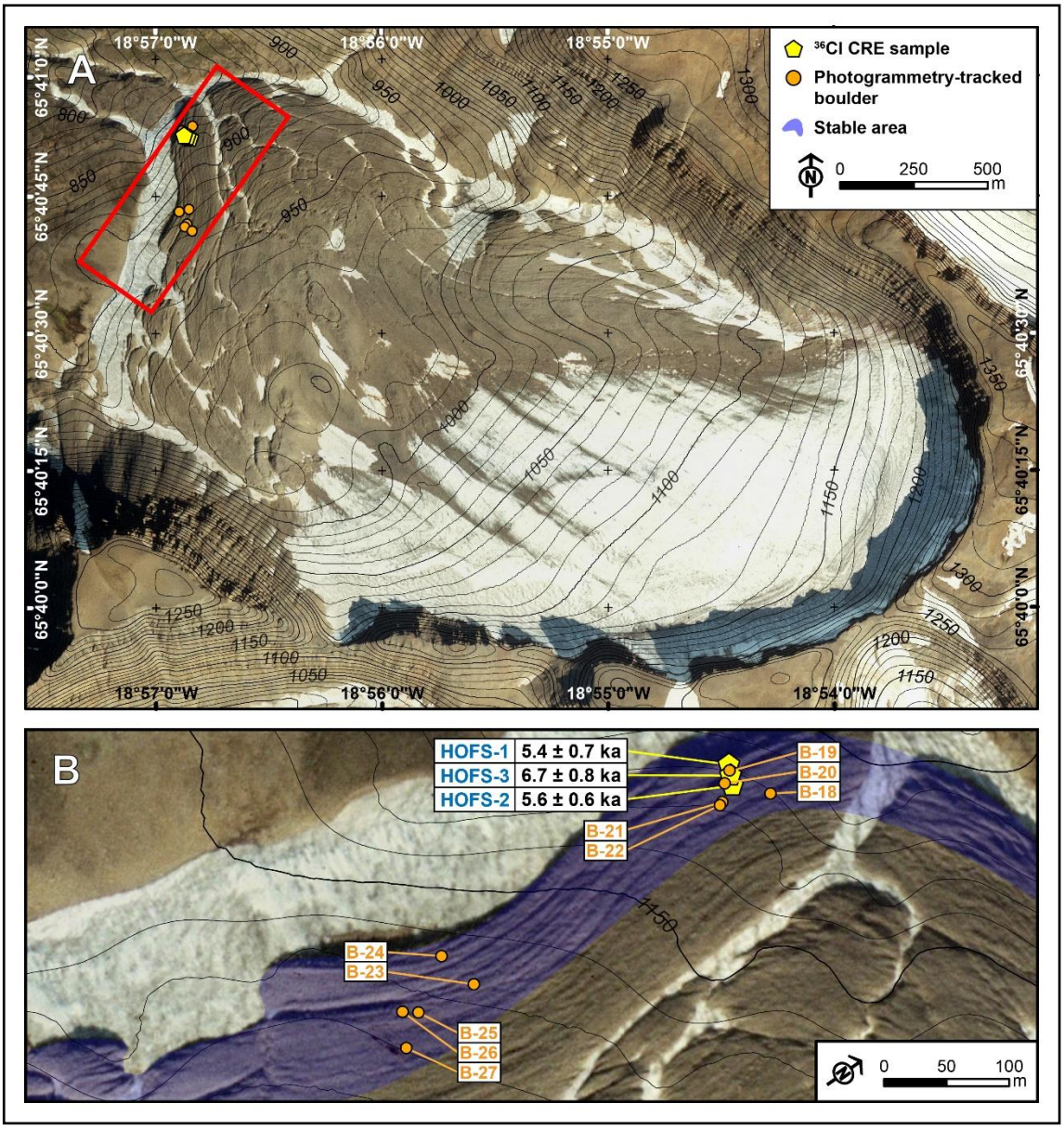

Figure 6.6. Overhead view of the Hofsjökull glacier complex and spatial distribution of ^{36}Cl CRE samples and photogrammetry-tracked boulders. Panel A shows the whole glacier complex (debris-free and debris-covered sectors). Panel B is a zoom of the frontal area. Stable area refers where it is known that the boulder movement is less than 0.37 m yr^{-1}.

Data from lacustrine and marine sediments, and sea level changes, suggest a cold period and glacial advances at the end of the Bølling interstadial, around 14 cal. ka BP (Ingólfsson et al. 1997; Pétursson et al. 2015; Patton et al. 2017). However, probably due to the intense paraglacial erosive activity, there is no geomorphological evidence of that cold episode in the Víðinesdalur valley or in the Fremri-Grjótárdalur and Hóladalur cirques. Lake sediments from the Torfadalsvatn lake, on the Skagi peninsula (west of the Skagafjörður fjord), show that temperatures rose to current levels during the Allerød interstadial in the Skagafjörður area (Rundgren 1995, 1999; Rundgren and Ingólfsson

1999). The Tröllaskagi glaciers, already reduced to their minimum extent in their cirques during the Bølling interstadial, may have retreated further.

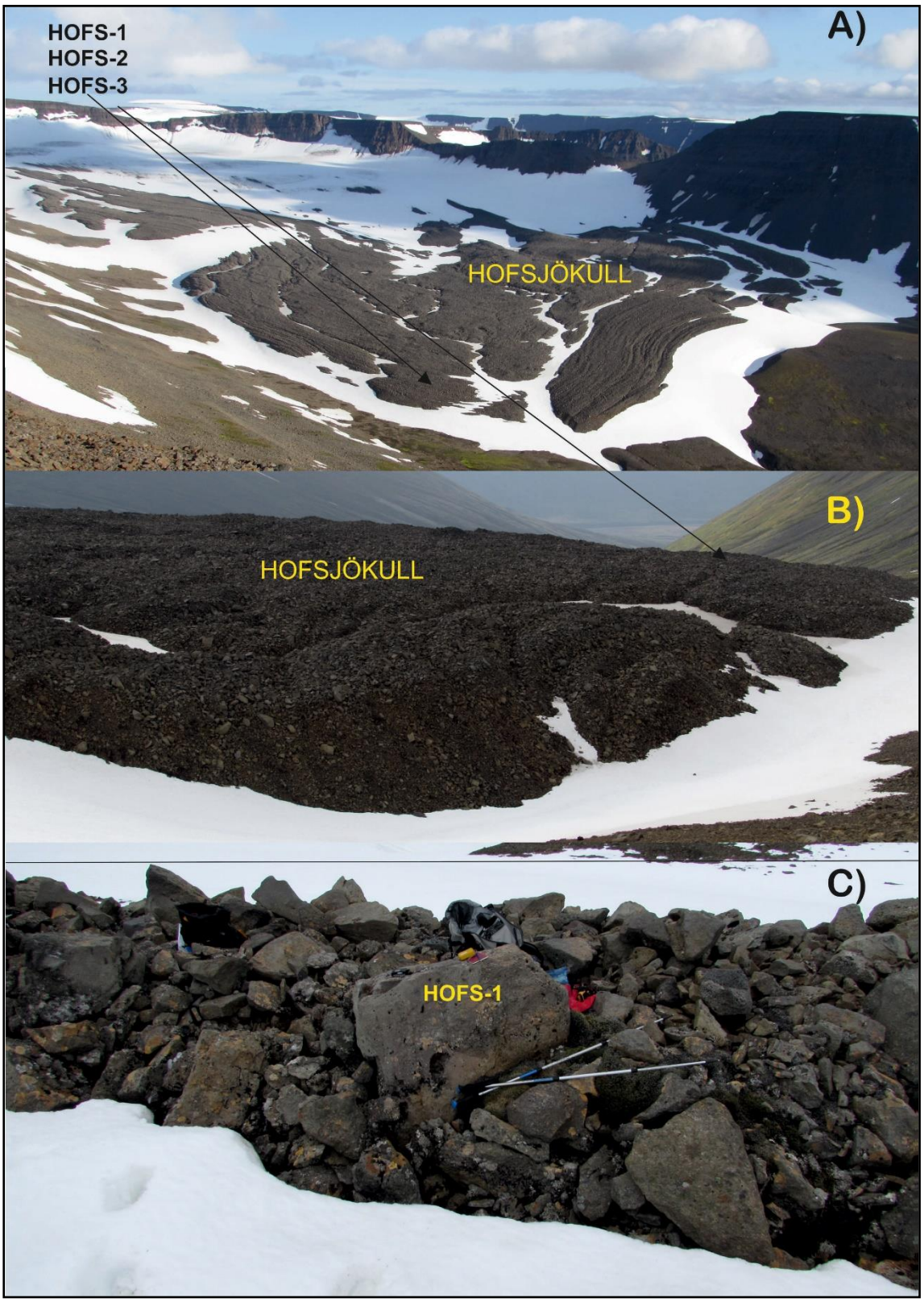

Figure 6.7. Field photos of Hofsjökull cirque. (A) Oblique view of the Hofsjökull debris-covered glacier from the southern summit area. (B) Close up view of the debris-covered glacier snout. (C) Sample HOFS-1 on a crest located in the frontal area of the debris-covered glacier.

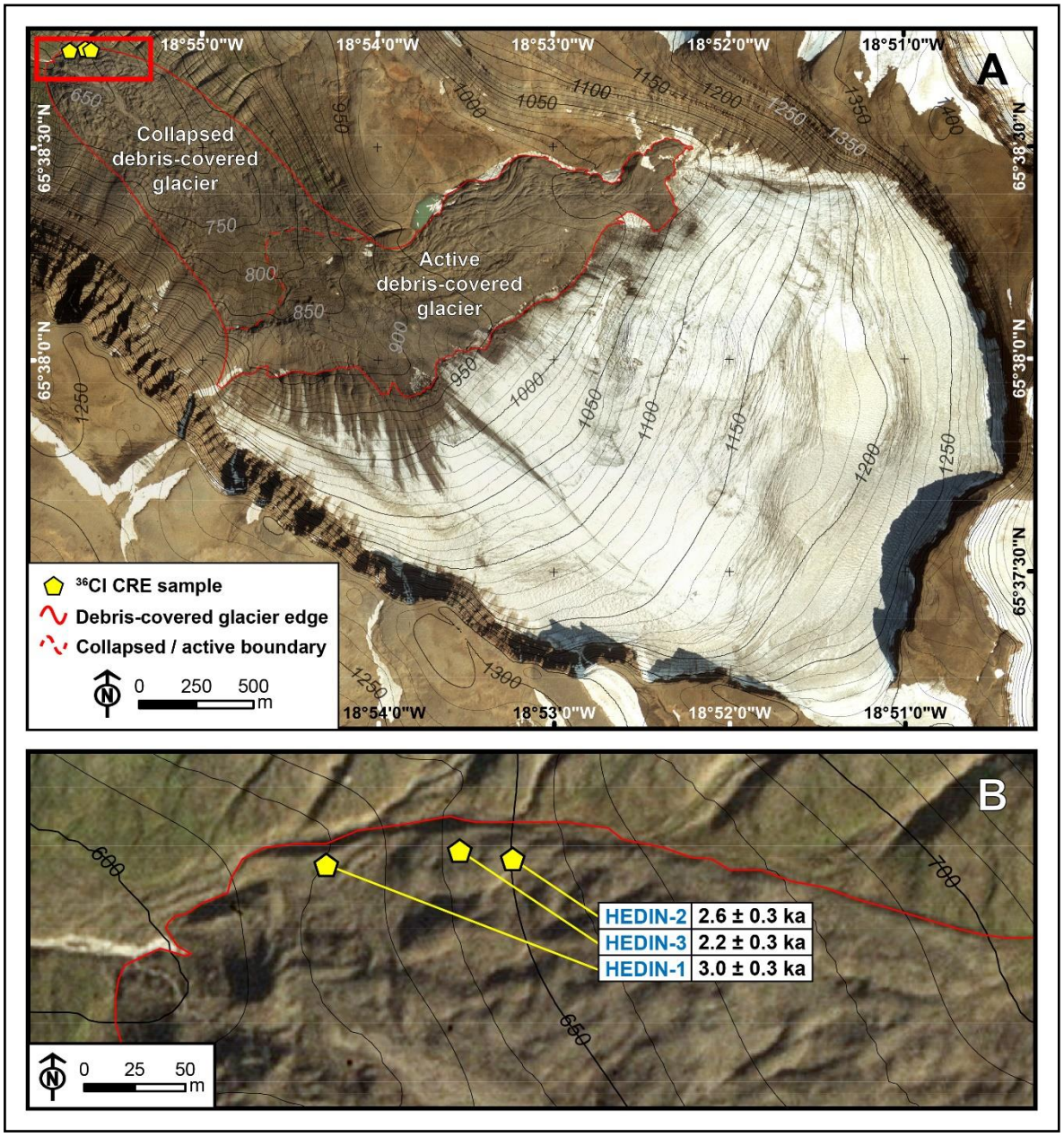

Figure 6.8. Overhead view of the Héðinsdalsjökull glacier complex and spatial distribution of ^{36}Cl CRE samples and photogrammetry-tracked boulders. Panel A shows the whole glacier complex (debris-free and fossil/active debris-covered sectors). Panel B is a zoom of the frontal area.

After the Allerød interstadial, during the Younger Dryas, major degradation of the biosphere and increased amounts of sea-ice occurred in northern Iceland (Rundgren 1995, 1999; Xiao et al., 2017). The glacial outlets descending from the IIS, reoccupied the main fjords of northern Iceland up to their middle parts according to shoreline and tephra distribution (Pétursson et al., 2015). This pattern has been confirmed in Skagafjörður with ^{36}Cl CRE ages of 12.7±0.9 and 11.9±0.9 ka BP for polished surfaces, when the front of the glaciers left the middle part of the fjord, 130 km from the current Hofsjökull ice cap (Andrés et al., 2019).

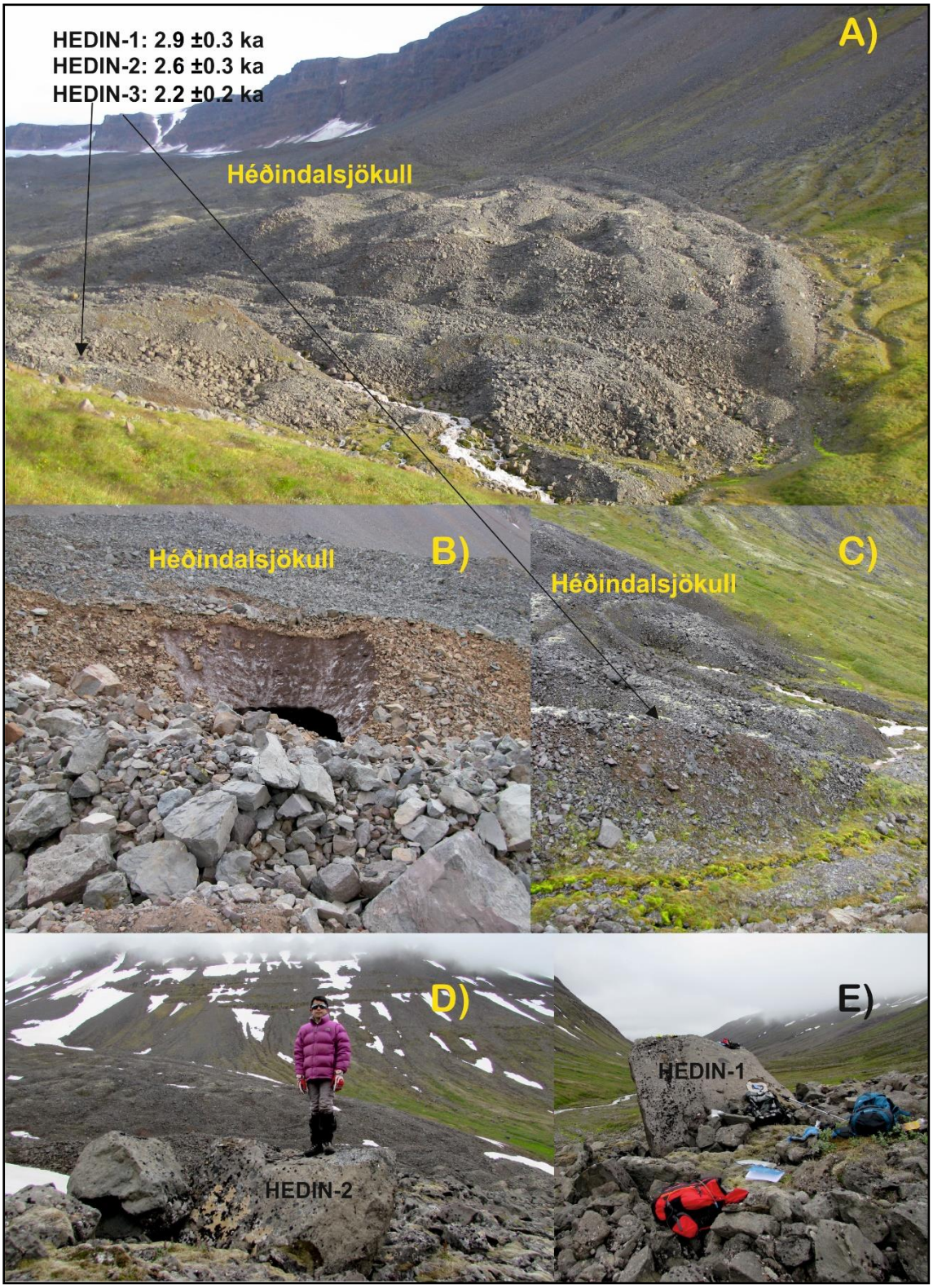

Figure 6.9. Field photos of Héðinsdalsjökull glacier. (A) Oblique view of the Héðinsdalsjökull debris-covered glacier from the south. (B) Middle sector of the debris-covered glacier with internal ice. (C) Snout of the debris-covered glacier in the current fossil stage. (D) Sample HEDIN-2 on a crest in the frontal area of the debris-covered glacier. (E) Sample HEDIN-1 on the crest in the frontal area of the debris-covered glacier.

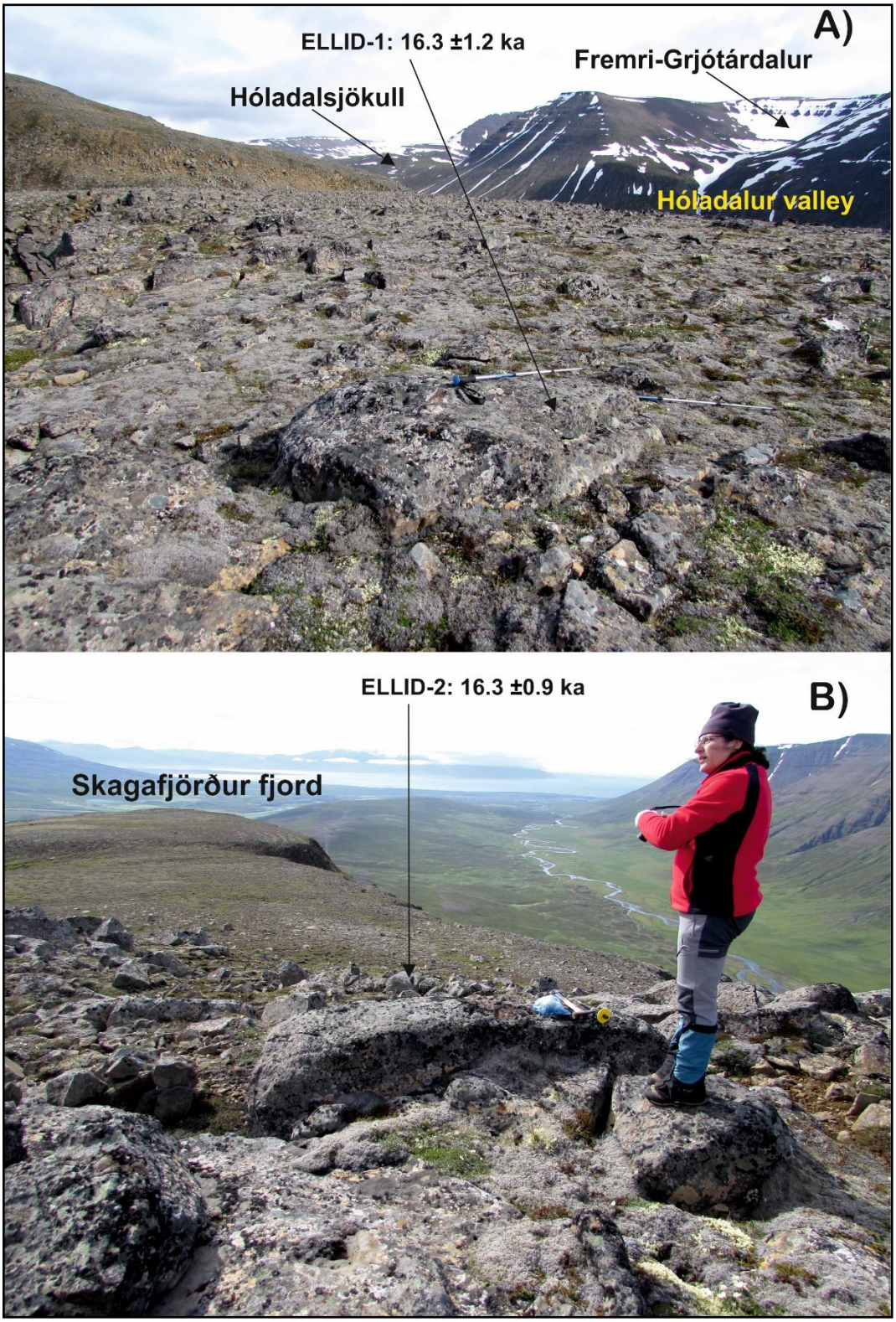

Figure 6.10. Field photo of the Elliði polished surface. (A) Location of sample ELLID-1 viewed from the west, on the northern side of the Hóladalur valley. Hólajökull and Fremri-Grjótárdalur cirques at the bottom. (B) Location of sample ELLID-2 viewed from the east. The Skagafjörður fjord can be seen at the bottom. Ages results from samples: ELLID-1: 16.3±1.2 ka; ELLID-2:16.3±0.9 ka.

The last important advance or stagnation of the IIS outlets in northern Iceland was around 11 ka (Preboreal), when their fronts were located at the innermost parts of the fjords (Ingólfsson et al., 1997; Norðdahl and Einarsson, 2001; Norðdahl and Pétursson, 2005; Pétursson et al., 2015). ^{36}Cl CRE ages confirm the position of the outlet terminus close to the present shoreline in the Skagafjörður fjord (90 km from the current Hofsjökull ice-cap) at around 11 ka (Andrés et al., 2019). This last glacial advance was immediately followed by an abrupt retreat until the disappearance of the IIS within the current limits of the glaciers (Kaldal and Víkingsson, 1990; Andrews et al., 2000; Norðdahl and Einarsson, 2001; Geirsdóttir et al., 2002, 2009; Larsen et al. al., 2012; Pétursson et al., 2015; Harning, et al., 2016b). This has been also confirmed by CRE ^{36}Cl ages in Skagafjörður (Andrés et al., 2019).

Samples FDG-11 (11.3 ± 0.7 ka) from the Fremri-Grjótárdalur moraine, and HOL-1 (11.1 ± 1.1 ka) and HOL-2 (10.3 ± 0.7, ka) from the moraine in front of Hóladalsjökull glacier (Fig. 6.1), may represent a glacial advance or glacial front stagnation in the Hóladalur valley during the Preboreal, around 11 ka, similar to that observed at the bottom of the fjords. After this, the Hóladalur glaciers must have retreated very quickly, as occurred in the nearby ice-caps (Andrés et al., 2019), until the probably total disappearance of all the Icelandic glaciers at ~9 ka (Larsen et al., 2012; Geirsdóttir et al., 2018). This may also be the case of Drangajökull, in the NW (Harning et al., 2016a; Anderson et al, 2018a).

The ages of the moraine located in front of Fremri-Grjótárdalur fossil rock glaciers and the frontal sector of these rock glaciers show similar ages, according to their internal uncertainties. This fact would demonstrate the rapid disappearance of the small glaciers that occupied the cirque at the beginning of the Holocene and that the rock glaciers were formed shortly afterwards. The surface boulders of these rock glaciers acquired immediately the necessary “stabilization”, resulting in undisturbed exposure to radiation (Fig. 6.5). Hereafter, we will use the concept of “stabilization” in that sense along the discussion. The samples collected from the front of the western fossil rock glacier, at around 870 m a.s.l., yield ages around 10-11 ka. Samples from the front of the eastern fossil rock glacier, located between 940-990 m a.s.l., gave slightly younger ages, ~9.4 ka. (Table 6.5). The time difference between the stabilization of the frontal parts of those two glaciers (Figs. 6.3 and 5) can be explained by the altitude difference above the current level of permafrost (Wangensteen et al., 2006; Etzelmüller et al., 2007). The ages of the boulders from the fossil rock glaciers are similar or even slightly younger than those of the moraines that precede them, which makes us confident that the samples are not affected by cosmogenic inheritance from earlier exposure periods (Andrés et al., 2019), but in contrast with the evolution in other areas (Çiner et al., 2017). From the ages –and uncertainty ranges (up to

~1 ka)– of the moraine (11 ka) and the fossil rock glaciers (9-11 ka), it could be deduced that the rock glacier formation and development until its stabilization might have been very rapid or even it might have lasted for 2-4 ka.

The formation of rock glaciers immediately after deglaciation of the cirques may indicate that their origin is a consequence of the rapid transformation of debris-free glaciers into rock glaciers during the final deglaciation stages with their fronts stabilizing shortly afterwards (Humlum, 2000; Janke et al., 2015; Monnier and Kinnard, 2015; Andrés et al., 2016; and many others). This would reject the total dissaperance of the glaciers, the contrary to what it would occur during the HTM in other regions of Iceland (Kaldal and Víkingsson, 1991; Guðmundsson, 1997; Norðdahl et al., 2008; Geirsdóttir et al., 2009, 2018). CRE dating of frontal boulders of fossil rock glaciers and glacial polished bedrock on which they are supported has demonstrated in many mountain ranges that rock glaciers usually formed shortly after deglaciation, along with the stabilization of their fronts. This process has been observed in several areas of the Iberian Peninsula, such as Sierra Nevada (Palacios et al., 2016), Sierra de Guadarrama (Palacios et al., 2012), Sierra de la Demanda (Fernández-Fernández et al., 2017), the Cantabrian Mountains (Rodríguez-Rodríguez et al., 2017), the Central Pyrenees (Palacios et al., 2017) and the Eastern Pyrenees (Andrés et al., 2018), and also in the British Isles (Ballantyne et al., 2009), the Alps (Hippolyte et al., 2009; Moran et al., 2016), the Karçal Mountains in Lesser Caucasus (Dede et al., 2017) and in the New Zealand Southern Alps (Winkler and Lambiel, 2018).

The rapid formation of debris-covered glaciers and rock glaciers at the end of deglaciation and the early stabilization of their fronts has a logical explanation in many mountains (Winkler and Lambiel, 2018), but especially in the Tröllaskagi valleys (Fig. 6.11). Deglaciation and the disappearance of the ice imply the start of the cirque walls debutressing (Ballantyne, 2002). Consequently paraglacial processes accelerate following deglaciation yielding large amounts of boulders as shear stress increases on the slopes with the post glacial erosion, as it has been observed in other studied mountains (Ballantyne, 2002; Ballantyne et al.2009; Mercier, 2008; Oliva et al., 2016). Intense paraglacial activity just after deglaciation has been proposed in many valleys of Tröllaskagi, and has even been demonstrated by radiocarbon dating of several landslides (Mercier et al., 2013, 2017; Cossart et al., 2014; Coquin et al., 2015; Decaulne et al., 2016). The intense supply of material from the slopes derived from paraglacial activity can transform a retreating glacier into a rock glacier or debris-covered glacier (Johnson, 1980; Giardino and Vitek, 1988; Ackert, 1998; Janke et al., 2015; Anderson et al., 2018b; among others). In the same way, the decrease of the slope processes towrads the end of paraglacial activity may involve the slowdown of boulder accumulation and the stabilization of the rock glacier

(Humlum, 2000; Deline et al., 2015; Anderson and Anderson, 2016). In the context described, these Tröllaskagi rock glaciers could be framed in a paraglacial mountain landscape (Knight et al., 2018).

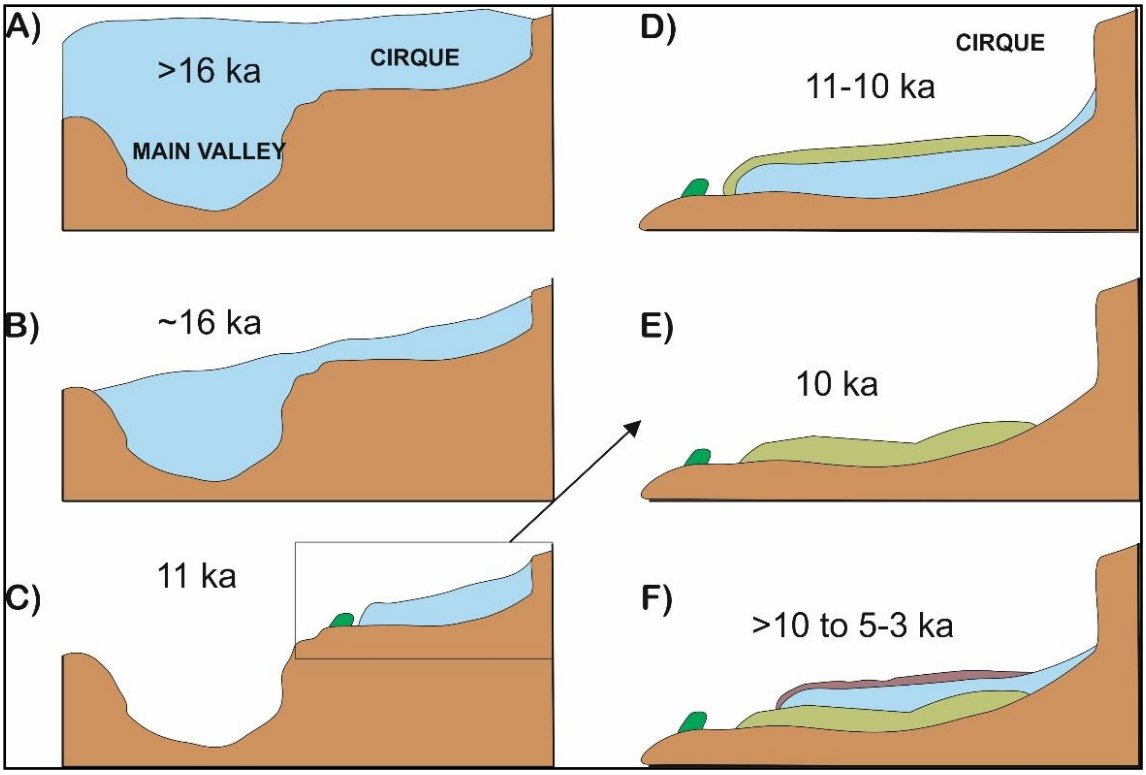

Figure 6.11. Idealized model about the evolution of glaciers in the Tröllaskagi mountains according to the CRE dating results. (A) The main valleys of the interior of Tröllaskagi were covered with ice before 16 ka, feeding the glacier outlet of Skagafjörður. (B) Around 16 ka a series begins of rapid, intense, glaciological and geomorphological processes; the sequence can be determined, but the uncertainty of the CRE results prevents an accurate timing of each specific moment. Deglaciation begins around 16 ka and glaciers in the interior of Tröllaskagi become disconnected from the Skagafjörður glacier outlet. (C) Subsequently, the main valleys are deglaciated with a small advance inside the cirques around 11 ka. (D) The first rock glacier generation forms around 11-10 ka. (E) The glacier fronts rapidly become inactive around 10 ka. (F) After 10 ka, a new generation of rock glaciers forms and their dynamics begin to stabilize 5-3 ka according to their altitude.

6.5.2 The exposure age of boulders in active rock glaciers and debris-covered glaciers and the climatic and geomorphological significance.

The CRE dating results from the front of the Fremri-Grjótárdalur rock glacier yielded ages of 2-6 ka (Table 6.5, Figs. 6.2 and 6.5), with two boulders around 5-6 ka. This rock glacier is considered active (Farbrot et al., 2007; Wangensteen et al., 2006; Kellerer-Pirklbauer et al., 2007, 2008b). In a recent study, the mobility of its blocks was restricted to less than 0.15 m yr^{-1} of horizontal displacement and -0.37 m in sinking during 14 years (Tanarro et al., 2019). This work confirms that the current mobility of the sampled boulders

is very limited (Table 6.1). Even the boulders on rock glaciers and debris-covered glaciers with internal ice have along the last decades a minimum displacement rate, mainly related to subsidence. All these data confirm the present static character of the rock glacier, whose subsidence linked to the slow melting of the internal ice is practically the only dynamics (Tanarro et al., 2019).

Our information obtained about the almost null flow of these formations is limited to the last decades. However, we assume that the debris-covered and rock glaciers, although they contain internal ice, if they do not have flow, their superficial boulders will always keep the same surface exposed to the radiation, since they do not move or overturn. In fact, our CRE results show a long exposure of these surfaces to the cosmic radiation, which suggests that the Hólar debris-covered and rock glaciers have been static for a long period. This limited displacement may have allowed the sampled surfaces of the blocks to be exposed to cosmogenic radiation continuously from 5 ka. As a suggestion, this date of definitive stabilization could reflect the impact of the Holocene Thermal Maximum (HTM), which in Tröllaskagi entailed the maximum birch expansion between 8 and 5 ka BP, with temperatures higher than at present (1961-1990 series) (Wastl et al., 2001; Caseldine et al., 2006). According to lake sediment dating, the ice cap Drangajökull glacier, in northeast Iceland, had retreated compared to its current extent (Schomacker et al., 2016) or even disappeared (Harning et al., 2016a, 2018b) at that time, just as other central ice-caps (Anderson et al., 2018a; Geirsdóttir et al., 2018). A MAAT >3ºC above the present mean value would be required for this to occur (Anderson et al., 2018a; Geirsdóttir et al., 2018). We can therefore deduce that the Fremri-Grjótárdalur rock glacier flow ended during the HTM, when the headland glacier stopped feeding the tongue, composed of a mixture of debris and ice, which remained static, as it was above the permafrost level (Etzelmüller et al., 2007; Wangensteen et al., 2006).

In fact, with our data another interpretation is possible. The present Tröllaskagi rock glaciers with internal ice could be formed at the onset of the Neoglacial cooling, 5 ka ago (see synthesis in Geirsdóttir et al., 2018).

The comparison of our results with other cases is complicated, since the boulders on the top of an active rock glacier (Fig. 6.5) have only been dated very rarely by CRE. One of the rare occasions when boulders were dated was in the Southern Alps (Winkler and Lambiel, 2018). This work support our identification of the rock glacier boulders with the age of the rock glacier stabilization within CRE ages.

The results obtained in the Hofsjökull debris-covered glacier are similar to those of the stagnant ice rock glaciers in Fremri-Grjótárdalur. Three boulders at the glacier front

yielded similar ages between 5-7 ka, thus supporting its possible “stabilization” during the HTM. It is important to remember that these blocks belong to a 2-m-thick debris cover resting on about 20 m thick glacial ice as it was observed in the field. Their current boulder subsidence rates is of -0.55 m yr^{-1} and horizontal displacement ranges from 0.18 to 0.37 m yr^{-1}, probably derived from the subsidence processes, and their frontal limits do not advance along 50 years.

The CRE results obtained from the collapsed sector of the Héðinsdalsjökull debris-covered glacier, at 650 m a.s.l., yielded ages between 2 and 3 ka. This front is now completely static and has no internal ice. CRE dates previously obtained on fossil debris-covered glaciers suggest different timing of existence of those exposed to strong radiation (which lost the ice shortly after being formed) compared to nearby glaciers which are more shielded, with glacial activity lasting for thousands of years (Fernández-Fernández et al., 2017). Thus, our results may show the end of the most important Neoglacial advances in Tröllaskagi around 3.2 ka (Caseldine and Hatton, 1994; Stötter et al., 1999; Wastl et al., 2001 among others), as occurred in some sectors of Drangajökull (Harning et al., 2016a, 2018b), where lake records indicate severe cooling in Iceland (synthesis in Geirsdóttir et al., 2018). The other possibility is that the glacier stabilized after the end of the Little Ice Age, due to a temperature increase of 1-1.2 ºC (Anderson et al., 2018a; see Chapter 4). Since then, the front of the Héðinsdalsjökull debris-covered may have collapsed, as it is below the permafrost level, while internal ice still remains at present in its mid and upper sectors, above altitude 900 m a.s.l.

6.6. Conclusions.

Despite the few samples collected, the results are fully coherent from the geomorphological and chronostratigraphical point of view and with previous knowledge of the deglaciation in Iceland, coming mainly from lake sediment dating around the large ice-caps. Our results allow for preliminary reconstruction of the glacier behavior in valleys and cirques of the Tröllaskagi peninsula during and after the last deglaciation.

Just as in the Icelandic fjords, the valley glaciers in the Tröllaskagi peninsula began their retreat at around 16 ka. The glacier dynamics between the onset of deglaciation and the beginning of the Holocene cannot be determined at present, as there are no preserved glacial landforms between the terminal part of the valleys and the base of the cirques. Small moraines occur in these cirques, with ages apparently corresponding to the last glacial advance in the fjords, probably during the Preboreal, around 11 ka. After this date, the glaciers retreated abruptly, as in the rest of Iceland, triggering paraglacial processes on the

deglaciated walls, with the subsequent formation of debris-covered and rock glaciers with fronts which shortly stabilized, especially those at lower altitudes.

New rock glaciers and debris-covered glaciers were then formed at the upper sectors of the valleys, and previous glaciers re-advanced to form new tongues. These new formations still retain currently internal ice covered by debris, but display minimal dynamics, mainly related to subsidence. These limited dynamics allowed the boulder surfaces resting on the ice exposed to cosmic radiation. This indicates that these debris-covered glaciers and rock glaciers no longer accumulated ice in their head areas. This stabilization timing oscillates between 7 and 3 ka ago and may have been caused either by the HTM warm period or remobilization during the cold Neoglacial periods. To fully understand this evolution and its origin, more information must be collected. Nevertheless, this research demonstrates the enormous potential of CRE dating methods in the study of the past dynamics of debris-covered glaciers and rock glaciers both in the frame of the glacial landscape evolution and in the understanding of the debris-free glaciers transformation to debris-covered and rock glaciers.

Chapter 7.

Conclusions.

In the preceding chapters, the Doctoral Thesis has achieved the intended objectives, which can be summarized in three "groups": (i) new paleoclimate data, based on the peculiarities of the Tröllaskagi glaciers and the Icelandic climate, which broaden the understanding of the current climate change trend; (ii) new chronological data on glaciers that has helped to expand the knowledge of the evolution of the Tröllaskagi glaciers at the Late Holocene; and (iii) the application of a novel methodological sequence that precisely and justifiably combines different techniques and glacial parameters for the study of deglaciation.

This last section of the Thesis has been reserved to present in an orderly fashion: the relationships between glaciers and climatic tendency; glacial evolution during the Neoglacial; relationships between deglaciation and the formation of rock glaciers and debris-covered glaciers; the main methodological conclusions of the study; and future research perspectives.

7.1. Relationships between the recent evolution of glaciers and climate change.

To understand the relationships between the Tröllaskagi glaciers and climate, the Thesis has analysed (Chapter 4) the recent climate trend and the evolution of three Tröllaskagi debris-free glaciers (Gljúfurárjökull, western Tungnahryggsjökull and eastern Tungnahryggsjökull) from the end of the Little Ice Age (LIA) to 2005. The investigation has confirmed that the sharp end of the LIA coincided with an increase in temperature (summer and annual) sustained for more than 20 years (second warmest period in the analysed interval), which determined that most of the retreat and volume loss of the glaciers had occurred by 1946. This confirms the important control exerted by the temperature on the glaciers. The Thesis proves that the climate warming trend after the LIA was only reversed in 1951-1955, 1966-1973 and 1979-1986, with annual and summer temperatures below the average that determined the advance of the glaciers –at least between the eighties and

nineties– as shown by aerial photographs. The results of the investigation indicate that the last important glacial advance, initiated at the end of the seventies, occurred after 10 consecutive years with below average summer temperatures.

On the other hand, the Thesis has not been able to establish such clear relationships between the evolution of precipitation and glacial fronts. The research in Chapter 4 has shown that the increase in precipitation estimated in the warmer dates analysed (1946 and 2005) was not enough to reverse glacial retreat, at least immediately, although it did reduce the intensity of this retreat. On the contrary, the Thesis suggests that the increase in precipitation between 1985 and 1994, observed when comparing the quantities calculated by the glacier-climate models on both dates, could have been responsible for the continuous advance of the glaciers, even in the middle of the nineties despite being a warm period. In this way, this research shows that during the period analysed, precipitation has not controlled the evolution of glaciers as directly as temperature, but it has been able to have some influence on the reaction of glacial fronts, such as provoking their advance even in warm periods.

The glacier-climate models in the Thesis, however, have shown an estimated decrease in precipitation in cold periods and an increase in warm periods, corresponding to the predominant air masses and the influence of the ocean, where the presence or absence of sea ice can impede or favour convective processes, as has been suggested in Chapter 4. Likewise, there is also evidence of the close relationship between precipitation and changes in the North Atlantic Oscillation (NAO) mode, with increases in precipitation / accumulation in the positive phases of the NAO, and reduction in the negative phases. However, research has not been able to clarify the relationships between the changes in the NAO and the fluctuations of the glacial fronts, and only points out a possible association between the glacial retreat that occurred from the 1950s until the end of the 1970s, due to a long negative NAO phase.

7.2. The effects of Neoglaciation on the glaciers in Northern Iceland.

The cooling of the climate initiated at around 5 ka determined the formation of new cirque glaciers in the headwaters of the Tröllaskagi valleys. In response to sudden climate cooling, these glaciers advanced in different phases before and after the LIA, some of which have been dated in Chapter 5 through the application of Cosmic-Ray Exposure (CRE) and lichenometric dating methods.

As a result, the Thesis provides new results that complete the limited knowledge of glacial evolution prior to the LIA in Tröllaskagi. The findings refute the results of previous glacial chronologies based on lichenometric dating. This new data rectifies the traditional hypothesis according to which the maximum glacial advance of the Late Holocene culminated in the LIA, which, in fact, did occur in other ice caps of the south, centre and northwest of Iceland. This Thesis demonstrates the existence of extensive glacial advances towards 1.6 and 1.3 ka in Vesturdalur and Austurdalur that coincides with an important cold period in Europe known as "Dark Ages Cold Period". These results have important paleaoclimatic implications, since they did not occur in the coldest period of the Neoglacial era, experienced between 0.7 and 0.1 ka, that is, during the LIA. Therefore, these neoglacial advances, more extensive than those of the LIA, could derive from increases in accumulation in glacial cirques, either by an increase in precipitation or by overfeeding (snow blowing, avalanches, etc.). On the other hand, the fact that the maximum Neoglacial advances occurred before the LIA could be motivated by a shorter response time in the Tröllaskagi glaciers, compared to the ice-caps, whose maximum expansion occurred later.

Chapter 5 of the Thesis has also shown that the glaciers of Vesturdalur and Austurdalur began their advance during the LIA long before what had been proposed in Tröllaskagi, developing their maximum extension during the 15th and 17th centuries at the latest. The results have allowed us to date several moraines from the 15th century (second third of the LIA), which indicates the great sensitivity of these glaciers to the climatic variability of the LIA. In addition, the combination of dating with geomorphological mapping suggests that the maximum advance of the LIA did not occur in the coldest period (last third, eighteenth-nineteenth centuries), but before. Therefore, the Thesis suggests that these more extensive advances could be attributed more to solar forcing or precipitation increase than decrease in temperatures.

On the other hand, low temperatures, in conjunction with solar or volcanic forcing, or the presence of sea ice, could have triggered the different advances of the last third of the LIA, which have been dated from the 19th century using lichenometry. These advances occurred in the decades of the 1830s, 1840s, 1860s and 1890s.

7.3. The formation of rock glaciers in the context of deglaciation.

Sudden changes in climate in the form of warming not only determined the retreat of the glaciers, but also their transformation when the headwalls and slopes were ice-free. Consequently, paraglacial dynamics began, which were highly active on the Tröllaskagi slopes. Paraglacial activity caused large volumes of rocks to fall from the walls onto the

retreated glaciers and this determined their transformation into debris-covered or rock glaciers.

Due to the existence of some polished thresholds in the interfluves, the Thesis was able to determine the deglaciation of the Kolbeinsdalur-Viðinesdalur valley system at around 16 ka. The existence of moraines inside the cirques (Fremri Grjótárdalur, Hóladalur), dating back to 11 ka, indicates that these glaciers were disconnected from Icelandic Ice Sheet in the form of alpine glaciers, at least from the Allerød interstadial (13.9-12.9 ka). On the other hand, the age of the fossil rock glaciers of Fremri-Grjótárdalur has been set at around 11-9 ka, which indicates that the moraine abandonment, the transformation of the glaciers into rock glaciers and the stabilization of their fronts happened quickly, just after deglaciation, at the beginning of the Holocene. These ages also demonstrate the intensity of the paraglacial processes, initiated along with the deglaciation of the slopes, coinciding with what happened in other nearby valleys. This dynamism transformed the glaciers of Hóladalur, Hofsdalur and Héðinsdalur into debris-covered glaciers.

After the rock glaciers of Fremri-Grjótárdalur collapsed and stabilized at 11-9 ka, new rock glaciers were formed in the cirques, which currently still are formed by internal ice, but which are completely static. This state made it possible to date their stabilization back to around 7-5 ka. The limited flow of the debris-covered glacier of Hofsdalur also allowed the dating of the stabilization of its front, which also occurred between 7 and 5 ka. For both cases, the Thesis offers a double interpretation: (i) the impact of the Holocene Thermal Maximum on these glaciers, with the consequent reduction of the flow and stabilization; or (ii) the origin of both formations during Neoglaciation. In contrast, the collapse of the front of the debris-covered glacier of Héðinsdalur occurred later, between 3 and 2 ka, coinciding with the end of major Neoglacial advances.

Therefore, the application of CRE dating in this thesis has improved the understanding of the deglaciation of the main valleys of Tröllaskagi and the subsequent process of transformation from debris-free glaciers into debris-covered or rock glaciers. These landforms, despite their lower dynamism and climate sensitivity, have been used as indicators of climate change. Front stabilizations are indicative of warm periods or reduction of precipitations and their dating has allowed us to evaluate the timing and impact of the climatic changes in this type of glaciers.

However, it should be noted that despite the information obtained through the dating, it is complicated to reconstruct in greater detail the deglaciation sequence of the main valleys due to the intensity of the geomorphological processes on slopes and the deposition of post-glacial sediments. The activity of these geomorphological agents implies the

degradation of glacial landforms, as glacial thresholds and moraines, which would be potentially datable.

7.4. Proposal of a new methodological strategy for the study of the evolution of glaciers as indicators of climate change.

The success of the results depends on the precise application and integration of the different techniques that make up the methodological body of the research. In this sense, the thesis proposes a methodological sequence that allows the use of glaciers as indicators of climate change and sources of palaeoclimatic information. On the one hand, the Thesis has managed to use the current glaciers as a direct record of the recent evolution of the climate –periods of warming and cooling–, through the analysis of its recent trends –periods of retreat and advance–. On the other hand, from the study and reconstruction of former glaciers (palaeoglaciers), the Thesis has been able to determine the climatic conditions that made their existence possible (palaeoclimate).

The methodological sequence of the Thesis is a complex structure that integrates techniques of a different nature. The discussion in Chapter 3 of the Thesis about the advantages and disadvantages of each technique ensures its applicability and suitability in the future. Therefore, the methodology used by the Thesis and the results that derive from it can be considered valid.

This thesis proposes a versatile methodology with great potential for application in contrasting areas, since it does not include methods designed only for a specific glacier or areas. The study of glaciers as indicators of climate change based only on one single variable –for example, the variations of their front– is discouraged. Therefore, this study required the analysis of different complementary parameters related to climate such as area, volume or ELA. This research also required the combination of different methods that make it possible to monitor the changes experienced by glaciers over time and understand the relationships of these changes with the climate system. In this sense, the Thesis has applied complementary techniques such as photointerpretation, geomorphological cartography, palaeoglacier reconstruction, palaeoclimatic reconstruction, and lichenometric and CRE dating.

In the study of the recent glacier trends (Chapter 4), the Thesis has shown that multitemporal aerial photographs are very useful for analysing the evolution of glaciers since the LIA, without depending on the state of conservation of the moraines, which is essential in such a geomorphological dynamic environment. However, the scarce availability of aerial

photographs of the glaciers studied –only 1946, 1985, 1994 and 2000– limited their potential to record the impact of short-lived climatic disturbances on small glaciers, as in the case of 1951-1955 and 1974-1978, cold and warm, respectively. However, as could be seen in Chapter 5 with the Neoglacial and LIA advances, geomorphological photointerpretation, especially the identification of moraines, has been essential in the reconstruction of the locations of glacial fronts on dates without photographic records. In this same chapter, the Thesis also reinforces the role of aerial photography to solve some of the most problematic points of lichenometric dating, such as knowledge of lichen colonization periods.

The Thesis has correctly selected the glacial parameters that affected the variations in the geometry of the glaciers and the fluctuations of their fronts. This is the case of volumes, whose changes are consistent with that observed in the glacial areas and glacial front locations. Chapter 3 of the Thesis makes a correct adjustment of the morphometric and glaciological parameters (glacier width, slope, lateral drag, flow and mass balance) that define the exponential relationship between area and volume ($V \propto cS^{\gamma}$). They lead to the theoretical value of the exponent $\gamma = 1.375$, which is close to the empirical value observed in current glaciers ($\gamma \approx 1.36$). However, the estimation of the volumes has been limited due to the small number of glaciers studied and the lack of knowledge of the constant "*c*" value that modulates the theoretical relationship between area and volume in Tröllaskagi. On the other hand, as observed in Chapter 4, the glaciers were not in equilibrium with the climate in the analysed periods, since they were retreating or advancing, which could have distorted the calculations.

The Thesis shows (Chapters 4 and 5) a good correspondence between the trend of the glacial volumes obtained according to the area volume scaling approach in recent dates and that derived from palaeoglacier reconstruction by the application of numerical physical-based models. In addition, the Thesis studied the evolution of glaciers and the ELA with consistent results in the reconstructions of palaeoglacier, both through numerical models and using a cartographic approach. In this sense, the Thesis highlights the importance of the ELA parameter in the analysed glaciers as a powerful indicator of climate change. In fact, ELA variations after the LIA are consistent with climatic fluctuations recorded in the Akureyri climatological series (Chapters 4 and 5). Nevertheless, the Thesis also suggested that the real results could be underestimated when comparing the evolution of the summer temperature with the variations of the ELA. Therefore, it also highlights the need to consider changes in precipitation, as well as the role of snow drifting, especially when the glaciers are on the leeward side of a plateau.

The thesis has enriched the climatic information that can be derived from the ELAs through the application of glacier-climate models. As observed in the palaeoclimatic reconstructions in Chapter 4, these models were essential for the knowledge of climatic conditions (temperature and precipitation as the most influential variables in the mass balance) under which the glaciers existed and for obtaining information on the impact of the climatic fluctuations. In this same chapter, the Thesis highlights the utility of these models in determining changes in the patterns of regional atmospheric circulation.

In Chapter 5, the Thesis has been able to establish the timing of the culmination of advances or stabilizations of glaciers as indicative of climatic phases propitious to glacial expansion, either as a result of periods of cooling or increased precipitation. Chapter 6 reinforces the suitability of CRE dating of the stabilization of rock glaciers, as stages of evolution indicative of changes in climate.

In order to fulfil the main objective of improving knowledge of the evolution of glaciers during the Late Holocene, Chapter 5 of the Thesis required the combination of several complementary dating techniques (CRE dating, lichenometry and historical aerial photographs). The Thesis has dated both recent glacial phases, such as those corresponding to the LIA and older Neoglacial ones, at temporal scales of tens, hundreds and thousands of years. Chapter 5 of the Thesis has also shown that the superimposed and coordinated test of different techniques such as lichenometry, fieldwork and aerial photography, avoids obtaining anomalous results derived from the intrinsic technical limitations of each dating method. This is the case, for example, of lichenometry in Iceland, whose results tend to underestimate the ages of the moraines and does not allow the dating of moraines prior to the last phases of the LIA. However, Chapter 5 combined this technique with aerial photographs and field observations as a means of validating the ages of recent advances and the growth rate of *Rhizocarpon geographicum*. With this approach, the Thesis also reviewed the period of colonization of lichens of this species in Tröllaskagi (15-20 years), until now based on assumptions. As an important novelty, the Thesis has introduced a new alternative species of lichen as for lichenometric dating, *Porpidia* cf. *soredizodes*, with a shorter colonization period (10-15 years) and faster growth, estimated to be found for the first time in northern Iceland at 0.737 mm yr^{-1}, although it still requires more research.

However, the Thesis has shown a limitation in the potential of dating by surface exposure through cosmogenic isotopes (^{36}Cl) and lichenometry in the valleys of Tröllaskagi, given the high slope dynamism –debris-flows and landslides, fundamentally–. This issue considerably limited the number of samples dated in Chapter 5, which in some cases

affected the ambiguity of results, complicating the interpretation of glacial evolution. In this case, the Thesis has opted for a thorough on-site geomorphological investigation and detailed cartography of moraines to identify potentially better-preserved moraines without signs of re-mobilization or deterioration, as potentially reliable datable landforms.

7.5. Proposals for future research topics: Tröllaskagi as a laboratory in the study of climate change.

Although the Doctoral Thesis has achieved the main objectives established at the beginning, new problems have arisen during the course of the investigation that would require more attention in the future to improve the knowledge of the relationships between glaciers and climate. For example, it is necessary to gain a better understanding of the patterns of wind directions and subsequent accumulation of snow into glacial cirques. This is a key issue that should be considered in the glaciers located at the foot of a plateau, in which a significant percentage of snow accumulation results from wind deflation. Improving this knowledge requires, on the one hand, a longer analysis of climatological series (precipitation and wind), and on the other, the delimitation of those plateau areas surrounding the cirques that contribute to glacial accumulation.

Further research is also needed into the relationships between fluctuations in the NAO and the response of glaciers. This issue will contribute to a better understanding of the effects that changes in regional atmospheric circulation cause in glaciers. This study involves monitoring a longer period and recording the positions of the glacier fronts with a higher temporal resolution, which allows us to observe the response of the glaciers to fluctuations of the NAO index. The understanding of the NAO-glacier relationships will, among other things, help us determine which changes in atmospheric patterns triggered the most important Neoglacial advances, or why the maximum glacial advance of the LIA occurred in some areas prior to the 17-19th centuries despite not coinciding with the coldest phases.

For a better understanding of the climate of the LIA, the palaeoclimatic reconstructions existing in Tröllaskagi should be reviewed. Traditionally, they have been based on the reconstruction of glaciers and paleo-ELAs in the phase of the maximum advance of the LIA, dated to have occurred at the end of the 19th century using lichenometry, which was associated with instrumental climatic data at the end of the same century. However, the technique used in this Thesis, dating trough cosmogenic isotopes, indicates that the LIA maximum occurred several centuries earlier, so other alternative palaeoclimatic proxies must be used in the future work.

Additionally, the Thesis showed large age uncertainties in some of the moraines investigated, either as a result of post-glacial reworking from geomorphological processes on slopes, or overlapping advances. Therefore, it will be necessary to take a larger number of samples to improve the glacial chronologies in moraines with discrepant ages. CRE should also be applied in Gljúfurárdalur and other nearby valleys to complete the knowledge of the impact of the Neoglaciation on debris-free glaciers. This will enable us to verify when the Neoglacial maximum took place in Tröllaskagi from information on a larger number of valleys. The reconstruction of the deglaciation and subsequent formation of rock glaciers and debris-covered glaciers requires an extensive application of CRE dating in nearby cirques with similar landforms to those already studied (moraines, active and inactive rock glaciers and debris-covered glaciers).

Finally, in order to improve the application of lichenometric dating, it is necessary to monitor the colonization and growth rates of the species *Rhizocarpon geographicum* and *Porpidia* cf. *soredizodes*. It will also be interesting to correlate the lichen growth rates to the evolution of environmental conditions (temperature and precipitation), when lichenometric dating is applied.

References.

Ackert, Jr., R.P., 1998. A rock glacier/debris-covered glacier system at Galena Creek, Absaroka mountains, Wyoming. Geogr. Ann. Ser. A, Phys. Geogr. 80, 267–276.

Adhikari, S., Marshall, S.J., 2012. Glacier volume-area relation for high-order mechanics and transient glacier states. Geophysical Research Letters 39, 1–6.

Ahlmann, H.W., 1924. Le Niveau De Glaciation Comme Fonction De L'accumulation D'humidité Sous Forme Solide. Geogr. Ann. 6, 223–272.

Alley, R.B., Ágústsdóttir, A.M., 2005. The 8k event: cause and consequences of a major Holocene abrupt climate change. Quat. Sci. Rev. 24, 1123–1149.

Andersen, C., Koç, N., Moros, M., 2004. A highly unstable Holocene climate in the subpolar North Atlantic: evidence from diatoms. Quat. Sci. Rev. 23, 2155–2166.

Anderson, L.S., Anderson, R.S., 2016. Modeling debris-covered glaciers: response to steady debris deposition. Cryosph. 10, 1105–1124.

Anderson, L.S., Flowers, G.E., Jarosch, A.H., Aðalgeirsdóttir, G.T., Geirsdóttir, Á., Miller, G.H., Harning, D.J., Thorsteinsson, T., Magnússon, E., Pálsson, F., 2018a. Holocene glacier and climate variations in Vestfirðir, Iceland, from the modeling of Drangajökull ice cap. Quat. Sci. Rev. 190, 39–56.

Anderson, R.S., Anderson, L.S., Armstrong, W.H., Rossi, M.W., Crump, S.E., 2018b. Glaciation of alpine valleys: The glacier–debris-covered glacier–rock glacier continuum. Geomorphology 311, 127-142.

Andrés, N., Gómez-Ortiz, A., Fernández-Fernández, J.M., Tanarro, L.M., Salvador-Franch, F., Oliva, M., Palacios, D., 2018. Timing of deglaciation and rock glacier origin in the southeastern Pyrenees: a review and new data. Boreas 47, 1050–1071.

Andrés, N., Palacios, D., Saemundsson, Þ., Brynjólfsson, S., Fernández-Fernández, J.M., 2019. The rapid deglaciation of the Skagafjörður fjord, northern Iceland. Boreas 48, 92–106.

Andrés, N., Tanarro, L.M., Fernández, J.M., Palacios, D., 2016. The origin of glacial alpine landscape in Tröllaskagi Peninsula (North Iceland). Cuad. Investig. Geográfica 42, 341–368.

Andresen, C.S., Bond, G., Kuijpers, A., Knutz, P.C., Björc, S., 2005. Holocene climate variability at multidecadal time scales detected by sedimentological indicators in a shelf core NW off Iceland. Mar. Geol. 214, 323–338.

Andrews, J.T., Giraudeau, J., 2003. Multi-proxy records showing significant Holocene environmental variability: the inner N. Iceland shelf (Húnaflói). Quat. Sci. Rev. 22, 175–193.

Andrews, J.T., Harðardóttir, J., Helgadóttir, G., Jennings, A.E., Geirsdóttir, Á., Sveinbjörnsdóttir, Á.E., Schoolfield, S., Kristjánsdóttir, G.B., Smith, L.M., Thors, K., Syvitski, J., 2000. The N and W Iceland Shelf: Insights into Last Glacial Maximum ice extent and deglaciation based on acoustic stratigraphy and basal radiocarbon AMS dates. Quat. Sci. Rev. 19, 619-631.

Arróniz-Crespo, M., Pérez-Ortega, S., De Los Ríos, A., Green, T.G.A., Ochoa-Hueso, R., Casermeiro, M.Á., De La Cruz, M.T., Pintado, A., Palacios, D., Rozzi, R., Tysklind, N., Sancho, L.G., 2014. Bryophyte-cyanobacteria associations during primary succession in recently deglaciated areas of Tierra del Fuego (Chile). PLoS One 9, 15–17.

Azócar, G.F., Brenning, A., 2010. Hydrological and geomorphological significance of rock glaciers in the dry Andes, Chile (27°-33°S). Permafr. Periglac. Process. 21, 42–53.

Bachrach, T., Jakobsen, K., Kinney, J., Nishimura, P., Reyes, A., Laroque, C.P., Smith, D.J., 2004. Dendrogeomorphological assessment of movement at hilda rock glacier, banff national park, canadian rocky mountains. Geogr. Ann. Ser. A, Phys. Geogr. 86, 1–9.

Bahr, D.B., 1997. Global distributions of glacier properties: A stochastic scaling paradigm. Water Resour. Res. 33, 1669–1679.

Bahr, D.B., Meier, M.F., Peckham, S.D., 1997. The physical basis of glacier volume-area scaling. J. Geophys. Res. Solid Earth 102, 20355–20362.

Bahr, D.B., Pfeffer, W.T., Kaser, G., 2015. A review of volume-area scaling of glaciers. Rev. Geophys. 53, 95–140.

Bahuguna, I.M., Kulkarni, A.V., Nayak, S., Rathore, B.P., Negi, H.S., Mathur, P., 2007. Himalayan glacier retreat using IRS 1C PAN stereo data. Int. J. Remote Sens. 28, 437–442.

Bakke, J., Nesje, A., 2017. Equilibrium Line Altitude (ELA). In: Singh, V.P., Singh, P., Haritashya, U.K. (Eds.), Encyclopedia of Snow, Ice and Glaciers. Springer, The Netherlands, pp. 268-277.

Ballantyne, C.K., 1989. The Loch Lomond Readvance on the isle of Skye, Scotland: Glacier reconstruction and palaeoclimatic implications. J. Quat. Sci. 4, 95–108.

Ballantyne, C.K., 2002. Paraglacial geomorphology. Quat. Sci. Rev. 21, 1935–2017.

Ballantyne, C.K., Schnabel, Ch., Xu, S., 2009. Exposure dating and reinterpretation of coarse debris accumulations (‘rock glaciers’) in the Cairngorm Mountains, Scotland. J. Quat. Sci. 24, 19-31.

Barker, S., Knorr, G., Vautravers, M.J., Diz, P., Skinner, L.C., 2010. Extreme deepening of the Atlantic overturning circulation during deglaciation. Nat. Geosci. 3, 567–571.

Barsch, D., 1996. Rockglaciers. Springer-Verlag Berlin Heidelberg, Berlin, 331 pp.

Benedict, J.B. 1973. Chronology cirque glaciation, Colorado Front Range. Quat. Res. 3, 584-599.

Benn, D.I., Bolch, T., Hands, K., Gulley, J., Luckman, A., Nicholson, L.I., Quincey, D., Thompson, S., Toumi, R., Wiseman, S., 2012. Response of debris-covered glaciers in the Mount Everest region to recent warming, and implications for outburst flood hazards. Earth-Sci. Rev. 114, 156–174.

Benn, D.I., Hulton, N.R.J., 2010. An Excel™ spreadsheet program for reconstructing the surface profile of former mountain glaciers and ice caps. Comput. Geosci. 36, 605–610.

Benn, D.I., Lehmkuhl, F., 2000. Mass balance and equilibrium-line altitudes of glaciers in high-mountain environments. Quat. Int. 65–66, 15–29.

Benn, D.I., Owen, L.A., Osmaston, H.A., Seltzer, G.O., Porter, S.C., Mark, B., 2005. Reconstruction of equilibrium-line altitudes for tropical and sub-tropical glaciers. Quat. Int. 138–139, 8–21.

Benson, L., Madole, R., Phillips, W., Landis, G., Thomas, T., Kubik, P., 2004. The probable importance of snow and sediment shielding on cosmogenic ages of north-central Colorado Pinedale and pre-Pinedale moraines. Quat. Sci. Rev. 23, 193–206.

Berger, J., Krainer, K., Mostler, W., 2004. Dynamics of an active rock glacier (Ötztal Alps, Austria). Quat. Res. 62, 233–242.

Bergþórsson, P., 1969. An Estimate of Drift Ice and Temperature in Iceland in 1000 Years. Jökull 19, 94-101.

Bibby, T., Putkonen, J., Morgan, D., Balco, G., Shuster, D.L., 2016. Million year old ice found under meter thick debris layer in Antarctica. Geophys. Res. Lett. 43 (13), 6995e7001.

Bickerton, R.W., Matthews, J.A., 1992. On the accuracy of lichenometric dates: an assessment based on the “Little Ice Age’’ moraine sequence of Nigardsbreen, southern Norway. The Holocene 2, 227–237.

Bjerknes, J., Solberg, H., 1922. Life cycle of cyclones and the polar front theory of atmospheric circulation. Geophys. Publ. 3, 1–18.

Björnsson, H., 1971. Bægisarjökull, North Iceland. Results of glaciological investigations 1967–68. Part I. Mass balance and general meteorology. Jökull 21, 1–23.

Björnsson, H., 1978. The surface area of glaciers in Iceland. Jökull 28, 31.

Björnsson, H., 1979. Glaciers in Iceland. Jökull 29, 74–80.

Björnsson, H., 2003. The annual cycle of temperature in Iceland, Technical Report 03037. Icelandic Meteorology Office, Reykjavík, 45 pp.

Björnsson, H., Pálsson, F., 2008. Icelandic glaciers. Jökull 58, 365–386.

Black, J., Miller, G.H., Geirsdóttir, Á., 2006. Diatoms as proxies for a fluctuating Holocene ice cap margin in Hvítárvatn, central Iceland, in: Eos Trans. AGU 87, Fall Meeting Supplement, Abstract PP41C–08.

Black, T.A., 1990. The Holocene fluctuation of the Kvíárjökull glacier, southeastern Iceland. Unpublished MA thesis. University of Colorado.

Böðvarsson, G. 1955. On the flow of ice-sheets and glaciers. Jökull 5, 1-8.

Bond, G., 2001. Persistent Solar Influence on North Atlantic Climate During the Holocene. Science 294, 2130–2136.

Bosson, J.B., Lambiel, C., 2016. Internal Structure and Current Evolution of Very Small Debris-Covered Glacier Systems Located in Alpine Permafrost Environments. Front. Earth Sci. 4.

Bradwell, T., 2001. A new lichenometric dating curve for Southeast Iceland. Geogr. Ann. Ser. A Phys. Geogr. 83, 91–101.

Bradwell, T., 2004a. Lichenometric dating in southeast Iceland: The size- frequency approach. Geogr. Ann. Ser. A Phys. Geogr. 86, 31–41.

Bradwell, T., 2004b. Annual Moraines and Summer Temperatures at Lambatungnajökull, Iceland. Arctic, Antarct. Alp. Res. 36, 502–508.

Bradwell, T., Armstrong, R.A., 2006. Growth rates of Rhizocarpon geographicum lichens: a review with new data from Iceland. J. Quat. Sci. 22, 311–320.

Bradwell, T., Dugmore, A.J., Sudgen, D.E., 2006. The Little Ice Age glacier maximum in Iceland and the North Atlantic Oscillation: evidence from Lambatungnajökull, southeast Iceland. Boreas 35, 61–80.

Bradwell, T., Sigurđsson, O., Everest, J., 2013. Recent, very rapid retreat of a temperate glacier in SE Iceland. Boreas 42, 959–973.

Braithwaite, R.J., 2008. Temperature and precipitation climate at the equilibrium-line altitude of glaciers expressed by the degree-day factor for melting snow. J. Glaciol. 54, 437–444.

Braithwaite, R.J., Raper, S.C.B., Chutko, K., 2006. Accumulation at the equilibrium-line altitude of glaciers inferred from a degree-day model and tested against field observations. Ann. Glaciol. 43, 329–334.

Brenning, A., 2005. Geomorphological, hydrological and climatic significance of rock glaciers in the Andes of Central Chile (33-35°S). Permafr. Periglac. Process. 16, 231–240.

Briner, J.P., Tulenko, J.P., Young, N. E., Baichtal, J.F., Lesnek, A., 2017. The last deglaciation of Alaska. Cuad. Investig. Geográfica, 43(2), 429-448.

Brückner, E., 1886. Die Hohern Tauern und ihre Eisbedeckung. Zeitschrift des Deutsch-Österreichische Alpenvereins 17, 163–187.

Brückner, E., 1887. Die Höhern der Schneelinie und ihre Bestimmung. Meteorol. Zeitschrift 4, 31–32.

Brugger, K.A., 2006. Late Pleistocene climate inferred from the reconstruction of the Taylor River glacier complex, southern Sawatch Range, Colorado. Geomorphology 75, 318–329.

Brynjólfsson, S., Ingólfsson, Ó., Schomacker, A., 2012. Surge fingerprintings of cirque glaciers at Tröllaskagi peninsula, North Iceland. Jökull 62, 153–168.

Brynjólfsson, S., Schomacker, A., Guðmundsdóttir, E.R., Ingólfsson, Ó., 2015b. A 300-year surge history of the Drangajökull ice cap, northwest Iceland, and its maximum during the Little Ice Age. The Holocene 25(7), 1076-1092.

Brynjólfsson, S., Schomacker, A., Ingólfsson, Ó., Keiding, J.K., 2015a. Cosmogenic 36Cl exposure ages reveal a 9.3 ka BP glacier advance and the Late Weichselian-Early Holocene glacial history of the Drangajökull region, northwest Iceland. Quat. Sci. Rev. 126, 140–157.

Burn, M.J., Holmes, J., Kenedy, L.M., Bain, A., Marshall, J.D., Perdikaris, S., 2016. A sediment-based reconstruction of Caribbean effective precipitation during the 'Little Ice Age' from Freshwater Pond, Barbuda. The Holocene 26(8), 1237-1247.

Campos, N., Tanarro, L.M., Palacios, D., Zamorano, J.J., 2019. Slow dynamics in debris-covered and rock glaciers in Hofsdalur, Tröllaskagi Peninsula (northern Iceland). Geomorphology 342, 61–77.

Capt, M., Bosson, J.B.B., Fischer, M., Micheletti, N., Lambiel, C., 2016. Decadal evolution of a very small heavily debris-covered glacier in an Alpine permafrost environment. J. Glaciol. 62, 535–551.

Carr, S., Coleman, C., 2007. An improved technique for the reconstruction of former glacier mass-balance and dynamics. Geomorphology 92, 76–90.

Carr, S.J., Lukas, S., Mills, S.C., 2010. Glacier reconstruction and mass-balance modelling as a geomorphic and palaeoclimatic tool. Earth Surf. Process. Landforms 35, 1103–1115.

Caseldine, C., 1983. Resurvey of the margins of Gljúfurárjökull and the chronology of recent deglaciation. Jökull 33, 111–118.

Caseldine, C., 1987. Neoglacial glacier variations in northern Iceland: Examples from the Eyjafjörður area. Arct. Alp. Res. 19, 296–304.

Caseldine, C., Geirsdóttir, Á., Langdon, P., 2003. Efstadalsvatn – a multi-proxy study of a Holocene lacustrine sequence from NW Iceland. J. Paleolimnol. 30, 55–73.

Caseldine, C., Hatton, J., 1994. Environmental change in Iceland. Münchener Geogr. Abhandlungen. R. B Bd. B 12 41–62.

Caseldine, C., Langdon, P., Holmes, N., 2006. Early Holocene climate variability and the timing and extent of the Holocene thermal maximum (HTM) in northern Iceland. Quat. Sci. Rev. 25, 2314–2331.

Caseldine, C., Stotter, J., 1993. "Little Ice Age'' glaciation of Tröllaskagi peninsula, northern Iceland: climatic implications for reconstructed equilibrium line altitudes (ELAs)." The Holocene 3, 357–366.

Caseldine, C.J., 1985a. The Extent of Some Glaciers in Northern Iceland during the Little Ice Age and the Nature of Recent Deglaciation. Geogr. J. 151, 215–227.

Caseldine, C.J., 1985b. Survey of Gljúfurárjökull and features associated with a glacier burst in Gljúfurárdalur, Northern Iceland. Jökull 35, 61-68.

Caseldine, C.J., 1988. Fluctuations of Gljúfurárjökull, Northern Iceland 1983-1987. Jökull 38, 32-34.

Caseldine, C.J., 1990. A review of dating methods and their application in the development of a Holocene glacial chronology for Northern Iceland, in: Gletscher- Und Landschaftsgeschichtliche Untersuchungen in Nordisland. pp. 59–82.

Caseldine, C.J., 1991. Lichenometric dating, lichen population studies and Holocene glacial history in Tröllaskagi, Northern Iceland, in: Maizels, J.K., Caseldine, C. (Eds.), Environmental Change in Iceland: Past and Present. Glaciology and Quaternary Geology, Vol 7. Springer, Dordrecht, pp. 219–233.

Caseldine, C.J., Cullingford, R.A., 1981. Recent mapping of Gljúfurárjökull and Gljúfurárdalur. Jökull, 11–22.

Castañeda, I.S., Smith, L.M., Kristjánsdóttir, G.B., Andrews, J.T., 2004. Temporal changes in Holocene δ18O records from the northwest and central North Iceland Shelf. J. Quat. Sci. 19, 321–334.

Chandler, B.M.P., Evans, D.J.A., Roberts, D.H., 2016b. Recent retreat at a temperate Icelandic glacier in the context of the last ~80 years of climate change in the North Atlantic region. Arktos 2, 24.

Chandler, B.M.P., Evans, D.J.A., Roberts, D.H., Ewertowski, M., Clayton, A.I., 2016a. Glacial geomorphology of the Skálafellsjökull foreland, Iceland: A case study of 'annual' moraines. J. Maps 12, 904–916.

Chandler, B.M.P., Lukas, S., 2017. Reconstruction of Loch Lomond Stadial (Younger Dryas) glaciers on Ben More Coigach, north-west Scotland, and implications for reconstructing palaeoclimate using small ice masses. J. Quat. Sci. 32, 475–492.

Chen, J., Ohmura, A., 1990. Estimation of Alpine glacier water resources and their change since the 1870s, in: Lang H., M.A. (Ed.), Hydrology in Mountainous Regions I. IAHS; Publication, 193, pp. 127–135.

Chen, T., Robinson, L.F., Burke, A., Southon, J., Spooner, P., Morris, P.J., Ng, H.C., 2015. Synchronous centennial abrupt events in the ocean and atmosphere during the last deglaciation. Science 349, 1537–1541.

Chenet, M., Roussel, E., Jomelli, V., Grancher, D., 2010. Asynchronous Little Ice Age glacial maximum extent in southeast Iceland. Geomorphology 114, 253–260.

Church, J.A., Gregory, J.M., Huybrechts, P., Kuhn, M., Lambeck, K., Nhuan, M.T., Quin, D., Woodworth, P.L., 2001. Changes in sea level, in: Houghton, J.T., Ding, Y., Griggs, D.J., Noguer, M., Van der Linden, P.J., Dai, X., Maskell, K., Johnson, C.A. (Eds.), Climate Change 2001: The Scientific Basis. Cambridge University Press, Cambridge, pp. 639–693.

Çiner, A., Sarikaya, M.A., Yildirim, C., 2017. Misleading old age on a young landform? The dilemma of cosmogenic inheritance in surface exposure dating: Moraines vs. rock glaciers. Quat. Geochronol. 42, 76-88.

Cogley, J.G., Hock, R., Rasmussen, L.A., Arendt, A.A., Bauder, A., Braithwaite, R.J., Jansson, P., Kaser, G., Möller, M., Nicholson, L., Zemp, M., 2011. Glossary of Glacier Mass Balance and Related Terms. IHP-VII Technical Documents in Hydrology No. 86, IACS Contribution No. 2, UNESCO-IHP, Paris.

Colucci, R.R., 2016. Geomorphic influence on small glacier response to post-Little Ice Age climate warming: Julian Alps, Europe. Earth Surf. Process. Landforms 41, 1227–1240.

Colucci, R.R., Žebre, M., 2016. Late Holocene evolution of glaciers in the southeastern Alps. J. Maps 12, 289–299.

Coquin, J., Mercier, D., Bourgeois, O., Cossart, E., Decaulne, A., 2015. Gravitational spreading of mountain ridges coeval with Late Weichselian deglaciation: Impact on glacial landscapes in Tröllaskagi, northern Iceland. Quat. Sci. Rev. 107, 197–213.

Cossart, E., Mercier, D., Decaulne, A., Feuillet, T., Jónsson, H.P., Sæmundsson, Þ., 2014. Impacts of post-glacial rebound on landslide spatial distribution at a regional scale in northern Iceland (Skagafjörður). Earth Surf. Process. Landforms 39, 336–350.

Crochet, P., Jóhannesson, T., Jónsson, T., Sigurðsson, O., Björnsson, H., Pálsson, F., Barstad, I., 2007. Estimating the Spatial Distribution of Precipitation in Iceland Using a Linear Model of Orographic Precipitation. J. Hydrometeorol. 8, 1285–1306.

Cropper, T., Hanna, E., Valente, M.A., Jónsson, T., 2015. A daily Azores–Iceland North Atlantic Oscillation index back to 1850. Geosci. Data J. 2, 12–24.

D'Agata, C., Zanutta, A., 2007. Reconstruction of the recent changes of a debris-covered glacier (Brenva Glacier, Mont Blanc Massif, Italy) using indirect sources: Methods, results and validation. Glob. Planet. Change 56, 57–68.

Dahl, S.O., Nesje, A., 1992. Paleoclimatic implications based on equilibrium-line altitude depressions of reconstructed Younger Dryas and Holocene cirque glaciers in inner Nordfjord, western Norway. Palaeogeogr. Palaeoclimatol. Palaeoecol. 94, 87–97.

Davis, B.A.S., Brewer, S., Stevenson, A.C., Guiot, J., 2003. The temperature of Europe during the Holocene reconstructed from pollen data. Quat. Sci. Rev. 22, 1701–1716.

Decaulne, A., 2016. Lichenometry in Iceland, results and application. Géomorphologie Reli. Process. Environ. 22, 77–91.

Decaulne, A., Cossart, E., Mercier, D., Feuillet, T., Coquin, J., Jónsson, H.P., 2016. An early Holocene age for the Vatn landslide (Skagafjörður, central northern Iceland): Insights into the role of postglacial landsliding on slope development. The Holocene 26, 1304-1318.

Decaulne, A., Saemundsson, T., 2006. Geomorphic evidence for present-day snow-avalanche and debris-flow impact in the Icelandic Westfjords. Geomorphology 80, 80–93.

Dede, V., Cicek, I., Sarikaya, M. A., Ciner, A., Uncu, L., 2017. First cosmogenic geochronology from the Lesser Caucasus: late Pleis- tocene glaciation and rock glacier development in the Karçal Valley, NE Turkey. Quat. Sci. Rev. 164, 54–67.

Delaloye, R., Perruchoud, E., Avian, M., Kaufmann, V., Bodin, X., Hausmann, H., Ikeda, A., Kääb, A., Kellerer-Pirklbauer, A., Krainer, K., Lambiel, C., Mihajlovic, D., Staub, B., Roer, I., Thibert, E., 2008. Recent Inter annual Variations of Rock Glacier Creep in the European Alps, in: Ninth International Conference on Permafrost. Fairbanks, Alaska, United States, pp. 343–348.

Deline, P., Akçar, N., Ivy-Ochs, S., Kubik, P.W., 2015. Repeated Holocene rock avalanches onto the Brenva Glacier, Mont Blanc massif, Italy: A chronology. Quat. Sci. Rev. 126, 186-200.

Delunel, R., Bourlès, D.L., van der Beek, P.A., Schlunegger, F., Leya, I., Masarik, J., Paquet, E., 2014. Snow shielding factors for cosmogenic nuclide dating inferred from long-term neutron detector monitoring. Quat. Geochronol. 24, 16–26.

Dickson, R.R., Lamb, H.H., Malmberg, S.A., Colebrook, J.M., 1975. Climatic reversal in northern North Atlantic. Nature 256, 479–482.

Dickson, R.R., Meincke, J., Malmberg, S.A., Lee, A.J., 1988. The “great salinity anomaly” in the Northern North Atlantic 1968-1982. Prog. Oceanogr. 20, 103–151.

Dietz, A.J., Wohner, C., Kuenzer, C., 2012. European Snow Cover Characteristics between 2000 and 2011 Derived from Improved MODIS Daily Snow Cover Products. Remote Sens. 4, 2432–2454.

Diolaiuti, G., D’Agata, C., Meazza, A., Zanutta, A., Smiraglia, C., 2009. Recent (1975-2003) changes in the Miage debris-covered glacier tongue (Mont Blanc, Italy) from analysis of aerial photos and maps. Geogr. Fis. e Din. Quat. 32, 117–127.

Dong, G., Zhou, W., Yi, C., Zhang, L., Li, M., Fu, Y., Zhang, Q., 2017. Cosmogenic 10Be surface exposure dating of ‘Little Ice Age’ glacial events in the Mount Jaggang area, central Tibet. The Holocene 27(10), 1516-1525.

Dugmore, A.J., 1989. Tephrochronological studies of Holocene glacial fluctuations in South Iceland, in Oerlemans, J. (Ed.): Glacier Fluctuations and Climatic Change, pp. 37–55.

Dugmore, A.J., Cook, G.T., Shore, J.S., Newton, A.J., Edwards, K.J., Larsen, G., 1995. Radiocarbon Dating Tephra Layers in Britain and Iceland. Radiocarbon 37, 379–388.

Dunai, T.J., 2010. Cosmogenic Nuclides. Cambridge University Press, Cambridge. 187 pp.

Dunai, T.J., Binnie, S.A., Hein, A.S., Paling, S.M., 2014. The effects of a hydrogen-rich ground cover on cosmogenic thermal neutrons: Implications for exposure dating. Quat. Geochronol. 22, 183–191.

Eddudóttir, S.D., Erlendsson, E., Tinganelli, L., Gísladóttir, G., 2016. Climate change and human impact in a sensitive ecosystem: the Holocene environment of the Northwest Icelandic highland margin. Boreas 45, 715–728.

Eddy, J.A., 1976. The Maunder Minimum. Science 192 (4245), 1189–1202.

Einarsson, M.Á., 1984. Climate of Iceland. In: van Loon, H. (Ed.), World Survey of Climatology: 15: Climates of the Oceans. Elsevier, Amsterdam, pp. 673-697.

Einarsson, M.A., 1991. Temperature conditions in Iceland 1901-1990. Jökull 41, 1–20.

Einarsson, T., 1968. Jarðfræði – Saga Bergs og Lands. Mál og menning, Reykjavík. 335 pp.

Eiríksson, J., Knudsen, K.L., Haflidason, H., Henriksen, P., 2000. Late-glacial and Holocene palaeoceanography of the North Icelandic shelf. J. Quat. Sci. 15, 23–42.

Emmer, A., Loarte, E.C., Klimeš, J., Vilímek, V., 2015. Recent evolution and degradation of the bent Jatunraju glacier (Cordillera Blanca, Peru). Geomorphology 228, 345–355.

Eriksen, H.Ø., Rouyet, L., Lauknes, T.R., Berthling, I., Isaksen, K., Hindberg, H., Corner, G.D., 2018. Recent Acceleration of a Rock Glacier Complex, Ádjet, Norway, Documented by 62 Years of Remote Sensing Observations. Geophys. Res. Lett. 45 (16), 8314-8323.

Etzelmüller, B., Farbrot, H., Guðmundsson, Á., Humlum, O., Tveito, O.E., Björnsson, H., 2007. The regional distribution of mountain permafrost in Iceland. Permafr. Periglac. Process. 18, 185–199.

Evans, D.J.A., Archer, S., Wilson, D.J.H., 1999. A comparison of the lichenometric and Schmidt hammer dating techniques based on data from the proglacial areas of some Icelandic glaciers. Quat. Sci. Rev. 18, 13–41.

Evans, D.J.A., Ewertowski, M., Orton, C., 2016a. Eiríksjökull plateau icefield landsystem, Iceland. J. Maps 12, 747–756.

Evans, D.J.A., Ewertowski, M., Orton, C., 2016b. Fláajökull (north lobe), Iceland: active temperate piedmont lobe glacial landsystem. J. Maps 12, 777–789.

Evans, D.J.A., Orton, C., 2015. Heinabergsjökull and Skalafellsjökull, Iceland: active temperate piedmont lobe and outwash head glacial landsystem. J. Maps 11, 415–431.

Evans, D.J.A., Twigg, D.R., Rea, B.R., Shand, M., 2007. Surficial geology and geomorphology of the Brúarjökull surging glacier landsystem. J. Maps 3, 349–367.

Everest, J., Bradwell, T., Jones, L., Hughes, L., 2017. The geomorphology of Svínafellsjökull and Virkisjökull-Falljökull glacier forelands, southeast Iceland. J. Maps 13, 936–945.

Eythórsson, J., 1931. On the present position of the glaciers in Iceland: some preliminary studies and investigations in the summer 1930. Vísindafélag Isl, Rit, p 10, Reykjavik.

Eythórsson, J., 1935. On the Variations of Glaciers in Iceland. Geogr. Ann. 17, 121–137.

Farbrot, H., Etzelmüller, B., Guðmundsson, Á., Humlum, O., Kellerer-Pirklbauer, A., Eiken, T., Wangensteen, B., 2007. Rock glaciers and permafrost in Tröllaskagi, northern Iceland. Z. Geomorph. N.F. (Suppl. 51), 1–16.

Farinotti, D., Huss, M., Bauder, A., Funk, M., Truffer, M., 2009. A method to estimate ice volume and ice thickness distribution of alpine glaciers. J. Glaciol. 55, 422–430.

Federici, P.R., Stefanini, C.S., 2001. Evidence and chronology of the Little Ice Age in the Argentera Massif (Italian Maritime Alps). Zeitschrift für Gletscherkd. und Glazialgeol. Band 37, 35–48.

Fernández-Fernández, J.M., Palacios, D., García-Ruiz, J.M., Andrés, N., Schimmelpfennig, I., Gómez-Villar, A., Santos-González, J., Álvarez-Martínez, J., Arnáez, J., Úbeda, J., Léanni, L., Aumaître, G., Bourlès, D., Keddadouche, K., 2017b. Chronological and geomorphological investigation of fossil debris-covered glaciers in relation to deglaciation processes: A case study in the Sierra de La Demanda, northern Spain. Quat. Sci. Rev. 170, 232–249.

Feuillet, T., Coquin, J., Mercier, D., Cossart, E., Decaulne, A., Jónsson, H.P., Sæmundsson, Þ., 2014. Focusing on the spatial non-stationarity of landslide predisposing factors in northern Iceland. Prog. Phys. Geogr. 38, 354–377.

Fink, D., Vogt, S., Hotchkis, M., 2000. Cross-sections for 36Cl from Ti at Ep=35–150 MeV: Applications to in-situ exposure dating. Nucl. Instruments Methods Phys. Res. Sect. B Beam Interact. with Mater. Atoms 172, 861–866.

Flowers, G.E., Björnsson, H., Geirsdóttir, Á., Miller, G.H., Black, J.L., Clarke, G.K.C., 2008. Holocene climate conditions and glacier variation in central Iceland from physical modelling and empirical evidence. Quat. Sci. Rev. 27, 797–813.

Flowers, G.E., Björnsson, H., Geirsdóttir, Á., Miller, G.H., Clarke, G.K.C., 2007. Glacier fluctuation and inferred climatology of Langjökull ice cap through the Little Ice Age. Quat. Sci. Rev. 26, 2337–2353.

Francou, B., Vincent, C., 2007. Les glaciers à l'épreuve du climat, IRD Editions.

Fuchs, M.C., Bohlert, R., Krbetschek, M., Preusser, F., Egli, M., 2013. Exploring the potential of luminescence methods for dating Alpine rock glaciers. Quat. Geochronol. 18, 17-33.

Gabbud, C., Micheletti, N., Lane, S.N., 2016. Response of a temperate alpine valley glacier to climate change at the decadal scale. Geogr. Ann. Ser. A, Phys. Geogr. 98, 81–95.

Gachev, E., Stoyanov, K., Gikov, A., 2016. Small glaciers on the Balkan Peninsula: State and changes in the last several years. Quat. Int. 415, 33–54.

Galanin, A.A. Lytkin, V.M. Fedorov, A.N. Kadota, T. 2014, Kriosfera Zemli, XVIII (2), 64–74.

Gardner, A.S., Moholdt, G., Cogley, J.G., Wouters, B., Arendt, A.A., Wahr, J., Berthier, E., Hock, R., Pfeffer, W.T., Kaser, G., Ligtenberg, S.R.M., Bolch, T., Sharp, M.J., Hagen, J.O., Van Den Broeke, M.R., Paul, F., 2013. A reconciled estimate of glacier contributions to sea level rise: 2003 to 2009. Science 340, 852–857.

Geirsdóttir, Á., Andrews, J.T., Ólafsdóttir, S., Helgadótti, G., Hardardóttir, J., 2002. A 36 Ky record of iceberg rafting and sedimentation from north-west Iceland. Polar Res. 21, 291–298.

Geirsdóttir, Á., Miller, G.H., 2004. Hlý og köld tíma- bil lesin úr setlögum íslenskra stöðuvatna. Raunvísin- daþing í Reykjavík, Ágrip Jarðvísindi og Landfræði, 5.

Geirsdóttir, Á., Miller, G.H., Andrews, J.T., Harning, D.J., Anderson, L.S., Thordarson, T., 2018. The onset of Neoglaciation in Iceland and the 4.2 ka event. Clim. Past Discuss. 1–33.

Geirsdóttir, Á., Miller, G.H., Axford, Y., Sædís Ólafsdóttir, 2009. Holocene and latest Pleistocene climate and glacier fluctuations in Iceland. Quat. Sci. Rev. 28, 2107–2118.

Geirsdóttir, Á., Miller, G.H., Larsen, D.J., Ólafsdóttir, S., 2013. Abrupt Holocene climate transitions in the northern North Atlantic region recorded by synchronized lacustrine records in Iceland. Quat. Sci. Rev. 70, 48–62.

Giardino, J.R., Vitek, J.D., 1988. The significance of rock glaciers in the glacial periglacial landscape continuum. J. Quat. Sci. 3 (1), 97-103.

Gibson, M.J., Glasser, N.F., Quincey, D.J., Rowan, A.V., Irvine-Fynn, T.D., 2017. Changes in glacier surface cover on Baltoro glacier, Karakoram, north Pakistan, 2001–2012. J. Maps 13, 100–108.

Giraudeau, J., Cremer, M., Manthé, S., Labeyrie, L., Bond, G., 2000. Coccolith evidence for instabilities in surface circulation south of Iceland during Holocene times. Earth Planet. Sci. Lett. 179, 257–268.

Gjermundsen, E.F., Mathieu, R., Kääb, A., Chinn, T., Fitzharris, B., Hagen, J.O., 2011. Assessment of multispectral glacier mapping methods and derivation of glacier area changes, 1978–2002, in the central Southern Alps, New Zealand, from ASTER satellite data, field survey and existing inventory data. J. Glaciol. 57, 667–683.

Glasser, N.F., Jansson, K.N., Duller, G.A.T., Singarayer, J., Holloway, M., Harrison, S., 2016. Glacial lake drainage in Patagonia (13-8 kyr) and response of the adjacent Pacific Ocean. Sci. Rep. 6, 21064.

Glenn, J.W., 1958. The flow law of ice: A discussion of the assumptions made in glacier theory, their experimental foundations and consequences, in: International Association of Scientific Hydrology. International Association of Scientific Hydrology Publication 47 (Symposium at Chamonix 1958 — Physics of the Movement of the Ice), pp. 171–183.

Gordon, J.E., Sharp, M., 1983. Lichenometry in dating recent glacial landforms and deposits, southeast Iceland. Boreas 12, 191–200.

Gross, G., Kerschner, H., Patzelt, G., 1978. Methodische Untersuchungen über die Schneegrenze in alpinen Gletschergebieten. Zeitschrift für Gletscherkd. und Glazialgeol. 12, 223–251.

Grove, J.M., 1988. The Little Ice Age. Routledge, London, 502 pp.

Grove, J.M., 2001. The initiation of the “Little Ice Age” in regions round the North Atlantic. Clim. Change 48, 53–82.

Guðmundsson, H.J., 1997. A review of the Holocene environmental history of Iceland. Quat. Sci. Rev. 16, 81–92.

Häberle, T., 1991. Holocene Glacial History of the Hörgárdalur Area, Tröllaskagi, Northern Iceland, in: Maizels, J.K., Caseldine, C. (Eds.), Environmental Change in Iceland: Past and Present. Glaciology and Quaternary Geology, Vol 7. Springer, Dordrecht, pp. 193–202.

Häberle, T., 1994. Glacial, Late Glacial and Holocene History of the Hörgárdalur Area, Tröllaskagi, Northern Iceland, in: Stöttter, J., Wilhelm, F. (Eds.), Environmental Change in Iceland. Münchener Geographische Abhandlungen, Reihe B, pp. 133–145.

Haeberli, W., 1995. Glacier Fluctuations and Climate Change Detection. Geogr. Fis. e Din. Quat. 18, 191–199.

Haeberli, W., Brandova, D., Burga, C., Egli, M., Frauenfelder, R., Kääb, A., Maisch, M., Mauz, B., Dikau, R., 2003. Methods for absolute and relative age dating of rockglacier surfaces in alpine permafrost, in: Phillips, M., Springman, S., Arenson, L. (Eds.), Proceedings of the 8th International Conference on Permafrost 2003, Zürich, pp. 343-348.

Haeberli, W., Hallet, B., Arenson, L., Elconin, R., Humlum, O., Kääb, A., Kaufmann, V., Ladanyi, B., Matsuoka, N., Springman, S., Vonder Mühll, D., 2006. Permafrost creep and rock glacier dynamics. Permafr. Periglac. Process. 17 (3), 189-214

Haeberli, W., Huggel, C., Paul, F., Zemp, M., 2013. 13.10 Glacial Responses to Climate Change. In: Shroder, J.F. (Ed.), Treatise on Geomorphology. Academy Press, San Diego, pp. 152–175.

Hallsdóttir, M., 1995. On the pre-settlement history of Icelandic vegetation. Icelandic Agric. Sci. 9, 17–29.

Hambrey, M.J., Quincey, D.J., Glasser, N.F., Reynolds, J.M., Richardson, S.J., Clemmens, S., 2008. Sedimentological, geomorphological and dynamic context of debris-mantled glaciers, Mount Everest (Sagarmatha) region, Nepal. Quat. Sci. Rev. 27, 2361–2389.

Hamilton, S.J., Whalley, W.B., 1995a. Preliminary results from the lichenometric study of the Nautardálur rock glacier, Tröllaskagi, northern Iceland. Geomorphology 12, 123–132.

Hamilton, S.J., Whalley, W.B., 1995b. Rock glacier nomenclature: A re-assessment. Geomorphology 14, 73–80.

Hannesdóttir, H., Björnsson, H., Pálsson, F., Aðalgeirsdóttir, G., Guðmundsson, S., 2015b. Changes in the southeast Vatnajökull ice cap, Iceland, between ~ 1890 and 2010. The Cryosphere 9, 565–585.

Hannesdóttir, H., Björnsson, H., Pálsson, F., Aðalgeirsdóttir, G., Guðmundsson, S., 2015a. Variations of southeast Vatnajökull ice cap (Iceland) 1650-1900 and reconstruction of the glacier surface geometry at the Little Ice Age maximum. Geogr. Ann. Ser. A, Phys. Geogr. 97, 237–264.

Hansen, B., Meincke, J., 1979. Eddies and meanders in the Iceland-Faroe Ridge area. Deep Sea Res. Part A. Oceanogr. Res. Pap. 26, 1067–1082.

Harning, D.J., Geirsdóttir, Á., Miller, G.H., 2018a. Punctuated Holocene climate of Vestfirðir, Iceland, linked to internal/external variables and oceanographic conditions. Quat. Sci. Rev. 189, 31–42.

Harning, D.J., Geirsdóttir, Á., Miller, G.H., Anderson, L., 2016 b. Episodic expansion of Drangajökull, Vestfirðir, Iceland, over the last 3 ka culminating in its maximum dimension during the Little Ice Age. Quat. Sci. Rev. 152, 118–131.

Harning, D.J., Geirsdóttir, Á., Miller, G.H., Zalzal, K., 2016 a. Early Holocene deglaciation of Drangajökull, Vestfirðir, Iceland. Quat. Sci. Rev. 153, 192–198.

Harning, D.J., Thordarson, T., Geirsdóttir, Á., Zalzal, K., Miller, G.H., 2018b. Provenance, stratigraphy and chronology of Holocene tephra from Vestfirðir, Iceland. Quat. Geochronol. 46, 59–76.

Harris, T., Tweed, F.S., Knudsen, Ó., 2004. A polygenetic landform at Stígá, Öræfajökull, southern Iceland. Geogr. Ann. Ser. A Phys. Geogr. 86, 143–154.

Harrison, S.P., Prentice, I.C., Bartlein, P.J., 1992. Influence of insolation and glaciation on atmospheric circulation in the North Atlantic sector: Implications of general circulation model experiments for the Late Quaternary climatology of Europe. Quat. Sci. Rev. 11, 283–299.

Helama, S., Jones, P.D., Briffa, K.R., 2017. Dark Ages Cold Period: A literature review and directions for future research. The Holocene 27, 1600–1606.

Heyman, J., Stroeven, A.P., Harbor, J.M., Caffee, M.W., 2011. Too young or too old: Evaluating cosmogenic exposure dating based on an analysis of compiled boulder exposure ages. Earth Planet. Sci. Lett. 302, 71–80.

Hippolyte, J.C., Bourlès, D., Braucher, R., Carcaillet, J., Léanni, L., Arnold, M., Aumaitre, G., 2009. Cosmogenic 10Be dating of a sackung and its faulted rock glaciers, in the Alps of Savoy (France). Geomorphology 108, 312-320

Hjort, C., Ingólfsson, Ó., Norðdahl, H., 1985. Late Quaternary geology and glacial history of Hornstrandir, Northwest Iceland: a reconnaissance study. Jökull 35, 9–29.

Holmes, N., Langdon, P.G., Caseldine, C.J., Wastegård, S., Leng, M.J., Croudace, I.W., Davies, S.M., 2016. Climatic variability during the last millennium in Western Iceland from lake sediment records. The Holocene 26, 756–771.

Holmlund, P., 1987. Mass Balance of Storglaciaren during the 20th Century. Geogr. Ann. Ser. A Phys. Geogr. 69, 439.

Holzhauser, H., Magny, M., Zumbuühl, H.J., 2005. Glacier and lake-level variations in west-central Europe over the last 3500 years. The Holocene 15, 789–801.

Hooker, T.N., Brown, D.H., 1977. A photographic method for accurately measuring the growth of crustose and foliose saxicolous lichens. Lichenol. 9, 65–75.

Houghton, J.T., Meira Filho, L.G., Callander, B.A., Harris, N., Kattenberg, A., Maskell, K., 1996. Climate Change 1995: The Science of Climate Change. Contribution of Working Group I to the Second Assessment Report of the Intergovernmental Panel on Climate Change. Published for the Intergovernmental Panel on Climate Change, Cambridge University Press, Cambridge.

Hubbard, A., Sugden, D., Dugmore, A., Norddahl, H., Pétursson, H.G., 2006. A modelling insight into the Icelandic Last Glacial Maximum ice sheet. Quat. Sci. Rev. 25, 2283–2296.

Hughes, P.D., 2008. Response of a Montenegro glacier to extreme summer heatwaves in 2003 and 2007. Geogr. Ann. Ser. A Phys. Geogr. 90, 259–267.

Hughes, P.D., 2009a. Loch Lomond Stadial (Younger Dryas) glaciers and climate in Wales. Geol. J. 44, 375–391.

Hughes, P.D., 2009b. Twenty-first Century Glaciers and Climate in the Prokletije Mountains, Albania. Arctic, Antarct. Alp. Res. 41, 455–459.

Hughes, P.D., Braithwaite, R.J., 2008. Application of a degree-day model to reconstruct Pleistocene glacial climates. Quat. Res. 69, 110–116.

Hughes, P.D., Woodward, J.C., Gibbard, P.L., 2006. Late Pleistocene glaciers and climate in the Mediterranean. Glob. Planet. Change 50, 83–98.

Hughes, P.D., Woodward, J.C., van Calsteren, P.C., Thomas, L.E., Adamson, K.R., 2010. Pleistocene ice caps on the coastal mountains of the Adriatic Sea. Quat. Sci. Rev. 29, 3690–3708.

Humlum, O., 1998. The climatic significance of rock glaciers. Permafr. Periglac. Process. 9, 375–395.

Humlum, O., 2000. The geomorphic significance of rock glaciers: estimates of rock glacier debris volumes and headwall recession rates in West Greenland. Geomorphology 35, 41–67.

Hurrell, J.W., 1995a. Decadal Trends in the North Atlantic Oscillation: Regional Temperatures and Precipitation. Science 269, 676–679.

Hurrell, J.W., 1995b. Transient Eddy Forcing of the Rotational Flow during Northern Winter. J. Atmos. Sci. 52, 2286–2301.

Icelandic Glaciological Society, 2017. Glacier termini variations data. Available at: http://spordakost.jorfi.is (last access: 27/06/2017).

Icelandic Meteorological Office, 2017. Climatological data. Available at: http://en.vedur.is/climatology/data/ (last access: 29/06/2017).

Icelandic Road and Coastal Administration, 2017. Climatological data. Available at: http://www.road.is/ (last access: 29/06/2017).

Ingólfsson, O., 1991. A review of the late Weichselian and early Holocene glacial and environmental history of Iceland, in: J. Maizels, C. Caseldine (Eds.), Environmental Change in Iceland: Past and Present, Kluwer Academic Publishers, Dordrecht, pp. 13-29.

Ingólfsson, Ó., Benediktsson, Í.Ö., Schomacker, A., Kjær, K., Brynjólfsson, S., Jónsson, S.A., Korsgaard, N.J., Johnson, M., 2016. Glacial geological studies of surge type glaciers in Iceland – Research status and future challenges. Earth-Science Rev. 152, 37-69.

Ingólfsson, Ó., Björck, S., Hafliðason, H., Rundgren, M. 1997. Glacial and climatic events in Iceland reflecting regional North Atlantic climatic shifts during the Pleistocene-Holocene transition. Quat. Sci. Rev. 16, 1135-1144.

Ingólfsson, O., Norðdahl, H., 2001. High Relative Sea Level during the Bolling Interstadial in Western Iceland: A Reflection of Ice-Sheet Collapse and Extremely Rapid Glacial Unloading. Arctic, Antarct. Alp. Res. 33, 231.

Innes, J.L., 1985. Lichenometry. Prog. Phys. Geogr. 9(2), 187-254.

Institute of Marine Research, Norway, 2017. Available at: http://www.imr.no/en/imr (last access: 20/06/2017).

Ipsen, H.A., Principato, S.M., Grube, R.E., Lee, J.F., 2018. Spatial analysis of cirques from three regions of Iceland: implications for cirque formation and palaeoclimate. Boreas 47, 565–576.

Ivy-Ochs, S., Synal, H.-A., Roth, C., Schaller, M., 2004. Initial results from isotope dilution for Cl and 36Cl measurements at the PSI/ETH Zurich AMS facility. Nucl. Instruments Methods Phys. Res. Sect. B Beam Interact. with Mater. Atoms 223–224, 623–627.

Jacob, T., Wahr, J., Pfeffer, W.T., Swenson, S., 2012. Recent contributions of glaciers and ice caps to sea level rise. Nature 482, 514–518.

Jaksch, K., 1970. Beobachtungen in den Gletschervorfeldern des Sólheima und Siðujökull im Sommer 1970. Jökull 20.

Jaksch, K., 1975. Das Gletschervorfeld des Sólheimajökull. Jökull 25, 34–38.

Jaksch, K., 1984. Das Gletcshervorfeld des Vatnajökull am Oberflauf des Djúpá, Südisland. Jökull 34, 97–103.

James, W.H.M., Carrivick, J.L., 2016. Automated modelling of spatially-distributed glacier ice thickness and volume. Comput. Geosci. 92, 90–103.

Janke, J.R., Bellisario, A.C., Ferrando, F.A., 2015. Classification of debris-covered glaciers and rock glaciers in the Andes of central Chile. Geomorphology 241, 98–121.

Janke, J.R., Regmi, N.R., Giardino, J.R., Vitek, J.D., 2013. 8.17 Rock glaciers, in: Shroder, J. (Ed.), Treatise in Geomorphology, Volume 8. Elsevier, pp. 238-273.

Jansen, H.L., Simonsen, J.S., Dahl, S.O., Bakke, J., Nielsen, P.R., 2016. Holocene glacier and climate fluctuations of the marine ice cap Høgtuvbreen, northern Norway. The Holocene 26(5), 736-755.

Jiang, H., Muscheler, R., Björck, S., Seidenkrantz, M.S., Olsen, J., Sha, L., Sjolte, J., Eiríksson, J., Ran, L., Knudsen, K.L., Knudsen, M.F., 2015. Solar forcing of Holocene summer sea-surface temperatures in the northern North Atlantic. Geology 43, 203–206.

Jiskoot, H., Curran, C.J., Tessler, D.L., Shenton, L.R., 2009. Changes in Clemenceau Icefield and Chaba Group glaciers, Canada, related to hypsometry, tributary detachment, length–slope and area–aspect relations. Ann. Glaciol. 50, 133–143.

Johannessen, O.M., 1986. Brief Overview of the Physical Oceanography, in: Hurdle, B.G. (Ed.), The Nordic Seas. Springer New York, New York, NY, pp. 103–128.

Jóhannesson, H., Sæmundsson, K., 1989. Geological map of Iceland. 1:500.000. Bedrock. Icelandic Institute of Natural History, Reykjavik.

Jóhannesson, T., 1986. The Response Time of Glaciers in Iceland to Changes in climate. Ann. Glaciol. 8, 100–101.

Jóhannesson, T., Raymond, C., Waddington, E., 1989b. Time-scale adjustment of glaciers to changes in mass balance. J. Glaciol. 35, 355-369.

Jóhannesson, T., Raymond, C.F., Waddington, E.D., 1989a. A Simple Method for Determining the Response Time of Glaciers. In: Oerlemans, J. (Ed.), Glacier Fluctuations and Climatic Change. Proceedings of the Symposium on Glacier Fluctuations and Climatic Change, Held in Amsterdam, 1-5 June 1987. pp. 343–352.

Jóhannesson, T., Sigurðsson, O., 1998. Interpretation of glacier variations in Iceland 1930-1995. Jökull 45, 27–33.

Johnson, P.G., 1980. Rock glaciers: glacial and non-glacial origins. World Glacier Inventory - inventaire mondial des Glaciers, in Proceedings of the Riederalp Workshop, September 1978: Actes de l'Atelier de Riederalp, vol. 126. International Association of Scientific Hydrology, pp. 285–293.

Jomelli, V., Lane, T., Favier, V., Masson-Delmotte, V., Swingedouw, D., Rinterknecht, V., Schimmelpfennig, I., Brunstein, D., Verfaillie, D., Adamson, K., Leanni, L., Mokadem, F., Aumaître, G., Bourlès, D.L., Keddadouche, K., 2016. Paradoxical cold conditions during the medieval climate anomaly in the Western Arctic. Sci. Rep. 6, 32984.

Jones, D.B., Harrison, S., Anderson, K., Selley, H.L., Wood, J.L., Betts, R.A., 2018. The distribution and hydrological significance of rock glaciers in the Nepalese Himalaya. Glob. Planet. Change 160, 123–142.

Jónsson, O., 1976. Berghlaup. Ræktunarfélag Norðurlands, Akureyri.

Kääb, A., 2005. Remote Sensing of Mountain Glaciers and Permafrost Creep. Physical Geography Series 48, 266 pp.

Kääb, A., Huggel, C., Fischer, L., Guex, S., Paul, F., Roer, I., Salzmann, N., Schlaefli, S., Schmutz, K., Schneider, D., Strozzi, T., Weidmann, Y., 2005. Remote sensing of glacier- and permafrost-related hazards in high mountains: an overview. Nat. Hazards Earth Syst. Sci. 5, 527–554.

Kaldal, I., Víkingsson, S., 1991. Early Holocene deglaciation in Central Iceland. Jökull 40, 51–66.

Kaldybayev, A., Chen, Y., Vilesov, E., 2016. Glacier change in the Karatal river basin, Zhetysu (Dzhungar) Alatau, Kazakhstan. Ann. Glaciol. 57, 11–19.

Kellerer-Pirklbauer, A., 2012. The Schmidt-Hammer as a Relative Age Dating Tool for Rock Glacier Surfaces. Quat. Int. 279–280, 239.

Kellerer-Pirklbauer, A., Kaufmann, V., 2012. About the relationship between rock glacier velocity and climate parameters in central Austria. Austrian J. Earth Sci. 105, 94–112.

Kellerer-Pirklbauer, A., Lieb, G.K., Avian, M., G., J., 2008b. The response of partially debris-covered valley glaciers to climate change: the example of the Pasterze glacier (Austria) in the period 1964 to 2006. Geogr. Ann. Ser. A, Phys. Geogr. 90, 269–285.

Kellerer-Pirklbauer, A., Lieb, G.K., Kaufmann, V., 2017. The Dösen Rock Glacier in Central Austria: A key site for multidisciplinary long-term rock glacier monitoring in the Eastern Alps. Austrian J. Earth Sci. 110.

Kellerer-Pirklbauer, A., Wangensteen, B., Farbrot, H., Etzelmüller, B., 2008a. Relative surface age-dating of rock glacier systems near Hólar in Hjaltadalur, northern Iceland. J. Quat. Sci. 23, 137–151.

Kenner, R., 2019. Geomorphological analysis on the interaction of Alpine glaciers and rock glaciers since the Little Ice Age. L. Degrad. Dev. 30, 580–591.

Kenner, R., Phillips, M., Limpach, P., Beutel, J., Hiller, M., 2018. Monitoring mass movements using georeferenced time-lapse photography: Ritigraben rock glacier, western Swiss Alps. Cold Reg. Sci. Technol. 145, 127–134.

Kern, Z., László, P., 2010. Size specific steady-state accumulation-area ratio: An improvement for equilibrium-line estimation of small palaeoglaciers. Quat. Sci. Rev. 29, 2781–2787.

Kirkbride, M.P., 2000. Ice-marginal geomorphology and Holocene expansion of debris-covered Tasman Glacier, New Zealand, in: Nakawo, M., Raymond, C. F., Fountain, A. (Eds.), Debris-Covered Glaciers. IAHS; Publication 264, pp. 211–217.

Kirkbride, M.P., 2002. Icelandic climate and glacier fluctuations through the termination of the “Little Ice Age”. Polar Geogr. 26, 116–133.

Kirkbride, M.P., 2011. Debris-Covered Glaciers. In: Singh, V.P., Singh, P., Haritashya, U.K. (Eds.), Encyclopedia of Snow, Ice and Glaciers. Springer Netherlands, Dordrecht, pp. 180–182.

Kirkbride, M.P., Dugmore, A.J., 2001a. Timing and significance of mid-Holocene glacier advances in Northern and Central Iceland. J. Quat. Sci. 16, 145–153.

Kirkbride, M.P., Dugmore, A.J., 2001b. Can lichenometry be used to date the “Little Ice Age” glacial maximum in Iceland? Clim. Change 48, 151–167.

Kirkbride, M.P., Dugmore, A.J., 2006. Responses of mountain ice caps in central Iceland to Holocene climate change. Quat. Sci. Rev. 25, 1692–1707.

Kirkbride, M.P., Dugmore, A.J., 2008. Two millennia of glacier advances from southern Iceland dated by tephrochronology. Quat. Res. 70, 398–411.

Kjær, K.H., Korsgaard, N.J., Schomacker, A., 2008. Impact of multiple glacier surges - a geomorphological map from Brúarjökull, East Iceland. J. Maps 4, 5–20.

Klein, A.G., Isacks, B.L., 1998. Alpine glacial geomorphological studies in the central Andes using Landsat Thematic Mapper images. Glacial Geology and Geomorphology rp01.

Knight, J., Harrison, S., Jones, D.B., 2018. Rock glaciers and the geomorphological evolution of deglacierizing mountains. Geomorphology 311, 127–142.

Knudsen, K., Jiang, H., Jansen, E., Eiríksson, J., Heinemeier, J., Seidenkrantz, M.-S., 2004. Environmental changes off North Iceland during the deglaciation and the Holocene: foraminifera, diatoms and stable isotopes. Mar. Micropaleontol. 50, 273–305.

Koblet, T., Gärtner-Roer, I., Zemp, M., Jansson, P., Thee, P., Haeberli, W., Holmlund, P., 2010. Reanalysis of multi-temporal aerial images of Storglaciären, Sweden (1959-99) - Part 1: Determination of length, area, and volume changes. The Cryosphere 4, 333–343.

Koc Karpuz, N., Schrader, H., 1990. Surface sediment diatom distribution and Holocene paleotemperature variations in the Greenland, Iceland and Norwegian Sea. Paleoceanography 5, 557–580.

Koch, L., 1945. The East Greenland Ice. Medd. Grønl. 130, 1–374.

Konrad, S.K., Clark, D.C. 1998. Evidence for an Early Neoglacial Glacier Advance from Rock Glaciers and Lake Sediments in the Sierra Nevada, California, U.S.A. Arctic, Antarct. Alp. Res. 30 (3), 272-284.

Krainer, K., Bressan, D., Dietre, B., Haas, J.N., Hajdas, I., Lang, K., Mair, V., Nickus, U., Reidl, D., Thies, H., Tonidandel, D., 2015. A 10,300-year-old permafrost core from the active rock glacier Lazaun, southern Ötztal Alps (South Tyrol, northern Italy). Quat. Res. 83, 324–335.

Kugelmann, O., 1991. Dating Recent Glacier Advances in the Svarfaðardalur-Skíðadalur Area of Northern Iceland by Means of a New Lichen Curve, in: Maizels, J.K., Caseldine, C. (Eds.), Environmental Change in Iceland: Past and Present. Glaciology and Quaternary Geology, Vol 7. Springer, Dordrecht, pp. 203–217.

Lamb, H.H., 1965. The early medieval warm epoch and its sequel. Palaeogeogr. Palaeoclimatol. Palaeoecol. 1, 13–37.

Larsen, D.J., Geirsdóttir, Á., Miller, G.H., 2015. Precise chronology of Little Ice Age expansion and repetitive surges of Langjökull, central Iceland. Geology 43, 167–170.

Larsen, D.J., Miller, G.H., Geirsdóttir, Á., Ólafsdóttir, S., 2012. Non-linear Holocene climate evolution in the North Atlantic: A high-resolution, multi-proxy record of glacier activity and environmental change from Hvítárvatn, central Iceland. Quat. Sci. Rev. 39, 14–25.

Larsen, D.J., Miller, G.H., Geirsdóttir, Á., Thordarson, T., 2011. A 3000-year varved record of glacier activity and climate change from the proglacial lake Hvítárvatn, Iceland. Quat. Sci. Rev. 30, 2715–2731.

Le Roy, M., Deline, P., Carcaillet, J., Schimmelpfennig, I., Ermini, M., 2017. 10Be exposure dating of the timing of Neoglacial glacier advances in the Ecrins-Pelvoux massif, southern French Alps. Quat. Sci. Rev. 178, 118–138.

Lehner, F., Born, A., Raible, C.C., Stocker, T.F., 2013. Amplified Inception of European Little Ice Age by Sea Ice-Ocean Atmosphere Feedbacks. J. Clim. 26, 7586-7602.

Leonard, E.M., Laabs, B.J.B., Schweinsberg, A.D., Russell, C.M., Briner, J.P., Young, N.E., 2017. Deglaciation of the Colorado Rocky Mountains following the Last Glacial Maximum. Cuad. Investig. Geográfica 43, 497–526.

Li, Y., Li, Y., Harbor, J., Liu, G., Yi, C., Caffee, M.W., 2016. Cosmogenic10Be constraints on Little Ice Age glacial advances in the eastern Tian Shan, China. Quat. Sci. Rev. 138, 105–118.

Licciardi, J. M., and Pierce, K. L, 2018. History and dynamics of the Greater Yellowstone Glacial System during the last two glaciations. Quat. Sci. Rev. 200, 1-33.

Licciardi, J.M., Denoncourt, C.L., Finkel, R.C., 2008. Cosmogenic 36Cl production rates from Ca spallation in Iceland. Earth Planet. Sci. Lett. 267, 365–377.

Licciardi, J.M., Kurz, M.D., Curtice, J.M., 2006. Cosmogenic 3He production rates from Holocene lava flows in Iceland. Earth Planet. Sci. Lett. 246, 251–264.

Licciardi, J.M., Kurz, M.D., Curtice, J.M., 2007. Glacial and volcanic history of Icelandic table mountains from cosmogenic 3He exposure ages. Quat. Sci. Rev. 26, 1529–1546.

Lie, O., Dahl, S.O., Nesje, A., 2003. A Theoretical Approach to Glacier Equilibrium-Line Altitudes Using Meteorological Data and Glacier Mass-Balance Records from Southern Norway. The Holocene 13, 365–372.

Liestøl, O., 1967. Storbreen glacier in Jotunheimen, Norway. Norsk Polarinstitutt Skrifter nr. 141 1–63.

Lilleøren, K.S., Etzelmüller, B., Gärtner-Roer, I., Kääb, A., Westermann, S., Guðmundsson, Á., 2013. The Distribution, Thermal Characteristics and Dynamics of Permafrost in Tröllaskagi, Northern Iceland, as Inferred from the Distribution of Rock Glaciers and Ice-Cored Moraines. Permafr. Periglac. Process. 24, 322–335.

Lippl, S., Vijay, S., Braun, M., 2018. Automatic delineation of debris-covered glaciers using InSAR coherence derived from X-, C- and L-band radar data: a case study of Yazgyl Glacier. J. Glaciol. 64, 811–821.

Mackay, S.L., Marchant, D.R., 2016. Dating buried glacier ice using cosmogenic 3He in surface clasts: Theory and application to Mullins Glacier, Antarctica. Quat. Sci. Rev. 140, 75-100.

Mackintosh, A.N., Dugmore, A.J., Hubbard, A.L., 2002. Holocene climatic changes in Iceland: Evidence from modelling glacier length fluctuations at Sólheimajökull. Quat. Int. 91, 39–52.

Maizels, J.K., Dugmore, A.J., 1985. Lichenometric dating and tephrochronology of sandur deposits, Sólheimajökull area, southern Iceland. Jökull 35, 69–77.

Mal, S., Singh, R.B., Schickhoff, U., 2016. Estimating Recent Glacier Changes in Central Himalaya, India, Using Remote Sensing Data, in: Singh, R.B., Schickhoff, U., Mal, S. (Eds.) Climate Change, Glacier Response, and Vegetation Dynamics in the Himalaya. Springer International Publishing, Cham, pp. 205–218.

Malmberg, S.A., 1969. Hydrographic changes in the waters between Iceland and Jan Mayen in the last decade. Jökull 19, 30–43.

Malmberg, S.A., 1985. The water masses between Iceland and Greenland. J. Mar. Res. Inst. 9, 127–140.

Malmberg, S.A., Valdimarsson, H., Mortensen, J., 1996. Long-time series in Icelandic waters in relation to physical variability in the northern North Atlantic. NAFO Sci. Counc. Stud. 69–80.

Marrero, S.M., Phillips, F.M., Caffee, M.W., Gosse, J.C., 2016. CRONUS-Earth cosmogenic 36Cl calibration. Quat. Geochronol. 31, 199–219.

Martin, H.E., Whalley, B., Orr, J., Caseldine, C., 1994. Dating and interpretation of rock glaciers using lichenometry, south Tröllaskagi, North Iceland. Münchener Geogr. Arb. 12, 205–224.

Martin, H.E., Whalley, W.B., Caseldine, C., 1991. Glacier Fluctuations and Rock Glaciers in Tröllaskagi, Northern Iceland, with Special Reference to 1946–1986, in: Maizels, J.K., Caseldine, C. (Eds.), Environmental Change in Iceland: Past and Present. Springer Netherlands, Dordrecht, pp. 255–265.

Marzeion, B., Cogley, J.G., Richter, K., Parkes, D., 2014. Attribution of global glacier mass loss to anthropogenic and natural causes. Science 345, 919–921.

Marzeion, B., Nesje, A., 2012. Spatial patterns of North Atlantic Oscillation influence on mass balance variability of European glaciers. The Cryosphere 6, 661–673.

Matthews, J.A., Shakesby, R.A., Fabel, D., 2017. Very low inheritance in cosmogenic surface exposure ages of glacial deposits: A field experiment from two Norwegian glacier forelands. The Holocene 27, 1406–1414.

Matthews, J.M., Nesje, A., Linge, H., 2013. Relict talus-foot rock glaciers at Øyberget, upper Ottadalen, Southern Norway: Schmidt hammer exposure ages and palaeoenvironmental implications. Permafr. Periglac. Process. 24 (4), 336-346.

Mayewski, P.A., Rohling, E.E., Curt Stager, J., Karlén, W., Maasch, K.A., David Meeker, L., Meyerson, E.A., Gasse, F., van Kreveld, S., Holmgren, K., Lee-Thorp, J., Rosqvist, G.,

Rack, F., Staubwasser, M., Schneider, R.R., Steig, E.J., 2004. Holocene climate variability. Quat. Res. 62, 243–255.

Mayr, E., Hagg, W., 2019. Debris-Covered Glaciers, in: Heckmann, T., Morche, D. (Eds.), Geomorphology of Proglacial Systems. Geography of the Physical Environment. Springer, Cham, pp. 59–71.

Meier, M.F., Bahr, D.B., 1996. Counting Glaciers: Use of Scaling Methods to Estimate the Number and Size Distribution of the Glaciers of the World, in: Colbeck, S.C. (Ed.), Glaciers Ice Sheets and Volcanoes A Tribute to Mark F. Meier. pp. 89–94.

Merchel, S., Bremser, W., Alfimov, V., Arnold, M., Aumaître, G., Benedetti, L., Bourlès, D.L., Caffee, M., Fifield, L.K., Finkel, R.C., Freeman, S.P.H.T., Martschini, M., Matsushi, Y., Rood, D.H., Sasa, K., Steier, P., Takahashi, T., Tamari, M., Tims, S.G., Tosaki, Y., Wilcken, K.M., Xu, S., 2011. Ultra-trace analysis of 36Cl by accelerator mass spectrometry: an interlaboratory study. Anal. Bio- anal. Chem. 40 (9), 3125-3132.

Mercier, D., 2008. Paraglacial and paraperiglacial landsystems; concepts, temporal scales and spatial distribution. Géomorphologie Reli. Process. Environ. 14, 223-233.

Mercier, D., Coquin, J., Feuillet, T., Decaulne, A., Cossart, E., Jónsson, H.P., Sæmundsson, Þ., 2017. Are Icelandic rock-slope failures paraglacial? Age evaluation of seventeen rock-slope failures in the Skagafjörður area, based on geomorphological stacking, radiocarbon dating and tephrochronology. Geomorphology 296, 45–58.

Mercier, D., Cossart, E., Decaulne, A., Feuillet, T., Jónsson, H.P., Sæmundsson, Þ., 2013. The Höfðahólar rock avalanche (sturzström): chronological constraint of paraglacial landsliding on an Icelandic hillslope. The Holocene 23, 432–446.

Meyer, H.H., Venzke, J.F., 1985. Der Klængshóll-Kargletscher in Nordisland. Natur and Museum 115, 29–46.

Meyer, V.D., Barr, I.D., 2017. Linking glacier extent and summer temperature in NE Russia - Implications for precipitation during the global Last Glacial Maximum. Palaeogeogr. Palaeoclimatol. Palaeoecol. 470, 72–80.

Miller, G.H., Brigham-Grette, J., Alley, R.B., Anderson, L., Bauch, H.A., Douglas, M.S.V., Edwards, M.E., Elias, S.A., Finney, B.P., Fitzpatrick, J.J., Funder, S. V., Herbert, T.D., Hinzman, L.D., Kaufman, D.S., MacDonald, G.M., Polyak, L., Robock, A., Serreze, M.C., Smol, J.P., Spielhagen, R., White, J.W.C., Wolfe, A.P., Wolff, E.W., 2010. Temperature and precipitation history of the Arctic. Quat. Sci. Rev. 29, 1679–1715.

Miller, G.H., Geirsdóttir, Á., Zhong, Y., Larsen, D.J., Otto-Bliesner, B.L., Holland, M.M., Bailey, D.A., Refsnider, K.A., Lehman, S.J., Southon, J.R., Anderson, C., Björnsson, H., Thordarson, T., 2012. Abrupt onset of the Little Ice Age triggered by volcanism and sustained by sea-ice/ocean feedbacks. Geophys. Res. Lett. 39, 1–5.

Mills, S.C., Grab, S.W., Rea, B.R., Carr, S.J., Farrow, A., 2012. Shifting westerlies and precipitation patterns during the Late Pleistocene in southern Africa determined using glacier reconstruction and mass balance modelling. Quat. Sci. Rev. 55, 145–159.

Möller, M., Schneider, C., 2010. Calibration of glacier volume–area relations from surface extent fluctuations and application to future glacier change. J. Glaciol. 56, 33–40.

Monnier, S., Kinnard, C., 2015. Reconsidering the glacier to rock glacier transformation problem: new insights from the central Andes of Chile. Geomorphology 238, 47-55.

Moran, A.P., Ivy-Ochs, S., Vockenhuber, C., Kerschner, H., 2016. Rock Glacier development in the Northern Calcareous Alps at the Pleistocene-Holocene boundary. Geomorphology 273, 178-188.

Moros, M., Andrews, J.T., Eberl, D.D., Jansen, E., 2006. Holocene history of drift ice in the northern North Atlantic: Evidence for different spatial and temporal modes. Paleoceanography 21, 1–10.

Müller, H.N., 1984. Spätglazlale Gletscherschwankungen in den westlichen Schweizer Alpen (Simplon-Süd und Val de Nendaz, Wallis) und im nordisländischen Tröllaskagi-Geblrge (Skidadalur). Niifels 158–177.

National Land Survey of Iceland, 2015. Climatological data. Available at: http://www.lmi.is/en/ (last access: 13/06/2015).

Nesje, A., 1992. Topographical effects on the equilibrium-line-altitude on glaciers. GeoJournal 27, 383–391.

Nesje, A., Bakke, J., Dahl, S.O., Lie, Ø., Matthews, J.A., 2008. Norwegian mountain glaciers in the past, present and future. Glob. Planet. Change 60, 10–27.

Nesje, A., Dahl, S.O., 2003. The 'Little Ice Age' – only temperature? The Holocene 13, 139–145.

Nesje, A., Lie, Ø., Dahl, S.O., 2000. Is the North Atlantic Oscillation reflected in Scandinavian glacier mass balance records? J. Quat. Sci. 15, 587–601.

Norðdahl, H., 1991a. Late Weichselian and early Holocene deglaciation history of Iceland. Jökull 40, 27-50.

Norðdahl, H., 1991b. A review of the glaciation maximum concept and the deglaciation of Eyjafjörður, North Iceland, in: J. Maizels, C. Caseldine (Eds.), Environmental Changes in Iceland: Past and Present, Kluwer Academic Publishers, Dordrecht, pp. 31-47.

Norðdahl, H., Einarsson, T., 2001. Concurrent changes of relative sea-level and glacier extent at the Weichselian–Holocene boundary in Berufjörður, Eastern Iceland. Quat. Sci. Rev. 20, 1607–1622.

Norðdahl, H., Ingólfsson, Ó., 2015. Collapse of the Icelandic ice sheet controlled by sea-level rise? Arktos 1, 13.

Norðdahl, H., Ingólfsson, Ó., Pétursson, H.G., Hallsdóttir, M., 2008. Late Weichselian and Holocene environmental history of Iceland. Jökull 343–364.

Norðdahl, H., Pétursson, H. G., 2005. Relative sea level changes in Iceland. New aspects of the Weichselian deglaciation of Iceland, in: Caseldine, C., Russel, A., Harðardóttir, J., Knudsen, O. (Eds.) Developments in Quaternary Sciences, vol. 5 Iceland — Modern Processes and Past Environments, Elsevier, Amsterdam, pp. 25–78.

Nye, J.F., 1952. A Methods of Calculating the Thickness of the Ice-Sheets. Nature 169, 529–530.

Oerlemans, J., 2005. Extracting a climate signal from 169 glacier records. Science 308, 675–677.

Ogilvie, A., 1996. Sea-ice conditions off the coasts of Iceland A.D. 1601-1850 with special reference to part of the Maunder Minimum period (1675-1715). AmS-Varia 25, 9–12.

Ogilvie, A.E.J., 1984. The past climate and sea-ice record from Iceland, Part 1: Data to A.D. 1780. Clim. Change 6, 131–152.

Ogilvie, A.E.J., 1991. Climatic changes in Iceland A.D. 865 to 1598. Acta Archaeol. 61, 233–251.

Ogilvie, A.E.J., 2005. 11. Local knowledge and travellers' tales: a selection of climatic observations in Iceland, in: Caseldine, C., Russell, A., Hardardottir, J. and Knudsen, O. (Eds.) Developments in Quaternary Sciences, vol. 5 Iceland — Modern Processes and Past Environments. Elsevier, Amsterdam, pp. 257–287.

Ogilvie, A.E.J., 2010. Historical climatology, climatic change, and implications for climate science in the twenty-first century. Clim. Change 100, 33-47.

Ogilvie, A.E.J., Jónsdóttir, I., 2000. Sea ice, climate, and Icelandic fisheries in the eighteenth and nineteenth centuries. Arctic 53, 383–394.

Ogilvie, A.E.J., Jónsson, T., 2001. "Little Ice Age" Research: a perspective from Iceland. Clim. Change 48, 9–52.

Ohmura, A., Kasser, P., Funk, M., 1992. Climate at the Equilibrium Line of Glaciers. J. Glaciol. 38, 397–411.

Ólafsdóttir, S., Jennings, A.E., Geirsdóttir, Á., Andrews, J., Miller, G.H., 2010. Holocene variability of the North Atlantic Irminger current on the south- and northwest shelf of Iceland. Mar. Micropaleontol. 77, 101–118.

Oliva, M., Ruiz-Fernández, J., Barriendos, M., Benito, G., Cuadrat, J.M., Domínguez-Castro, F., García-Ruiz, J.M., Giralt, S., Gómez-Ortiz, A., Hernández, A., López-Costas, O., López-Moreno, J.I., López-Sáez, J.A., Martínez-Cortizas, A., Moreno, A., Prohom, M., Saz, M.A., Serrano, E., Tejedor, E., Trigo, R., Valero-Garcés, B., Vicente-Serrano, S.M., 2018. The Little Ice Age in Iberian mountains. Earth-Science Rev. 177, 175–208.

Oliva, M., Serrano, E., Gómez-Ortiz, A., González-Amuchástegui, M. J., Nieuwendam, A.; Palacios, D., Pérez-Alberti, A., Pellitero, R., Ruiz-Fernández, J., Valcárcel, M., Vieira, G., Antoniades, D., 2016. Spatial and temporal variability of periglaciation of the Iberian Peninsula. Quat. Sci. Rev. 137, 176-199.

Orme, L.C., Husum, K., Van Nieuwenhove, N., Pearce, C., Divine, D., Seidenkrantz, M.-S., Born, A., Miettinen, A., Mohan, R., 2018. Subpolar North Atlantic sea surface temperature since 6 ka BP: Indications of anomalous ocean-atmosphere interactions at 4-2 ka BP. Quat. Sci. Rev. 194, 128–142.

Orvik, K.A., Skagseth, Ø., Mork, M., 2001. Atlantic inflow to the Nordic Seas: current structure and volume fluxes from moored current meters, VM-ADCP and SeaSoar-CTD observations, 1995–1999. Deep Sea Res. Part I Oceanogr. Res. Pap. 48, 937–957.

Orwin, J.F., Mckinzey, K.M., Stephens, M.A., Dugmore, A.J., 2008. Identifying moraine surfaces with similar histories using lichen size distributions and the U2 statistic, Southeast Iceland. Geogr. Ann. Ser. A Phys. Geogr. 90 A, 151–164.

Osborn, G., McCarthy, D., LaBrie, A., Burke, R., 2015. Lichenometric dating: Science or pseudo-science? Quat. Res. (United States) 83, 1–12.

Osmaston, H., 2005. Estimates of glacier equilibrium line altitudes by the Area×Altitude, the Area×Altitude Balance Ratio and the Area×Altitude Balance Index methods and their validation. Quat. Int. 138–139, 22–31.

Paasche, Ø., Olaf Dahl, S., Bakke, J., Løvlie, R., Nesje, A., 2007. Cirque glacier activity in arctic Norway during the last deglaciation. Quat. Res. 68, 387–399.

Palacios, D., Andrés, N., García-Ruiz, J. M., Schimmelpfennig, I., Campos, N., Léanni, L., Aster Team, 2017. Deglaciation in the central Pyrenees during the Pleistocene–Holocene transition: timing and geomorphological significance. Quat. Sci. Rev. 150, 110-129.

Palacios, D., Andrés, N., López-Moreno, J.I., García-Ruiz, J.M., 2015b. Late Pleistocene deglaciation in the upper Gállego valley, central Pyrenees. Quat. Res. 83, 397-414.

Palacios, D., Andrés, N., Marcos, J., Vázquez-Selem, L., 2012. Glacial landforms and their paleoclimatic significance in Sierra de Guadarrama, central Iberian Peninsula. Geomorphology 139-140, 67-78.

Palacios, D., Gómez-Ortiz, A., Alcalá-Reygosa, J., Andrés, N., Oliva, M., Tanarro, L.M., Salvador-Franch, F., Schimmelpfennig, I., Fernández-Fernández, J.M., Léanni, L., 2019. The challenging application of cosmogenic dating methods in residual glacial landforms: The case of Sierra Nevada (Spain). Geomorphology 325, 103–118.

Palacios, D., Gómez-Ortiz, A., Andrés, N., Salvador-Franch, F., Oliva, M., 2016. Timing and new geomorphologic evidence of the last deglaciation stages in Sierra Nevada (southern Spain). Quat. Sci. Rev. 150, 110-129.

Palacios, D., Gómez-Ortiz, A., Andrés, N., Vázquez-Selem, L., Salvador-Franch, F., Oliva, M., 2015a. Maximum extent of Late Pleistocene glaciers and last deglaciation of La Cerdanya mountains, southeastern Pyrenees. Geomorphology 231, 116-129.

Paterson, W.S.B., 1994. The Physics of Glaciers, 3rd Edition. Pergamon/Elsevier, London.

Patton, H., Hubbard, A., Bradwell, T., Schomacker, A., 2017. The configuration, sensitivity and rapid retreat of the Late Weichselian Icelandic ice sheet. Earth-Science Rev. 166, 223–245.

Pearce, D.M., Ely, J.C., Barr, L.D., Boston, C.M., 2017. 3.4.9 Glacier Reconstruction, in: Cook, S., Clarke, L., Nield, J. (Eds.), Geomorphological Techniques. British Society for Geomorphology, London, pp. 1–16.

Pellika, P., Rees, W.G., 2009. Remote Sensing of Glaciers. Techniques for Topographic, Spatial and Thematic Mapping of Glaciers. Taylor & Francis. 340 pp.

Pellitero, R., 2013. Evolución finicuaternaria del glaciarismo en el macizo de Fuentes Carrionas (Cordillera Cantábrica), propuesta cronológica y paleoambiental. Cuaternario y Geomorfología 27, 71–90.

Pellitero, R., Rea, B.R., Spagnolo, M., Bakke, J., Hughes, P., Ivy-Ochs, S., Lukas, S., Ribolini, A., 2015. A GIS tool for automatic calculation of glacier equilibrium-line altitudes. Comput. Geosci. 82, 55–62.

Pellitero, R., Rea, B.R., Spagnolo, M., Bakke, J., Ivy-Ochs, S., Frew, C.R., Hughes, P., Ribolini, A., Lukas, S., Renssen, H., 2016. GlaRe, a GIS tool to reconstruct the 3D surface of palaeoglaciers. Comput. Geosci. 94, 77–85.

Pelto, M., Capps, D., Clague, J.J., Pelto, B., 2013. Rising ELA and expanding proglacial lakes indicate impending rapid retreat of Brady Glacier, Alaska. Hydrol. Process. 27, 3075–3082.

Pétursson, H.G., Norðdahl, H., Ingólfsson, Ó., 2015. Late Weichselian history of relative sea level changes in Iceland during a collapse and subsequent retreat of marine based ice sheet. Cuad. Investig. Geográfica 41, 261-277.

Phillips, F. M., 2016. Cosmogenic nuclide data sets from the Sierra Nevada, California, for assessment of nuclide production models: I. Late Pleistocene glacial chronology. Quat. Geochronol. 35, 119-129.

Phillips, F.M., 2003. Cosmogenic 36Cl ages of Quaternary basalt flows in the Mojave Desert, California, USA. Geomorphology 53, 199–208.

Porter, S.C., Denton, G.H., 1967. Chronology of neoglaciation in the North American Cordillera. Am. J. Sci. 265, 177–210.

Potter, N.J., Steig, E.J., Clark, D.H., Speece, M.A., Clark, G.M., Updike, A.B., 1998. Galena Creek rock glacier revisited—new observations on an old controversy. Geogr. Ann. Ser. A, Phys. Geogr. 80, 251–265.

Principato, S.M., Geirsdóttir, Á., Jóhannsdóttir, G.E., Andrews, J.T., 2006. Late Quaternary glacial and deglacial history of eastern Vestfirðir, Iceland using cosmogenic isotope (36Cl) exposure ages and marine cores. J. Quat. Sci. 21, 271–285.

Qureshi, M.A., Yi, C., Xu, X., Li, Y., 2017. Glacier status during the period 1973–2014 in the Hunza Basin, Western Karakoram. Quat. Int. 444, 125–136.

Rabatel, A., Bermejo, A., Loarte, E., Soruco, A., Gomez, J., Leonardini, G., Vincent, C., Sicart, J.E., 2012. Can the snowline be used as an indicator of the equilibrium line and mass balance for glaciers in the outer tropics? J. Glaciol. 58, 1027–1036.

Rabatel, A., Dedieu, J.P., Christian, V., 2016. Spatio-temporal changes in glacier-wide mass balance quantified by optical remote sensing on 30 glaciers in the French Alps for the period 1983–2014. J. Glaciol. 62, 1153–1166.

Radić, V., Hock, R., Oerlemans, J., 2007. Volume-area scaling vs flowline modelling in glacier volume projections. Ann. Glaciol. 46, 234–240.

Rangecroft, S., Harrison, S., Anderson, K., 2015. Rock glaciers as water stores in the Bolivian Andes: an assessment of their hydrological importance. Arctic, Antarct. Alp. Res. 47(1), 89-98.

Rea, B.R., 2009. Defining modern day Area-Altitude Balance Ratios (AABRs) and their use in glacier-climate reconstructions. Quat. Sci. Rev. 28, 237–248.

Reimer, P.J., Bard, E., Bayliss, A., Beck, J.W., Blackwell, P.G., Ramsey, C.B., Buck, C.E., Cheng, H., Edwards, R.L., Friedrich, M., Grootes, P.M., Guilderson, T.P., Haflidason, H., Hajdas, I., Hatté, C., Heaton, T.J., Hoffmann, D.L., Hogg, A.G., Hughen, K.A., Kaiser, K.F., Kromer, B., Manning, S.W., Niu, M., Reimer, R.W., Richards, D.A., Scott, E.M., Southon, J.R., Staff, R.A., Turney, C.S.M., van der Plicht, J., 2013. IntCal13 and Marine13 Radiocarbon Age Calibration Curves 0–50,000 Years cal BP. Radiocarbon 55, 1869–1887.

Renssen, H., Goosse, H., Crosta, X., Roche, D.M., 2010. Early Holocene Laurentide ice sheet deglaciation causes cooling in the high-latitude southern hemisphere through oceanic teleconnection. Paleoceanography 25, 1–15.

Renssen, H., Seppä, H., Crosta, X., Goosse, H., Roche, D.M., 2012. Global characterization of the Holocene Thermal Maximum. Quat. Sci. Rev. 48, 7–19.

Renssen, H., Seppä, H., Heiri, O., Roche, D.M., Goosse, H., Fichefet, T., 2009. The spatial and temporal complexity of the Holocene thermal maximum. Nat. Geosci. 2, 411–414.

Robb, C., Willis, I., Arnold, N., Guðmundsson, S., 2015. A semi-automated method for mapping glacial geomorphology tested at Breiðamerkurjökull, Iceland. Remote Sens. Environ. 163, 80–90.

Robson, B.A., Nuth, C., Dahl, S.O., Hölbling, D., Strozzi, T., Nielsen, P.R., 2015. Automated classification of debris-covered glaciers combining optical, SAR and topographic data in an object-based environment. Remote Sens. Environ. 170, 372–387.

Roca-Valiente, B., Hawksworth, D.L., Pérez-Ortega, S., Sancho, L.G., Crespo, A., 2016. Type studies in the Rhizocarpon geographicum group (Rhizocarpaceae, lichenized Ascomycota). Lichenologist 48, 97–110.

Rodewald, M., 1967. Recent Variations of North Atlantic Sea Surface Temperatures (SST) and the “Type-Tendencies” of the Atmospheric Circulation. ICNAF Redb. 1854, 6–23.

Rodríguez-Rodríguez, L., Jiménez-Sánchez, M., Domínguez-Cuesta, M.J., Rinterknecht, V., Pallàs, R., Bourlès, D., 2016. Chronology of glaciations in the Cantabrian Mountains (NW Iberia) during the Last Glacial Cycle based on in situ-produced 10Be. Quat. Sci. Rev. 138, 31–48.

Rodríguez-Rodríguez, L., Jiménez-Sánchez, M., Domínguez-Cuesta, M.J., Rinterknecht, V., Pallàs, R., Aster Team, 2017. Timing of last deglaciation in the Cantabrian Mountains (Iberian Peninsula; North Atlantic region) based on in situ-produced 10Be exposure dating. Quat. Sci. Rev. 171, 166-181.

Rogers, J.C., 1985. Atmospheric Circulation Changes Associated with the Warming over the Northern North Atlantic in the 1920s. J. Clim. Appl. Meteorol. 24, 1303–1310.

Rogers, J.C., 1990. Patterns of Low-Frequency Monthly Sea Level Pressure Variability (1899-1986) and Associated Wave Cyclone Frequencies. J. Clim. 3, 1364–1379.

Rogers, J.C., Van Loon, H., 1979. The Seesaw in Winter Temperatures between Greenland and Northern Europe. Part II: Some Oceanic and Atmospheric Effects in Middle and High Latitudes. Mon. Weather Rev. 107, 509–519.

Rosenwinkel, S., Korup, O., Landgraf, A., Dzhumabaeva, A., 2015. Limits to lichenometry. Quat. Sci. Rev. 129, 229-238.

Rundgren, M. 1999. A summary of the environmental history of the Skagi peninsula, northern Iceland, 11,300-7800 BP. Jökull 47, 1-19.

Rundgren, M., 1995. Biostratigraphic Evidence of the Allerød-Younger Dryas-Preboreal Oscillation in Northern Iceland. Quat. Res. 44, 405–416.

Rundgren, M., Ingólfsson, Ó. 1999. Plant survival in Iceland during periods of glaciations. Journal of Biogeography 26, 387-396.

Russell, A.J., Knight, P.G., Van Dijk, T.A.G.P., 2001. Glacier surging as a control on the development of proglacial, fluvial landforms and deposits, Skeiðarársandur, Iceland. Glob. Planet. Change 28, 163–174.

Sæmundsson, K., Kristjansson, L., McDougall, I., Watkins, N.D., 1980. K-Ar dating, geological and paleomagnetic study of a 5-km lava succession in northern Iceland. J. Geophys. Res. Solid Earth 85, 3628–3646.

Sæmundsson, Þ., Morino, C., Helgason, J.K., Conway, S.J., Pétursson, H.G., 2018. The triggering factors of the Móafellshyrna debris slide in northern Iceland: Intense precipitation, earthquake activity and thawing of mountain permafrost. Sci. Total Environ. 621, 1163–1175.

Sagredo, E.A., Lowell, T. V., Kelly, M.A., Rupper, S., Aravena, J.C., Ward, D.J., Malone, A.G., 2017. Equilibrium line altitudes along the Andes during the Last millennium: Paleoclimatic implications. The Holocene 27, 1019–1033.

Sahsamanoglou, H.S., 1990. A contribution to the study of action centres in the North Atlantic. Int. J. Climatol. 10, 247–261.

Sancho, L.G., Palacios, D., Green, T.G.A., Vivas, M., Pintado, A., 2011. Extreme high lichen growth rates detected in recently deglaciated areas in Tierra del Fuego. Polar Biol. 34, 813–822.

Sancho, L.G., Pintado, A., Navarro, F., Ramos, M., De Pablo, M.A., Blanquer, J.M., Raggio, J., Valladares, F., Green, T.G.A., 2017. Recent Warming and Cooling in the Antarctic Peninsula Region has Rapid and Large Effects on Lichen Vegetation. Sci. Rep. 7, 5689.

Santos-González, J., Redondo-Vega, J.M., González-Gutiérrez, R.B., Gómez-Villar, A., 2013. Applying the AABR method to reconstruct equilibrium-line altitudes from the last glacial maximum in the Cantabrian Mountains (SW Europe). Palaeogeogr. Palaeoclimatol. Palaeoecol. 387, 185–199.

Scapozza, C., Lambiel, C., Bozzini, C., Mari, S., Conedera, M., 2014. Assessing the rock glacier kinematics on three different timescales: A case study from the southern Swiss Alps. Earth Surf. Process. Landforms 39, 2056–2069.

Schaefer, J.M., Denton, G.H., Kaplan, M., Putnam, A., Finkel, R.C., Barrell, D.J.A., Andersen, B.G., Schwartz, R., Mackintosh, A., Chinn, T., Schlüchter, C., 2009. High-frequency Holocene glacier fluctuations in New Zealand differ from the northern signature. Science 324, 622–625.

Schildgen, T.F., Phillips, W.M., Purves, R.S., 2005. Simulation of snow shielding corrections for cosmogenic nuclide surface exposure studies. Geomorphology 64, 67–85.

Schilling, D.H., Hollin, J.T., 1981. Numerical reconstructions of valley glaciers and small ice caps, in: Denton, G.H., Hughes, T.J. (Eds.), Last Great Ice Sheets. Willey, New York, USA, pp. 207–220.

Schimmelpfennig, I., 2009. Cosmogenic 36Cl in Ca and K rich minerals: analytical developments, production rate calibrations and cross calibration with 3He and 21Ne. Ph. D. Thesis, Université Aix-Marseille III, France.

Schimmelpfennig, I., Benedetti, L., Finkel, R., Pik, R., Blard, P.H., Bourlès, D., Burnard, P., Williams, A., 2009. Sources of in-situ36Cl in basaltic rocks. Implications for calibration of production rates. Quat. Geochronol. 4, 441–461.

Schimmelpfennig, I., Benedetti, L., Garreta, V., Pik, R., Blard, P.H., Burnard, P., Bourlès, D., Finkel, R., Ammon, K., Dunai, T., 2011. Calibration of cosmogenic 36Cl production rates from Ca and K spallation in lava flows from Mt. Etna (38°N, Italy) and Payun Matru (36°S, Argentina). Geochim. Cosmochim. Acta 75, 2611–2632.

Schimmelpfennig, I., Schaefer, J.M., Akçar, N., Ivy-Ochs, S., Finkel, R.C., Schlüchter, C., 2012. Holocene glacier culminations in the Western Alps and their hemispheric relevance. Geology 40, 891–894.

Schimmelpfennig, I., Schaefer, J.M., Akçar, N., Koffman, T., Ivy-Ochs, S., Schwartz, R., Finkel, R.C., Zimmerman, S., Schlüchter, C., 2014b. A chronology of Holocene and Little Ice Age glacier culminations of the Steingletscher, Central Alps, Switzerland, based on high-sensitivity beryllium-10 moraine dating. Earth Planet. Sci. Lett. 393, 220–230.

Schimmelpfennig, I., Schaefer, J.M., Putnam, A.E., Koffman, T., Benedetti, L., Ivy-Ochs, S., Team, A., Schlüchter, C., 2014a. 36Cl production rate from K-spallation in the European Alps (Chironico landslide, Switzerland). J. Quat. Sci. 29, 407–413.

Schomacker, A., Benediktsson, Í.Ö., Ingólfsson, Ó., 2014. The Eyjabakkajökull glacial landsystem, Iceland: Geomorphic impact of multiple surges. Geomorphology 218, 98–107.

Schomacker, A., Brynjólfsson, S., Andreassen, J.M., Gudmundsdóttir, E.R., Olsen, J., Odgaard, B.V., Håkansson, L., Ingólfsson, O., Larsen, N.K., 2016. The Drangajökull ice cap, northwest Iceland, persisted into the early-mid Holocene. Quat. Sci. Rev. 148, 66-84.

Schomacker, A., Krüger, J., Larsen, G., 2003. An extensive late Holocene glacier advance of Kötlujökull, central south Iceland. Quat. Sci. Rev. 22, 1427–1434.

Seppä, H., Bjune, A.E., Telford, R.J., Birks, H.J.B., Veski, S., 2009. Last nine-thousand years of temperature variability in Northern Europe. Clim. Past 5, 523–535.

Serreze, M.C., 1995. Climatological aspects of cyclone development and decay in the Arctic. Atmosphere-Ocean 33, 1–23.

Sharp, M., Dugmore, A., 1985. Holocene glacier fluctuations in eastern Iceland. Zeitschrift fur Gletscherkd. und Glazialgeol. 21, 341–349.

Sigurðsson, O., 1998. Glacier variations in Iceland 1930-1995. Jökull 45, 3–25.

Sigurðsson, O., 2005. 10. Variations of termini of glaciers in Iceland in recent centuries and their connection with climate, in: Caseldine, C., Russell, A., Harðardóttir, J., Knudsen,

Ó.B.T. (Eds.), Developments in Quaternary Sciences, vol. 5 Iceland — Modern Processes and Past Environments, Elsevier, Amsterdam, pp. 241–255.

Sigurðsson, O., Jónsson, T., Jóhannesson, T., 2007. Relation between glacier-termini variations and summer temperature in Iceland since 1930. Ann. Glaciol. 46, 170–176.

Sigurðsson, O., Williams, R.S., 2008. Geographic Names of Iceland's Glaciers: Historic and Modern. US Geol. Surv. Prof. Pap. 1746 1–42.

Sissons, J.B., 1974. A Late-Glacial Ice Cap in the Central Grampians, Scotland. Trans. Inst. Br. Geogr. 95.

Sissons, J.B., Sutherland, D.G., 1976. Climatic Inferences from Former Glaciers in the South-East Grampian Highlands, Scotland. J. Glaciol. 17, 325–346.

Solomina, O.N., Bradley, R.S., Hodgson, D.A., Ivy-Ochs, S., Jomelli, V., Mackintosh, A.N., Nesje, A., Owen, L.A., Wanner, H., Wiles, G.C., Young, N.E., 2015. Holocene glacier fluctuations. Quat. Sci. Rev. 111, 9–34.

Solomina, O.N., Bradley, R.S., Jomelli, V., Geirsdottir, A., Kaufman, D.S., Koch, J., McKay, N.P., Masiokas, M., Miller, G., Nesje, A., Nicolussi, K., Owen, L.A., Putnam, A.E., Wanner, H., Wiles, G., Yang, B., 2016. Glacier fluctuations during the past 2000 years. Quat. Sci. Rev. 149, 61–90.

Stefansson, U., 1962. North Icelandic waters. Rit Fiskid. 3, 1–269.

Stone, J.O., 2000. Air pressure and cosmogenic isotope production. J. Geophys. Res. Solid Earth 105, 23753–23759.

Stone, J.O., Allan, G.L., Fifield, L.K., Cresswell, R.G., 1996. Cosmogenic chlorine-36 from calcium spallation. Geochim. Cosmochim. Acta 60, 679–692.

Stone, J.O., Fifielde, K., Vasconcelos, P., 2005. Terrestrial chlorine-36 production from spallation of iron, in: Abstract of 10th International Conference on Accelerator Mass Spectrometry. Berkeley, CA.

Stötter, J., 1990. Geomorphologische und landschaftsgeschichtliche Untersuchungen im Svarfaðardalur-Skiðadalur, Tröllaskagi, N-Island. Münchener Geogr. Abhandlungen 9, 1–166.

Stötter, J., 1991. New Observations on the Postglacial Glacial History of Tröllaskagi, Northern Iceland, in: Maizels, J.K., Caseldine, C. (Eds.), Environmental Change in Iceland: Past and Present. Glaciology and Quaternary Geology, Vol 7. Springer, Dordrecht, pp. 181–192.

Stötter, J., Wastl, M., Caseldine, C., Häberle, T., 1999. Holocene palaeoclimatic reconstruction in northern Iceland: Approaches and results. Quat. Sci. Rev. 18, 457–474.

Striberger, J., Björck, S., Holmgren, S., Hamerlík, L., 2012. The sediments of Lake Lögurinn - A unique proxy record of Holocene glacial meltwater variability in eastern Iceland. Quat. Sci. Rev. 38, 76–88.

Styllas, M.N., Schimmelpfennig, I., Ghilardi, M., Benedetti, L., 2016. Geomorphologic and paleoclimatic evidence of Holocene glaciation on Mount Olympus, Greece. The Holocene 26, 709–721.

Sutherland, D.G., 1984. Modern glacier characteristics as a basis for inferring former climates with particular reference to the Loch Lomond Stadial. Quat. Sci. Rev. 3, 291–309.

Swanson, T.W., Caffee, M.L., 2001. Determination of 36Cl production rates derived from the well-dated deglaciation surfaces of Whidbey and Fidalgo Islands, Washington. Quat. Res. 56, 366–382.

Tanarro, L.M., Palacios, D., Andrés, N., Fernández-Fernández, J.M., Zamorano, J.J., Sæmundsson, Þ., Brynjólfsson, S., 2019. Unchanged surface morphology in debris-covered glaciers and rock glaciers in Tröllaskagi peninsula (northern Iceland). Sci. Total Environ. 648, 218–235.

Tanarro, L.M., Palacios, D., Zamorano, J.J., Andrés, N., 2018. Proposal for geomorphological mapping of debris-covered and rock glaciers and its application to Tröllaskagi Peninsula (Northern Iceland). J. Maps 14, 692–703.

Tangborn, W., 1980. Two Models for Estimating Climate–Glacier Relationships in the North Cascades, Washington, U.S.A. J. Glaciol. 25, 3–21.

Thompson, A., Jones, A., 1986. Rates and causes of proglacial river terrace formation in southeast Iceland: an application of lichenometric dating techniques. Boreas 15, 231–246.

Thompson, D., Tootle, G., Kerr, G., Sivanpillai, R., Pochop, L., 2011. Glacier Variability in the Wind River Range, Wyoming. J. Hydrol. Eng. 16, 798–805.

Thorarinsson, S., 1956. On the variations of Svinafellsjokull, Skaftafellsjokull and Kviarjokull in Oraefi. Jokull 6, 1–15.

Úbeda, J., 2011. El impacto del cambio climático en los glaciares del complejo volcánico Nevado Coropuna, (Cordillera Occidental de los Andes Centrales). PhD Thesis. Universidad Complutense de Madrid, Servicio de Publicaciones, Madrid, 583 pp.

Van de Wal, R.S.W., Wild, M., 2001. Modelling the response of glaciers to climate change by applying volume-area scaling in combination with a high resolution GCM. Clim. Dyn. 18, 359–366.

Van der Veen, C.J., 1999. Fundamentals of glacier dynamics. Balkema, Rotterdam. 462 pp.

Vázquez-Selem, L., Lachniet, M.S., 2017. The deglaciation of the mountains of Mexico and Central America. Cuad. Investig. Geográfica 43, 553-570.

Veettil, B.K., Wang, S., Bremer, U.F., de Souza, S.F., Simões, J.C., 2017. Recent trends in annual snowline variations in the northern wet outer tropics: case studies from southern Cordillera Blanca, Peru. Theor. Appl. Climatol. 129, 213–227.

Wagner, S., Zorita, E., 2005. The influence of volcanic, solar and CO2 forcing on the temperatures in the Dalton Minimum (1790-1830): A model study. Clim. Dyn. 25, 205–218.

Wangensteen, B., Guðmundsson, Á., Eiken, T., Kääb, A., Farbrot, H., Etzelmüller, B., 2006. Surface displacements and surface age estimates for creeping slope landforms in Northern and Eastern Iceland using digital photogrammetry. Geomorphology 80, 59–79.

Wanner, H., Beer, J., Bütikofer, J., Crowley, T.J., Cubasch, U., Flückiger, J., Goosse, H., Grosjean, M., Joos, F., Kaplan, J.O., Küttel, M., Müller, S.A., Prentice, I.C., Solomina, O.,

Stocker, T.F., Tarasov, P., Wagner, M., Widmann, M., 2008. Mid- to Late Holocene climate change: an overview. Quat. Sci. Rev. 27, 1791–1828.

Wastl, M., Stötter, J., 2005. 9. Holocene glacier history, in: Caseldine, C., Russell, A., Harðardóttir, J., Knudsen, Ó.B.T. (Eds.), Developments in Quaternary Sciences, vol. 5 Iceland — Modern Processes and Past Environments, Elsevier, Amsterdam, pp. 221–240.

Wastl, M., Stotter, J., Caseldine, C., 2001. Reconstruction of Holocene Variations of the Upper Limit of Tree or Shrub Birch Growth in Northern Iceland Based on Evidence from Vesturardalur-Skidadalur, Trollaskagi. Arctic, Antarct. Alp. Res. 33, 191.

Whalley, W.B., Douglas, G.R., Jonsson, A., 1983. The magnitude and frequency of large rockslides in Iceland in the postglacial. Geogr. Ann. Ser. A., Phys. Geogr. 65, 99–110.

Whalley, W.B., Hamilton, S., Palmer, C., Gordon, J., Martin, H.E., 1995a. The dynamics of rock glaciers: data from Tröllaskagi, North Iceland. In: Slaymaker, O. (Ed.), Steepland Geomorphology. John Wiley & Sons, pp. 129–145.

Whalley, W.B., Palmer, C.F., Hamilton, S.J., Martin, H.E., 1995b. An Assessment of Rock Glacier Sliding Using Seventeen Years of Velocity Data: Nautárdalur Rock Glacier, North Iceland. Arct. Alp. Res. 27, 345–351.

Wiles, G.C., Barclay, D.J., Young, N.E., 2010. A review of lichenometric dating of glacial moraines in Alaska. Geogr. Ann. Ser. A Phys. Geogr. 92, 101–109.

Winkler, S., 2003. A new interpretation of the date of the “Little Ice Age” glacier maximum at Svartisen and Okstindan, northern Norway. The Holocene 13, 83–95.

Winkler, S., 2009. First attempt to combine terrestrial cosmogenic nuclide (10Be) and Schmidt hammer relative-age dating: Strauchon Glacier, Southern Alps, New Zealand. Cent. Eur. J. Geosci. 1, 274–290.

Winkler, S., Lambiel, C., 2018. Age constraints of rock glaciers in the Southern Alps/New Zealand – Exploring their palaeoclimatic potential. The Holocene 28, 778–790.

Wirz, V., Gruber, S., Purves, R.S., Beutel, J., Gärtner-Roer, I., Gubler, S., Vieli, A., 2016. Short-term velocity variations at three rock glaciers and their relationship with meteorological conditions. Earth Surf. Dyn. 4, 103–123.

Xiao, X., Zhao, M., Knudsen, K.L., Sha, L., Eiríksson, J., Gudmundsdóttir, E., Jiang, H., Guo, Z., 2017. Deglacial and Holocene sea–ice variability north of Iceland and response to ocean circulation changes. Earth Planet. Sci. Lett. 472, 14–24.

Young, N.E., Schweinsberg, A.D., Briner, J.P., Schaefer, J.M., 2015. Glacier maxima in Baffin Bay during the Medieval Warm Period coeval with Norse settlement. Sci. Adv. 1.

Zhong, Y., Miller, G.H., Otto-Bliesner, B.L., Holland, M.M., Bailey, D.A., Schneider, D.P., Geirsdóttir, A., 2011. Centennial-scale climate change from decadally-paced explosive volcanism: a coupled sea ice-ocean mechanism. Clim. Dyn. 37, 2373–2387.

Zreda, M., England, J., Phillips, F., Elmore, D., Sharma, P., 1999. Unblocking of the Nares Strait by Greenland and Ellesmere icesheet retreat 10,000 years ago. Nature 398, 139–142.

Zweck, C., Zreda, M., Desilets, D., 2013. Snow shielding factors for cosmogenic nuclide dating inferred from Monte Carlo neutron transport simulations. Earth Planet. Sci. Lett. 379, 64–71.

UNIVERSIDAD
COMPLUTENSE
MADRID

GFAM